

$2_s + 2_s$ REACTIONS AT TRANSITION METALS

Thesis by

MICHAEL L. STEIGERWALD

In Partial Fulfillment of the Requirements
for the Degree of
Doctor of Philosophy

California Institute of Technology
Pasadena, California
1984

(Submitted September 12, 1983)

*Si possent homines, proinde ac sentire videntur
 pondus inesse animo quod se gravitate fatiget,
 e quibus id fiat causis quoque nocere et unde
 tanta mali tamquam moles in pectore constet,
 haud ita vitam agerent, ut nunc plerumque videmus
 quid sibi quisque velit nescire et quaerere semper
 commutare locum, quasi onus deponere possit.
 Exit saepe foras magnis ex aedibus ille,
 esse domi quem pertaesumst, subitoque revertit,
 quippe foris nilo melius qui sentiat esse.
 Currit agens mannos ad villam praecipitanter,
 auxilium tectis quasi ferre ardentibus instans;
 oscitat extemplo, tetigit cum lumina villae,
 aut abit in somnum gravis atque obliviam quaerit,
 aut etiam properans urbem petit atque revisit.
 Hoc se quisque modo fugit, at quem scilicet, ut fit,
 effugere haud potis est, ingratis haeret et odit,
 propterea morbi quia causam non tenet aeger;
 quam bene si videat, iam rebus quisque relictis
 naturam primum studeat cognoscere rerum,
 temporis aeterni quoniam, non unius horae,
 ambigitur status, in quo sit mortalibus omnis
 aetas, post mortem quae restat cumque, manenda.*

Titus Lucretius Carus

"De Rerum Natura"

III. 1052-1075

Acknowledgements

I sincerely thank the California Institute, the National Science Foundation, and the Sun Oil Company for financial support.

I have been at Caltech a long time. Among the myriad of things I've learned here, I've realized that modern science, and the practice of it, are certainly not what I had expected before I came here. The natural philosophy of which Lucretius spoke suffers when its fruits are forced to turn a profit--no matter what form that profit may take. Bummer.

I am compelled to judge Caltech. It is an excellent place to realize a scientific training. It is at best only a fair place in which one may become educated.

I look back to thank those who have given me their friendship, encouragement, and support. Dave Evans first interested me in chemistry--I don't think he knew what he was doing.

Tony Rappé has taught me so much, mostly about the practical side of faith.

Ken Doxsee helped me enjoy my stay here more than he knows.

I hope Bosco Lee finds what he's looking for.

Bob Grubbs helped me learn so much about chemistry. His patience has not been misplaced.

Bill Goddard is an amazing man. The ability to appreciate hare-brained notions for their redeeming features and thereby to impose some--but not too much--discipline on sometimes unruly thoughts must be treasured. Taking calculated risks is part of the job, but taking calculated leaps of faith puts spirit into the whole thing.

Lists are odious--one always forgets important people. To all who have added so much to my life in California go my thanks. I cannot forget the Weenies, especially Barry and Art, who made summertime more than just another season.

Very special thanks go Adria who always does so much to remind me about people and life and being happy.

The best thing Caltech ever did for me, by bunches, was to introduce me to Mary. Words of thanks will never suffice.

ABSTRACT

A study of the suprafacial 2 + 2 reaction at transition metal centers is presented. It is demonstrated that this reaction is allowed and proceeds with a low activation energy if the reacting transition metal-to-substituent bond is covalent, nonpolar, and has a large component at transition nickel d-orbital character. These chains are evinced by examination of $2_s + 2_s$ reactions at M-H bonds. Those systems in which M can use d orbitals show lower barriers to the $2_s + 2_s$ reaction than those in which M cannot use d orbitals.

The importance of the electronic structure of the metal-to-substituent bond is highlighted by a study of dichlorotitanacyclopropane. This molecule, being a metallacyclopropane, can undergo $2_s + 2_s$ reactions which one unavailable to a simple olefin.

Studies concerning the importance of $2_s + 2_s$ reactivity in the organic chemistry of nickel, and in the Ziegler-Natta polymerization of simple olefins are presented.

It is suggested that the principle of maximum bonding (the Woodward-Hoffmann rules) implies the conservation of transition metal covalency in low-energy catalytic cycles.

TABLE OF CONTENTS

	<u>Page</u>
<u>Chapter 1:</u> Reactions of D_2 with Cl_2TiH^+ , Cl_2TiH and Cl_2SCH	1
I. Introduction	2
II. Results and Discussion	4
III. Appendix: Details of the Calculations	8
IV. Tables and Figures	11
V. References and Notes	23
<u>Chapter 2:</u> Reactions of D_2 with Main Group Hydrides	26
I. Introduction	27
II. Results	29
III. Discussion	33
IV. Conclusion	55
V. Appendix: Details of the Calculations	56
VI. Tables and Figures	59
VII. References and Notes	85
<u>Chapter 3:</u> Dichlorotitanacyclopropane	92
I. Introduction	93
II. Results and Discussion	95
III. Conclusions	106
IV. Appendix: Details of the Calculations	107
V. Tables and Figures	113
VI. References and Notes	139
<u>Chapter 4:</u> Reaction of Cl_2ZrH with D_2	145
I. Introduction	146
II. Results	147
III. Discussion	149
IV. Conclusion	153
V. Appendix: Details of the Calculations	156
VI. Tables and Figures	157
VII. References and Notes	175

	<u>Page</u>
<u>Chapter 5:</u> Effect of Hybridization on Reactions at Transition Metals	179
I. Hybridization of Atomic Orbitals on Transition Metals	180
II. Shapes of Hybrid Orbitals	183
III. Bonding to Hybrid Orbitals	185
IV. The Nature of the Chemical Bond	188
V. Figures	192
VI. References and Notes	207
<u>Chapter 6:</u> Carbon-Carbon Bond Cleavage in Nickelacyclopentanes	211
I. $2_s + 2_s$ Reactions in the Organic Chemistry of Nickel	212
II. Previous Work	222
III. Hypothesis	225
IV. Transphos - 2,11-bis(diphenylphosphino- methyl)benzo[c]phenanthrene	226
V. Attempted Synthesis of (transphos)- nickelacyclopentane	228
VI. Experimental Section	241
VII. Figures	251
VIII. References and Notes	260
<u>Chapter 7:</u> Concerning the Mechanism of Ziegler- Natta Polymerization of Simple Olefins	267
I. Isotope Effects on Propagation Rates	268
II. Appendix: Elaboration on Footnote 17	270
Conclusion	280

Chapter 1. Reactions of D_2 with Cl_2TiH^+ , Cl_2TiH and Cl_2Sch .

Introduction

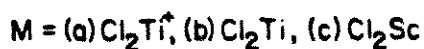
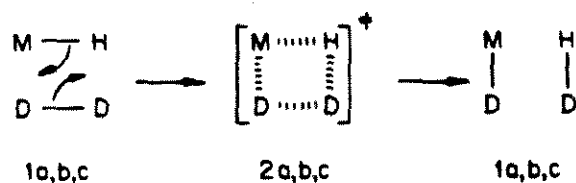
The Woodward-Hoffmann orbital symmetry rules have had a profound effect on the understanding of organic reactions,¹ but attempts to generalize these rules to organic reactions mediated by transition metals have not led to specific results of comparable utility.² It is generally assumed that there are no particular reactions that are symmetry-forbidden for transition metal systems. For example, [2s + 2s] reactions such as migratory insertion pervade organometallic chemistry,³ whereas analogous reactions are known to be forbidden in strictly organic systems. Our belief (*vide infra*) is that the detailed nature of the metal-hydrogen and metal-carbon *covalent* bond is critical to the process of these now allowed reactions. An appreciation of the transition-metal-ligand covalent bond is now emerging⁴ that allows us to go beyond the simple standards of allowed and forbidden and to begin predicting relative rates of particular organometallic reactions. In this paper we outline some recent studies of concerted reactions of transition metals. We find that low activation barriers for reactions such as (1) will result when the M-Z bond is nonpolar and covalent, involving strictly d-character in the metal center.



Our analysis of molecules and their reactions is based on simple valence bond wavefunctions supplemented by *ab initio* generalized valence bond (GVB) calculations.⁵ Within this description, a chemical bond is formed by the overlap of two one-electron orbitals,⁶ and a reaction results from the delocalization of one or more previously localized

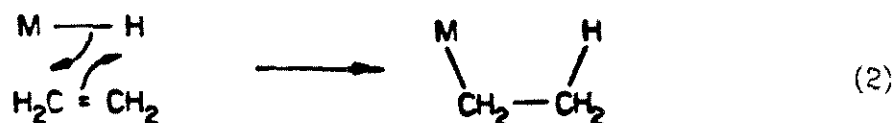
bonds across several centers, and the subsequent relocation to give the bonds of the products. The Pauli principle governs the course of these delocalizations, and in so doing provides selection rules for reactivity.⁷

In order to investigate the nature of these reactive orbital delocalizations in the organometallic migratory insertion reaction, we have studied the three reactions shown in Scheme I.



Scheme I

These simple exchange reactions are expected to be electronically quite similar to the more traditional $[2_s + 2_s]$ reactions such as insertion of an olefin into a metal-hydrogen bond (2).



The study of this sequence was chosen to answer three questions:

- 1) Does the indicated exchange proceed with a low activation barrier, and, if so, how?
- 2) What is the effect of the Lewis acidity of the metal center on this activation barrier?

- 3) What is the effect of spectator electrons (such as the unpaired electron of Cl_2TiH) on this activation barrier?

Results and Discussion

In order to answer these questions, we have determined accurate wavefunctions for the reactants (1a,b,c) and compared them with analogous wavefunctions for the indicated transition states (2a,b,c). The geometries of these species were optimized and are reported in Tables I and II. Throughout this study, the chloride ligands, being simply model anionic ligands, were held fixed at the values shown. The four-center transition states were assumed to have C_{2v} symmetry, and the geometries were optimized with this constraint. The activation barriers are quoted in Table III.

From Table III one sees that these three reactions proceed with low activation barriers (with that of the titanium cation being conspicuously lower), and hence the reactions are allowed. Examination of the active orbitals along the reaction path indicate why this is so. Figure 1 shows the four active one-electron orbitals as they move from reactants to products. We see that the original bond pairs (Ti-H and H-H) are retained throughout the reaction. At the transition state, one of these bonds becomes a three-center bond on the three hydrogens; the other a three-center bond on the titanium and its two neighboring hydrogens. As the reaction proceeds to products, these delocalized bonds relocalize to form the bonds characteristic of the products. The change in bond pair overlaps (Table IV) substantiates our assertion that the two active bonds are retained throughout these reactions.

It is critical to note that the two three-center bonds of the transition state are orthogonal to one another, as demanded by the Pauli principle.

It is in this ability that transition metals outdo main group elements. Examining the pericyclic $[2_s + 2_s]$ cyclodimerization of ethylene (Figure 2), we see that the two active bonds in the reactants (the C-C π bonds) *cannot* delocalize to give two three-center bonds in the transition state that are mutually orthogonal. Either the two delocalized bonds are not orthogonal (forbidden by the Pauli principle) or one of the bonds is forced to be broken at the transition state (the definition of a forbidden reaction). It is the shape and availability of the transition metal d-orbital that allows the orthogonal delocalization to occur.

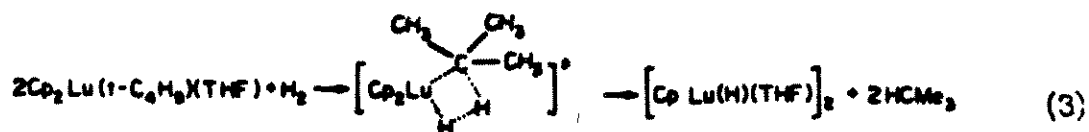
Based on these considerations, we believe that the more metal d-character in the M-Z bond [Eq. (1)], the lower the activation barrier for the exchange reaction and analogous insertions. This is because any metal s- or p-character in the active bond must be removed on going to the X \cdots M \cdots Z three-center bond in the symmetrical transition state, leading to increased activation energy (see Table IV), and this change in optimal orbital hybridization about the metal will be energetically costly. This contributes to the explanation for the very low barrier for exchange in the $(\text{Cl}_2\text{TiH})^+$ system. The metal orbital in this Ti-H bond is $\sim 90\%$ d in character, whereas in the other two cases, the corresponding metal orbital is only 50-70% d (Table I, Figures 1, 3, and 4).

In comparing the reaction of $(\text{Cl}_2\text{TiH})^+$ with the isoelectronic Cl_2ScH , we see that the effect of increasing the intrinsic Lewis acidity of the metal center is to decrease the barrier height for the exchange reaction. One explanation for this is given above. The more electronegative the metal center, the more d-character in the active bond,⁸ and therefore the lower energy of the transition state. A second point is that the overlap of the two bonding orbitals in $(\text{Cl}_2\text{TiH})^+$ is quite low (0.44) compared

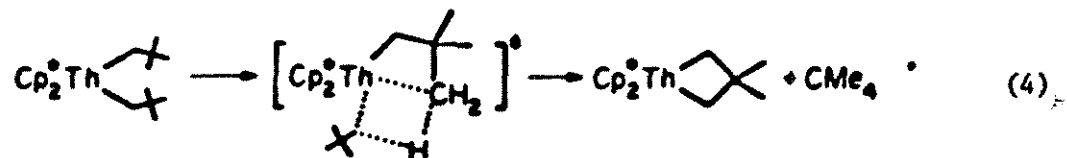
with that in Cl_2ScH (0.74). This indicates that the TiH bond in $(\text{Cl}_2\text{TiH})^+$ is significantly weaker than the Sc-H bond in Cl_2ScH . This would imply a correspondingly lower barrier for the exchange reaction. Finally, even though H_2 is not a particularly good Lewis base, a donor/acceptor interaction (to the extent of an additional transfer of 0.21 electrons from the new H_2 to the Cl_2TiH fragment) stabilizes the cationic transition state.

Comparison of the exchange reactions of Cl_2ScH and Cl_2TiH shows the effect of the odd electron on titanium. In order to transform from the metal bonding orbital in the reactant to that at the transition state, the reactant orbital must mix with some of the d-orbital, which is singly-occupied in the case of Cl_2TiH , but empty in the case of the Cl_2ScH . Equivalently, the odd electron in $\text{Cl}_2\text{Ti(H)(D)}_2$ must be in an orbital that is orthogonal to the $\text{H}\cdots\text{Ti}\cdots\text{D}$ and $\text{H}\cdots\text{D}\cdots\text{D}$ bonds. This orthogonality requirement results in energetic destabilization and is absent in the case of $\text{Cl}_2\text{Sc(H)(D)}_2$. In this case our calculations indicate that this mixing is of moderate energetic cost, 4.3 kcal (even though the orbital energy of the singly-occupied orbital changes from -0.5314 hartree in Cl_2TiH to -0.5153 hartree in Cl_2TiH_3 , a destabilization of 10.1 kcal/mol). We expect that such spectator d-electrons may have even greater effect upon reaction barriers in other systems.

These results may have distinct implications for our appreciation of known organometallic processes. For example, we expect that the exchange of H for D between $\text{Cp}_2^*\text{ZrH}_2$ and D_2 ,⁹ the direct hydrogenolysis of lanthanide alkyl complexes,¹⁰



and the thermolysis of $\text{Cp}_2^+\text{Th}(\text{CH}_2\text{CMe}_3)_2$.¹¹



proceeds by a direct four-center concerted mechanism, as in these model studies. Furthermore, these results suggest that the titanium site in Ziegler-Natta polymerization¹² is more active if it is a *cationic* Ti(IV) rather than a neutral Ti(III). In this way, our work underscores the suggestion that one of the functions of the Lewis acidic cocatalysts used in Ziegler-Natta polymerization is to remove an anionic ligand such as Cl^- from the sphere of the metal.¹³

Appendix: Details of the Calculations

Appendix

These calculations were performed at the fully *ab initio* level. All titanium, scandium, and hydrogen orbitals (core as well as valence) were optimized explicitly. Geometries were optimized at the calculational levels outlined in Tables I and II. Valence double zeta basis sets were used on the metals, and unscaled triple zeta sets on each hydrogen atom.¹⁴ The chlorine atoms were described by valence minimum basis sets that were optimized for Cl_2TiH_2 , and the chlorine core electrons were described by an *ab initio* effective potential.¹⁵ The geometries of the Cl_2MH_3 species were optimized using the GVB gradient program of Low and Goddard.¹⁶

In determining the barrier height (Table III) we calculated the GVB-PP(2/4) wavefunction at the saddle point, included the two additional spin eigenfunctions characteristic of a full GVB wavefunction (i.e., GVB-RCI), and then carried out a CI calculation allowing all single excitations from the six GVB-RCI configurations to all virtual orbitals. This procedure relaxes all orbital orthogonality and spin-coupling restrictions involved in interactions of the orbitals and is expected to yield accurate barriers. In the limits of the reactant and product species, the above wavefunction reduces to a GVB(1/2) wavefunction on H_2 plus the following wavefunction on Cl_2MH . Starting with GVB-PP(1/2) and including the third configuration of the RCI, we include all single excitations into the full virtual space. For Cl_2ScH and Cl_2TiH^+ , this reduces to GVB-PP, but for Cl_2TiH there are additional spin-coupling terms arising from the extra electron.

As a control, we calculated the barrier for the exchange reaction of $\text{H} + \text{D}_2 \rightarrow \text{HD} + \text{D}$. Using this method, we calculate a barrier of 14.6 kcal/mol for this reaction. The most accurate calculations available show

this barrier to be 9.90 kcal/mol.¹⁷ These comparisons indicate that our calculations should yield barriers that are systematically ~5 kcal/mol high.

Table I. Geometries of Cl_2MH . a, b)

Complex	θ (ClTiCl)	$r(\text{Cl-Ti})$	$r(\text{TiH})$	Mulliken Populations in M-H bond pair		
				M (valence d)	M (valence s and p)	H
$\text{Cl}_2\text{TiH}^\oplus$	(140°)	(2.328 Å)	1.80 Å ^{c)}	1.07	0.22	0.71
Cl_2TiH	(140°)	(2.328 Å)	1.70 Å	0.70	0.37	0.87
Cl_2ScH	(142°)	2.35 Å	1.78 Å	0.55	0.44	0.98

a) Values in parentheses are not optimized. Other parameters were optimized using a wavefunction having a correlated [GVB(1/2)] M-H sigma bond.

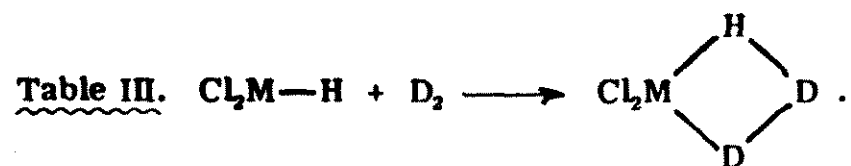
b) $\text{Cl}_2\text{TiH}^\oplus$ was found to be planar. Cl_2TiH and Cl_2ScH were subsequently assumed to be planar.

c) When the Ti-H bond length was optimized at the Hartree-Fock level, a value of 1.58 Å was found. Intrapair correlation is critical in this calculation.

Table II: Geometries of $\text{Cl}_2\text{M}(\text{H})(\text{D})_2$. a, b)

Complex	r_1	r_2	θ	α
$\text{Cl}_2\text{Ti}^{\oplus}(\text{H})(\text{D})_2$	1.782 Å	0.992 Å	62°	134°
	(1.750 Å)	0.993 Å	64°	137°)
$\text{Cl}_2\text{Ti}(\text{H})(\text{D})_2$	1.8459 Å	1.0284 Å	65°	148°
$\text{Cl}_2\text{Sc}(\text{H})(\text{D})_2$	1.887 Å	1.014 Å	62°	149°

- a) In each case the Cl_2M fragment was held fixed at the values from the Cl_2MH molecule.
- b) C_{2v} symmetry was assumed for all complexes.
- c) The geometry of $\text{Cl}_2\text{Ti}(\text{H})(\text{D})_2$ and that of $\text{Cl}_2\text{SC}(\text{H})(\text{D})_2$ were optimized using gradient techniques at the Hartree-Fock level. Owing to the inaccuracy of the Hartree-Fock prediction of the Ti-H bond length in $\text{Cl}_2\text{Ti}^{\oplus}$, this optimization technique could not be used for $\text{Cl}_2\text{Ti}^{\oplus}(\text{H})(\text{D})_2$. This reported geometry results from a point-by-point geometry search at the GVB(2/4) level and is therefore only approximate. The geometry in parentheses is the result of this Hartree-Fock gradient optimization.



Reactant	Barrier Height	Mulliken Populations				
		Transition State D...M...H Bond			Total on hydrogens in MH_3	
		s	p	d	Terminal	Central
$\text{Cl}_2\text{TiH}^\oplus$	2 kcal/mol ^{a)}	0.0	0.06	1.09	0.70	0.82
Cl_2TiH	21.7 kcal/mol	0.0	0.11	0.72	0.93	0.82
Cl_2ScH	17.4 kcal/mol	0.0	0.13	0.61	1.00	0.80

^{a)} Upper limit; see footnote c), Table II.

Table IV. GVB Pair Overlaps in Active Bonds.

System	Reactants		Transition State	
	M-H	H-H	H···M···D	H···D···D
\oplus Cl ₂ TiH	0.44	0.80	0.54	0.84
Cl ₂ TiH	0.66	0.80	0.72	0.84
Cl ₂ ScH	0.74	0.80	0.77	0.84

Figure 1. GVB orbitals for the $\text{Cl}_2\text{Ti}^+-\text{H} + \text{D}_2 \rightarrow \text{Cl}_2\text{Ti}^+-\text{D} + \text{HD}$ reaction. (i) Reactants. (ii) Transition state. (iii) Products. Solid lines indicate positive amplitude and dashed lines indicate negative amplitude. The spacing between contours is 0.05 a.u.

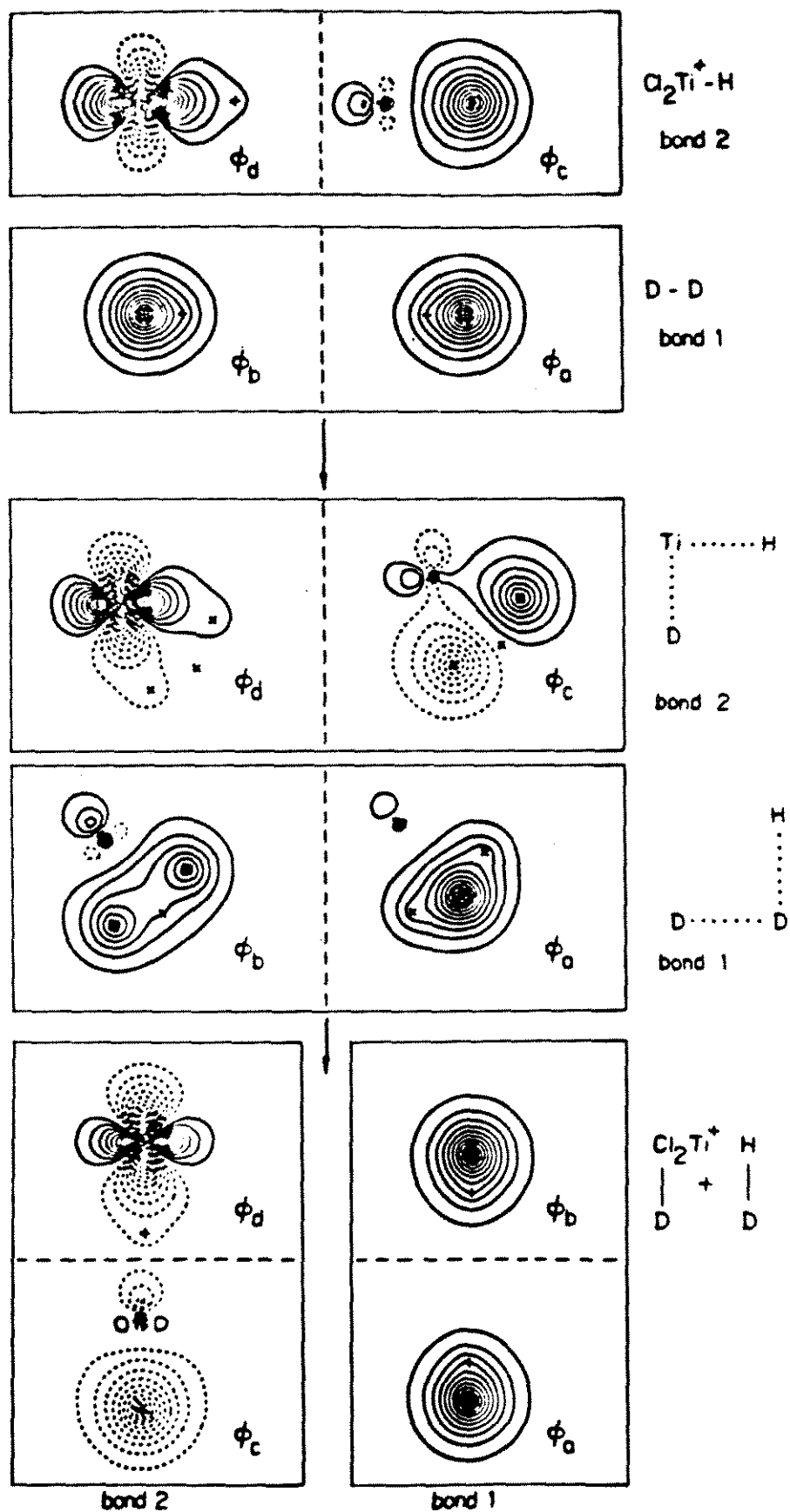


Figure 2. Valence bond orbitals for the $C_2H_4 + C_2H_4 \rightarrow$ cyclobutane reaction. (i) Reactants. (ii) Transition state. (iii) Products.

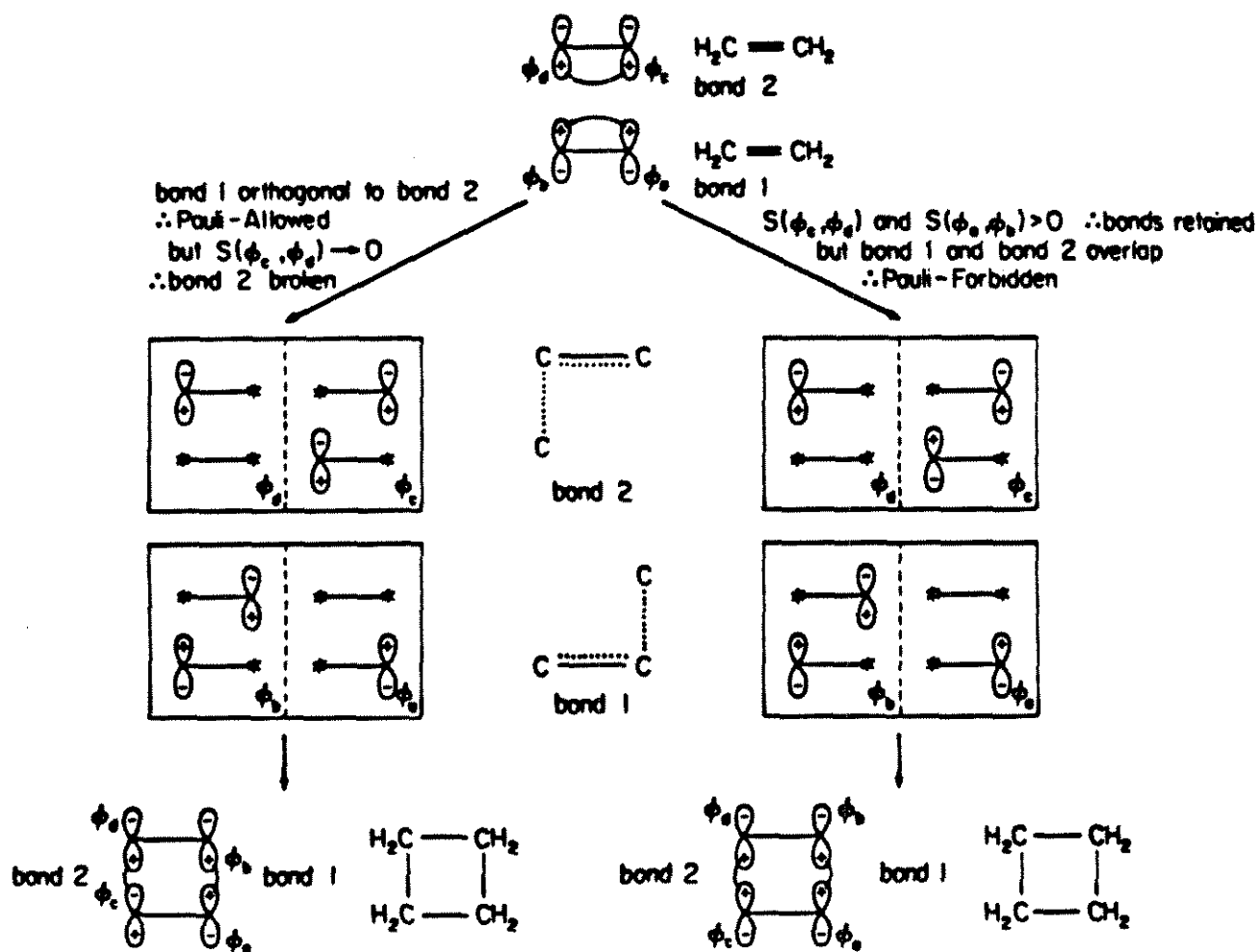


Figure 3. GVB orbitals describing the Sc-H bond of Cl_2ScH . The spacing between contours is 0.05 a.u.

Sc-H bond in Cl ScH

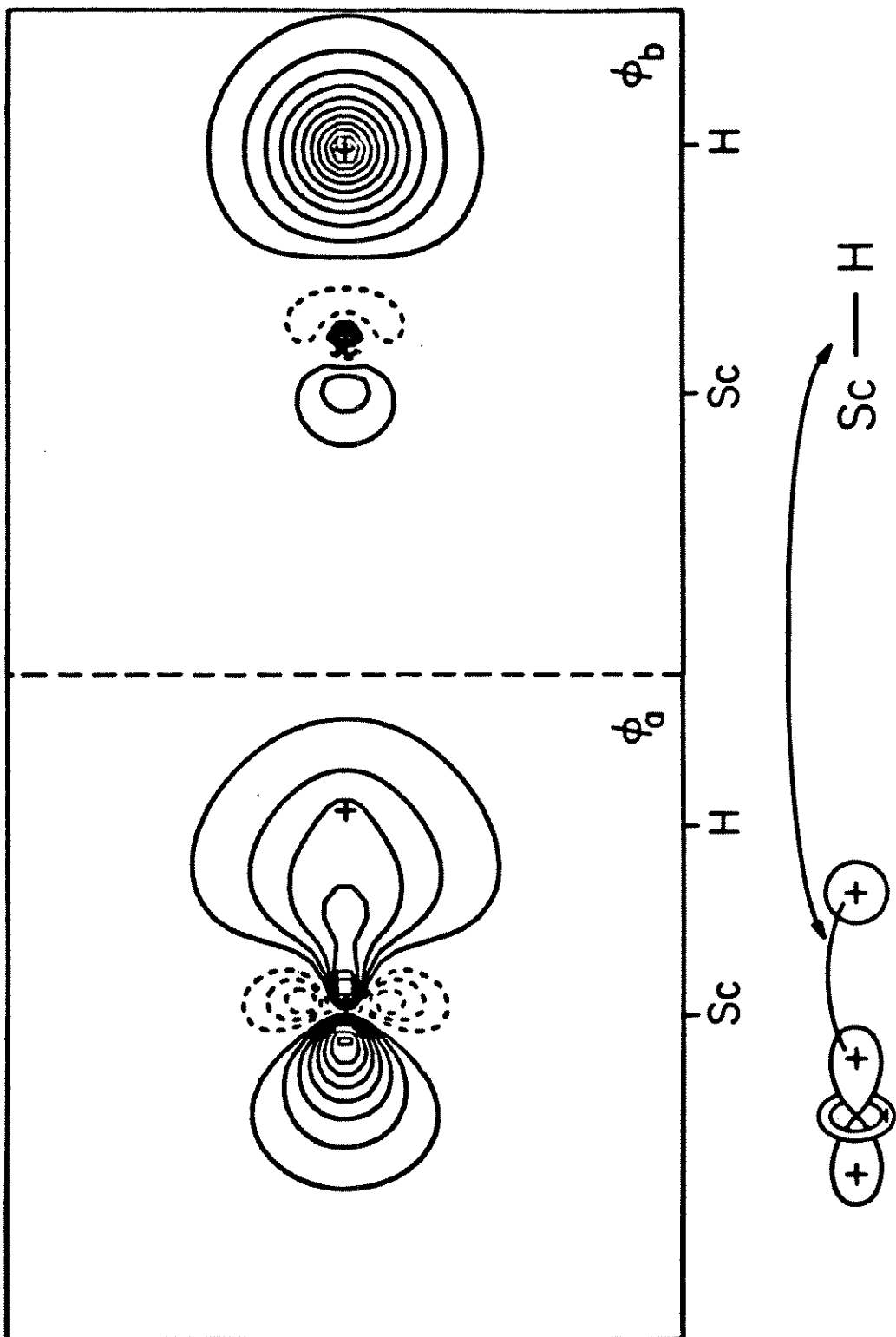
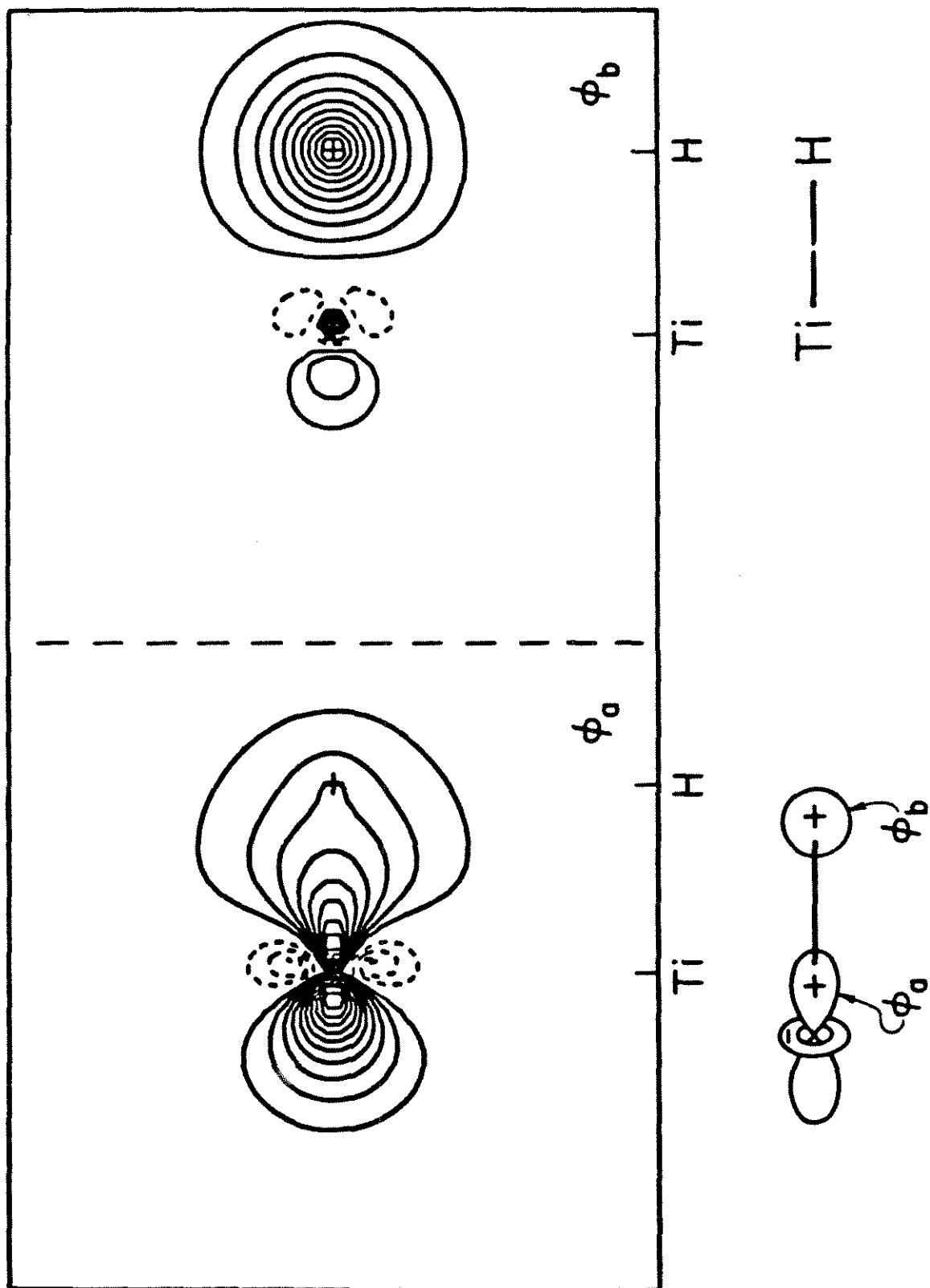


Figure 4. GVB orbitals describing the Ti-H bond of Cl_2TiH . The spacing between contours is 0.05 a.u.

Ti—H σ bond in Cl_2TiH



References and Notes

- (1) Woodward, R. B.; Hoffmann, R. "The Conservation of Orbital Symmetry"; Academic Press: New York, 1970.
- (2) Mango, F. D.; Schachtschneider, J. H. *J. Am. Chem. Soc.*, **1971**, *93*, 1123-1130; Pearson, R. G. *Chem. Brit.*, **1976**, *12*, 160.
- (3) See, for example, Collman, J. P.; Hegedus, L. S. "Principles and Applications of Organotransition Metal Chemistry", University Science Books: Mill Valley, California, 1980.
- (4) A. K. Rappe and W. A. Goddard III, *J. Am. Chem. Soc.*, **1982**, *104*, 297-299, 448-456, 3287-3294.
- (5) Goddard III, W. A.; Dunning, Jr., T. H.; Hunt, W. J.; Hay, P. J. *Accts. Chem. Res.*, **1973**, *6*, 368-376.
- (6) Pauling, L. "The Nature of the Chemical Bond", Cornell University Press: Ithaca, New York, 1960.
- (7) Goddard III, W. A. *J. Am. Chem. Soc.*, **1972** *94*, 793-807.
- (8) In almost all transition metal atoms, single ionization results in the removal of an electron from the valence s orbital rather than from the valence d orbital (Moore, C. E. "Atomic Energy Levels"; National Standard Reference Data Series, NBS 35; U. S. Government Printing Office: Washington, DC, 1971.) Therefore, electronegative substituents (e.g., Cl) will bond to a transition metal using the more easily ionized valence s orbital of the metal, thereby making a more polar (and stronger) bond. This will have less valence s space (and, consequently, relatively more valence d space) for the electronegative substituents (e.g., H) to use in bonding. In general, higher positive charge on the metal (due either to electronegative substituents or

to ionization) will indicate that less valence s and more valence d space will be available for subsequent bonding. Higher positive charge on M also indicates a higher electronegativity at M, and hence our statement in the text.

- (9) Bercaw, J. E. *Advan. Chem. Ser.*, **1978**, *167*, 136-148.
- (10) Evans, W. J.; Meadows, J. H.; Wayda, A. L.; Hunter, W. E.; Atwood, J. L. *J. Am. Chem. Soc.*, **1982**, *104*, 2008-2014.
- (11) Bruno, J. W.; Marks, T. J.; Day, V. W. *J. Am. Chem. Soc.*, **1982**, *104*, 7357-7360.
- (12) Cossee, P. *J. Catal.*, **1964**, *3*, 80.
- (13) Boor, Jr., J. "Ziegler-Natta Catalysts and Polymerizations", Academic Press, Inc.: New York, 1979.
- (14) The metal basis sets are from Rappe', A. K.; Smedley, T. A.; Goddard III, W. A. *J. Phys. Chem.*, **1981**, *85*, 2607-2611. The hydrogen basis used is a triple zeta contraction of the Huzinaga (unscaled) six primitive basis. See Dunning, Jr., T. H.; Hay, P. J. In "Modern Theoretical Chemistry: Methods of Electronic Structure Theory", Schaefer III, H. F., Ed.; Plenum Press: New York, 1977; Vol. 3 and references therein.
- (15) (a) Goddard III, W. A.; Rappe', A. K. In "Potential Energy Surfaces and Dynamics Calculations"; Truhlar, D. G., Ed.; Plenum Press: New York, 1981, pp 661-684; (b) Rappe', A. K.; Smedley, T. A.; Goddard III, W. A. *J. Phys. Chem.*, **1981**, *85*, 1662-1666.
- (16) Low, J. J.; Goddard III, W. A., unpublished results. The GVB gradient program is based on HONDO [Dupuis, M.; King, H. F. *J. Chem. Phys.*, **1978**, *68*, 3998-4004]; Gaussian 80 (Binkley, J. S.; Whiteside, R. A.;

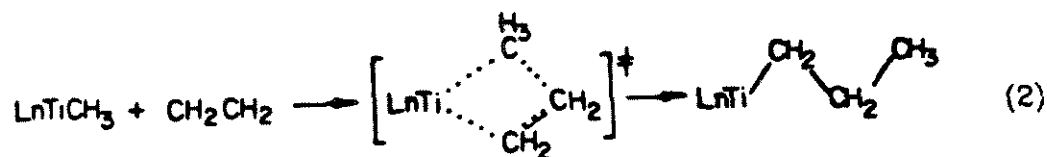
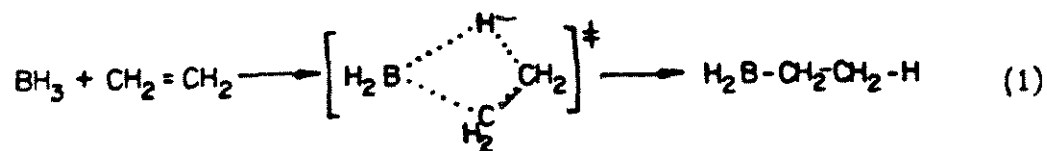
Krishnan, R.; Seeger, R; DeFrees, D. J.; Schlegel, H. B.; Topiol, S. W.; Kahn, L. R.; Pople, J. A.); and the vibrational analysis programs of McIntosh, D. F.; Peterson, M. R. (Quantum Chemistry Program Exchange #342).

- (17) Siegbahn, P.; Liu, B. *J. Chem. Phys.*, 1978, 68, 2547.

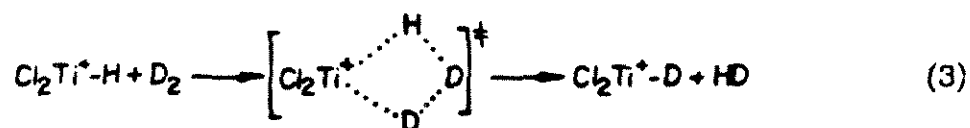
Chapter 2. Reactions of D₂ with Main Group Hydrides.

I. Introduction

For the concerted reactions of simple hydrocarbons, it is well-known (from the Woodward-Hoffmann rules) that the suprafacial 2 + 2 reaction is forbidden.¹ However, for a number of reactions involving main group metals or transition metals, the simplest mechanisms consistent with experiment invoke cyclic, four-center transition states. Examples include the hydroboration of olefins² [Eq. (1)] and the Cossee Arlman mechanism for Ziegler-Natta polymerization³ [Eq. (2)],

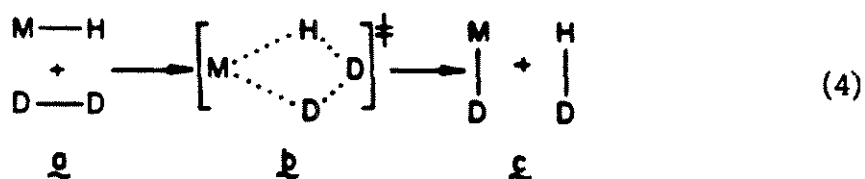


Recently we have examined several examples of the four-center reaction at transition metals such as the H/D exchange reaction in Eq. (3).⁴ In that work we showed that



to achieve a low activation energy it is critical that the bond to the transition metal be covalent and nonpolar and involve substantial d-orbital character on the metal. If this situation occurs, the reacting bonds [Ti-H and D-D in Eq. (3)] are retained in the transition state, leading to a low activation barrier. This view that the transition metal mediated suprafacial 2 + 2 reaction will proceed at lower activation energy if the metal-to-ligand bond in the reactants (M-H, M-CR₃, etc.) is nonpolar is at variance

with the belief that polar bonds are more reactive than nonpolar ones,⁵ and at variance with the notion that a *vacant* orbital of p character (as in trivalent boron, trivalent aluminum, divalent magnesium, monovalent alkali metals, and so forth) serves the same role in promoting the $2_s + 2_s$ reaction as a *vacant* d orbital at a transition metal.⁶ In order to test these ideas concerning selection rules for $2_s + 2_s$ reactions, we have performed *ab initio* quantum chemical calculations of activation enthalpies for a set of $2_s + 2_s$ reactions [Eq. (4)] involving *polar* M-H bonds in systems that do *not* allow the use of valence d-orbitals by the reacting atoms.



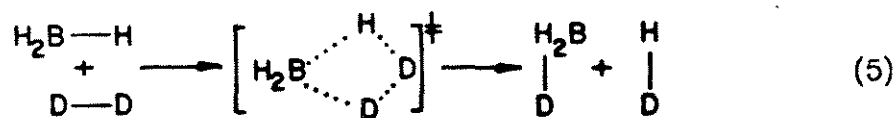
We find that *except* for the case of BH_3 , the transition state [Eq. (4), structure **b**] is polar (M^+H_3^-), making the reaction look like a hydride-transfer (or heterolytic activation of H_2).⁷ Only in the case of BH_3 is the transition state [Eq. (4) structure **b**, $\text{M} = \text{H}_2\text{B}$] nonpolar and covalent. We thus find two limiting cases, the "nonpolar" and the "polar" reactions, where (1) the relative rates of the *nonpolar reactions* can be related to the valence-s-to-valence-p excitation on M and the ability of this π state of M to form strong π bonds, and (2) the relative rates of the *polar reactions* can be related to the ionization potential of M.

II. Results

Using methods described in the Appendix, we calculated the activation barrier heights (Table I) for the reactions in Eq. (4). Here we see that there are two sets of reactions: the allowed reactions ($E_{\text{act}} \approx 24\text{-}34$ kcal/mol), and the forbidden reactions ($E_{\text{act}} \geq 40$ kcal/mol). The objective of our analysis will be to understand what makes one reaction "allowed" and another "forbidden", and to provide ways to estimate the activation energy for a reaction based on spectroscopic properties of the reactants.

We used generalized valence bond (GVB)⁸ wavefunctions to obtain activation barriers for these reactions. In the GVB model, each chemical bond in a molecule is described by two *overlapping*, one-electron orbitals, just as in the simple valence bond formalism; however, in GVB calculations, these one-electron orbitals are allowed to optimize their hybridization and delocalization. An example, the GVB orbitals for the H-H bond in H_2 are shown together with the 1s orbital of H atom in Figure 1. Each orbital in the H-H bond looks similar to but not exactly the same as the 1s orbital of the atom. (In fact, the overlap of a GVB orbital of H_2 and an atomic 1s on the same center is 0.988.)⁹ Thus, the GVB method has the interpretability of simple valence bond and the quantitative benefit of self-consistent field optimization. The **atomic** nature of GVB one-electron orbitals allows the facile qualitative as well as quantitative description of bond forming and bond breaking processes, and hence this particular orbital description is used.

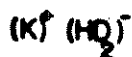
In Figure 2 we illustrate the method, showing the four one-electron orbitals that are active in the H/D exchange reaction between BH_3 and D_2 [Eq. (5)].



The optimal description of the B-H bond shows one electron localized in what is predominantly a 1s orbital on H, (φ_{2b}), and one electron localized in a predominantly sp^2 hybrid orbital on B, (φ_{2a}). These orbitals (φ_{2a} and φ_{2b}) have an overlap at 0.83, indicative of a strong bond. The bond in D_2 is formed by the overlap ($S = 0.80$) of the two orbitals, φ_{1a} and φ_{1b} . Each of these two orbitals is predominantly a localized hydrogen 1s orbital.

At the transition state for this reaction, the pair of orbitals, φ_{1a} and φ_{1b} , which started the reaction as the D-D bond, has delocalized over the D-D-H region of the $\text{H}_2\text{B}(\text{H})(\text{D})_2$ molecule, retaining a high overlap. Similarly, the pair of orbitals (φ_{2a} and φ_{2b} , which started the reaction describing the B-H bond, has delocalized over the H-B-D region, also retaining a high overlap. The delocalization of covalent bonds at the transition state thus results in two three-center two-electron covalent bonds [bonds 1 and 2 in Figure 2(ii)].

In contrast, we show the results of our study of the reaction of KH with D_2 in Figure 3. This reaction involves the reorganization of four active orbitals, φ_{1a} and φ_{1b} (the D-D bond), and φ_{2a} and φ_{2b} (the KH bond), just as above. As in the $\text{BH}_3 + D_2$ reaction, the D-D bond delocalizes over the D-D-H region in the transition state. In this case, however, the K-H bond delocalizes not over the H-K-D region but just on the "terminal" H and D atoms. Therefore, the transition state for the KH + D_2 reaction looks like $\text{K}^+(\text{HD}_2)^-$, 1,



1

i.e., an *ionic* bond of K^+ to H_3^- , whereas for the $H_3B + D_2$ reaction, the transition state is best described as a covalent bond between the H_2B *radical* and the H_3 *radical*. The changes in GVB orbital overlaps in the two active bonds in each reaction studied are shown in Table II.

Our studies of the other eight reactions showed that in each case three of the active orbitals (the two describing the $H \cdots D \cdots D$ bond and one of the orbitals describing the $H \cdots M \cdots D$ bond, the orbital distributed uniformly over just the two "terminal" hydrogens) were essentially identical (for example, compare Figures 2 and 3, φ_{1a} , φ_{1b} , and φ_{2a} at the transition states). For this reason we show only the fourth active orbital (φ_{2b}) for each of these other eight reactions in Figure 4. In order to assess the role of charge in determining the properties of the transition states, the Mulliken populations¹⁰ of the atoms of the reactants and of the transition states are shown in Table III. The parameters describing the optimum geometries of the MH_3 complexes are reported in Table IV together with the geometrical parameters optimized for the reactants (M-H and H_2).

The wavefunctions and populations at the transition state should be compared with the corresponding quantities of the reactants (M-H and H_2), as shown in Figure 2 for BH_3 and in Figure 1 for KH. It is important to note that the KH bond is found to be quite *polar*, as is apparent because both orbitals of the KH bond are localized on hydrogen. This is in contradistinction to the case of H_2B-H in which one orbital is centered on H while the other orbital remains on boron. (For comparison, the valence s orbital on K atom and the sp^2 orbital on free BH_2 ¹¹ are shown in Figure 5.)

On the other hand, the *other* orbital of the two-electron bond is essentially a hydrogen 1s orbital in each of the cases we studied. Thus the M-H bond goes from the nonpolar extreme to the polar (M^+H^-) extreme, based solely on the character of the optimized "M-centered" orbital. In a covalent bond, this orbital is localized on the metal (as in BH_3), whereas in an ionic bond it is localized on the H. These "M-centered" orbitals for the various M-H bonds are shown in Figure 6. All of the alkalis (Li, Na, K, Rb) lead to quite polar bonds; however, the B-H bond is nonpolar while Al-H bond is polar. The Be-H bond is intermediate in polarity between the LiH and BH bonds. Transition metals that cannot use d orbitals in the M-H bonds (d^{10} Cu and d^5 Mn) are quite polar. This can be contrasted with cases such as Cl_2ZrH_2 (Figure 7)¹² where the bond is quite nonpolar and covalent with mainly d character on the metal. A more quantitative measure of these charge transfer effects is provided by the Mulliken populations in Table III.

III. Discussion

A. Geometries of the MH_3 Transition State

Perusal of Table IV shows that the geometry changes on going from $MH + H_2$ to the four-center transition state are similar for all cases. The reactive M-H bonds lengthen by 0.1 to 0.2 Å, while the H-H bond increases (from 0.74 in H_2)¹³ by 0.31 to 0.36 Å. The H-H-H angle in MH_3 lies in the range 150-160°. These values for $r(H-H)$ and $\vartheta(H-H-H)$ should be compared with our calculated values of 0.919 Å and 180°, respectively, for the H_3 radical¹⁴ and 1.079 Å and 180°, respectively, for the H_3^- anion.¹⁵ Based on the electronic structure of the MH_3 complexes (see Figures 2, 3, and 4), there is little directed valence toward the H_3 unit at M in the MH_3 complexes, and thus the HMH angle ranges from 46° to 99°, imposing no independent requirements on the transition state geometries.

The reaction of BH_3 is unique. The HBH angle internal to the exchanging units is significantly larger (99° versus 50° to 80° for the other reaction) than the corresponding angles in all the other exchange reactions. Similarly, the H-H-H angle is significantly smaller than the average (132° versus 145° to 169°). This is easily understood in terms of the electronic structure of this transition state (vide infra). The boron-centered orbital in the H-B-H bond (Figure 2, φ_{2b} of the transition state) shows a great deal of boron p-character. (In fact, removal of the boron p functions from the SCF calculations results in an increase in total energy of 74 kcal/mol, whereas the increase is only 24 kcal/mol for the corresponding exclusion in the case of H_2AlH_3 .¹⁵) The dominance of this p character implies a preferred H-B-H angle of 180°; however, this would require the rupture of the H_3 unit and thus the cleavage of the original D-D bond, thereby making the reaction forbidden. Thus there is a compromise between maximal H-

B-H bonding (180° at boron) and maximal H-H-H bonding (180° at the central H), yielding the 100° angle at boron and the 130° internal bond angle at H.

Corollary to this, comparison of the plots in Figures 2, 3, and 4, the Mulliken populations in Table III, and the geometries in Table IV shows a correlation between the polarization of the MH_3 transition state and the H-H-H angle. The more ionic transition states show the more open geometries as judged by the H-H-H angle.

B. *Electronics of the MH_3 Transition State*

In Figure 8 we show the three one-electron orbitals of H_3 at the optimum C_{2v} geometry of this molecule.¹⁴ Comparison of these orbitals with the orbitals of H_2BH_3 (Figure 2) and KH_3 (Figure 3) shows that the two *spiegel*¹⁶ H-H-H orbitals and one of the *unspiegel* H-M-H orbitals in both H_2BH_3 and KH_3 are very similar to the three corresponding one-electron orbitals of H_3 . Since these three orbitals are quite similar for all ten reactions studied, we can understand the electronics of these H-D exchange reactions by examining just the *fourth active orbital* of MH_3 . It is this orbital that gives the bonding between the H_3 fragment and the M center, stabilizes the MH_3 transition state, and therefore determines the activation barrier for the process. Since the H_3 orbital, which is available for bonding to M, is antisymmetric with respect to the plane bisecting the H-H-H angle (i.e., *unspiegel*), the orbital on M, to be used in the M- H_3 bond, must also be antisymmetric with respect to this plane (*unspiegel*) in order to have a good bond. These *unspiegel* orbitals on M are those depicted in Figure 4. These data indicate a convenient dichotomy in the discussion of these $2_s + 2_s$ reactions. In the case of $H_2BH + D_2$ (Figure 2), the fourth orbital on the transition state (φ_{2b}) is localized significantly on

the boron center. This plot as well as the Mulliken populations (Table III) indicate a *nonpolar* transition state, H_2BH_3 . In all nine other cases, the "M-centered" fourth orbital is not associated with the center M but rather is distributed equally between the two "terminal" hydrogens, giving rise to a polar transition state such as 1. The nonpolar and polar transition states will be discussed in turn.

1. Nonpolar Transition States

a. *Electronic Structure*

In the previous section we intimated that in the $2_s + 2_s$ reaction the transition state could be viewed as a complex formed between H_3 and M. We pointed out that the fourth active orbital must be an orbital that can overlap the *singly-occupied* unspiegel orbital of the H_3 fragment (φ_c of Figure 8) if the two reactive covalent bonds (M-H and H-H) of the reactants are to be retained at the transition state. If this unspiegel fourth orbital can be formed from *low-energy* orbitals on the M fragment, and if the overlap between this orbital and the unspiegel orbital of H_3 is large enough, a nonpolar three-center (H-M-H) bond can be formed, giving a nonpolar reaction. In earlier work,⁴ we reported such strong nonpolar bonds can be formed in cases where M is a transition metal, *if* the M-H bond of the reactant has significant d-character on the metal. This occurs because a metal d unspiegel orbital will be available to make the M- H_3 covalent bond at the transition state. This metallic d bonding orbital has positive and negative lobes at 90° to one another, thus accommodating square transition states. The requirement that the H_3 fragment be

intact at the transition state [equivalent to the requirement that the H-H (D-D) bond of the reactants be retained] establishes geometrical restrictions on the H-M-H angle that would seem to exclude s and p orbitals from functioning as the fourth orbital in these $2_s + 2_s$ reactions.

Figure 2 and Table III show that the $\text{BH}_3 + \text{D}_2$ reaction *does* proceed through a nonpolar transition state, and that the fourth active orbital (φ_{2b}) uses **only** p functions on boron. Figures 3 and 4 show that boron is distinctly different from the other cases. Only in the $\text{BH}_2 + \text{D}_2$ reaction is the fourth active orbital localized on the "metal" at the transition state. The Mulliken population analysis in Table III indicates that the H_2BH_3 transition state is not polar as are the other nine transition states. The polarization of H_2BH_3 is of the form **2**, *NOT 3*. This is reminiscent of the slight polarization noted for transition metal mediated H/D exchange reactions we reported earlier.⁴



The sequence of orbital plots in Figure 2 shows that the B-H and D-D bonds of the reactants are capable of smoothly moving to a pair of three-center, two-electron bonds at the $\text{H}_2\text{B(H)(D)}_2$ transition state. The bond pair ($\varphi_{2a}, \varphi_{2b}$) describes a *covalent* bond between the singly-occupied orbital of H_3 and an orbital that is substantially a boron 2p orbital (Figure 9). The overlap of the two orbitals constituting this three-center bond is indicative of significant bonding. In Figure 10 we show the plots for the two *one-electron* orbitals of the π -bond of ethylene.¹⁷ Note the general similarity between these orbitals and the orbitals (φ_{2a} and φ_{2b}) of the unspiegel bond in $(\text{H}_2\text{B})(\text{H}_3)$, especially as these two sets of orbitals differ

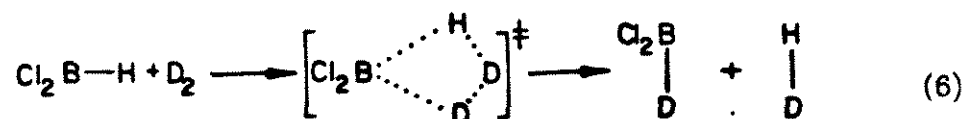
from the corresponding pair of orbitals in $(K)^+(H_3)^-$ (φ_{2a} and φ_{2b} in Figure 3). The fourth active orbital in $(H_2B)(H_3)$ (φ_{2b} of Figure 2) is a boron 2p orbital bonding to the unspiegel singly-occupied orbital of H_3 in the same way that the orbital, which is essentially a carbon 2p orbital on CH_2 , is bonding to a similar orbital on the neighboring CH_2 fragment in ethylene, giving rise to the C-C π bond. In this way we view the three-center, two-electron bond between H_2B and H_3 as a π bond. Thus, *the ability of a center M to sustain the nonpolar $2_s + 2_s$ reaction is intimately related to the ability of that center to form strong π bonds!*

b. *Relative Activation Barriers*

From Figure 4 it is apparent that while BH_3 can undergo a *nonpolar* $2_s + 2_s$ reaction with D_2 , Cl_2AlH and AlH_3 cannot. The unspiegel aluminum 3p orbital is just too diffuse to bond covalently to the unspiegel singly-occupied orbital of H_3 ¹⁸ (Figure 9). This highlights the general observation that second (and lower) row atoms are incapable of forming strong π bonds. (While ethylene is a remarkably stable molecule, the silicon analog, Si_2H_4 , shows, at best, a fleeting existence.¹⁹) Thus the transition state for a *nonpolar* $2_s + 2_s$ reaction will be stabilized (all else being equal) if one of the atoms in the four-centered complex is able to form strong " π " bonds, i.e., if M is either a first-row atom (an unsaturated complex of simple ligands about a first-row atom) or one of the set of transition metal centers that is capable of forming *alkylidene-type* π bonds to CH_2 ($M=CH_2$).²⁰ This is to say that not only must there be an unused valence orbital on M, but that orbital must have the size and shape to allow a high overlap with the unspiegel singly-occupied orbital of H_3 .

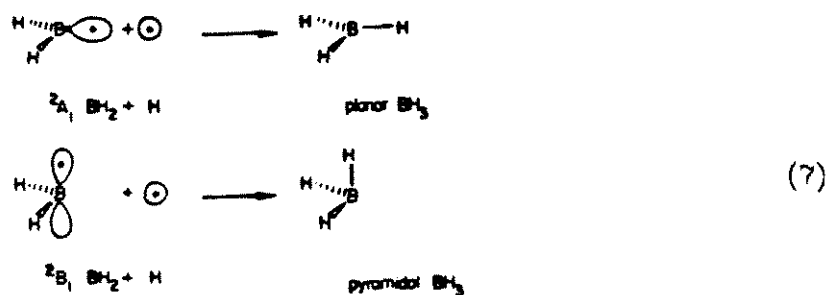
In order to form the required " π bond" to H_3 in Eq. (4), the center M must be in an electronic state that has the orbital of π symmetry (the

unspiegel orbital) singly-occupied. At the transition state in Eq. (5), the BH_2 fragment is in a configuration that separates to the excited (${}^2\text{B}_1$) state of (bent) BH_2 , *NOT* to the ground state (${}^2\text{A}_1$). The interaction between the ground state of H_2B and the ground state of H_3 , given a cyclic geometry, is *repulsive* because the singly-occupied orbital in the ground state of BH_2 is spiegel and therefore orthogonal to the unspiegel orbital of H_2 . This orthogonality defines the absence of bonding. In Figure 11 we show how the strength of the bond between BH_2 and H_3 may be decomposed conceptually into two fragments; viz., $\Delta E_1 + \Delta E_2$, where ΔE_1 is the "vertical" strength of the $\text{H}_2\text{B}-\text{H}_3$ bond, and ΔE_2 is the energy required to prepare the bonding state of BH_2 (${}^2\text{B}_1$, **6**) from the ground state (${}^2\text{A}_1$, **7**). Thus, when estimating *relative* barriers for *similar* $2_s + 2_s$ reactions, one may use this $\sigma \rightarrow \pi$ excitation energy as a guide. For example, at the geometry characteristic of the $(\text{H}_2\text{B})(\text{H}_3)$ transition state,²¹ we calculate the BH_2 (${}^2\text{A}_1 \rightarrow {}^2\text{B}_1$) excitation energy to be 33 kcal/mol (ΔE_2 in Figure 11). At an analogous geometry,²² we calculate the Cl_2B (${}^2\text{A}_1 \rightarrow {}^2\text{B}_1$) excitation energy to be 67 kcal/mol. We believe that the ability of ${}^2\text{B}_1$ (BH_2) and ${}^2\text{B}_1$ (BCl_2) to form π bonds is similar;²³ thus we predict that the activation barrier for the reaction in Eq. (6) will be



significantly higher than that for the reaction in Eq. (5).²⁴ In a similar way, we calculate the ${}^2\Sigma^+ \rightarrow {}^2\Pi$ excitation for BeH to be 64 kcal/mol.²⁵ This observation alone suggests that the $2_s + 2_s$ reaction of BeH_2 with D_2 should be higher in energy than the reaction of BH_3 with D_2 , as observed (Table I).

It is interesting to note that this $\sigma \rightarrow \pi$ excitation can be used to estimate the *relative* energies of distortion from planarity of a series of reactants M-H. Consider the case of BH_3 . We can form BH_3 by bonding the H atom to either the ground (${}^2\text{A}_1$) or excited (${}^2\text{B}_1$) state of bent BH_2 . Equation (7) shows that bonding to the ${}^2\text{A}_1$ state of BH_2 results in the planar geometry of BH_3 , but that



bonding to the ${}^2\text{B}_1$ state of bent BH_2 results in the highly distorted pyramidal form of BH_3 .²⁶ Bending BH_3 from planar corresponds to incorporating some fraction of the excited state of BH_2 . Thus the energy of the excited state gives a gauge of the energy needed to carry out this distortion and vice versa. The higher in energy the π state lies, the more difficult the distortion from planarity. Since the idealized transition state [Eq. (4b)] *requires* the angular distortion of the M-H bond, *the more difficult this distortion, the higher the activation barrier for the $2_s + 2_s$ reaction.*

Based on these considerations, we can construct estimates for the relative heats of formation of MH_3 transition states *of the nonpolar type* based either on the electronic spectroscopy of M, or on the vibrational spectroscopy (M-H bending mode) of MH.

2. Polar Transition States

a. Electronic Structure

Viewing the (M)(H_3) transition state as a bond between the H_3 radical

and the M radical (in a C_{2v} geometry) is convenient for analysis of the electronic structure of this (unstable) molecule. The "fourth electron" starts out in the bonding orbital on M in M-H, and at the transition state it forms a two-electron bond with the electron in the unspiegel orbital on H_3 . In the reactions we characterize as polar, this antisymmetric orbital on M is not sufficiently stable to hold the electron and form a covalent bond with H_3 . In these cases the fourth electron is transferred from M to H_3 to form a polar $M^+H_3^-$ state. Thus the $[M^+][H_3^-]$ state arises naturally in response to the energetic requirement of maximum bonding in the transition state.

Table IV shows that the optimum nuclear angle at the metal in MH_3 is between 50° and 100° for all cases. Only an orbital on M having high angular momentum (d, f, ..., orbitals) can position positive and negative lobes at such small angles to one another. In no cases studied are d orbitals available for bonding to the unspiegel orbital of H_3 . Therefore, either a three-center $p\pi$ bond must be formed (as in H_2BH_3) or electron transfer from M to H_3 is demanded. In the $KH + D_2$ reaction there is no valence d orbital available on potassium, and we do not expect the 2P state of K to form strong π bonds, so the only alternative is to form $[K^+][H_3^-]$. In Figure 12 we show the four one-electron orbitals describing H_3^- . Comparison of these orbitals with those of KH_3 substantiates our identification of $[K^+][H_3^-]$.

In all of the cases in Figure 4 we can identify the fourth active orbital of MH_3 with the diffuse antisymmetric orbital of H_3^- (ϕ_{2b} , Figure 12). Closer examination shows that there is some delocalization back from H_3^- to an unspiegel orbital on M^+ . For the main group complexes, this orbital must be p-like (Li 2p, Na 3p, etc.). In all of the main group reactions stu-

died, the needed unspiegel orbital is empty in the MH reactant, and may thus be used freely in the MH_3 complex. The extent of delocalization back from H_3^- to M^+ then depends on the energy of the $p\pi$ orbital, and the ability of H_3^- to use this orbital. The energies of the $p\pi$ orbitals may be estimated from atomic spectroscopy.²⁷ These excitation energies tend to increase as one goes to the left and as one goes down in the periodic table. These energetic considerations suggest the amount of back-delocalization will be greater for Li than for Rb, greater for B than for Al, and greater for B than for Li, in agreement with the results in Figure 3.

The ability of H_3^- to use the M $p\pi$ orbital relies on the effective size of this $p\pi$ orbital and on the size of the MH_3 molecule. The effective size of the orbital is merely a gauge of diffuseness. The more diffuse this orbital, the less fully the H_3^- orbitals can use it. This is simply because the energetic effectiveness of the delocalization is proportional to the overlap of the donor and acceptor orbitals.²⁸ The Al (3p) and B (2p) orbitals are plotted in Figure 9. From these plots one sees that the Al 3p orbital is much less concentrated in space and thus much less able to overlap the unspiegel orbitals of H_3^- . Thus the same orbital characteristic that makes the nonpolar transition state inaccessible in the reaction at AlH_3 (vide supra) disallows the "unspiegel" backbonding from H_3^- to H_2Al^+ .

The bond lengths in the MH_3 molecule are critical in determining the extent of back-donation from H_3^- onto the $p\pi$ orbital of M, owing to the exponential decrease of the overlap of the $p\pi$ and H_3^- orbitals with distance. These bond lengths are determined by the spatial extent of the valence orbitals, which are in turn determined by the size of the M core orbitals. Since the Li-H bonds are shorter than the Rb-H bonds, the back-donation from H_3^- to Li^+ is not insignificant, but the extent of the

analogous donation from H_3^- to Rb^+ is minimal (see Figure 4). A more direct effect of the core electrons on the π -backbonding can be seen in Figures 3 and 4. The four valence orbitals of MH_3 all must stay orthogonal to the core orbitals on M. This places particularly important constraints in the cases of H_2AlH_3 and CuH_3 where the antisymmetric H_3^- orbitals neatly outline the core region on M. The Pauli Principle-induced core-valence repulsion diminishes the stabilizing effect of H_3^- to M^+ delocalization. It is important to note that the cases showing the strongest π back donation (LiH_3 , BeH_4 , and BH_5) are first-row complexes in which the metallic cores are 1s orbitals. Since there are *no* core orbitals of unspiegel symmetry, the Pauli Principle is immediately satisfied with regard to this π backbonding. Therefore, there will *always* be the tendency for activation barriers in these 2 + 2 reactions to be smaller for first-row reactants than for the analogous lower row species (all else being equal). Our results (Table I) substantiate this.

In previous work⁴ we showed that the presence of transition metal valence d orbitals can render *nonpolar* $2_s + 2_s$ reactions to be allowed. Here we have presented data which show that the $2_s + 2_s$ reactions at $ClMnH$ and $Cu-H$ are both very high in activation energy (i.e., forbidden). What is the cause of this?

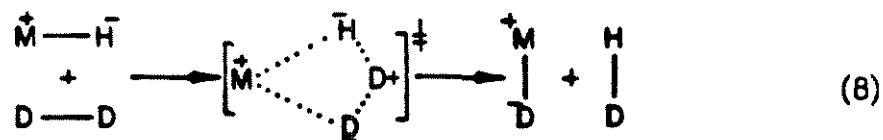
The bond in CuH is polar and is observed to involve only a small amount of d character on Cu (Figure 6). Similarly, the fourth orbital of the CuH_3 transition state uses only a very small amount of Cu d-space (Figure 4). In either case the five d orbitals on copper are filled and thus cannot be used further. Copper cannot take advantage of the valence d orbitals that separate the transition metals from the main group elements. These two cases emphasize our claim that transition metals can

render these $2_s + 2_s$ reactions allowed *only* if the d orbitals can be used effectively during the process.

In a similar way, the Mn-H bond in ClMn-H is polar, using an sp hybrid orbital on manganese and an s orbital on hydrogen. In the ClMnH₃ transition state, the "fourth electron" resides in an orbital that has only a small amount of metal character. The case of ClMnH is quite different from, say, that of Cl₂TiH because the five singly-occupied d orbitals are coupled into a particularly stable high-spin (sextet) state (recall Hund's Rule). Bonding to one of these orbital in either ClMnH or ClMnH₃ would cause an increase in the total electrostatic energy of the complex of 40 kcal/mol because of the Pauli Principle;²⁹ therefore, utilization of d⁵ Mn d-like functions is "forbidden" unless the spin state of the complex is changed. In the absence of a lower spin coupling, the Mn-H and MnH₃ bonds have essentially no d character. Therefore, even though the metallic valence d orbitals have the proper symmetry and spatial extent to stabilize the transition state for the $2_s + 2_s$ reaction, they are not used. In this way, the Mn of ClMnH is functionally *not* a transition metal. In both the reactions (ClMn-H and at Cu-H), *polar* transition states for the $2_s + 2_s$ reaction are observed, making these reactions look like hydride transfers or heterolytic H₂ activation. The available unspiegel orbital on the metal is 4p π -like, which in each case is too diffuse and too far away from the H₂⁻ fragment to be used in π back-donation; therefore these reactions behave like high-energy main group reactions.³⁰

b. *Relative Activation Barriers*

Our results indicate that one extreme of suprafacial $2 + 2$ reactivity is polar, as in Eq. (8).



In this case the "metal center" is cationic in the transition state; therefore we claim that the activation barrier for this *polar* $2_s + 2_s$ reaction will be lower when the "metal center" is more cationic in the reactants, i.e., when the M-H bond is more polar in the M^+H^- sense. As a direct corollary, the activation barrier for the $\text{MH} + \text{D}_2$ exchange reaction *that proceeds through a polar transition state* will be lower when the ionization potential of M is lower. This explains why the barrier for the exchange reaction at NaH is higher than that for the reaction at KH and RbH; why the barrier is higher for the reaction at Cl_2AlH than for that at H_2AlH ; and why the barriers for the exchange reaction at CuH and ClMnH are so high relative to the Group IA and Group IIA reactions.²⁷

This simple rule must be modified to include the effects of back donation from H_3^- to M^+ that will tend to stabilize the transition state and therefore lower the reaction barrier. For example, in Table I we find the exchange reaction at LiH to be 6.3 kcal/mol lower in energy than the corresponding reaction at NaH, despite the fact that $\text{IP}(\text{Li}) > \text{IP}(\text{Na})$,³¹ seemingly voiding our simple claim concerning relative rates and ionization potentials. Reference to Figure 4 will show that there is significantly more π backbonding from H_3^- to Li^+ than from H_3^- to Na^+ , as is expected owing to the greater ability of first-row atoms to form strong π bonds. Thus, the simplest description would say that the activation barriers for the LiH and NaH reactions should be roughly equal, but the intrusion of a slight bit of "nonpolar" reactivity into the polar reaction lowers the LiH + H_2 reaction barrier.

3. Resolution of the Dichotomy

The separation of the $2_s + 2_s$ reactions into two types, polar and nonpolar, is obviously an idealization and each of the reactions described in this work is a mixture of the two extremes. Thus the hydrogenolysis of RbH is clearly a polar reaction, and the hydrogenolysis of BH_3 is clearly nonpolar, but the hydrogenolysis of BeH_2 is less obviously one or the other. In all cases studied, the predictions have been clear, however. If a "metal" center can form the " π -bond" to the antisymmetric, singly-occupied orbital of H_3 (that is, if M is boron or a high-valent early transition metal), then the nonpolar route is accessible. If, on the other hand, M is easily ionized (i.e., if M is a Group IA metal), then a polar transition state is observed. Finally, if neither of the above requirements is met (e.g., $\text{M-H} = \text{Cl}_2\text{AlH}, \text{H}_2\text{AlH}, \text{ClMnH}, \text{CuH}, \text{HBeH}$), then the $2_s + 2_s$ reaction will have a high activation barrier.

C. *Qualitative Representation of the Transition State*

Throughout our analysis, we have found it quite helpful to conceptualize the transition state **not** as a complex of two reacting molecules but as a complex formed between two fragments (M and H_3) whose independent identity lies in a direction perpendicular to the reaction path. In this way we can appreciate the transition state as a molecule (albeit unstable) and understand its electronic structure and energetics with the same cognitive tools used in the study of stable molecules.

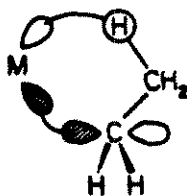
In the investigation of pericyclic reactions such as the $2_s + 2_s$ reaction, the two reactive fragments will contain delocalized valence bonds. In the present example, the H_3 fragment contains a bond that cannot be localized between just two centers. This delocalized valence bonding highlights the synchronous movement of two two-electron bonds in the

pericyclic process.

The dissection of the transition state into these two fragments is useful because we can examine each separately, qualitatively and quantitatively evaluating the factors affecting their energies. Having understood the separated units, we may then analyze the bonding of the two, which gives the transition state its structure. For example, the $(H_2B)(H_3)$ transition state is formed by a three-center bond between boron and its two neighbor hydrogens. In order to form this bond, the H_2B radical was excited to the unspiegel state and the H_3 unit was geometrically distorted so that its unspiegel orbital could overlap the boron orbital effectively. These adjustments of the fragments cost 33 kcal/mol and 12 kcal/mol, respectively. Below we outline how this energetic analysis can be used to extend our results.

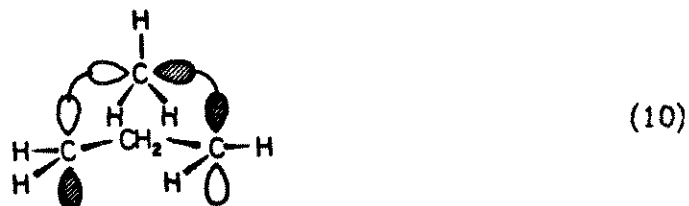
Similar dissection can be of assistance in envisioning transition states for other pericyclic reactions.

- i) The transition state for the insertion of olefins into metal-hydrogen bonds³² (vide infra) can be viewed as the bonding of the excited unspiegel state of the metal fragment to be a severely distorted ethyl radical (9).

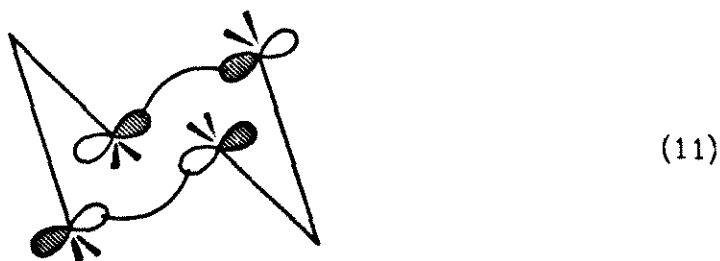


(9)

- ii) The transition state for the [1,3] sigmatropic shift of an allylic methyl group³³ may be viewed as the complex formed between an allylic radical and a (planar) CH_3 radical (10).



- iii) The [3,3] sigmatropic shift (Cope and Claisen rearrangements) may be visualized as proceeding through a transition state formed from two allylic radicals bound to one another via their respective unspiegel orbitals (11).³³



These diagrams show that this analytical scheme represents a valence bond relative of frontier orbital analysis.

Important aspects of these reactions (*relative* rates, selectivities, stereochemistry, etc.) could be explored by studying the ways in which the independent fragments (ethyl radical, allylic radicals, etc.) can be electronically and geometrically distorted and the energies needed to do so.

D. *Implications and Extensions*

In this work we have described the general features of $2_e + 2_e$ reactions carried on in the absence of available *valence* d orbitals at the unique center M. These studies have all involved the addition of the *non-polar* reagent H_2 to M-H bonds that were polar to a greater or lesser degree. Our studies have shown a spectrum of reactivities from the very polar four-center transition state characteristic of rubidium to the

nonpolar transition state of boron. We have shown how the nature of MH will determine the propensity to undergo the exchange reaction with D₂. We will now generalize these conclusions to other systems.

1. Alkali Metal Alkyls

Topologically there is not a great difference between the Li-H bond in lithium hydride and the Li-C bond in a saturated lithium alkyl³⁴ (see Figure 13). Aside from the obvious steric considerations then, the hydrogenation of LiH [Eq. (10)] should look much like the hydrogenation of LiR (R = alkyl). The major electronic difference in the 2_s + 2_s transition state for the direct hydrogenation of LiR is the increased electronegativity of carbon over hydrogen.³⁵ This increased electronegativity implies a greater ability to sustain charge; thus any process involving carbanionic behavior at the α carbon in a lithium alkyl will be lower in energy than the corresponding reaction of lithium hydride.

Lithium alkyls are known to react with hydrogen to give alkane and lithium hydride.³⁶ We hold that this reaction proceeds either through a direct four-center transition state analogous to Eq. (4) or through an oligomeric equivalent thereof. Vitale and San Filippo³⁷ have recently reported evidence that supports the four-membered, direct hydrogenolysis, cyclic transition state. They observe very large and negative values of ΔS^\ddagger for hydrogenolysis of n-octyl lithium with H₂ at 50° ≤ T ≤ 80°C. They interpret this as a suggestion of a highly structured transition state drawing a cyclic, four-membered species. They further observe that addition of n-donor bases (such as TMEDA) leads to substantial rate acceleration. The polar mechanism we invoke in the LiH/D₂ reaction is supported by this. Note that the LiH₃ transition state is polarized more than is the LiH reactant. Therefore the n-donor base is expected to sta-

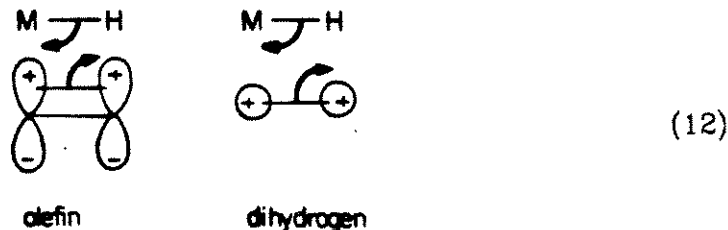
bilize the transition state more than the reactants, thereby lowering the activation barrier and increasing the reaction rate.

It is important to note here that the rate of hydrogenolysis of alkali metal alkyls increases in the order $\text{Li} < \text{K} < \text{Cs}$. This is directly in line with our prediction that the polar $2_s + 2_s$ transition state will be lower in energy if the ionization potential of the metal center is lower.³⁸

The polar mechanism nicely accommodates the essential features of the apparent $2_s + 2_s$ reactivity of the alkali metal alkyls.

2. Addition of M-H to Olefins

We may use the studies reported here as models for the corresponding reactions of metal hydrides with olefins. Equation (12) indicates the topological similarity of the two processes.

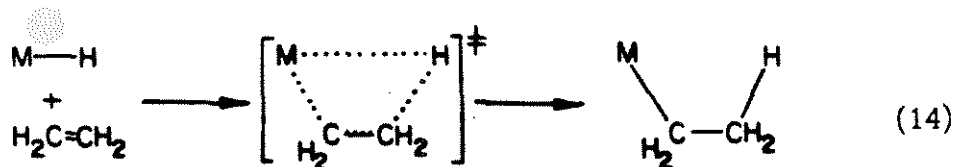


While the absolute energetics of olefin insertion will be different from the reaction with D_2 , the general trends will be similar.

Consider the analysis of the H/D exchange reactions given in Part B. There we thought of the MH_3 transition state as the complex formed between H_3 and M, and analyzed the stability of the transition state in terms of the type and strength of the bond formed between these two units. A strict analogy for the olefin/metal hydride reaction would analyze the bonding between M and $\text{CH}_2-\text{CH}_2-\text{H}$. Immediately one sees an interesting difference between the olefin and $\text{H}_2(\text{D}_2)$ reactions: whereas H_3 is not a stable molecule, the ethyl radical is (albeit reactive). This should

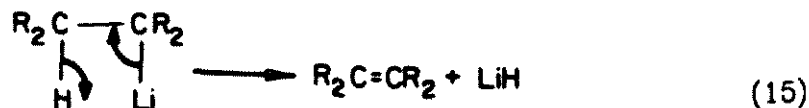
can see especially in the case of $\text{BH}_3 + \text{H}_2$ that the electronic optimum angle at boron in H_2BH_3 is 180° ; therefore 2 + 2 substrates that permit a larger internal angle at boron will react more quickly. Both simple estimates and Dewar's MNDO calculations⁴¹ show that an olefin does allow a greater internal angle (116.5°).⁴⁴

Based on the above arguments, we believe that addition of metal hydrides to olefins will occur by the same spectrum of reactivities, from nonpolar to polar, as the addition of these hydrides to H_2 . *When* concerted four-center transition states occur⁴⁵ [Eq. (14)],



those involving alkali metals will be polar (cf. LiH , NaH , KH , RbH), as will those involving alkali earths (cf. BeH_2) and those involving transition metals whose valence d orbitals are *NOT* available at the transition state (cf. ClMnH and CuH). The addition of $\text{R}_2\text{Al}-\text{H}$ across the π bond of an olefin will occur through a much more polar transition state than the corresponding addition of $\text{R}_2\text{B}-\text{H}$.

The addition of alkali metal hydrides to olefins is not an important reaction, but the reverse [Eq. (15)] is a common pathway for the thermolysis



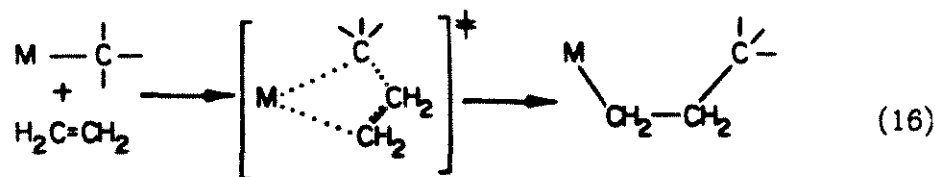
of organoalkali metal compounds.⁴⁶ The four-center transition state for this decomposition has been suggested, and evidence supporting this

structure has recently been reported.⁴⁷ It is interesting to note that this decomposition follows Zaitsev's Rule,⁴⁸ a rule that is consistent not only with E₁ elimination but also, in this case, with the *polar* four-center transition state in which positive charge develops transiently on the β-carbon.

The hydroboration² and hydroalumination⁴⁹ reactions have been extensively studied and used in organic synthesis. The hydroboration reaction is known to be more facile than the analogous hydroalumination reaction, which is consistent with our calculated barriers for the exchange reactions with D₂.⁵⁰ The exclusive cis-addition⁵¹ observed in both reactions implies an effective four-center transition state. The sense of addition in each case leads to placement of the "hydride" on the more substituted carbon of the incoming olefin.⁵² This has been attributed both to polarization^{52a} (of the form **3**) in the transition state and to steric effects.⁵³ Our results suggest the former to be more important in hydroalumination than in hydroboration, and that the latter effect dominates the directing of hydroboration.

3. Addition of Metal Alkyls to Olefins

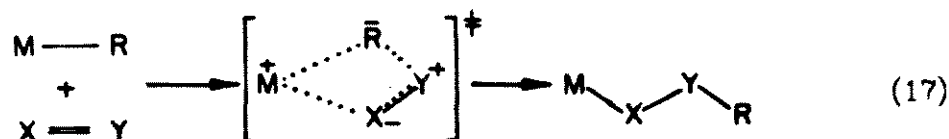
We combine the previous two sections to discuss the reaction shown in Eq. (16) and concentrate on the difference between trialkyl boron and trialkyl aluminum compounds.



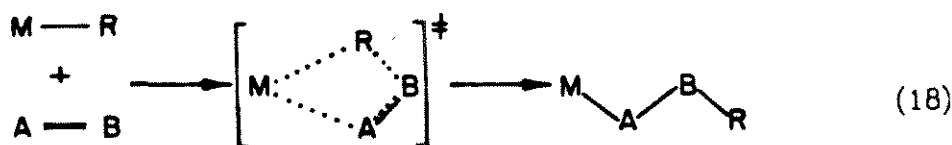
As a prelude to the discovery of transition metal-catalyzed stereoregular polymerization of simple olefins, Ziegler discovered that olefins will insert into the Al-C bond of trialkyl aluminum compounds⁵⁴ [Eq. (16), M=AlR₂].

Despite the fundamental similarity between the structures and reactivities of aluminum and boron compounds, no such insertion reaction is observed between simple olefins and trialkyl boron compounds,⁵⁵ this despite the fact that dialkyl boranes react much more quickly with olefin than do dialkyl alanes.⁵⁰ Our studies offer an explanation of this paradox.

As mentioned above, the predominant electronic difference between trivalent carbon and hydrogen in compounds of the form M-R (R = alkyl, hydrogen) is the greater electronegativity of carbon. Thus, in any reaction involving a polar transition state [Eq. (17),



one would expect a faster reaction for R = alkyl than for R = H *ignoring steric considerations*. In contrast to this, steric congestion and directed valence and carbon make frontside attack (insertion) of an olefin at a metal alkyl bond more difficult. For this reason we expect a strictly *non-polar* insertion reaction [Eq. (18)]



to proceed more quickly for R = H than for R = alkyl.

Our results on H/D exchange at BH₃ and AlH₃ show that trivalent boron tends to support *nonpolar* 2_s + 2_s reactions and that trivalent aluminum tends to support *polar* 2_s + 2_s reactions. Since there is not "*polar driving force*" to overcome the hampering effect of steric crowding at the transition state, we expect the B-H bond to be much more active than the B-CR₃ bond in 2_s + 2_s reactions. However, since the 2_s + 2_s

reactions at aluminum are *polar*, significantly more polar than at boron, transition state polarization will make the Al-CR₃ bond relatively more reactive than the B-CR₃ bond toward incoming olefin.

This is an example showing how the bisection of 2_s + 2_s reactivity into the polar and nonpolar extremes and the determination of which factors affect which reactivity patterns could be useful in the analysis and design of catalyst systems.

IV. Conclusion

We have examined ten pericyclic $2_s + 2_s$ reactions of H_2 with a metal hydride. In *none* of these cases were transition metal valence d orbitals used in the reactants, products, or transition state. We found these four-center reactions to be low energy (allowed) for the monomeric alkali metal hydrides, and in each case a polar $[M^+H_3^-]$ transition state obtained. We also found a low energy reaction at BH_3 that proceeds through a covalently bound, nonpolar transition state. We found the remaining five reactions to be sufficiently high in energy that we consider them to be "forbidden", even though all bonds are retained throughout each reaction. We assert that a low ionization potential of M promotes polar $2_s + 2_s$ reactions at M-H and that the ability of M to make π bonds promotes non-polar $2_s + 2_s$ reactions at M-H.

These "main group" reactions afford a useful counterpoint to the migratory insertion reactions of organotransition metal complexes.⁴

APPENDIX: Details of the Calculations

A. *Basis Sets and Effective Potentials*

Wavefunctions for species discussed in the text were calculated using the generalized valence bond technique⁸ and the GVB2P5 program.⁵⁶ These calculations were fully ab initio and all electrons were included in all of the calculations except those cases involving chlorine ligands. In these cases, the ten core electrons on chlorine were replaced by an ab initio effective potential.⁵⁷ Throughout these calculations, valence double zeta basis sets were used on the heavy atoms⁵⁸ and a triple zeta basis set was used on the hydrogen atoms.⁵⁹ The triple zeta basis was used so that the wavefunction could describe any charge on H (H^+ , H^- or neutral H atom) with equal facility. The valence electrons on chlorine were described using a minimal basis.⁶⁰

B. *Geometries*

The geometries of all of the active species (i.e., MH and MH_3) were optimized. These optimizations were all performed at the Hartree-Fock (HF) level except the cases of $ClMnH$ and $ClMnH_3$, which were performed at the GVB(1/2) and GVB(2/4) levels, respectively. The geometries of the simple diatomic molecules, of the simple binary molecules (BeH_2 , BH_3 , and AlH_3), and of the manganese-containing molecules were optimized in a point-by-point fashion, while the geometries of all other molecules were optimized using an HF-based gradient optimization program.⁶¹ A C_{2v} symmetry was assumed for all MH_3 complexes.

C. *Wavefunctions and Activation Barriers*

At the optimum geometry of MH, the GVB(1/2) wavefunction in which the M-H bond is described in a GVB sense was calculated. These calculations provided the GVB orbital plots shown in Figures 2, 3, and 6. At the

optimum geometry for each MH_3 complex, a GVB(2/4) wavefunction was calculated. In this wavefunction the two active bonds ($H \cdots H \cdots H$ and $H \cdots M \cdots H$) are described by four singly-occupied orbitals. One bond pair is symmetric (i.e., *spiegel*) with respect to reflection in the plane perpendicular to the plane of the reaction and containing M and the central hydrogen; the other bond pair is antisymmetric with respect to this reflection (*unspiegel*). Our studies of the reaction of Cl_2TiH^+ with D_2 indicated that this restriction is a valid one.⁴

In order to determine activation barriers for the exchange reactions, the total energies of $MH + H_2$ and $(M)(H_3)$ are compared; hence it is important to determine calculational schemes that will describe the three species *consistently*. We have found the following scheme useful. The $(M)(H_3)$ species is described by a configuration interaction (CI) wavefunction derived from the GVB(2/4)-PP wavefunction. The GVB-PP wavefunction was supplemented by the two additional spin eigenfunctions characteristic of a full GVB wavefunction (GVB-RCI). From this set of six spin eigenfunctions, all single excitations into the virtual orbitals were allowed. This results in a small CI (in the case of H_2BH_3 , this gives only 87 spatial configurations). This CI wavefunction allows relaxation of all orbital orthogonality and spin-coupling restrictions involved in interactions of the reactive orbitals and is expected to yield accurate barriers. In the limits of reactants and products, this wavefunction reduces to a GVB(1/2)-PP wavefunction on MH and on H_2 , except in the case of $ClMnH$ in which there are additional spin recoupling terms arising from the d^5 part of the wavefunctions. Total energies for the active species at the various levels of calculation are reported in Table V.

Using this calculation scheme and the simple triple zeta basis on

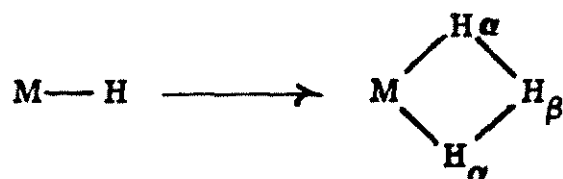
hydrogen, we calculate a barrier of 14.6 kcal/mol for the $\text{H} + \text{H}_2$ reaction.⁶² This compares favorably with the best available value of 9.90 kcal/mol.⁶³ Inclusion of a set of unscaled p functions on each hydrogen lowered this barrier to 13.3 kcal/mol. Addition of a set of unscaled p functions on the active hydrogen in the BH_3 and H_2 reaction lowered the activation barrier from 28.0 kcal/mol to 17.5 kcal/mol, but interestingly, the addition of a set of d function on boron lowered the barrier only 0.7 kcal/mol to 16.8 kcal/mol. We therefore believe that our activation barriers are systematically high by roughly 10 kcal/mol owing to the deficient basis on H, but that the inclusion of d functions in the valence region of the main group centers has a negligible effect. Thus, even when given the chance, the main group atoms do *not* use d orbitals. While our values for the activation barriers are thus only approximate in an absolute sense, we believe that the *relative* activation barriers are reliable.

Table I. Barrier heights for reaction 4.



M-H	ΔE (kcal/mol)
LiH	27.4
NaH	33.7
KH	27.8
RbH	25.7
BeH ₂	43.9
BH ₃	28.0
AlH ₃	46.0
Cl ₂ AlH	56.8
CuH	50.1
ClMnH	50.8

Table II. Mulliken populations.



M	Reactants		Products		
	M	H	M	H _α	H _β
Li	2.79	1.21	2.71	1.24	0.81
Na	10.62	1.38	10.30	1.43	0.84
K	18.53	1.47	18.17	1.48	0.86
Rb	36.52	1.48	36.20	1.47	0.86
HBe	1.20 + 3.60	1.20	1.19 + 3.59	1.21	0.81
H ₂ B	2 × 1.04 + 4.88	1.04	2 × 0.96 + 5.3	0.99	0.81
H ₂ Al	2 × 1.29 + 12.13	1.29	2 × 1.25 + 12.17	1.25	0.83
Cl ₂ Al	2 × 7.45 + 11.89	1.21	2 × 7.43 + 11.86	1.25	0.78
ClMn	7.43 + 24.37	1.20	7.41 + 24.33	1.24	0.78
Cu	28.82	1.18	28.6	1.29	0.77

Table III. GVB Pair Overlaps for the Active Bonds in the MH + D₂ Reactions.

GVB Orbital Overlaps			
System	M-H Bond	MH ₃ symmetric bond	MH ₃ antisymmetric bond
LiH ₃		0.84	0.86
LiH	0.73		
NaH ₃		0.83	0.86
NaH	0.69		
KH ₃		0.83	0.86
KH	0.67		
RbH ₃		0.81	0.85
RbH	0.66		
HBeH ₃		0.84	0.88
BeH ₂	0.82		
H ₂ BH ₃		0.84	0.87
BH ₂	0.83		
H ₂ AlH ₃		0.84	0.87
AlH ₃	0.80		
Cl ₂ AlH ₃		0.84	0.89
Cl ₂ AlH	0.80		
CuH ₃		0.83	0.87
CuH	0.72		
ClMnH ₃		0.83	0.90
ClMnH	0.77		
H ₂	0.80		
H ₃ ⁻		0.82	0.86
H ₃		0.86	

Table IV. Geometries and Geometry Changes in the Reaction $MH + D_2$.

M	M-H bond length ^a			H-H bond length ^{a, b}			
	Reactants	Transition State	Change	MH ₃	Δ ₁	Δ ₂	Δ ₃
	Li	1.654	1.744	0.079	1.053	0.311	0.134
Na	1.967	2.130	0.16	1.057	0.315	0.138	-0.022
K	2.434	2.543	0.109	1.060	0.318	0.141	-0.019
Rb	2.60	2.692	0.092	1.053	0.311	0.134	-0.026
HBe	1.335	1.479	0.144	1.070	0.328	0.151	-0.009
H ₂ B	1.18996	1.290	0.100	1.075	0.333	0.156	-0.004
H ₂ Al	1.5893	1.774	0.185	1.069	0.327	0.150	-0.010
Cl ₂ Al	1.5521	1.720	0.168	1.086	0.344	0.167	+0.007
ClMn	1.768	1.955	0.178	1.083	0.341	0.164	+0.004
Cu	1.577	1.819	0.242	1.115	0.375	0.196	+0.036

M	θ	α
Li	72.6°	157.9°
Na	59.1°	166.0°
K	48.0°	168.7°
Rb	46.0°	168.0°
HBe	87.2°	144.7°
H ₂ B	99.0°	131.8°
H ₂ Al	70.9°	148.8°
Cl ₂ Al	74.2°	145.0°
ClMn	65.2°	153°
Cu	74.1°	158.8°

a) Values in Å.

b) Δ₁ = difference between MH₃ H-H bond length and H-H length in H₂ (= 0.742 Å)

Δ₂ = difference between MH₃ H-H bond length and H-H length in H₂ (= 0.919 Å)

Δ₃ = difference between MH₃ H-H bond length and H-H length in H₂⁻ (= 1.079 Å)

Table V. Final Total Energies at Relevant Levels of Calculation.^{a)}

System	Hartree-Fock	GVB(n/2n) ^{b)}	RCI+Singles
LiH ₃	-9.060362	-9.077012	-9.091512
LiH	-7.969470	-7.986985	
NaH ₃	-163.238743	-163.255235	-163.269978
NaH	-162.175486	-162.154920	
KH ₃	-600.080723	-600.097366	-600.112417
KH	-598.988230	-599.009507	
RbH ₃	-2936.983706	-2937.000427	-2937.015670
RbH	-2935.887182	-2935.908615	
HBeH ₃	-16.864764	-16.820579	-16.833264
BeH ₂	-15.741709	-15.755146	
H ₂ BH ₃	-27.431873	-27.449934	-27.464450
BH ₃	-26.347127	-26.360925	
H ₂ AlH ₃	-244.354429	-244.370703	-244.384609
AlH ₃	-243.295144	-243.309851	
Cl ₂ AlH ₃	-1162.253917	-1162.269707	-1162.282227
Cl ₂ AlH	-1161.209153	-1161.224527	
CuH ₃	-1638.828178	-1638.844184	-1638.857591
CuH	-1637.770560	-1637.789636	
ClMnH ₃	-1607.750028	-1607.764943	-1609.780813
ClMnH	-1608.69266	-1608.708580	-1608.713610
H ₂	-1.12826	-1.148143	
H	-0.499940		
H ₃	-1.589972	-1.600247	-1.624308

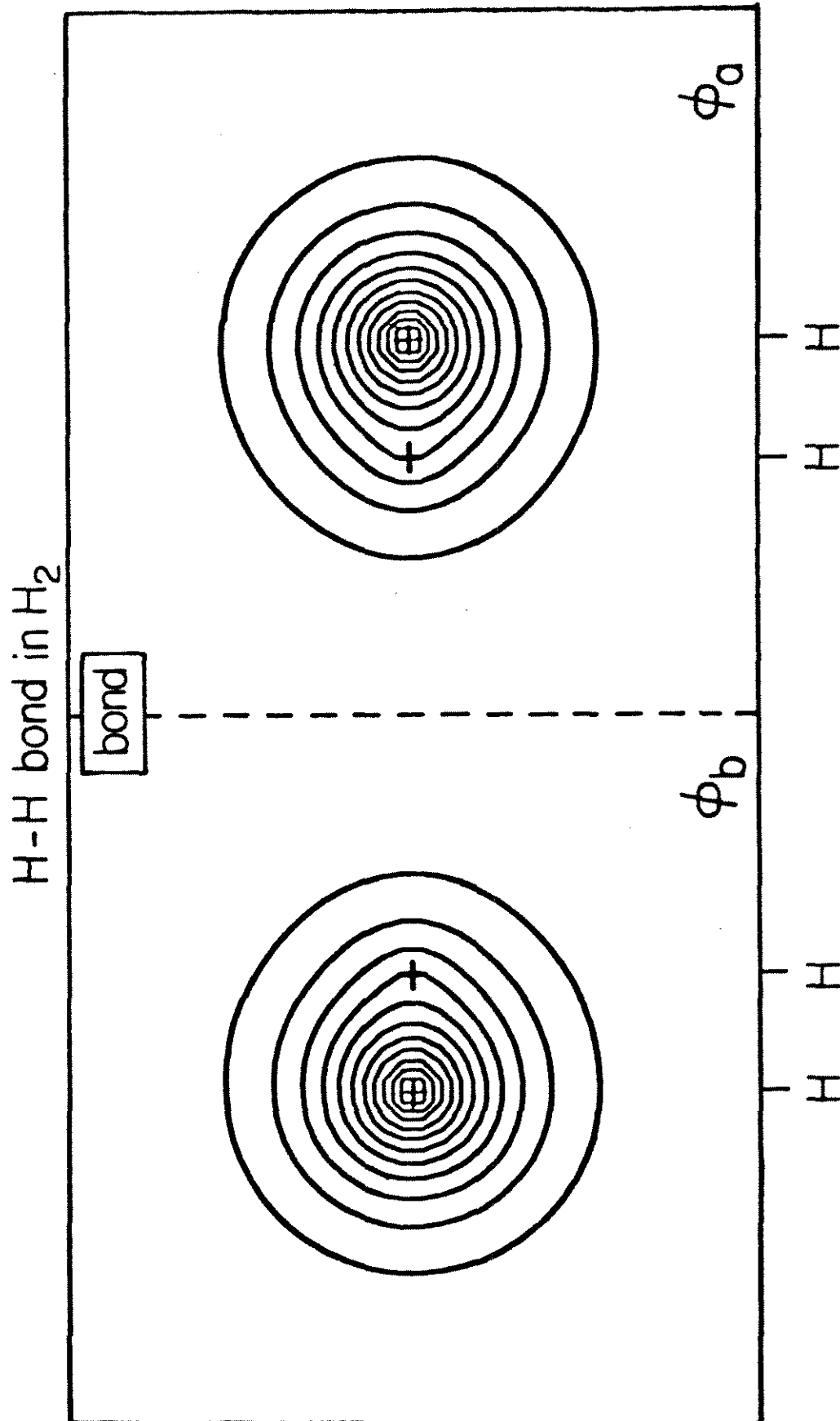


Figure 1. GVB orbitals describing the bond in H_2 . The separation between contours is 0.05 a.u.

Figure 2. GVB orbitals describing the reaction of BH_3 with D_2 . (i) Reactants. (ii) Transition state. (iii) Products. The separation between the contours is 0.05 a.u.

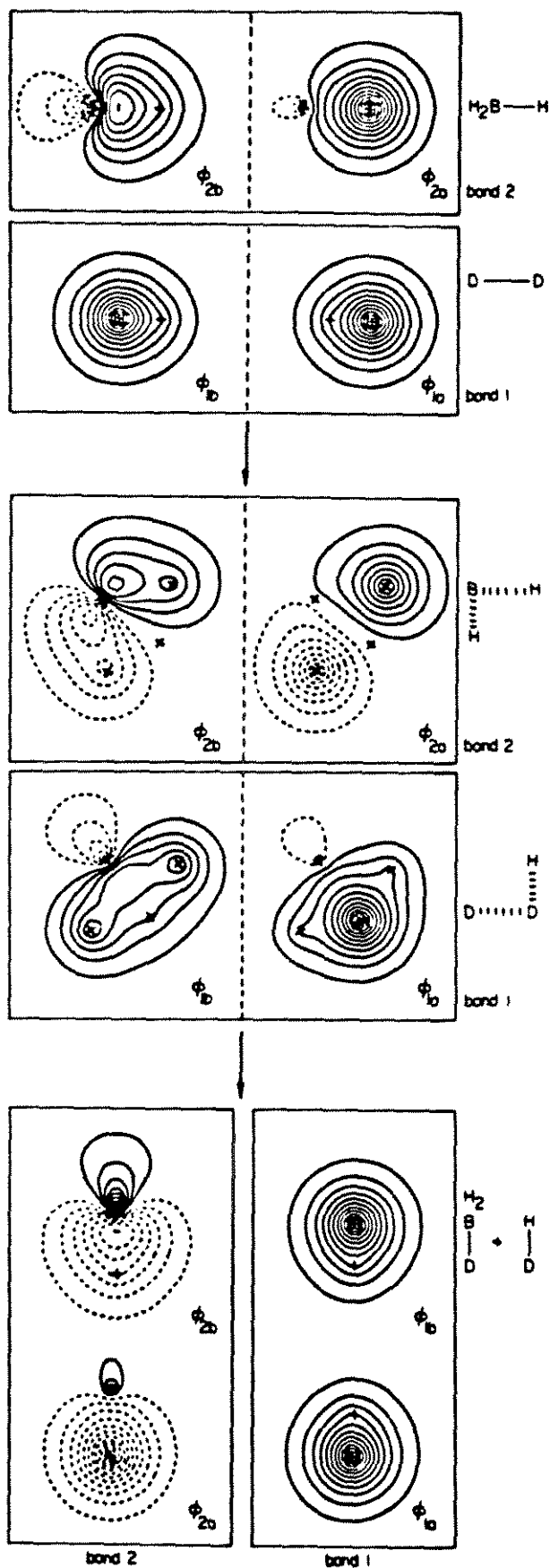


Figure 3. GVB orbitals describing the reaction of KH with D₂. (i) Reactants. (ii) Transition state. (iii) Products. The separation between contours is 0.05 a.u.

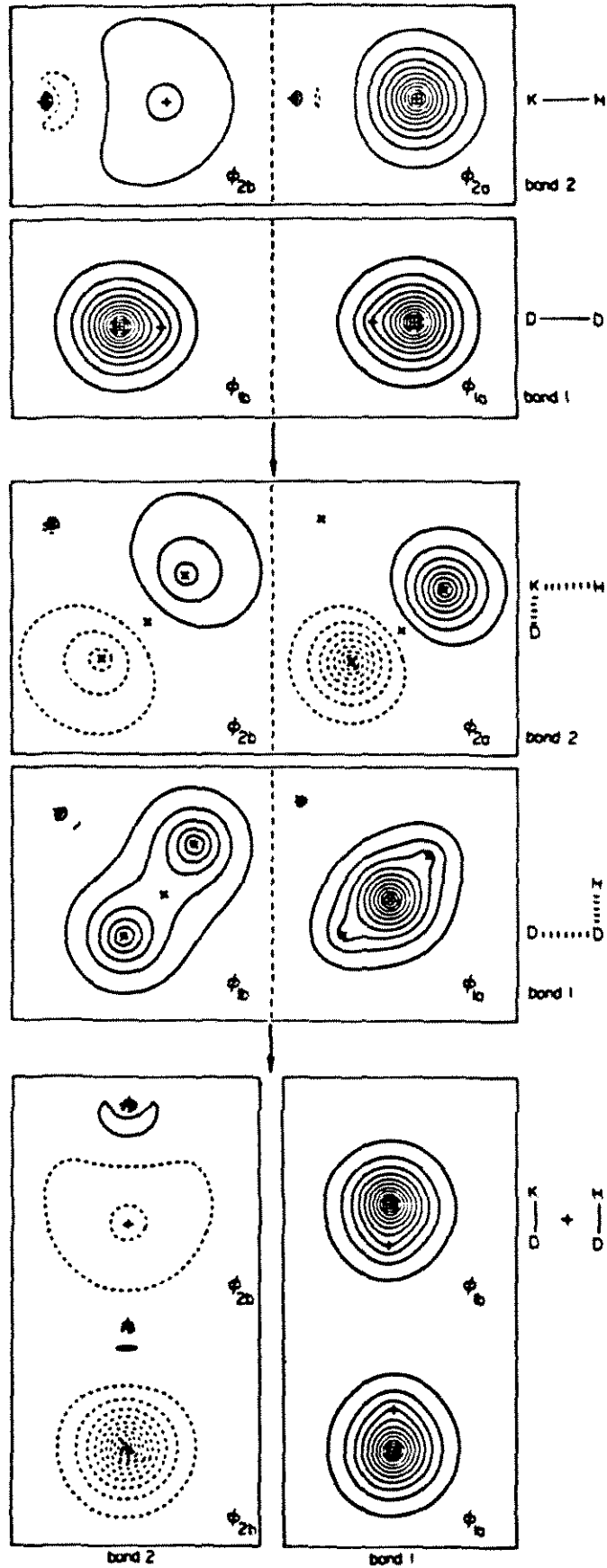


Figure 4. Fourth active GVB orbital describing the transition state of the reaction of MH with D₂ (see text). The separation between adjacent contours is 0.05 a.u.

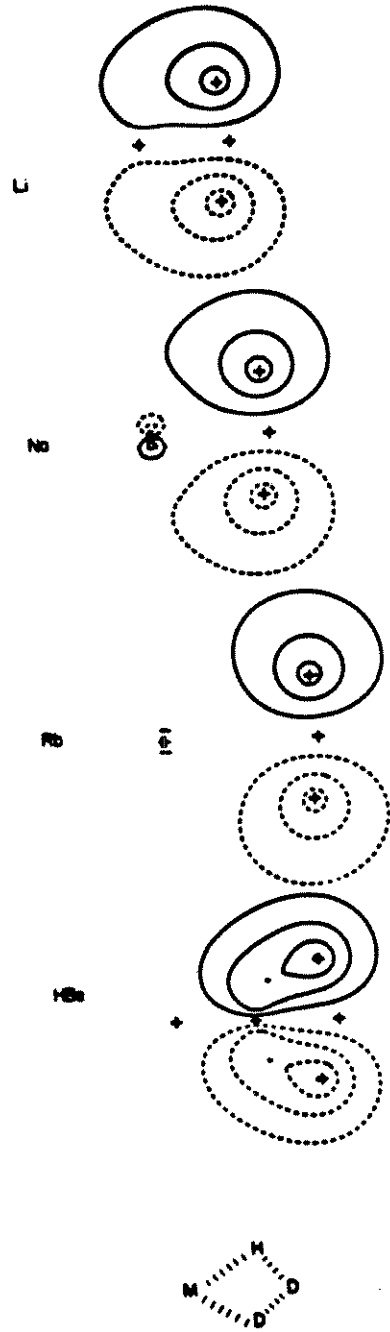
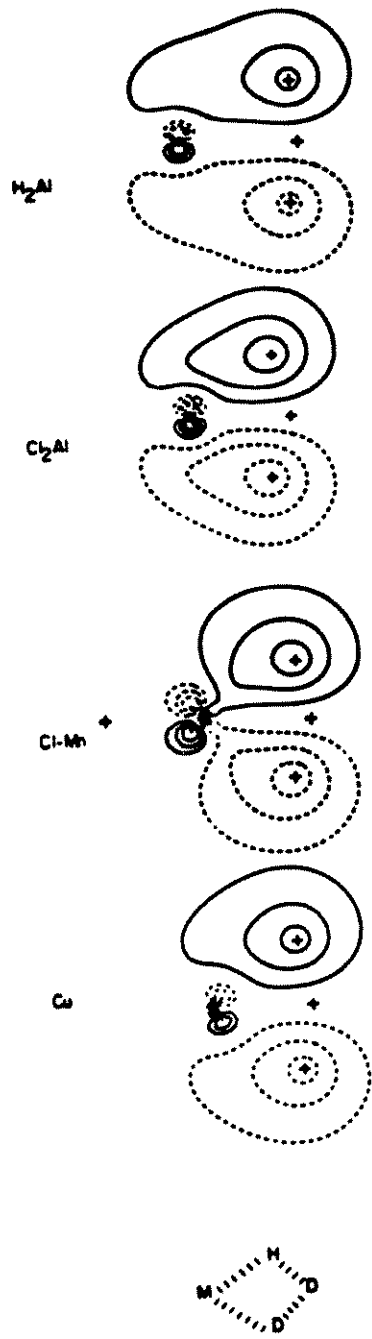
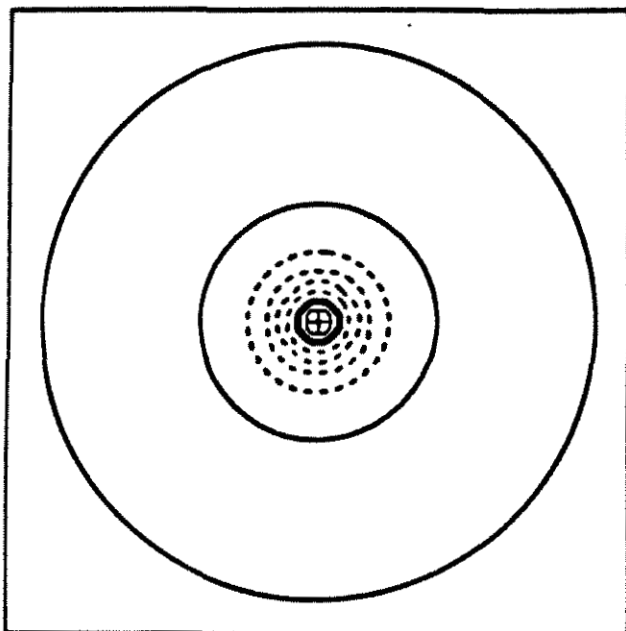
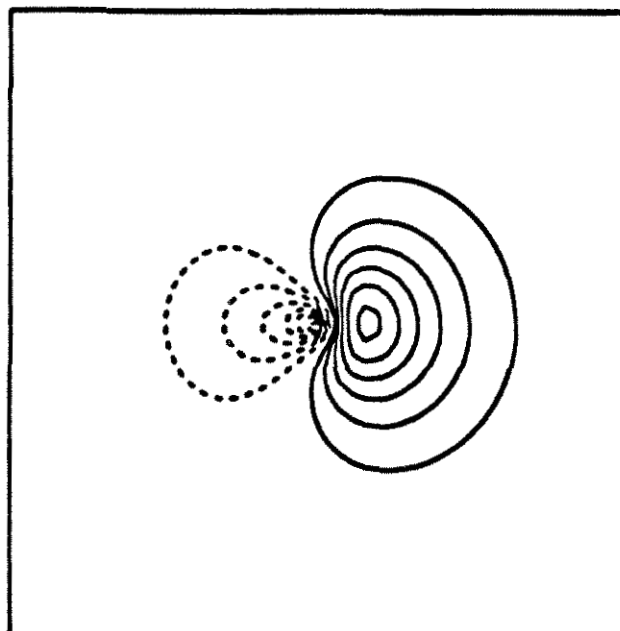


Figure 5. Singly-occupied orbitals. (a) The 4s orbital on K atom. The separation between adjacent contours is 0.025 a.u. (b) The sp^2 -type orbital in the BH_2 radical. The separation between adjacent contours is 0.05 a.u.

Singly Occupied Orbitals in K atom and BH_2 

K (4s)

 H_2B (2sp hybrid)

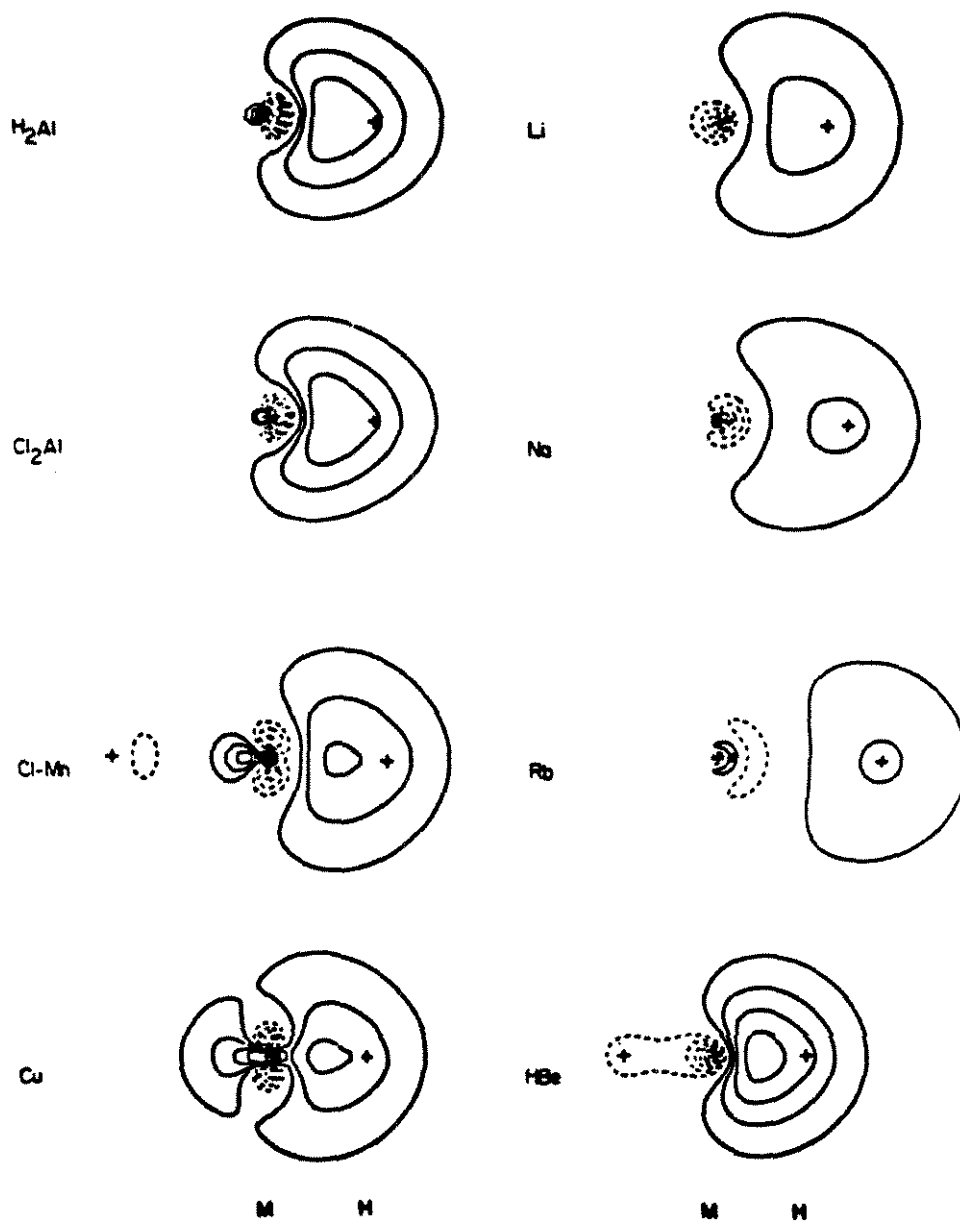


Figure 6. GVB orbital (singly-occupied) on M that participates in the M-H bond in MH. The separation between adjacent contours is 0.05 a.u.

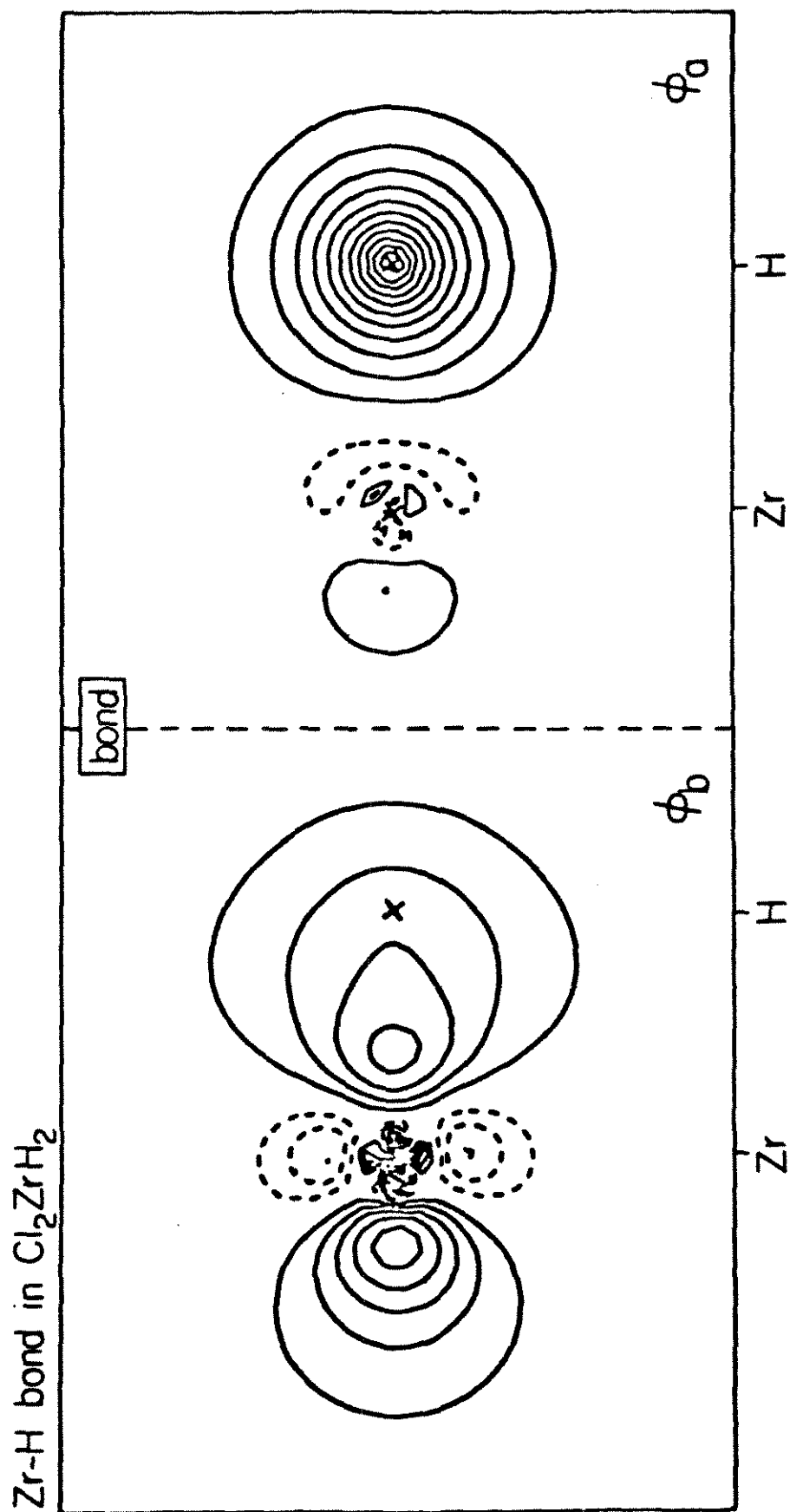


Figure 7. GVB orbitals describing a Zr-H bond in Cl_2ZrH_2 . The separation between adjacent contours is 0.05 a.u.

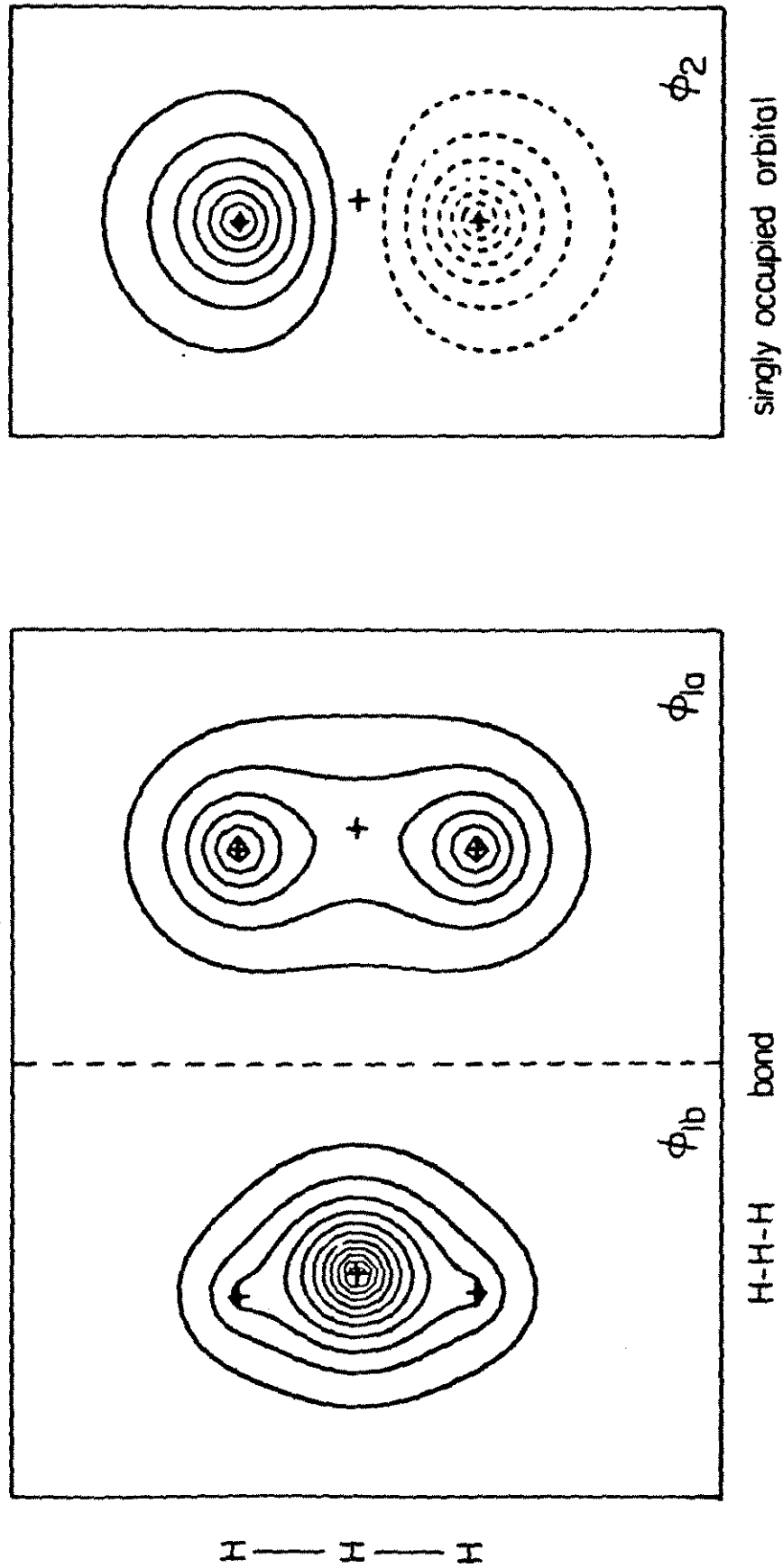
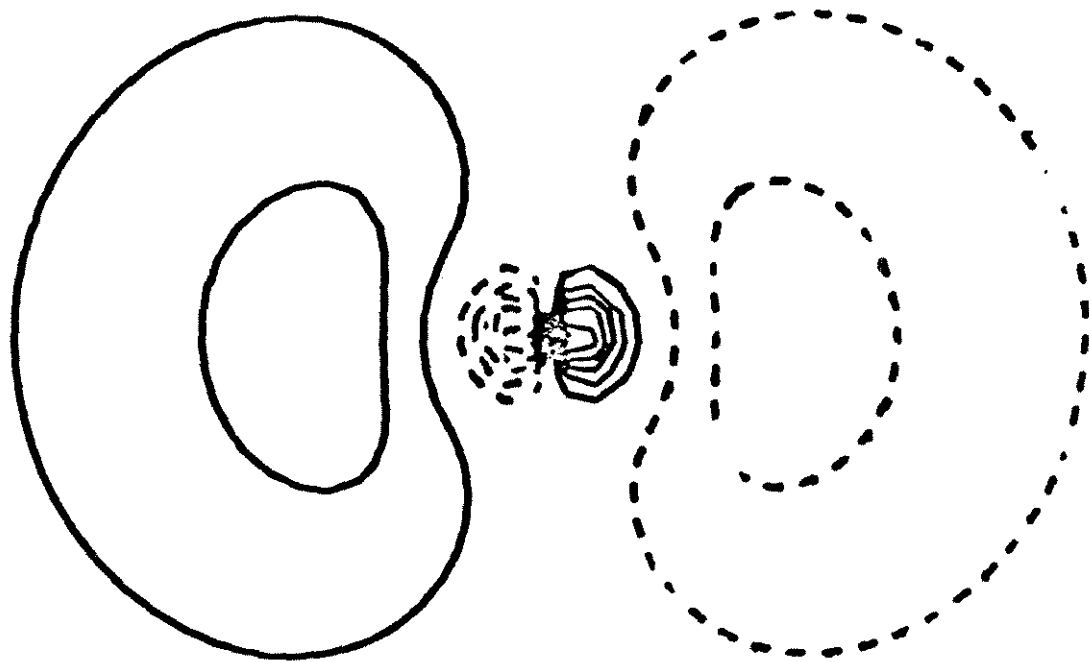
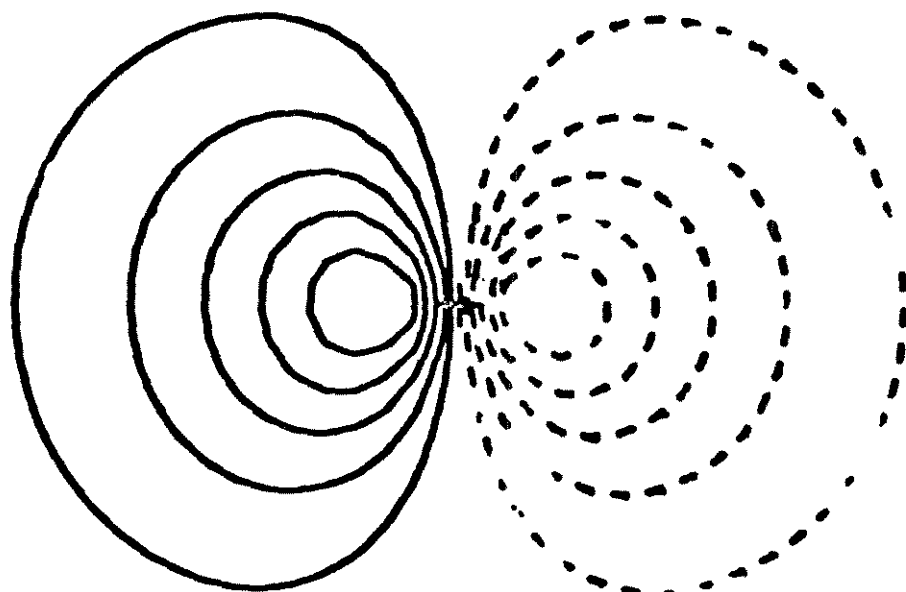


Figure 8. GVB orbitals describing H_3 . (a) The two orbitals of the delocalized spiegel bond. (b) The singly-occupied unspiegel orbital.

Figure 9. Atomic valence p orbitals on (a) boron and (b) aluminum. The separation between adjacent contours is 0.05 a.u.

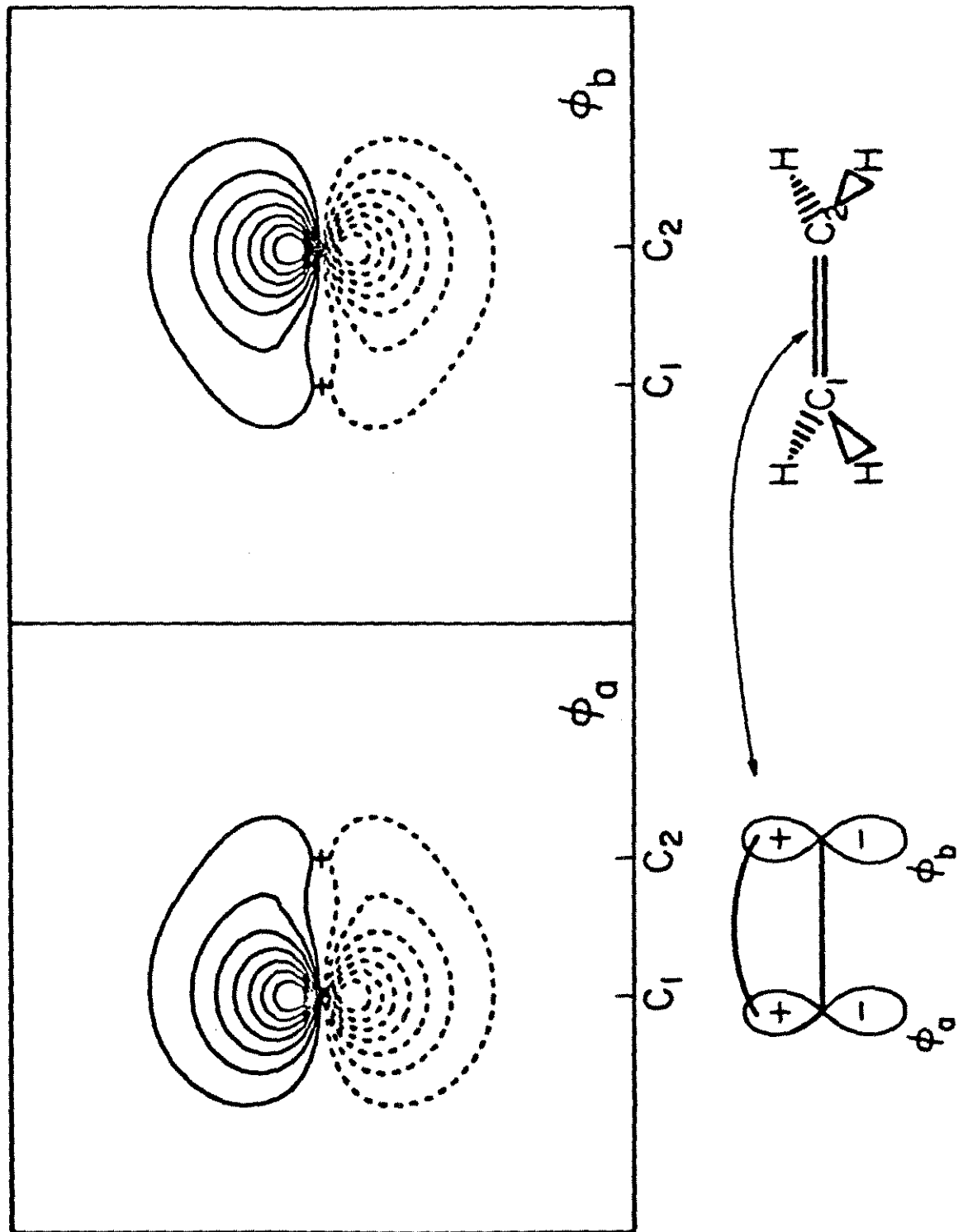


Al(3p)



B(2p)

Figure 10. GVB orbitals describing the C-C π bond in ethylene. The separation between adjacent contours is 0.05 a.u.

C—C π bond in ethylene

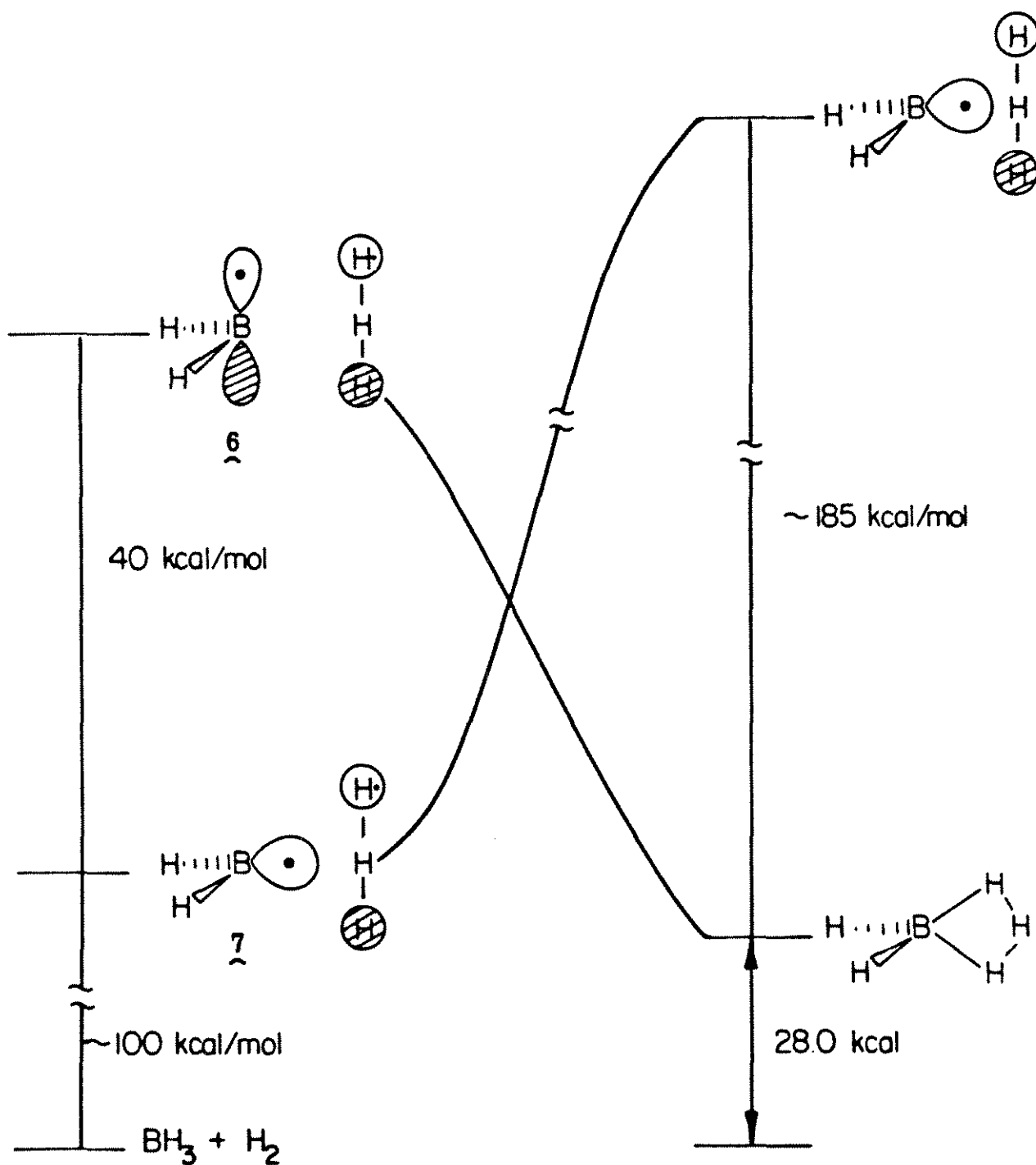


Figure 11. Schematic representation of the energetics of formation of the antisymmetric $\text{H}\cdots\text{B}\cdots\text{H}$ bond in H_2BH_3 .

Figure 12. GVB orbitals describing the two delocalized valence bonds of H_3^- . (a) The spiegel bond. (b) The unspiegel bond.

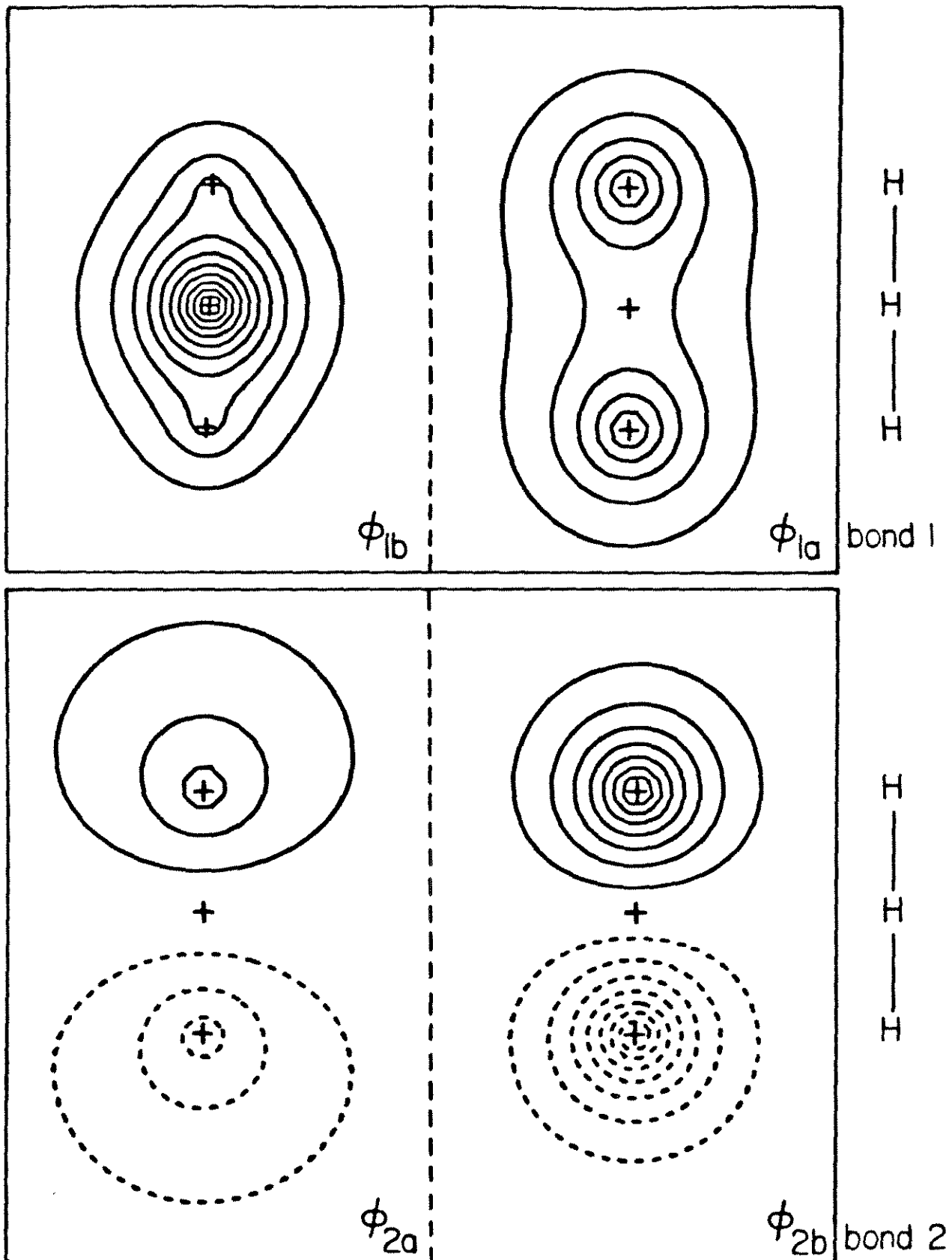
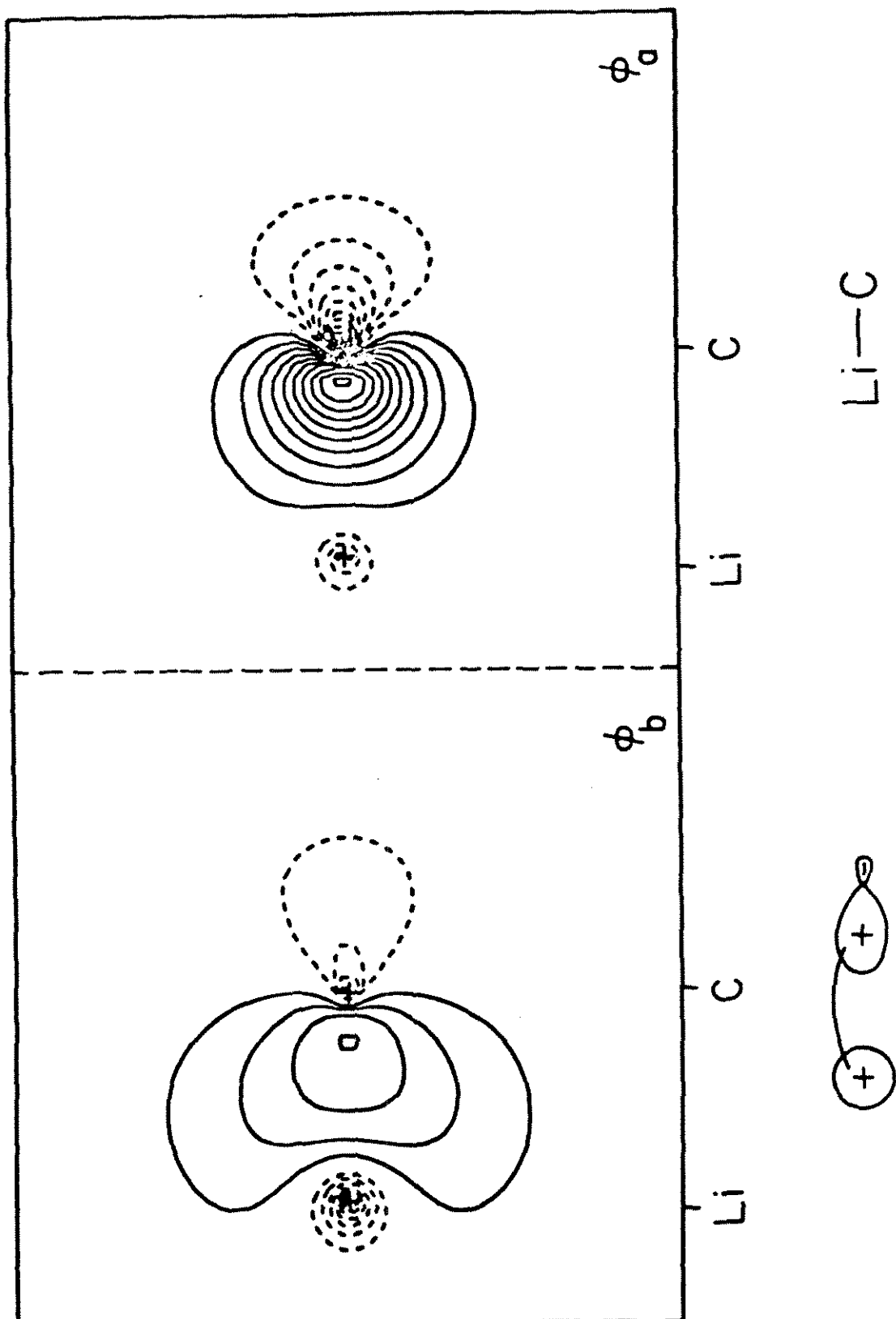


Figure 13. GVB orbitals describing the C-Li bond in methyllithium. The separation between adjacent contours is 0.05 a.u.

C—Li bond in methyllithium



References and Notes

- (1) R. B. Woodward and R. Hoffmann, "The Conservation of Orbital Symmetry", Verlag Chemie, Weinheim, 1971.
- (2) H. C. Brown, "Boranes in Organic Chemistry", Cornell University Press, Ithaca, New York, 1972.
- (3) P. Cossee, *Recl. Trav. Chim. Pays-Bas*, **85**, 1151 (1966); J. Boor, Jr., *Macromol. Rev.*, **2**, 115-268 (1967).
- (4) M. L. Steigerwald and W. A. Goddard III, *J. Am. Chem. Soc.*, in press.
- (5) R. G. Pearson, "Symmetry Rules for Chemical Reactions", Wiley Interscience, New York, 1976, p. 100.
- (6) Reference 5, p. 413.
- (7) See, for example, (a) P. J. Brothers, *Prog. Inorg. Chem.*, **28**, 1-67 (1981); (b) K. I. Gell and J. Schwartz, *J. Am. Chem. Soc.*, **100**, 3256 (1978).
- (8) W. A. Goddard III, T. H. Dunning, Jr., W. J. Hunt, and P. J. Hay, *Acc. Chem. Res.*, **6**, 368 (1973).
- (9) This calculation used a triple zeta basis on hydrogen (ref 59) and a simple GVB(1/2) wavefunction on H₂.
- (10) The significance and reliability of Mulliken populations is discussed in E. Steiner, "Determination and Interpretation of Molecular Wave Functions", Cambridge University Press, Cambridge, United Kingdom, 1976, Chapter 6.
- (11) For these calculations we set $\angle(\text{HBH}) = 120^\circ$ and $r(\text{B-H}) = 1.19 \text{ \AA}$. This is not very different from the observed values of 131° and 1.18 \AA , respectively.

- (12) The plots in Figure 7 are for the Zr-H bond in Cl_2ZrH_2 . Here the Mulliken population on H is 0.97. These hydrogens are not hydridic; M. L. Steigerwald and W. A. Goddard III, manuscript in preparation.
- (13) K. P. Huber and G. Herzberg, "Molecular Spectra and Molecular Structure. IV. Constants of Diatomic Molecules", Van Nostrand, New York, 1979.
- (14) Calculations on H_3 (H_3^-) were at the GVB(1/2) [GVB(2/4)] level and restricted to C_{2v} geometries. These geometries were optimized at the GVB level, using a triple zeta basis on hydrogen (ref 60).
- (15) In these calculations, only the p functions on B and Al that were in the plane of the reaction were excluded. The quoted energies are differences in total HF energies for the proper H_2MH_3 and those with the p functions removed.
- (16) We define the terms *spiegel* and *unspiegel* to mean symmetric with respect to reflection in a particular plane and antisymmetric with respect to such reflections, respectively. These terms are convenient generalizations of σ and π . The bond between M and H_3 may be considered to be a π bond with respect to M but a σ bond with respect to H_3 ; the *spiegel/unspiegel* nomenclature is precise.
- (17) The geometry of C_2H_4 was taken from "Landolt-Börnstein Numerical Data and Functional Relationships in Science and Technology. Group II. Atomic and Molecular Physics", Vol. 7; H.-H. Hellwege, Editor in Chief.
- (18) These plots are of p orbitals on the B and Al atoms that come from simple HF calculations.

- (19) See, for example, H. Sakurai, H. Sukaba, and Y. Nakadaira, *J. Am. Chem. Soc.*, **104**, 6156-6158 (1982), and references therein.
- (20) Transition metal alkylidenes have been defined [R. R. Schrock, *Acc. Chem. Res.*, **12**, 98-104 (1979)] and described as nucleophilic. The electronic structure of the M-C interaction has been shown to be that of a metal-carbon (σ - π) double bond [A. K. Rappe and W. A. Goddard III, *J. Am. Chem. Soc.*, **104**, 448-456 (1982)].
- (21) This is the vertical excitation with $r(\text{B-H}) = 1.184 \text{ \AA}$ and $\vartheta = 127.6^\circ$ (the H_2B geometry in H_2BH_3). At $R = 1.19 \text{ \AA}$ and $\vartheta = 120^\circ$ (the H_2B geometry in BH_3), this excitation is 40 kcal/mol. These excitation energies are differences in simple HF total energies.
- (22) For BCl_2 , $r(\text{B-Cl})$ was set at 1.70 \AA , and $\vartheta(\text{Cl-B-Cl})$ was set at 120° .
- (23) The related problem of cis-trans isomerization in olefin: the isomerization barrier of $(\text{H})(\text{D})\text{C}=\text{C}(\text{H})(\text{D})$ is 65 kcal/mol and the barrier in $(\text{Cl})(\text{H})\text{C}=\text{C}(\text{H})(\text{Cl})$ is 56.0 kcal/mol (S. W. Benson, "Thermochemical Kinetics", Second Edition, Wiley Interscience, New York, 1976, p 106). The ability of the two boron fragments to form unspiegel bonds should thus be commensurate. If anything, these data suggest the BCl_2 fragment will be less likely than BH_2 to form several bonds, making reaction 7 even less allowed.
- (24) (a) D. J. Pasto and Z.-Z. Kang, *J. Am. Chem. Soc.*, **89**, 295 (1967); (b) *ibid.*, **90**, 3797 (1968).
- (25) For BeH , $r(\text{Be-H})$ was set at 1.33 \AA . This is a single-configuration HF excitation energy.
- (26) W. A. Goddard III and L. B. Harding, *Ann. Rev. Phys. Chem.*, **29**, 363-396 (1978).

- (27) C. E. Moore, "Atomic Energy Levels", National Standard Reference Data Series, NBS 35; U. S. Government Printing Office, Washington, DC, 1971.
- (28) L. Pauling, "The Nature of the Chemical Bond", Third Edition, Cornell University Press, Ithaca, New York, 1960, p. 121.
- (29) The sextet d^5 core has a total two-electron energy of $5J_{d-d'} - 10K_{d-d'}$. Bonding to one of these d orbitals would result in a total two-electron energy of $5J_{d-d'} - 6K_{d-d'} - 4[(K_{d-d'})/2]$. Thus the coulombic energy, for example, increases by $2K_{d-d'}$. For $ClMnH$, $K_{d-d'} \approx 21$ kcal/mol.
- (30) "Organometallic" reactions such as oxidative addition, reductive elimination, and migratory insertion seem to occur via nucleophile/electrophile routes and organocopper centers. See (a) J. P. Collman and L. S. Hegehus, "Principles and Applications of Organotransition Metal Chemistry", University Books, Mill Valley, California, 1980, Chapter 11. Also, (b) "An Introduction to Synthesis Using Organocopper Reagents", G. H. Posner, Ed., Wiley Interscience, New York, 1980.
- (31) $IP(Li) = 5.390$ eV, $IP(Na) = 5.138$ eV; thus $\Delta(IP) = 6$ kcal/mol (ref 22).
- (32) (a) Reference 30(a), p. 294; (b) D. S. Matteson, "Organometallic Reaction Mechanisms of the Nontransition Elements", Academic Press, New York, 1974, Chapter 5.
- (33) See, for example, P. W. Alder, R. Baker, and J. M. Brown, "Mechanism in Organic Chemistry", Wiley Interscience, London, 1971, p. 249.

- (34) This is in regard to subsequent suprafacial reactivity at the Li-R bond.
- (35) Reference 28, p. 91.
- (36) Reference 46, p. 190.
- (37) A. A. Vitale and J. San Filippo, Jr., *J. Am. Chem. Soc.*, **104**, 7341-7343 (1982).
- (38) H. Gilman, A. L. Jacoby, and H. Ludeman, *J. Am. Chem. Soc.*, **60**, 2336-2338 (1938).
- (39) (a) G. S. Hammond, *J. Am. Chem. Soc.*, **77**, 334 (1955); (b) L. Salem, "Electrons in Chemical Reactions: First Principles", Wiley Interscience, New York, 1982, Chapter 2. Perusal of the data of Dewar and McKee (ref 41) shows that this is in fact the case. At their transition states for hydroboration, the nascent C-H bond has a length of 1.7-1.8 Å.
- (40) T. P. Fehlner, *J. Am. Chem. Soc.*, **93**, 6366-6373 (1971).
- (41) M. J. S. Dewar and M. L. McKee, *Inorg. Chem.*, **17**, 1075-1082 (1978).
- (42) S. W. Benson, "Thermochemical Kinetics", Second Edition, Wiley Interscience, New York, 1976, p. 106.
- (43) Reference 42, p. 289.
- (44) This value is an average of the values found by Dewar and McKee (ref 41).
- (45) See, for example, (a) A. H. Veefkind, F. Bickelhaupt, and G. W. Klumpp, *Recl. Trav. Chim. Pays-Bas*, **88**, 1058 (1969); (b) A. H. Veefkind, J. v. d. Schaaf, F. Bickelhaupt, and G. W. Klumpp, *J. Chem. Soc., Chem. Commun.*, 722 (1971).

- (46) J. Wakefield, "The Chemistry of Organolithium Compounds", Pergamon Press, Oxford, United Kingdom, 1974, Chapter 15.
- (47) M.-Y. Li and J. San Filippo, Jr., *Organometallics*, **2**, 554-555 (1983).
- (48) J. March, "Advanced Organic Chemistry: Reactions, Mechanism and Structure", McGraw-Hill, New York, 1968, p. 767.
- (49) T. Mole and E. A. Jeffery, "Organoaluminium Compounds", Elsevier, Amsterdam, 1972, Chapter 3.
- (50) Reference 47, p. 67.
- (51) Reference 2, Section XIV-6.
- (52) (a) Reference 2, Section XIV-5; (b) Reference 47, p. 69.
- (53) F. A. Carey and R. J. Sandberg, "Advanced Organic Chemistry. Part B. Reactions and Synthesis", Plenum Press, New York, 1977, p. 101.
- (54) K. Ziegler, *Angew. Chem.*, **64**, 323 (1952).
- (55) Reference 2, Sections XVI-3 and XVI-12.
- (56) R. A. Bair, W. A. Goddard III, A. F. Voter, A. K. Rappe', L. G. Yaffe, F.W. Bobrowicz, W. R. Wadt, P. J. Hay, and W. J. Hunt, GVB2P5 Program, unpublished. See R. A. Bair, Ph.D. Thesis, California Institute of Technology, 1980; F. W. Bobrowicz and W. A. Goddard III, In "Methods in Theoretical Chemistry," H. F. Schaefer III, Ed., Plenum Press, New York, 1979, Vol. 3, p. 77; W. J. Hunt, P. J. Hay, and W. A. Goddard III, *J. Chem. Phys.*, **57**, 738 (1972).
- (57) A. K. Rappe', T. A. Smedley, and W. A. Goddard III, *J. Phys. Chem.*, **85**, 1662 (1981).
- (58) A. K. Rappe', T. A. Smedley, and W.A. Goddard III, *J. Phys. Chem.*, **85**, 2607 (1981).

- (59) T. H. Dunning, Jr., and P. J. Hay, In "Modern Theoretical Chemistry: Methods of Electronic Structure Theory", H. F. Schaefer III, Ed., Plenum Press, New York, 1977, Vol. 3 and references therein.
- (60) W. A. Goddard III and A. K. Rappe', In "Potential Energy Surfaces and Dynamics Calculations", D. G. Truhlar, Ed., Plenum Press, New York, 1981, pp. 661-684.
- (61) J. J. Low and W. A. Goddard III, unpublished results. The GVB gradient program is based on HONDO [M. Dupuis, and H. F. King, *J. Chem. Phys.*, **68**, 3998-4004 (1978)]; Gaussian 80 (J. S. Binkely, R. A. Whiteside, R. Krishnan, R. Seeger, D. J. DeFrees, H. B. Schlegel, S. W. Topiol, L. R. Kahn, and J. A. Pople); and the vibrational analysis programs of D. F. McIntosh and M. R. Peterson, Quantum Chemistry Program Exchange No. 34, Department of Chemistry, Indiana University, Bloomington, Indiana.
- (62) At this level of calculation, we find H_3 to be linear with $r(H_1-H_2) = 0.919 \text{ \AA}$.
- (63) P. Siegbahn and B. Liu, *J. Chem. Phys.*, **68**, 2547 (1978).

Chapter 3. Dichlorotitanacyclopropane.

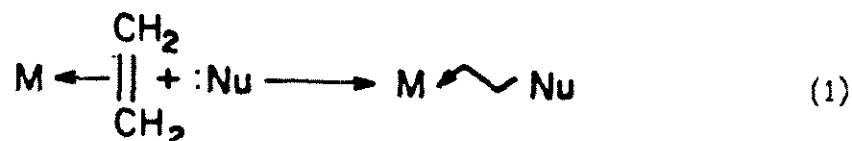
"If a substance is a hybrid of two or more structures, we might naturally suppose that its chemical reactions would be those characteristic of, at any rate, all the structures which have large weights".

-G. W. Wheland

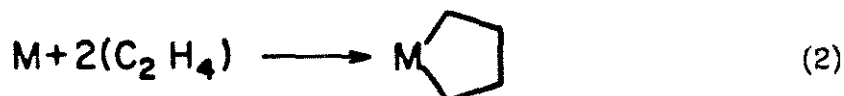
"Resonance in Chemistry"

I. Introduction

The chemistry of the enormous number of transition-metal olefin complexes reported in the literature is quite varied.¹ For example, in some cases transition metals are known to activate olefins toward nucleophilic attack (1),²



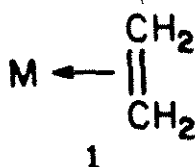
while in other systems, oxidative cycloaddition (2)



occurs.³ It is the case that metal systems that facilitate reaction (1) do not facilitate reaction (2) and vice versa.

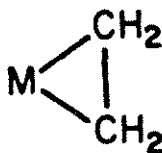
In an attempt to determine the electronic reason for the different reactivities of various metal-olefin complexes, we were led to examine whether a given metal-olefin complex should be regarded

(i) as a π -complex (1),



that is, an acid/base complex with donation of the C-C π -bonding electrons onto the metal supplemented by backbonding of the metal $d\pi$ electron pair into the antibonding orbital of the olefin π bond; or

(ii) as a metallacyclopropane (2)



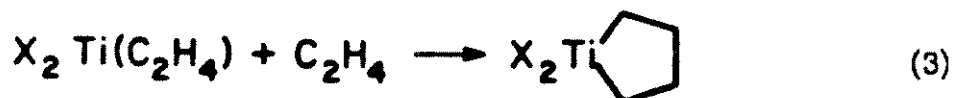
having two metal-carbon sigma bonds and only a single carbon-carbon bond.⁴

We have concluded that *some* metal-olefin complexes should be viewed as **1** and others should be viewed as **2**, and most importantly those species that are best described by **1** will show reactivity as in (1), and species that are described as **2** will show reactivity as in (2). We suggest that whether a complex has the form of **1** or **2** depends upon the metal, its oxidation state, the nature of the auxiliary ligands around the metal, and the nature of the olefin. This suggests strategies that one might use in designing systems that will show one type of reactivity in contrast to another.

Results and Discussion

A. Structure of a Metallacyclopropane

Complexes of the form $X_2Ti(C_2H_4)$ (X = anion ligand such as η^5 -cyclopentadienyl) have been reported to react with added olefin to give titanacyclopentanes [Eq. (3)]⁵



Inasmuch as the predominance of this mode of reactivity over the others open to these olefin complexes is difficult to predict using a simple acid/base model of the complexes 1,⁶ we undertook the detailed investigation of their electronic structure. As a model we chose $Cl_2Ti(C_2H_4)$ (3).

Using the procedure outlined in the Appendix [based on the generalized valence bond (GVB) method], we optimized the geometry of this complex. The resulting geometry is shown in Figure 1a. This calculated geometry should be compared with the structure of $Cp_2^*Ti(C_2H_4)$ (4) recently determined by Cohen, Auburn, and Bercaw^{5b} and shown in Figure 1b. The theory and experiment agree quite closely (disagreements of 0.02 Å in Ti-C and C-C bond lengths), indicating that the chlorine ligands in 3 are reasonable models for the Cp* ligands in 4.⁷

We also optimized the geometry of $Cl_2Ti(C_2H_4)$ using the Hartree-Fock (HF) method (the generalization of the molecular orbital method) and found the results shown in Figure 1c (5). This indicates that the electron correlation effects included in GVB⁸ must be taken into account for an accurate description of systems such as 3.

The optimum valence bond orbitals for the Ti-C and C-C bonds of 3 are shown in Figure 2 where we see that the wavefunction has the form of

a metallacycle, **2**. Here bond 1 is a *bent* sigma bond between a d orbital on the titanium and a p orbital on the upper carbon. Similarly, bond 2 is a *bent* sigma bond between a second titanium d orbital and a p orbital on the lower carbon. Bond 3 is a *bent* sigma bond between the two carbons of the CH₂CH₂ moiety. Thus the GVB wavefunction describes the electronics of a *strained* three-membered ring.⁹ The strain in the ring is obvious from Figure 2 because the C-Ti-C angle is seen to be 40° (both calculationally and experimentally), but the angle between the two bonding orbitals on Ti (ψ_{1a} and ψ_{2a} in Figure 2) is 75°. ¹⁰ This situation should be compared with our observation that in the unstrained system (Cl₂TiH₂, **6**), the H-Ti-H angle is 75°, and the angle between the two Ti-centered bonding orbitals (ψ_{1a} and ψ_{2a} in Figure 3) is also 75°. The orbitals of Figure 2 should also be compared with the C-C bond orbitals from cyclopropane (Figure 4). Here the C-C-C bond angle is 60°, but the angle between the two bonding orbitals at the same carbon is 100°. ¹¹ Our conclusion is that the Ti(C₂H₄) complexes (**3** and **4**) are *metallacyclopropanes, not π -complexes*.

B. Reactivity of a Metallacyclopropane

The distinction of an acid-base π -complex **1** from a metallacyclopropane **2** is not significant in a practical way unless one can see a clear difference in the reactivities of the two different forms. The question then is, what reactivity is expected from the dichlorotitanacyclopropane?

Recently we have examined exchange reactions of H₂ with several metal-hydrogen bonds¹² [Eq. (4)]



and found that the concerted, suprafacial 2 + 2 reaction shown in Eq. (5) is allowed

C. The Titanium-Olefin π Complex

In the above sections we argue that $\text{Cl}_2\text{Ti}(\text{C}_2\text{H}_4)$ and $\text{Cp}_2^*\text{Ti}(\text{C}_2\text{H}_4)$ should be viewed as titanacyclopropanes. We next must consider whether this form is significantly different from that of the classical π -complex.¹³ In order to explore this issue, we *restricted* the GVB calculations so that there would be two bonds between the carbon atoms (as in the free olefin) and a lone pair of electrons occupying a d orbital on the metal having the proper symmetry to donate from the metal to the π^* system of the olefin. The geometry preferred for this "Dewar-Chat-Duncanson"-type complex is that of Figure 1c. As would be expected, the π -complex 1 has a shorter C-C bond and a longer TiC bond than does the metallacycle 2 (compare Figures 1a and 1c). In fact, the C-C bond length in the π -complex form (Figure 1c) is quite close to the C-C bond length in Zeise's salt¹⁴ (Figure 8), long considered as a typical π -complex.

Energetic comparison shows the metallacycle form (at its optimum geometry, Figure 1a) to be 12 kcal/mol lower in energy than the π -complex form (at its preferred geometry, Figure 1c). This further substantiates our claim that 4 and $\text{Cl}_2\text{Ti}(\text{C}_2\text{H}_4)$ are best thought of as metallacycles.

D. The Reactivity of a π -Complex

The optimized GVB orbitals describing the π -complex are shown in Figure 9. Pair 1 (φ_{1a} and φ_{1b}) shows a basic C-C π bond delocalized onto the acidic metal, and Pair 2 (φ_{2a} and φ_{2b}) shows the delocalization of the basic doubly-occupied Ti d orbital into the acidic π^* orbital of the olefin. Pair 3 (φ_{3a} and φ_{3b}) shows the C-C sigma bond that has been distorted by the acid-base bonds of pairs 1 and 2. Note that the *simple* four-electron 2 + 2 suprafacial reaction described above is no longer allowed because

the ability of the transition metal to form the reactive metal-carbon "d bond" has been quenched. In this way the "transition-metal" character of the bonding has been eliminated and the "main group" Woodward-Hoffmann rules apply.¹⁵

These plots indicate that the C-C π bond and the Ti lone pair are still intact. The *spin-recoupling* that results in the disintegration of these two entities and subsequent formation of two metal-carbon bonds of the metallacycle has not occurred. We view this bonding as the interaction of two "closed-shell" molecules, Cl_2Ti (singlet) and C_2H_4 (as opposed to the bonding in the metallacyclopropane, which is the interaction of two higher spin fragments, "triplet" Cl_2Ti and "triplet" C_2H_4). This being the case, the chemistry of the π -complex should be dominated by "closed-shell" processes, i.e., reactions in which the electrons of a bonding pair delocalize *together* across the same paths. [This is distinct from the pericyclic reactions in which **one** member of each electronic pair delocalizes while the other remains localized (ideally) on one center^{1,12}].

It is known that when the central metal is an oxidized late transition metal [Pd(II) ,¹⁶ Pt(II) ,¹⁷ Fe(II) ¹⁸], the sense of acid-base bonding is acceptor-metal/donor-olefin. In these cases, the intrinsic Lewis acidity of the metal is transferred to the olefin, and thus the olefin is activated toward nucleophilic attack. Examples of this activation are shown in Figure 10. In cases where this mode of bonding obtains, the geometry of the olefinic ligand is not expected to deviate substantially from that of the free olefin. This is due to the persistence of the double bond between the two carbon atoms. Since this bond remains, the overlap between the two carbon $p\pi$ orbitals that form the olefinic π bond is still required and a short C-C internuclear distance results.

Complexes between simple unactivated olefins and highly reduced late transition metal centers (Ni^0 ,¹⁹ Fe^0 ,²⁰ Co^{-1} ,²¹ Pt^0 ²²) are also quite well known. The chief mode of reactivity of these complexes is olefin dissociation, and in this way these olefin complexes are usually used simply as sources of low-valent metals in homogeneous reactions.²³ These complexes react at the olefin with electrophiles such as proton acids, but extensive olefinic reactivity is absent in these complexes. These observations, as well as several quantum chemical studies and spectroscopic studies,²⁴ are consistent with the bonding in these complexes being of the acid/base type, in the sense donor-metal/acceptor-olefin.

Complexes of this form are expected to have C-C bond distances that are long relative to that of a normal C-C double bond. [For example, the C-C bond length in $(\text{P}\phi_3)_2\text{Ni}(\text{C}_2\text{H}_4)$ is 1.43 \AA ²⁵ and in $\text{Li}_2\text{Fe}(\text{C}_2\text{H}_4)_4$ is 1.43 \AA ²⁰; compare these with $r(\text{C-C}) = 1.34 \text{ \AA}$ in C_2H_4 .] This may be rationalized either by noting that occupation of the antibonding π^* orbital reduces the C-C bond order^{13b} or by noting that more effective stabilization of the metal-centered lone pair is realized if the two participating carbon $p\pi$ orbitals overlap the two lobes of the doubly-occupied d orbital more. This would tend to open the C-M-C angle more toward 90° (thus lengthening the C-C bond) and bend the CH_2 units out of the plane of the olefin.

E. Metallacycle versus π -Complexes

In the discussion above, we pointed out that there are two distinct forms for an $\text{M}(\text{C}_2\text{H}_4)$ complex, 1 and 2. We showed that the metallacycle form is preferred in 3 and 4. Of course, the full wavefunction of such a complex will be a mixture or *resonance* of these two forms.²⁶ We find the stabilization of this mixing to be 2 kcal/mol ,²⁷ further indicating that the metallacycle form is preferred. Even so, the less favored π -complex form

can play a role in chemistry, but only after paying a 12 kcal penalty due to loss of the favorable metallacycle character.

This situation is analogous to that of the enolate anion, which has two important resonance structures, **7** and **8**.



with their relative importance determined by the character of substituents and solvent.²⁸ Even when more stable, the use of structure **7** alone to describe the enolate would not explicitly recognize the oxygen-centered nucleophilicity of the molecule; similarly, exclusion of **7** from consideration would mask the carbon-centered nucleophilicity. The use of this concept of resonance of molecules is fruitful because each resonance structure has its own characteristic and distinct behavior. By determining which canonical form is more important in a given chemical structure, one may estimate the relative importance of the two manifolds of reactivity.²⁹ This being the case, it is necessary to come to an understanding of which physical characteristics of the constituent parts of a metal-olefin complex increase the importance of one canonical form over the other. In the same way that different chemical environments will enhance the importance of **7** or **8**, different environments (reaction medium, ligands, different metal centers, etc.) will favor **1** over **2**. To make our theory useful, we must outline rules for estimating the relative importance of **1** and **2**.

We can state rules for deciding when the metallacycle form will predominate over the π -complex form:

1) High-Spin Metal Fragment

The π -complex form requires a doubly-occupied d orbital on the metal that may backbond into the π^* space on the olefin.^{13b} Thus metals that have stable low-spin states (i.e., low-lying states with doubly-occupied d orbitals) will be more likely to form acid-base type complexes. Conversely, metal centers that prefer high-spin coupling of the valence d shells (such as $d^2 \text{Ti}^{\text{II}}$, $d^2 \text{Ta}^{\text{III}}$, and $d^2 \text{Nb}^{\text{III}}$)³⁰ will be more likely to form metallacyclopropanes. Thus, early transition metals will tend to form metallacycles and late metal will tend to form π complexes.³¹

2) Weak C-C π Bond in the Free Olefin

Formation of the metallacyclopropane requires the cleavage of a C-C π bond. Therefore the metallacyclopropane form will be more important as the C-C π bond of the free olefin is weaker. Thus, acetylenes and olefins with strained π bonds (methylenecyclopropane, cyclopropenes, norbornadiene, allenes, etc.)³² will be more likely to adopt a metallacycle form than will simple olefins. Also, olefins with electron-withdrawing substituents that weaken the C-C π bond will favor metallacyclopropane formation.³³ Since the C-C π -bond in C_2H_4 is one of the strongest C-C π -bonds known,³⁴ ethylene will be the olefin least likely to form a metallacyclopropane.

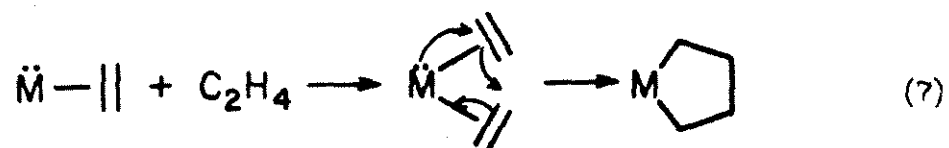
3) Strong M-C σ Bonds

Since the major force stabilizing the metallacyclopropane is the formation of metal-carbon covalent bonds, metal fragments that tend to make stronger covalent bonds will favor the metallacycle form. Thus Cl_2Ti will favor metallacyclopropane less than will Cl_2Zr or Cl_2Hf owing to the greater radial extent of the bonding orbitals of Cl_2Zr and

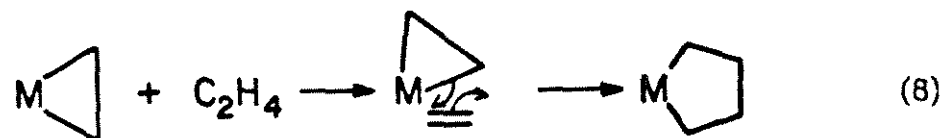
Cl_2Hf .³⁵ Late transition metals will favor metallacycles less than will corresponding early transition metals for the same reason.³⁵

F. Implications

When a complex having the form $\text{M}(\text{C}_2\text{H}_4)$ is judged by the above criteria to be predominantly metallacyclic, it should demonstrate chemistry associated with that of two *isolated*, and *strained*, metal carbon bonds. Therefore, we suggest that the oxidative cyclization reaction (2), which has been observed for $\text{M} = \text{Cp}_2^*\text{Zr}$,^{3c} Cp_2^*Ti ,^{5b} and CpCl_2Ta ^{3a} should be viewed NOT as a six-electron process [Eq. (7)]⁶

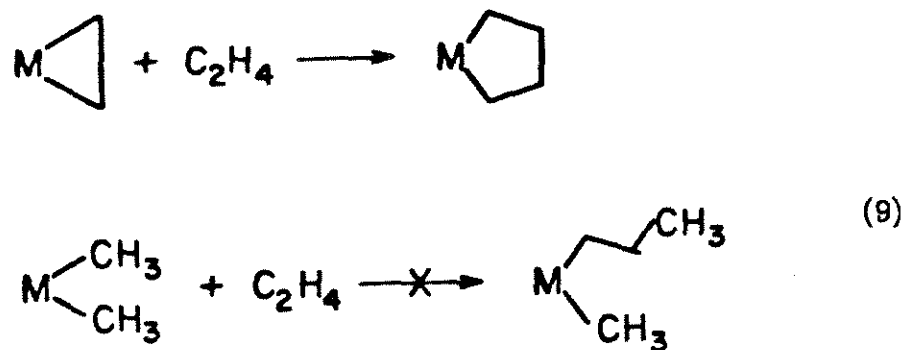


but rather as the simpler four-electron insertion process [Eq. (8)].

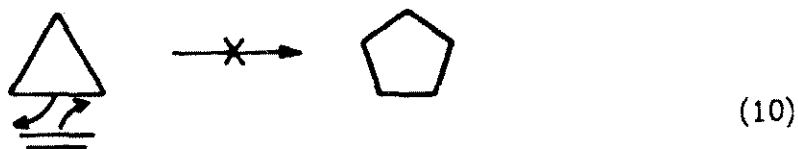


Furthermore, we suggest that reaction (2) is not oxidative at all; the "divalent" metal in the metallacyclopropane participates in the pericyclic migratory insertion reaction¹² to give the "divalent" metal in the metallacyclopentane.

Why is it that these metallacyclopropanes react with olefins (see Fig. 6), while the corresponding dialkyl complexes do not [Eq. (9)]?³⁶



The beautiful simplicity of the metallacyclopropane form is apparent in the plots of Figure 2. The *strain* in the three-membered ring, which is manifest in the valence bond description, stimulates the migratory insertion reaction. Cyclopropane itself is stable in the presence of simple olefins *only* because for carbon the $2_s + 2_s$ reaction is forbidden¹⁵ [Eq. (10)].

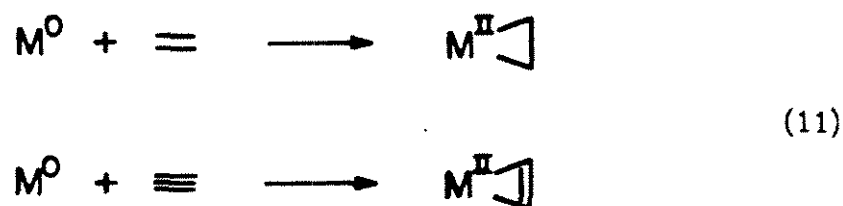


The presence of the metal at the apical site and, importantly, *the use of the metal valence d-orbitals in the covalent metal-carbon bond* allows the intrinsic strain of the three-membered ring to be relieved by a very simple $2 + 2$ reaction.

It is important to note that the metal fragments (Cp_2^*Ti , Cp_2^*Zr , CpCl_2Ta , etc.) affording the reaction shown in (2) are all expected to be high-spin d^2 species.³⁰ According to the first rule mentioned in Section II.E, the complex formed between each of these fragments and ethylene should be a metallacyclopropane.

There are also several examples in the literature where metal fragments that do *not* have high-spin d-shells promote "oxidative cycloaddition" to give metallacyclopentanes when they are treated with olefins.

Ni(0) and Ir(I) are especially effective^{3d,32} (Figure 11). In a similar way, low-valent group VIII metals are known to react with 2 equivalents of acetylene to give metallacyclopentadienes³⁷ (Figure 12). In all of these cases the metal is introduced into the (often catalytic) reaction sequence as a low-valent complex that is transformed to the higher-valent metallacyclic product. We suggest that the change in valency occurs upon the addition of the *first* equivalent of olefin (or acetylene) to give the metallacyclopropane (or -propene)^{33,38} [Eq. (11)].



Note that in all of the above cases the active π -bonds are *weak* ones (due to strain, electron-withdrawing substituents, or the intrinsic weakness of acetylene π bonds). This was mentioned above as the second criterion for predicting predominance of a metallacyclic structure over a π -complex form.

III. Conclusions

The GVB calculations on $\text{Cl}_2\text{Ti}(\text{C}_2\text{H}_4)$ lead to a metallacyclopropane resonance structure that predominates over the π -complex resonance structure. The chemistry expected from this metallacyclopropane form involves 2 + 2 suprafacial reactions with the strained Ti-C bond. This reactivity is consistent with experimental observation.

We have emphasized that the metallacyclopropane and π -complex forms are not truly separate and distinct; however, we expect that one form will take precedence over the other in any one system. This leads to the partitioning of the chemistry of olefin complexes into two classes, that of the metallacycle and that of the π -complex. The chemistry of the metallacyclopropane is dominated by $2_2 + 2_2$ -type reactions,¹² while the chemistry of the π -complex is dominated by acid-base reactions resulting from enhancement of the electrophilicity of the olefin.²

By examining the wavefunction of one metallacyclopropane in detail, we have been able to see the ring strain that is not at all apparent in the π -complex form. We have seen how this ring strain plays an important role in metallacyclopropane chemistry, owing to the suprafacial 2 + 2 reaction that, although forbidden in main group chemistry, is possible at a transition metal to carbon covalent bond!

APPENDIX: *Details of the Calculations*

A. *Basis Sets and Effective Potentials*

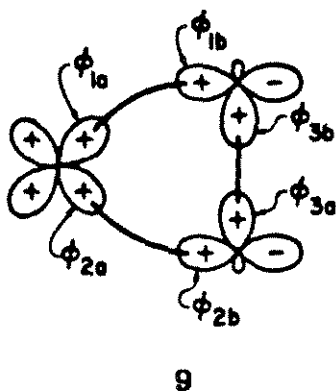
We calculated GVB(3/6) wavefunctions for the $\text{Cl}_2\text{Ti}(\text{C}_2\text{H}_4)$ complex. The titanium, carbon, and hydrogen centers were described in a fully ab initio, all-electron fashion, using valence double zeta basis sets on each.³⁹ The core electrons (1s,2s,2p) on chlorine were replaced with the SHC ab initio core effective potential,⁴⁰ and the valence electrons on chlorine were described using a minimal basis set optimized for molecular environments.⁴⁰

B. *Geometry Variation*

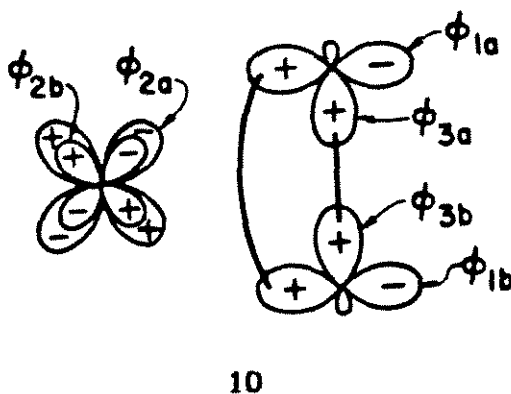
During the geometry searches, C_{2v} molecular symmetry was assumed. This is justified for several reasons. Firstly, all tetra- and divalent four-coordinate titanium complexes are pseudotetrahedral.⁴¹ It seems unlikely that the $\text{Cl}_2\text{Ti}(\text{C}_2\text{H}_4)$ complexes would deviate from this. Secondly, Bercaw and co-workers have studied $\text{Cp}_2^*\text{Ti}(\text{C}_2\text{H}_4)$ crystallographically and found that the ethylene moiety occupies two of the "tetrahedral sites" about the titanium atom.^{5b} Finally, our experience with similar complexes of titanium [Cl_2TiH_2 , Cl_2TiH , Cl_2TiH^+ , $\text{Cl}_2\text{Ti}=\text{CH}_2$, and $\text{Cl}_2\text{Ti}(\text{CH}_2)_3$] also indicates that there is little force driving the two "organic" ligands out of the plane that bisects the Cl-Ti-Cl angle.^{10,12}

Throughout these calculations, the Ti-Cl bond length was fixed at 2.328 Å, and the Cl-Ti-Cl angle was fixed at 142°. These are the parameters calculated for Cl_2TiH_2 ¹⁰ and since the chlorine ligands are used here singly as *model* "anionic" ligands, the fixing of their positions is justified. The C-H bonds in the complex were fixed at 1.091 Å and not varied, although the angle of depression of the methylene units was optimized.^{1c}

The geometry of the complex was optimized for the GVB-PP(3/6) level wavefunction in which the motions of three pairs of electrons are correlated. Each pair requires two valence bond-like orbitals so that six orbitals are used for the three pairs (hence, 3/6). These six electrons are the "active electrons" in this complex. This wavefunction has the flexibility to describe either the three bonds of a metallacyclopropane **9**



or the three pairs of a π -complex (a lone pair on the metal, a C-C sigma bond, and a C-C π bond) **10**



The geometry search was conducted as follows: (1) With $R(\text{CC}) = 1.432 \text{ \AA}$ and $R(\text{Ti-C}) = 2.14 \text{ \AA}$, the angle of depression of the CH_2 units from the ethylene plane was optimized at 21° . (2) With this angle set at 21° and

R(C-C) set at 1.432 Å, the Ti-C distance was bound to be 2.181 Å. (3) With the angle of depression set at 21° and R(Ti-C set at 2.181 Å, the carbon-carbon distance was optimized at 1.460 Å. In this way the structure shown in Figure 1a was found. [A similar geometry variation procedure using a purely HF (molecular orbital) wavefunction gave the geometry shown in Figure 1c.]

The GVB(3/6) wavefunction that was variationally determined is that wavefunction described by the orbitals in Figure 2. No symmetry or equivalence restrictions were placed on the wavefunction to force the metallacyclopropane structure.

Using symmetry restrictions, we were able to force the $\text{Cl}_2\text{Ti}(\text{C}_2\text{H}_4)$ system to have a wavefunction describing the π -complex form. This was done by requiring that two covalent bonds be retained between the two carbon atoms. As expected, the GVB(3/6) (π -complex) wavefunction prefers the geometry of Figure 1c (by 4.5 kcal/mol) over the geometry of Figure 1a.

It is valuable to examine the GVB orbitals describing these structures in more detail. Recall that in the valence bond formalism a covalent bond results from the overlap of two *singly-occupied* electronic orbitals, say φ_a and φ_b . Also recall that the valence bond wavefunction, ψ_{VB} , can be written as a sum of two molecular orbital configurations [Eq. (12)],

$$\psi^{\text{VB}} = (ab + ba) = (a + b)^2 - \lambda^2(a - b)^2 = \sigma^2 - \lambda^2\sigma^{*2} \quad (12)$$

where σ and σ^* correspond to bonding and antibonding localized molecular orbitals and $\lambda \sim 0.1$ for a strong bond (overlap = 0.8).⁴² The GVB pair lowering, ΔE , is the energetic destabilization realized in replacing the GVB pair ($\sigma^2 - \lambda^2\sigma^{*2}$) by the one configuration (molecular orbital) term (σ^2). A small overlap of the two GVB orbitals indicates large pair lowering energy,

and in this case a valence bond description is greatly preferred over the MO description.

In Table I we list these calculational results for the GVB(3/6) wavefunctions describing the metallacyclopropane and π -complex resonance structures. For comparison we include the analogous data for the two carbon-carbon bonds in ethylene,⁴³ the carbon-carbon bond in ethane,⁴³ the carbon-carbon bond in cyclopropane,⁴³ the titanium-carbon bond in $\text{Cl}_2\text{Ti}(\text{CH}_3)(\text{H})$,⁴⁴ and the lone pair on Ti in Cl_2Ti .⁴⁵

From these and other data we may generalize that Ti-C bonds are characterized by bond orbitals having an overlap of ~ 0.6 - 0.65 . This is significantly smaller than the overlap of bonding orbitals in a carbon-carbon σ bond (~ 0.8 - 0.85). Also, the inclusion of the second configuration (σ^*2) in the molecular wavefunction is energetically twice as important in the titanium-carbon bond as in the carbon-carbon bond.

Data in Table I indicate that the Ti-C bonds in the metallacyclopropane are quite similar to the "normal" Ti-C bond in $\text{Cl}_2\text{Ti}(\text{CH}_3)(\text{H})$. Contour plots of the orbitals of this TiC bond are shown in Figure 13. Comparison of these orbitals with the orbitals describing the Ti-C bond in the metallacyclopropane (Figure 2) shows the bent character of the latter bond. Similar plots of the orbitals of the C-C bond in ethane are shown in Figure 14. These two bonding orbitals point directly at one another, unlike the corresponding orbitals of the C-C bond in cyclopropane (Figure 4). Comparison of the two carbon-carbon bonds with the two titanium-carbon bonds shows that there is the same relationship between the two Ti-C bonds as between the two C-C bonds. In this way an evaluation of these GVB *wavefunctions* makes the strain in the titanacyclopropane apparent.

The nonpolarity of the Ti-C bonds in both the metallacyclopropane

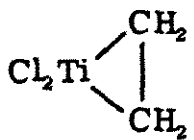
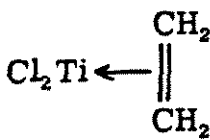
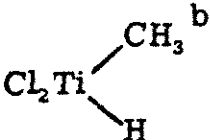
and $\text{Cl}_2\text{Ti}(\text{CH}_3)(\text{H})$ is also apparent from the plots of the GVB orbitals. Note that in each case there is one orbital that is centered on the metal atom and one orbital centered on the carbon. As a contrasting example, the two GVB orbitals for the Cr-H bond of the d^5 sextet state of CrH^{46} are shown in Figure 15. This bond is polar ($\text{Cr}^+ \rightarrow \text{H}^-$) because both orbitals (φ_a and φ_b) are centered on the hydrogen. Not surprisingly, this polarity also results in a higher overlap (0.77) in this bond than in a typical nonpolar M-H bond (overlap = 0.62 in the Ti-H bond in Cl_2TiH_2).

Finally, we can assess the shape of the titanium bonding orbital in the metallacyclopropane by plotting the amplitude of this orbital in the plane perpendicular to the Ti-C-C ring and along one of the Ti-C bond axes. This plot is shown in Figure 16. From this it is apparent that the Ti bonding orbital is shaped like a d_{z^2} orbital, just as in $\text{Cl}_2\text{Ti}^+-\text{H}$, $\text{Cl}_2\text{Ti}-\text{H}$, Cl_2TiH_2 , $\text{Cl}_2\text{Ti}(\text{CH}_3)(\text{H})$, $\text{Cl}_2\text{Ti}(\text{CH}_2)_3$, $\text{Cl}_2\text{Sc}-\text{H}$, Cl_2ZrH , and Cl_2ZrH_2 .^{10,12,47} The shape of this bonding orbital is critical when evaluating the propensity of this bond to participate in $2 + 2$ reactions, as mentioned in the above text. The fact that there is a ring of negative amplitude about the waist of the "dumbbell" of positive amplitude in this orbital means that the $2_s + 2_s$ substrate can approach the reaction bond from any azimuthal direction to form the quadrilateral transition state required for the pericyclic reaction.

The wavefunction that describes the π -complex form is not surprising. The orbitals in Figure 17 show a doubly-occupied d orbital in the singlet state of Cl_2Ti . Comparison of these plots with the corresponding plots for the π -complex form of $\text{Cl}_2\text{Ti}(\text{C}_2\text{H}_4)$ shows only minor changes. The changes observed in the two carbon-carbon bonds in the C_2H_4 unit, when complexed to the metal, are not surprising. These bond orbitals in the

π -complex indicate some distortion from the normal double bond in ethylene (Figure 18), but the ring strain is not nearly as clearly demonstrated here as in the metallacyclopropene form. Furthermore, it is not clear from the π -complex wavefunction that the ring strain is actually relieved *along* the 2 + 2 reaction pathway. In this way the ring strain, a *thermodynamic* quantity, can at least qualitatively be related to the *kinetics* of the 2 + 2 migratory insertion reaction.

Table I. Parameters characterizing GVB orbital pairs mentioned in this study.

Molecule	Electron Pair	GVB Orbitals	
		Overlap	$\Delta \epsilon$ (kcal/mol)
	C-C bond	0.85	8.2
	Ti-C bond	0.63	19.5
	C-C π bond	0.72	12.6
	C-C σ bond	0.87	6.3
	Ti lone pair	0.84	3.1
Ethane	C-C bond	0.83	9.4
Cyclopropane	C-C bond	0.81	10.0
Ethylene	C-C π bond	0.64	9.5
	C-C σ bond	0.88	6.3
$\text{Cl}_2\text{Ti}^{\text{a}}$	Ti lone pair	0.89	1.9
	Ti-C bond	0.64	23.2

^a Reference 45.

^b Reference 44.

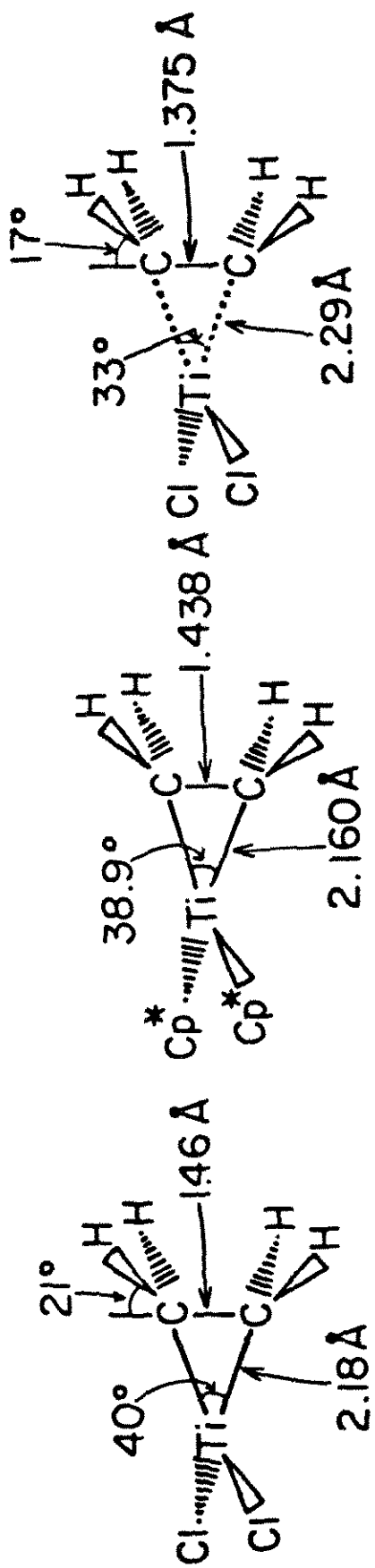


Figure 1. Calculated and observed geometries of complexes $X_2Ti(C_2H_4)$.
 (a) Dichlorotitanacyclopropane (this work). (b) $Cp_2^*Ti(C_2H_4)$ (ref 5b). (c)
 Dichlorotitanium (ethylene) (this work).

Figure 2. GVB orbitals describing the valence space of dichlorotitanacyclopropane. Spacing between contours is 0.05 a.u. The characteristic dimension of the plot is $6.0 a_0$.

Valence Bonds in Dichlorotitanacyclopropane

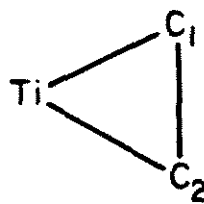
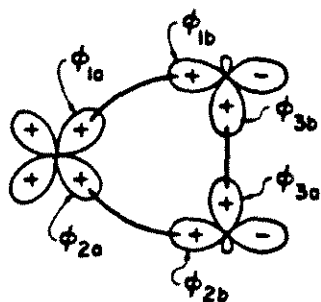
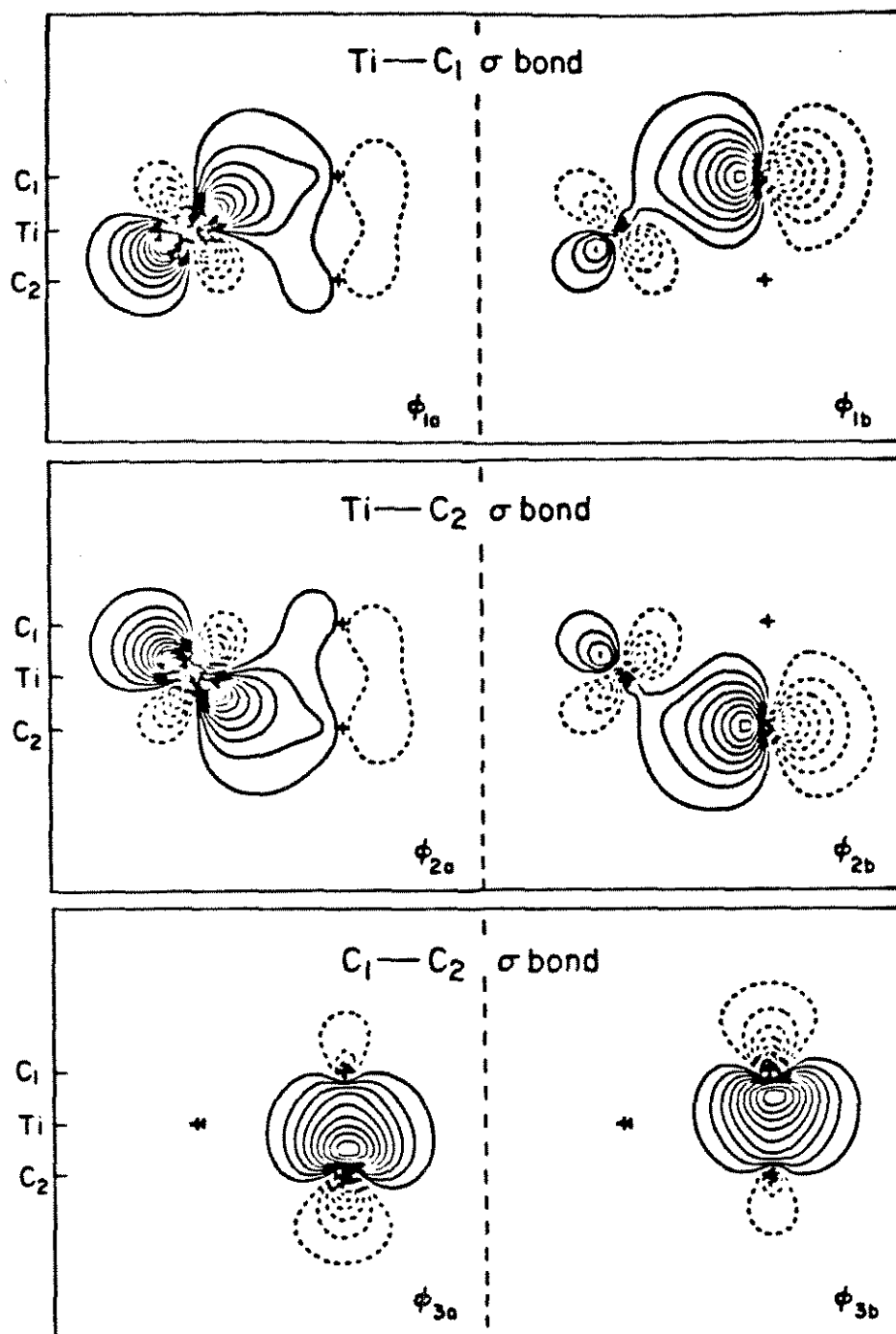
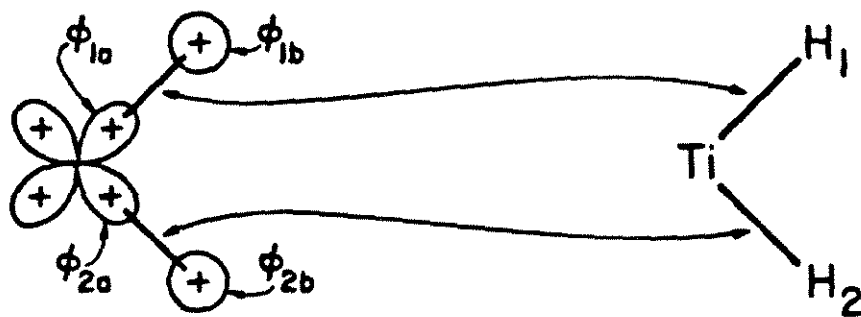
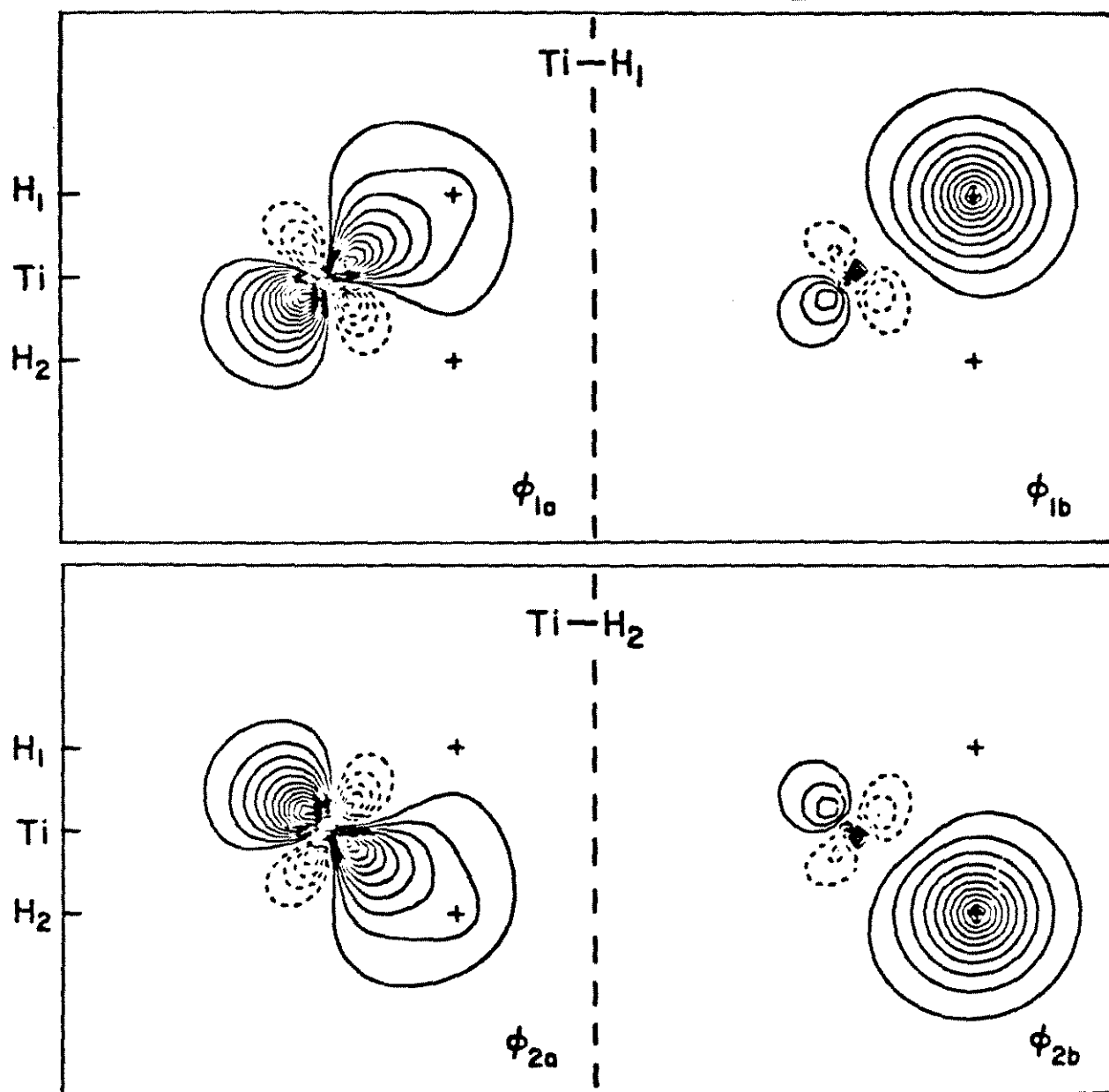


Figure 3. Plots of the two Ti-H bonds in Cl_2TiH_2 (ref 10). Spacing between contours is 0.05 a.u., and the characteristic dimension of the plots is 6.0 a_0 .

Ti-H bonds in Cl_2TiH_2 

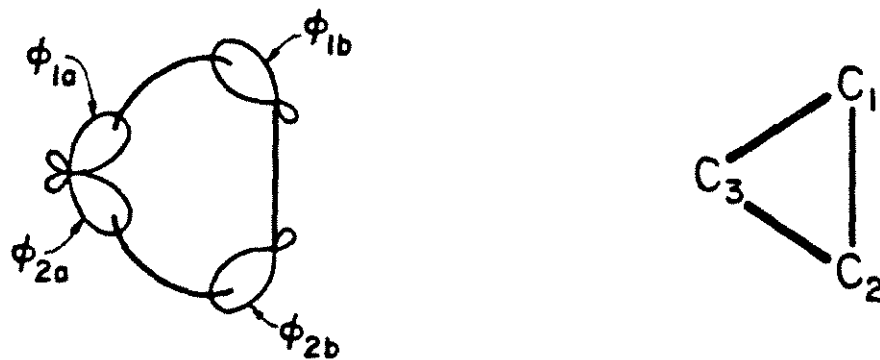
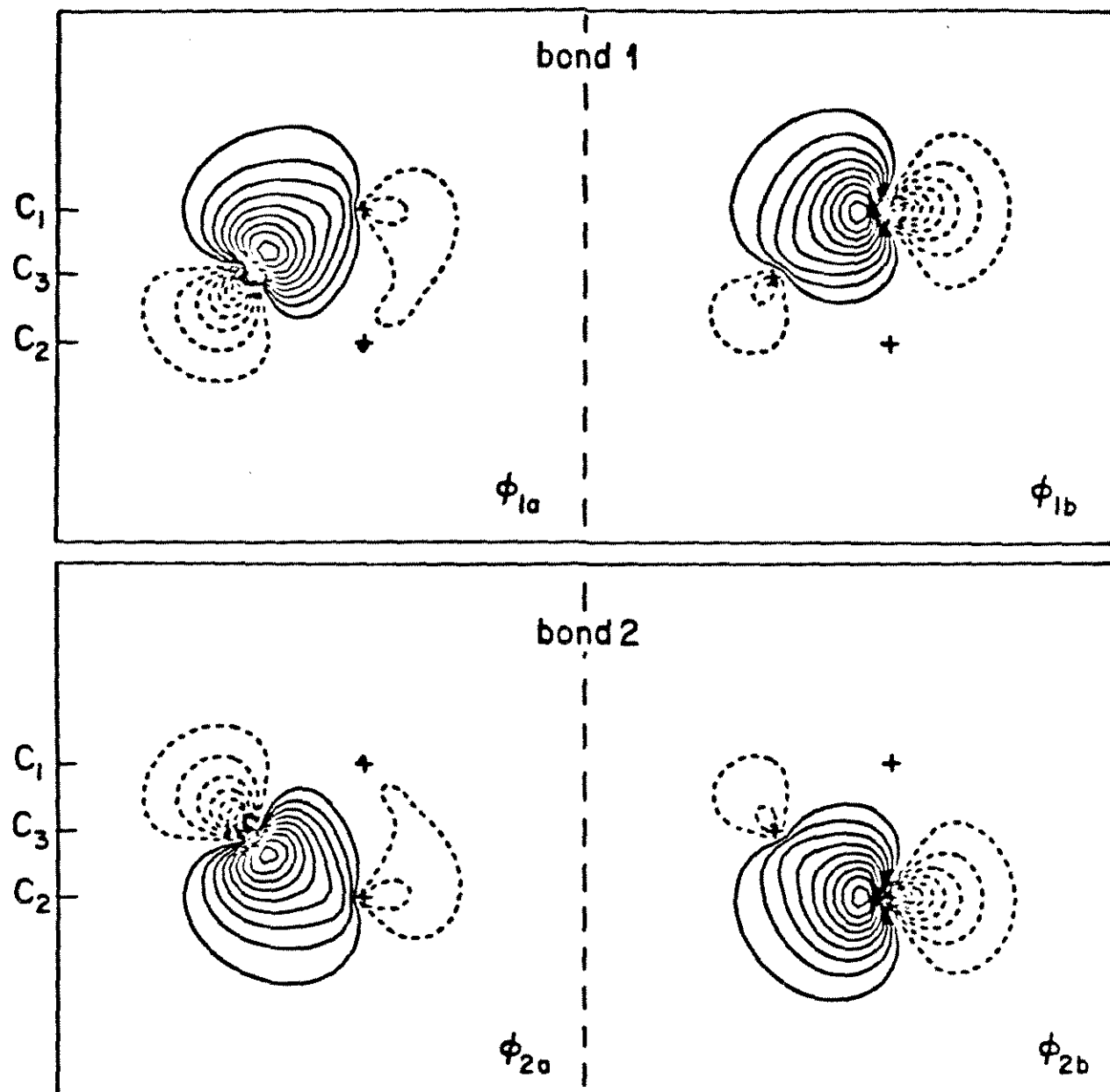
C-C σ bonds in cyclopropane

Figure 4. Plots of two of the C-C bonds in cyclopropane.

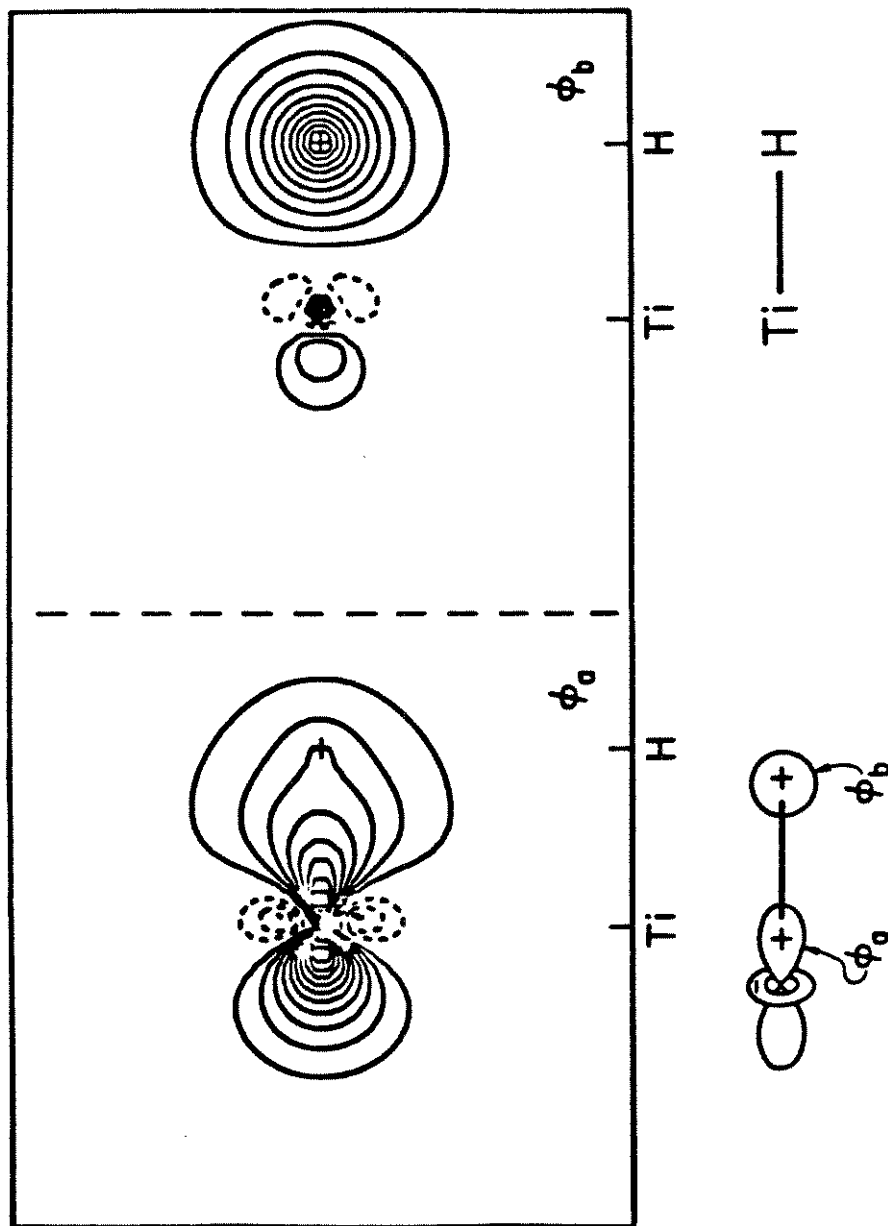
Ti-H σ bond in Cl_2TiH 

Figure 5. GVB orbitals describing the Ti-H bond in $\text{Cl}_2\text{Ti-H}$.

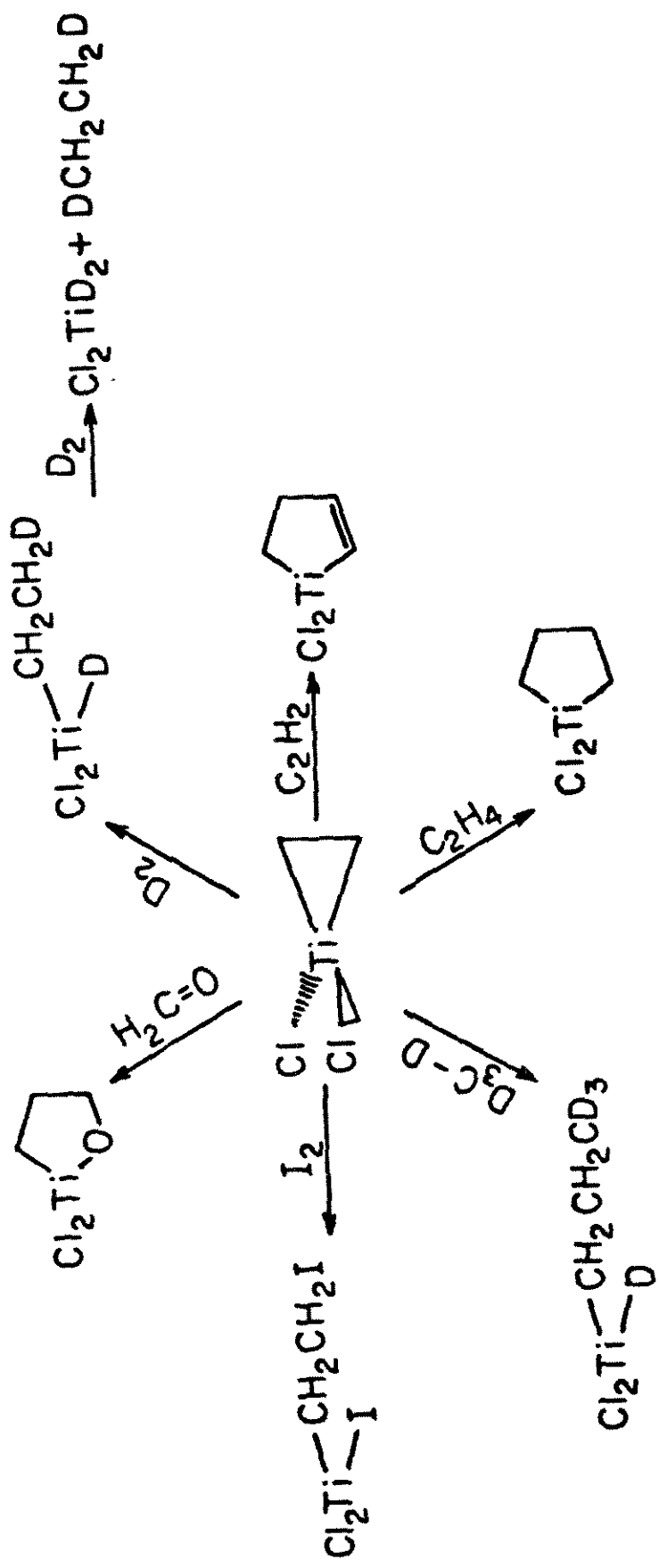
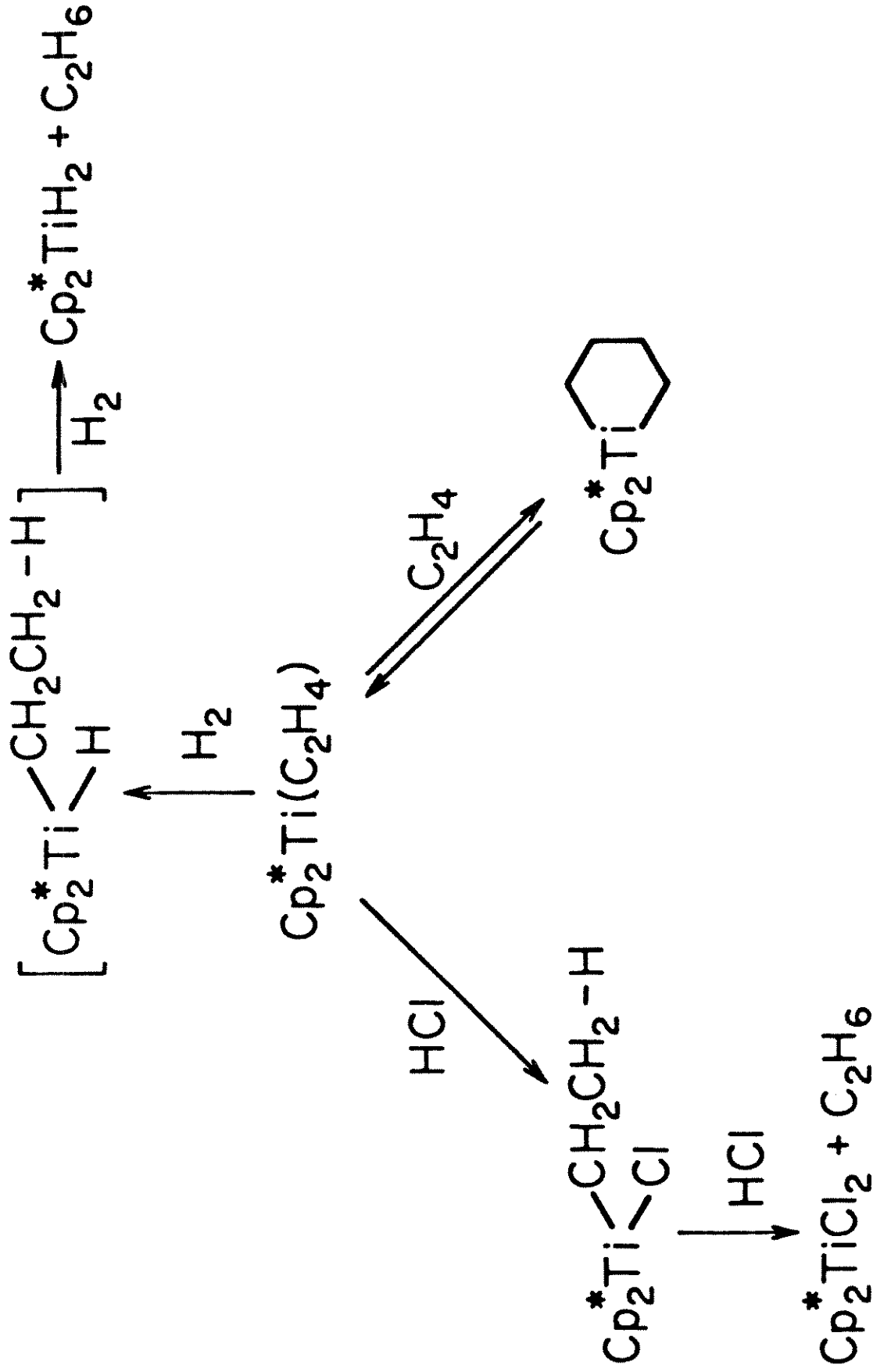


Figure 6. Expected reactions of dichlorotitanacyclopentane.

Figure 7. Observed reactions of $\text{Cp}_2^* \text{Ti}(\text{C}_2\text{H}_4)$ (ref 5b).

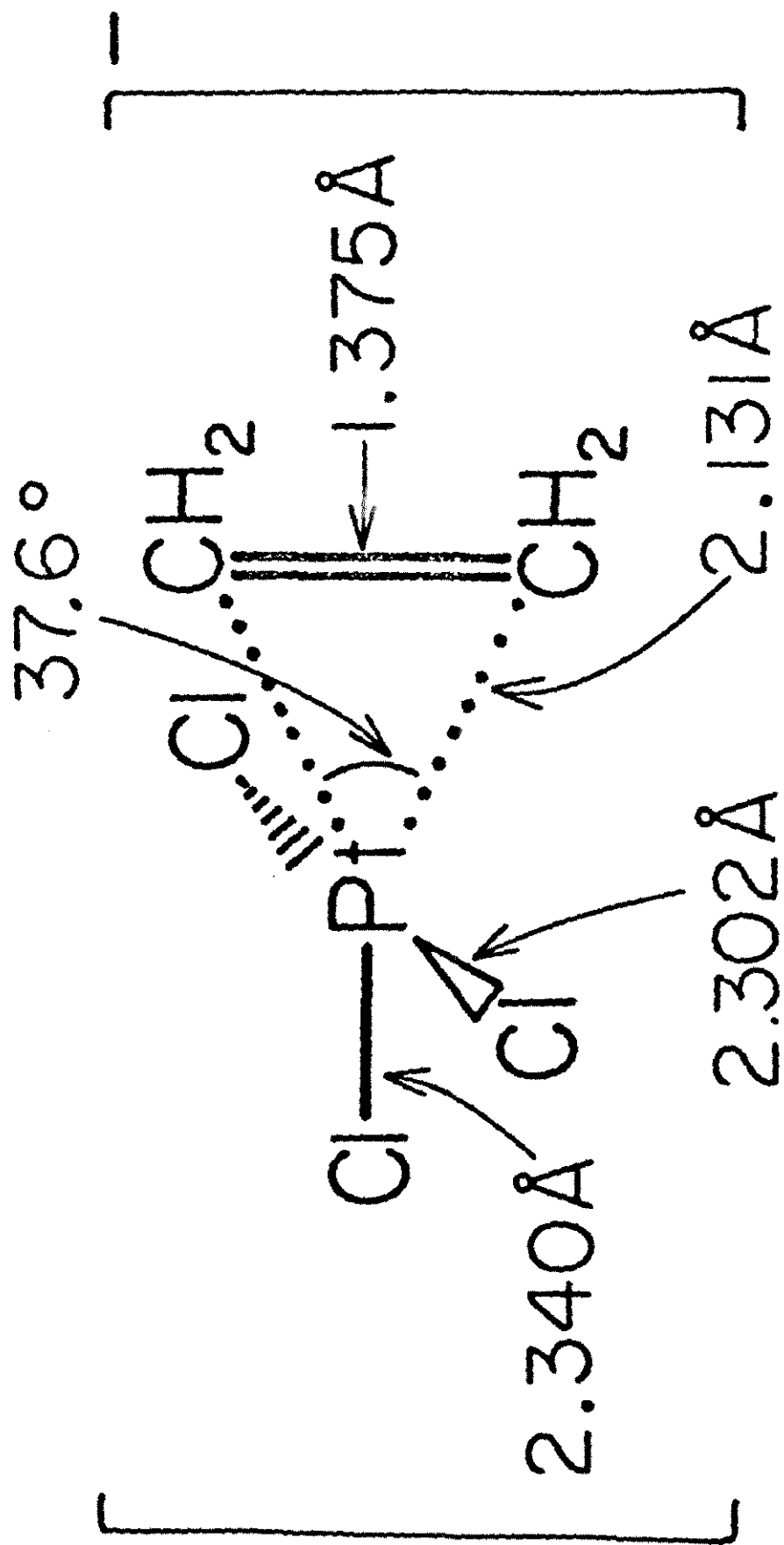
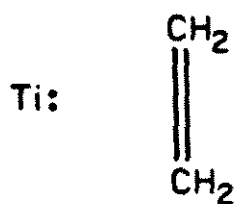
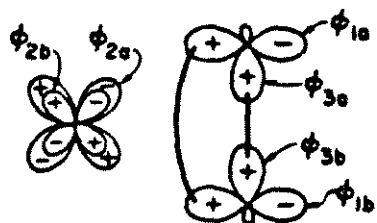
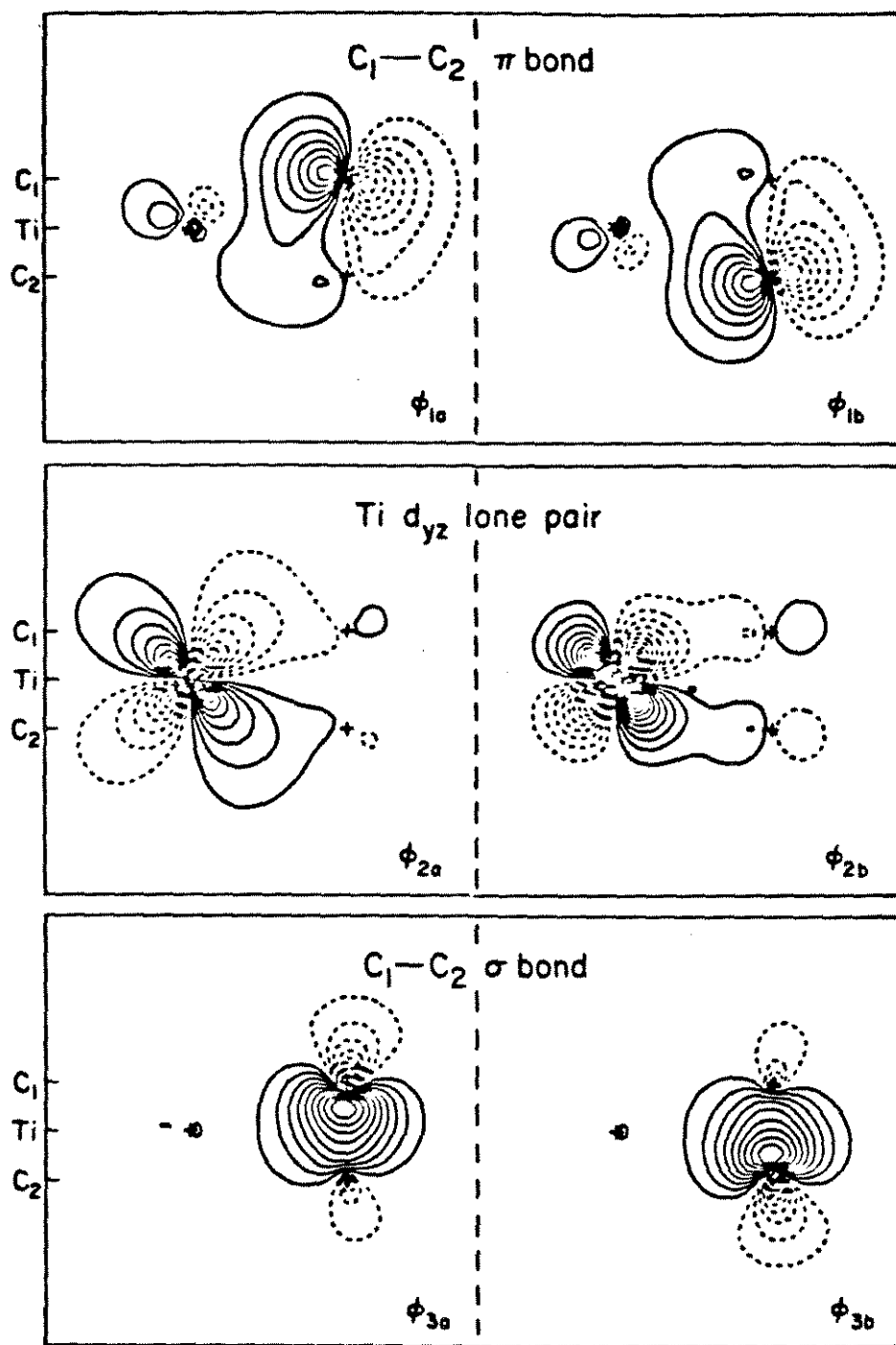


Figure 8. Structure of Zeise's salt (ref 14).

Figure 9. GVB orbitals describing the valence space of dichlorotitanium (ethylene). Spacing between the contours is 0.05 a.u., and the characteristic dimension of the plots is $6.0 a_0$.

Valence bonds in Ti- π complex

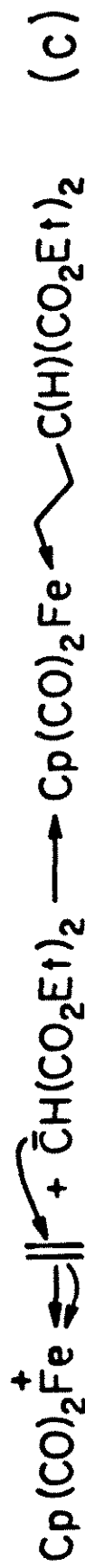
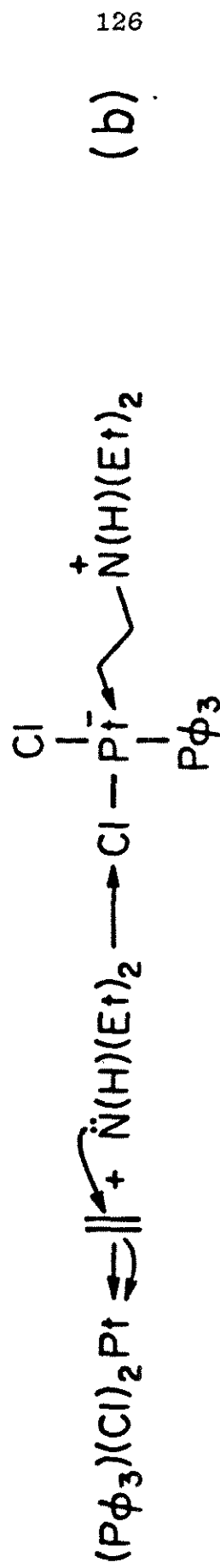
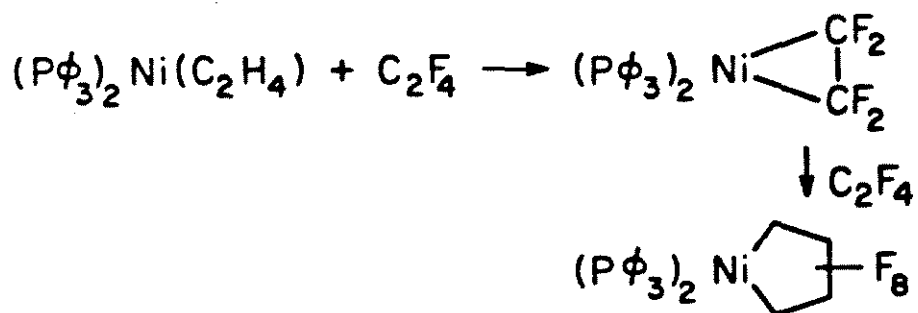
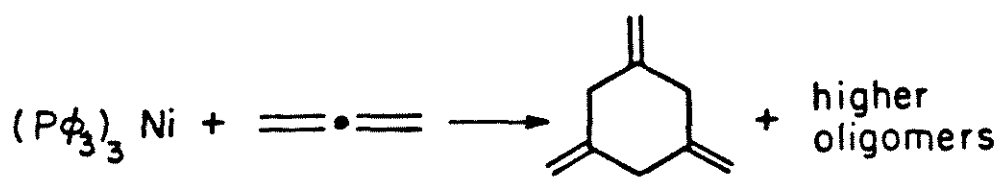
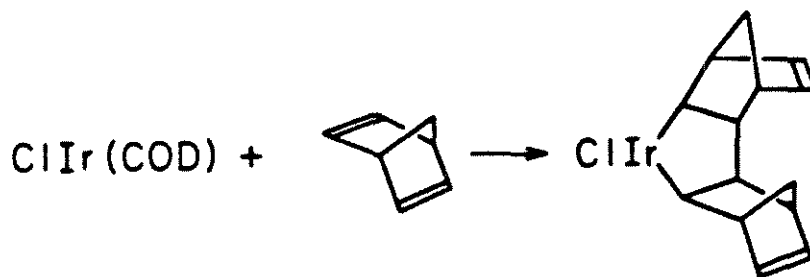
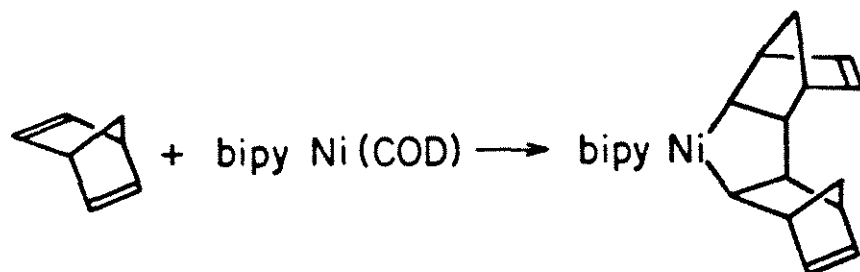
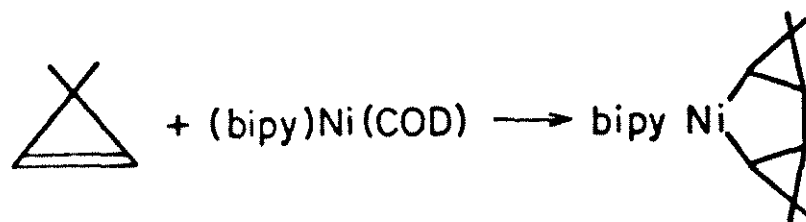
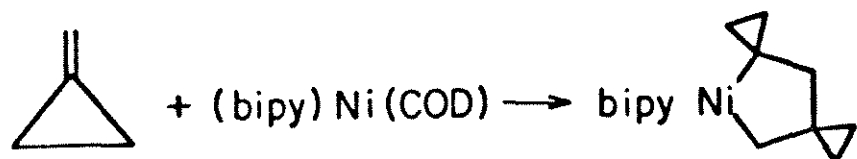


Figure 10. Some representative reactions of metal-olefin π complexes.

Figure 11. Some reaction of low-valent Group VIII metals with olefin having weak π bonds.



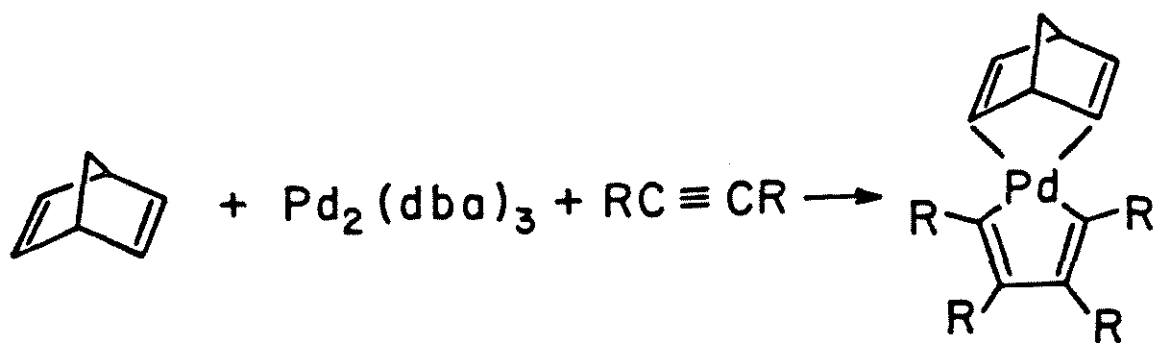
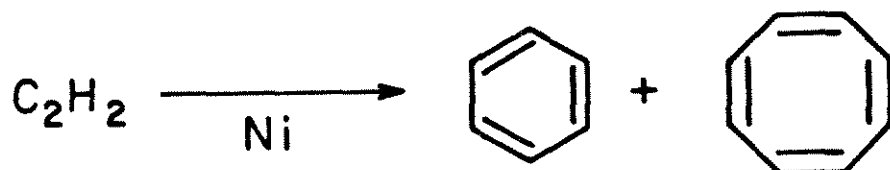
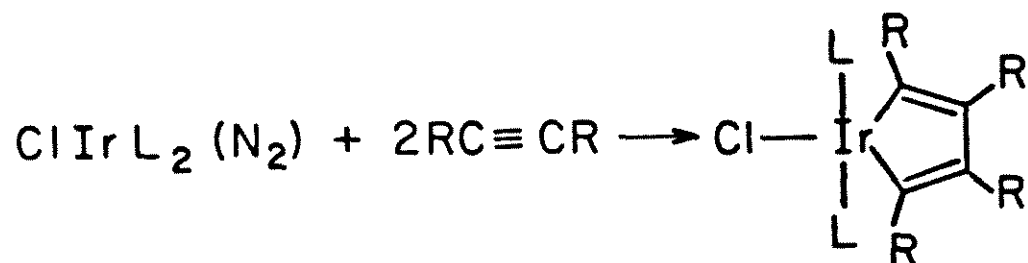
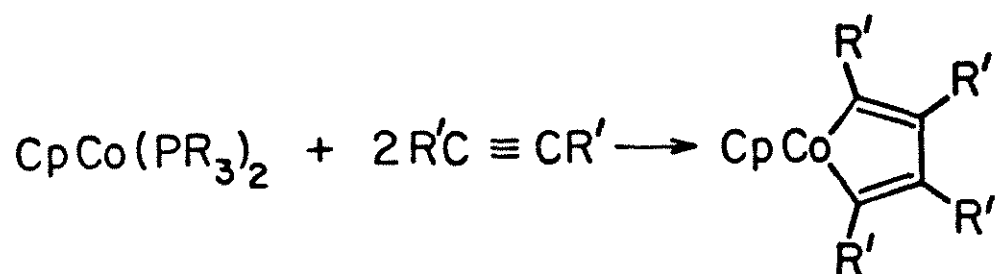
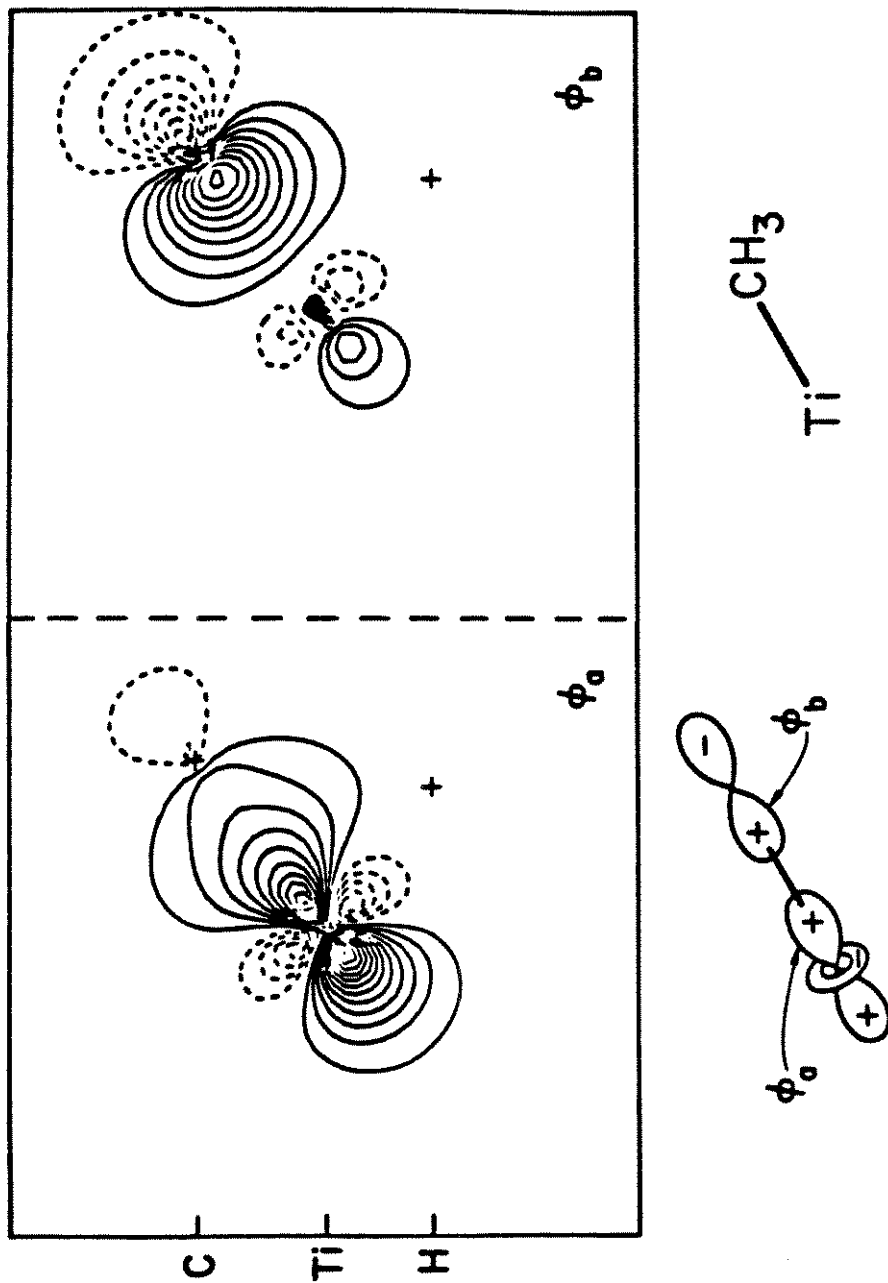


Figure 12. Some reactions of low-valent Group VIII metals with acetylenes.

Figure 13. GVB orbitals describing the Ti-C bond in $\text{Cl}_2\text{Ti}(\text{H})(\text{CH}_3)$. Spacing between the contours is 0.05 a.u., and the characteristic dimension of the plots is $6.0 a_0$.

Ti—C bond in $\text{Cl}_2\text{Ti}(\text{CH}_3)(\text{H})$ 

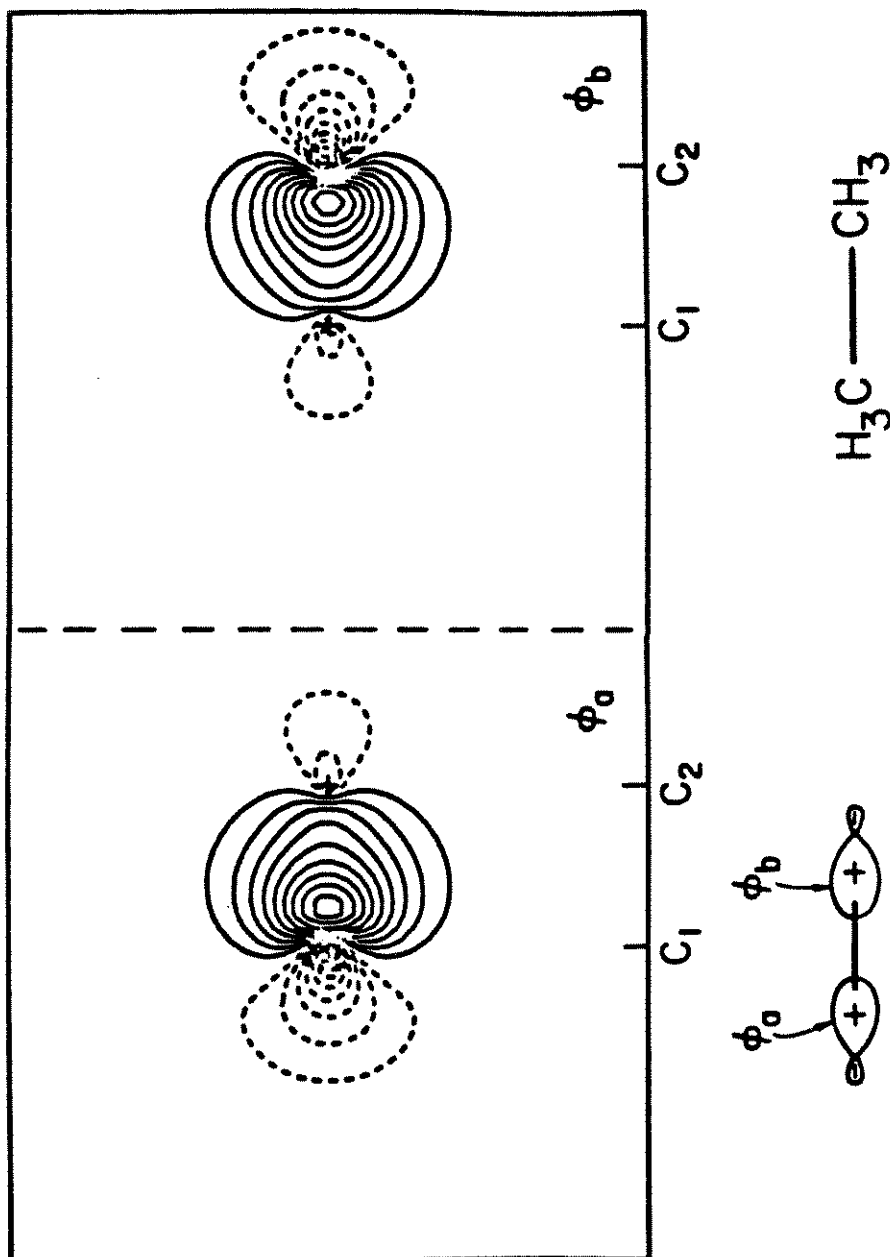
C—C σ bond in ethane

Figure 14. GVB orbitals describing the C-C bond in ethane.

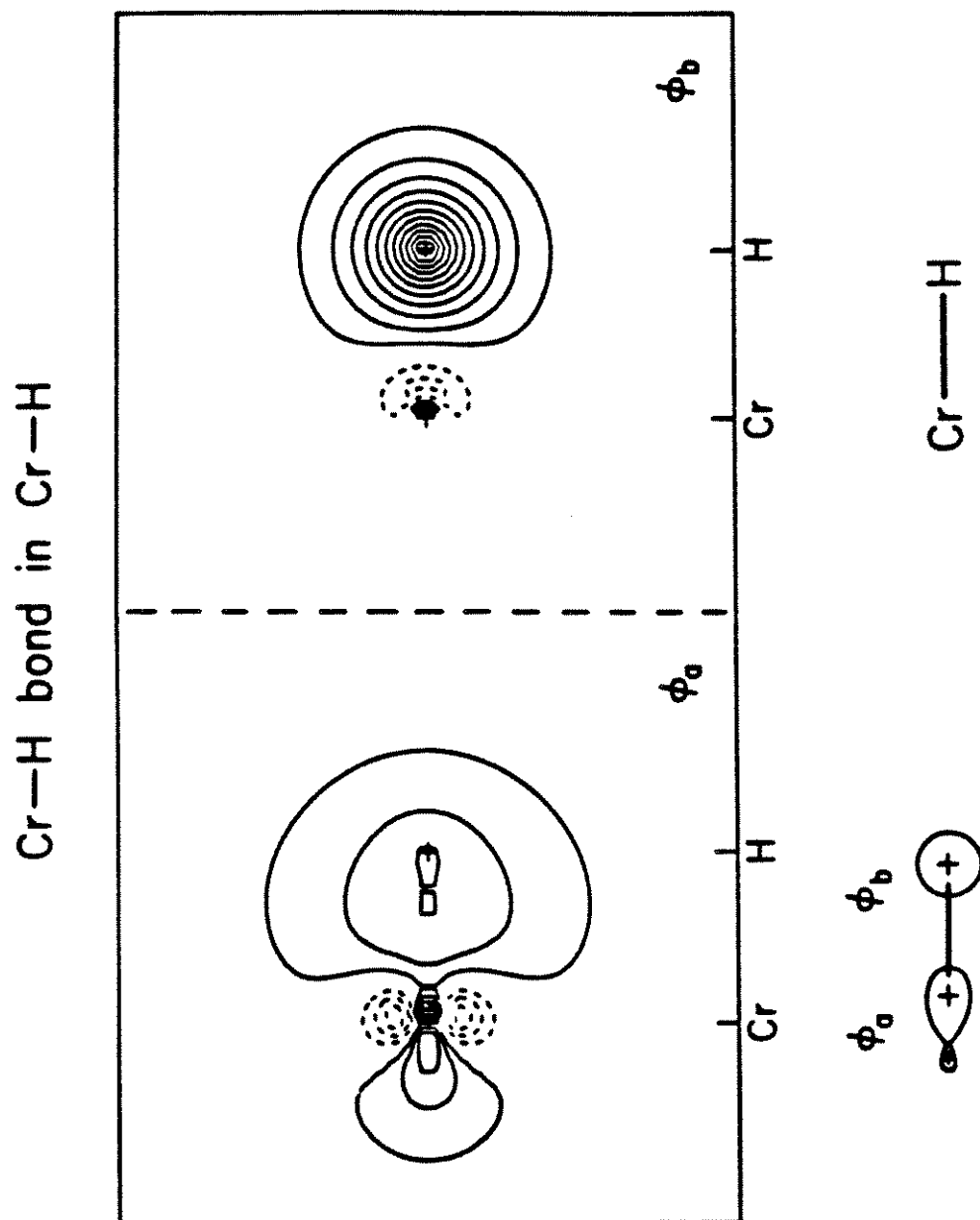
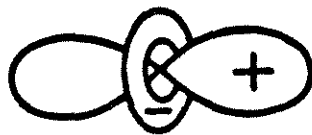
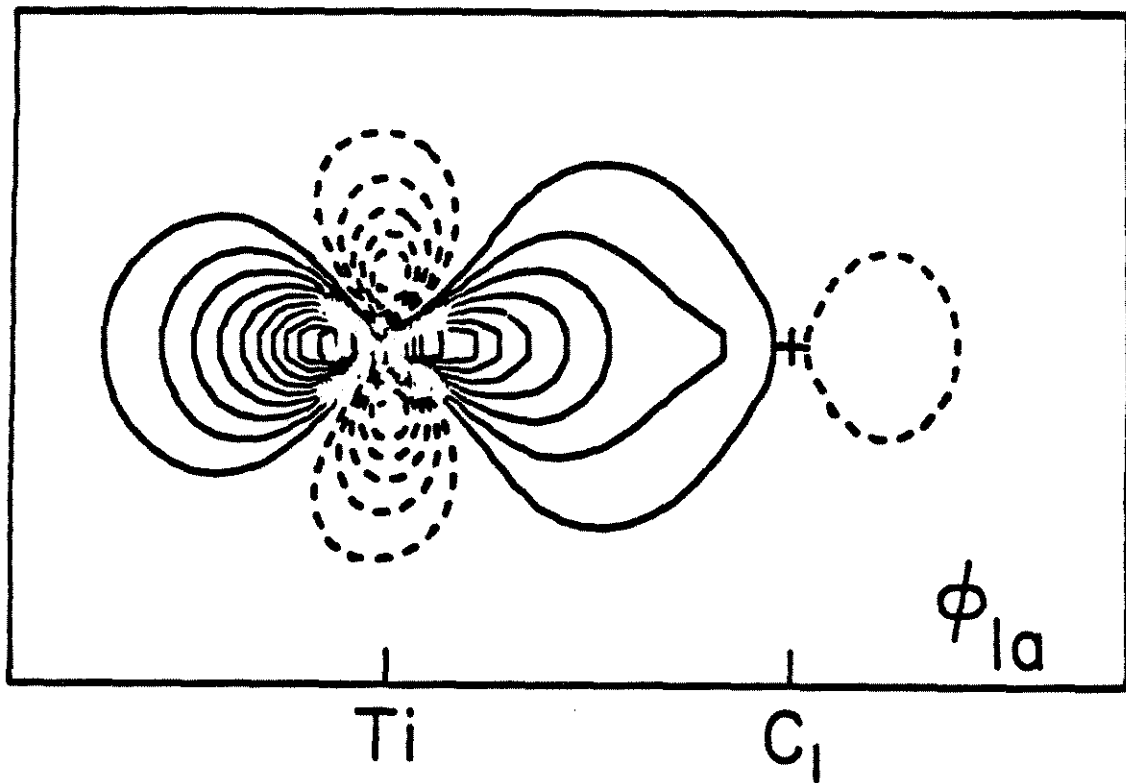


Figure 15. GVB orbitals describing the Cr-H bond in CrH.

Figure 16. Plot of the Ti-centered GVB orbital in the Ti-C σ bond in dichlorotitanacyclopropane. The plane of this plot is perpendicular to the plane of the Ti-C-C ring and contains the Ti and C atoms of the bond.



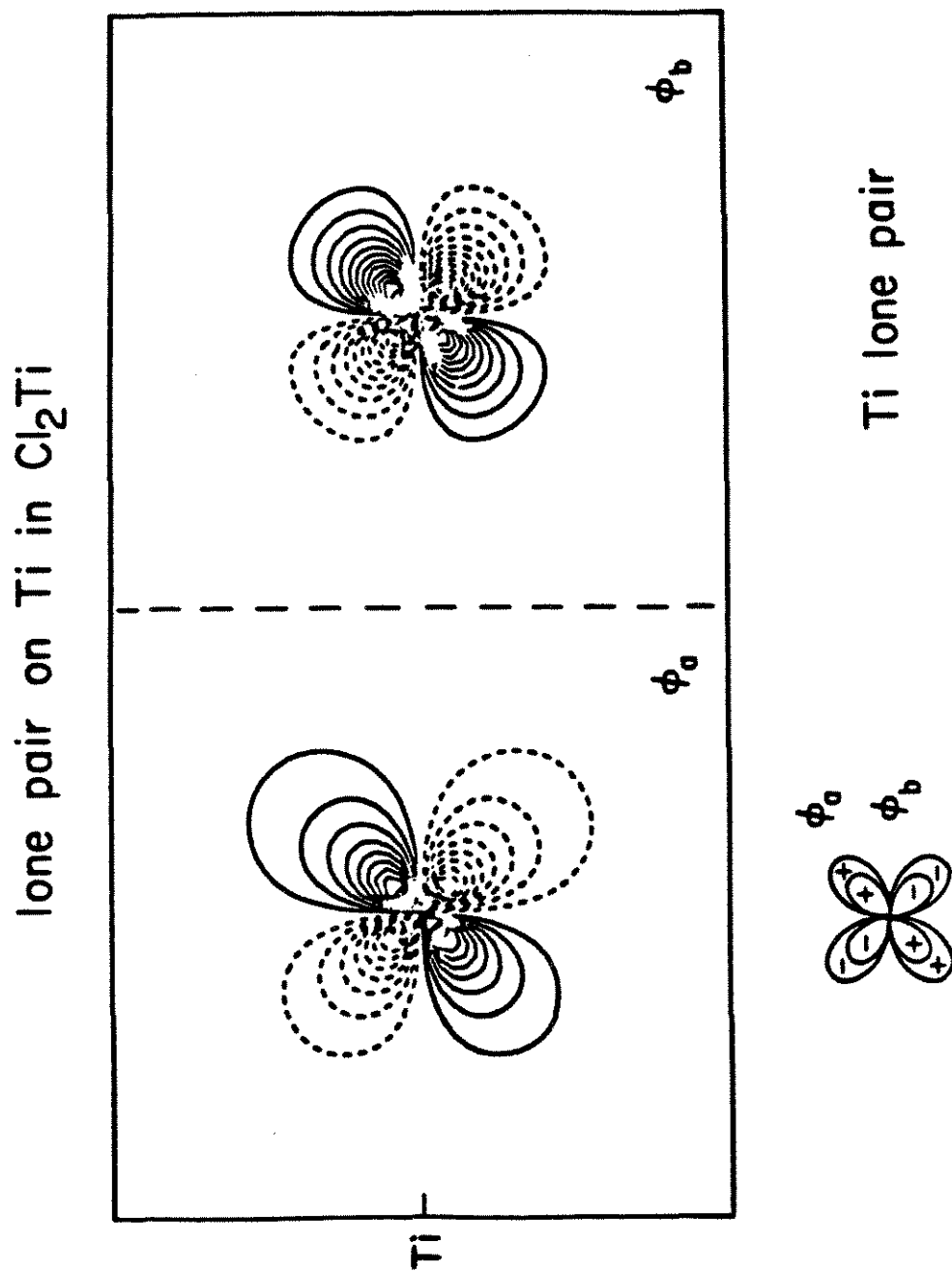
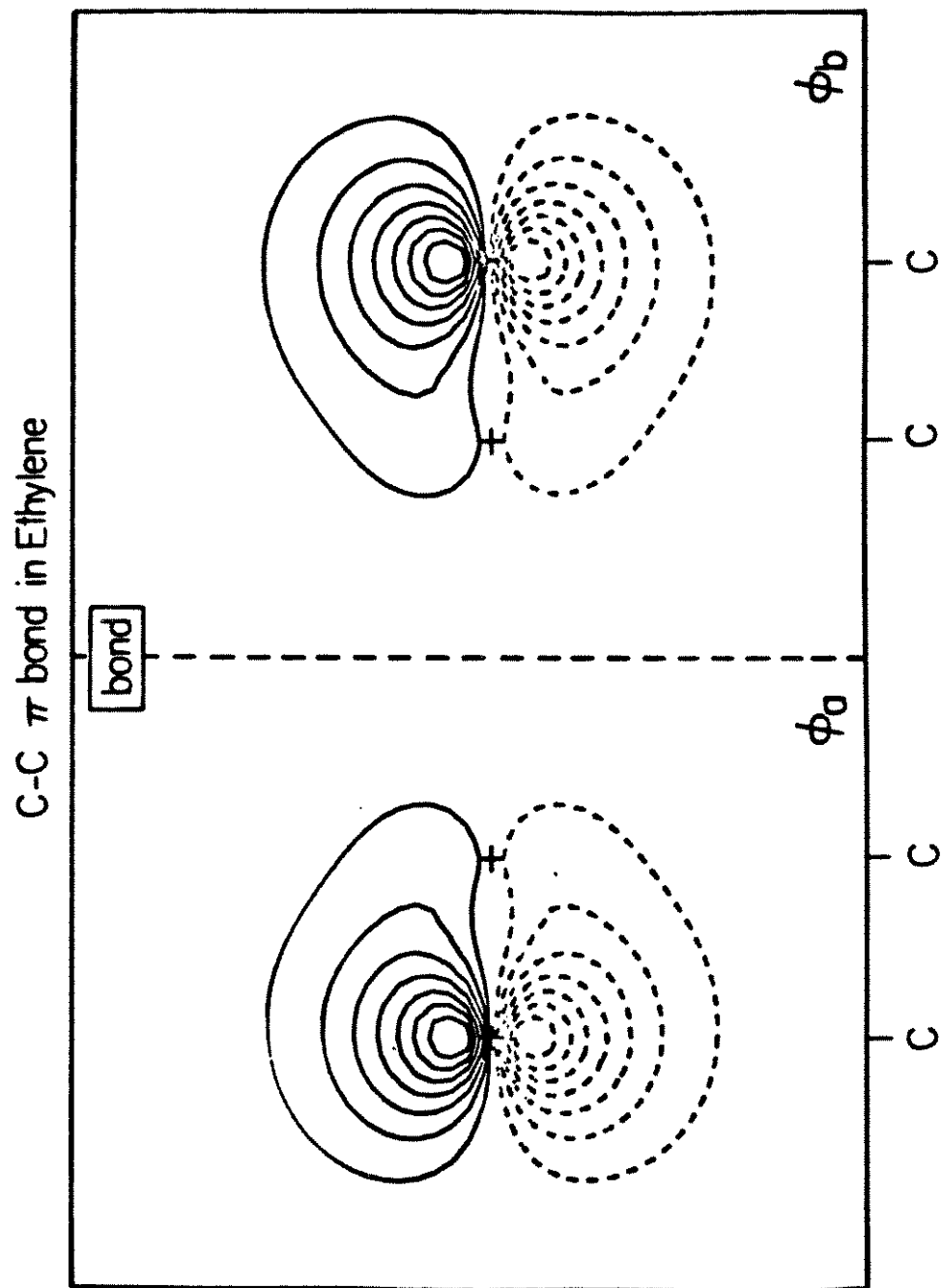


Figure 17. Lone pair on (bent) TiCl_2 .

Figure 18. GVB orbitals describing the π bond in ethylene. The spacing between the contours is 0.05 a.u., and the characteristic dimension of the plots is $6.0 a_0$.



References and Notes

- (1) (a) "Transition Metal Organometallic Chemistry in Organic Synthesis", H. Alper, Ed., Academic Press, New York, 1976, Vol. 1; (b) M. L. H. Green, "Organometallic Compounds. The Transition Elements", Chapman and Hall, London, 1968, Vol. 1, Chapter 1; (c) S. D. Ittel and J. A. Ibers, *Adv. Organomet. Chem.*, **14**, 33 (1976); (d) G. Henrici-Olive and S. Olive, "Coordination and Catalysis", Verlag Chemie, Weinheim, 1977; (e) J. P. Collman and L. S. Hegedus, "Principles and Applications of Organotransition Metal Chemistry", University Science Books, Mill Valley, California, 1980, Chapter 3.
- (2) See, for example, ref 1c, Chapter 12, and references therein.
- (3) (a) R. R. Schrock, S. McLain, and J. Sancho, *Pure Appl. Chem.*, **52**, 729 (1980); (b) G. Erber and K. Kropp, *J. Am. Chem. Soc.*, **101**, 3659 (1979); (c) D. R. McAlister, D. K. Erwin, and J. E. Bercaw, *ibid.*, **100**, 5966 (1978); (c) A. P. Fraser, P. H. Bird, S. A. Bezman, J. R. Shapley, R. White, and J. A. Osborn, *ibid.*, **95**, 597 (1973); (e) J. X. McDermott, M. E. Wilson, and G. M. Whitesides, *ibid.*, **98**, 6529 (1976).
- (4) The question of π complex versus metallacycle is not a new one. See (a) M. J. S. Dewar and G. P. Ford, *J. Am. Chem. Soc.*, **101**, 783 (1979); (b) T. A. Albright, R. Hoffmann, J. C. Thibeault, and D. L. Thorn, *ibid.*, **101**, 3801 (1979); (c) B. Åkermark, M. Almemarte, J. Almlöf, J.-E. Bäckvall, B. Roos, and Å. Stogå, *ibid.*, **99**, 4617 (1977).
- (5) (a) See ref 3(e); (b) S. A. Cohen, P. R. Auburn, and J. E. Bercaw, *J. Am. Chem. Soc.*, **105**, 1135 (1983); (c) S. A. Cohen, Ph.D. Thesis, California Institute of Technology (1982).

- (6) See, however, (a) F. D. Mango and J. H. Schachtschneider, *J. Am. Chem. Soc.*, **93**, 1123 (1971); (b) R. G. Pearson, "Symmetry Rules for Chemical Reactions", Wiley-Interscience, New York, 1976, p. 423; (c) J. W. Lauher and R. Hoffmann, *J. Am. Chem. Soc.*, **98**, 1729-1742 (1976).
- (7) Using $[EA(x) + \frac{1}{R(M-X)}] = \alpha(X)$ as a gauge of the propensity for X to form ionic bonds to M, and using $R(\text{Ti-Cp}) = 2.08 \text{ \AA}$ [G. Fachinetti, C. Floriani, F. Marchetti, and M. Mellini, *J. Chem. Soc., Dalton Trans.*, 1398 (1978)], $r(\text{Ti-Cl}) = 2.328 \text{ \AA}$ (this work), $EA(\text{Cl}) = 3.62 \text{ eV}$ [H. Hotop and W. C. Lineberger, *J. Phys. Chem. Ref. Data*, **4**, 539 (1975)], and $EA(\text{C}_5\text{H}_5) = 2.2 \text{ eV}$ [H. N. Rosenstock, K. Draxl, B. W. Steiner, and J. T. Herron, *ibid.*, **6**, 736 (1977)], one sees that $\alpha(\text{Cl}) = 9.8 \text{ eV}$ and $\alpha(\text{Cp}) = 9.1 \text{ eV}$. Thus the tendency of Cp and Cl to form ionic bonds is similar, and the gross features of the electronic structure of metal complexes with these ligands should be similar.
- (8) W. A. Goddard III, T. H. Dunning, Jr., W. J. Hunt, and P. J. Hay, *Acc. Chem. Res.*, **6**, 368-376 (1973).
- (9) S. W. Benson, "Thermochemical Kinetics", Wiley-Interscience, New York, 1976, Second Edition, p. 60.
- (10) A. K. Rappe' and W. A. Goddard III, *J. Am. Chem. Soc.*, **104**, 297 (1982).
- (11) This angle is measured from the plots shown in Figure 6 and is the angle between the lines of maximum amplitude of the two orbitals on the same center.
- (12) M. L. Steigerwald and W. A. Goddard III, *J. Am. Chem. Soc.*, in press.

- (14) R. A. Love, T.F. Koetzle, G. S. B. Williams, L. C. Andrews, and R. Bau, *Inorg. Chem.*, **14**, 2653 (1975).
- (15) R. B. Woodward and R. Hoffmann, "The Conservation of Orbital Symmetry", Verlag Chemie, Weinheim, 1971.
- (16) G. W. Parshall, "Homogeneous Catalysis", Wiley Interscience, New York, 1980, Chapter 6 and p. 25.
- (17) N. Belluco, "The Organometallic and Coordination Chemistry of Platinum", Academic Press, New York, 1974, p. 374.
- (18) M. Rosenblum, *Acc. Chem. Res.*, **7**, 122 (1974).
- (19) (a) K. Jonas, K. R. Pörschke, C. Krüger, and Y.-H. Tsay, *Angew. Chem. Int. Ed. Engl.*, **15**, 621 (1976); (b) P. W. Jolly and G. Wilke, "The Organic Chemistry of Nickel", Academic Press, New York, 1974, Vol. 1.
- (20) (a) K. Jonas, L. Schieferstein, C. Krüger, and Y.-H. Tsay, *Angew. Chem. Int. Ed. Engl.*, **18**, 550 (1979); (b) A. Carbonaro, A. Greco, and G. Dall'asta, *J. Organomet. Chem.*, **20**, 177-186 (1969).
- (21) K. Jonas, *Adv. Organomet. Chem.*, **19**, 97 (1981).
- (22) P.-T. Cheng, C. D. Cook, S. C. Nyburg, and K. Y. Wan, *Inorg. Chem.*, **10**, 2210 (1971).
- (23) (a) E. Uhlig and D. Walther, *Coord. Chem. Rev.*, **33**, 3 (1980); (b) Reference 17, p. 465.
- (24) (a) K. Kitaura, S. Sakati, and K. Morokuma, *Inorg. Chem.*, **20**, 2292 (1981); (b) K. Jonas and C. Krüger, *Angew. Chem. Int. Ed. Engl.*, **19**, 520 (1980); (c) T. H. Upton and W. A. Goddard III, *J. Am. Chem. Soc.*, **100**, 321 (1978).

- (25) (a) P.-T. Cheng, C. D. Cook, C. H. Koo, S. C. Nyburg, and M. T. Shiomi, *Acta Crystallogr., Sect. B*, **27**, 1909 (1971); (b) W. Dreissig and H. Dietrich, *Acta Crystallogr., Sect. B*, **24**, 108 (1968).
- (26) (a) L. Pauling, "The Nature of the Chemical Bond", Cornell University Press, Ithaca, New York, 1960, Third Edition; (b) G. W. Wheland, "Resonance in Organic Chemistry", Wiley & Sons, New York, 1955; (c) C. A. Russell, "The History of Valence", Leichestor University Press, Leichestor, United Kingdom, 1971.
- (27) Calculations performed using the method reported by A. F. Voter and W. A. Goddard III, *Chem. Phys.*, **57**, 253 (1981).
- (28) (a) H. O. House, "Modern Synthetic Reactions", W. A. Benjamin Co., Menlo Park, California, 1972, Second Edition, pp. 520-530; (b) J. March, "Advanced Organic Chemistry: Reactions, Mechanisms and Structure", McGraw-Hill, New York, 1968, Chapter 2.
- (29) Reference 26(b), Chapter 8, especially §8.2.
- (30) (a) C. J. Balhausen, "Introduction to Ligand Field Theory", McGraw-Hill, New York, 1962; (b) C. E. Moore, "Atomic Energy Levels", National Bureau of Standards Reference Data Series, NBS 35, U. S. Government Printing Office, Washington, DC, 1971.
- (31) Reference 1(e), p. 109.
- (32) (a) M. J. Doyle, M. McMeeking, and P. Binger, *J. Am. Chem. Soc., Chem. Commun.*, 376 (1976); (b) P. Binger, M. J. Doyle, J. McMeeking, C. Krüger, and Y.-H. Tsay, *J. Organomet. Chem.*, **135**, 405 (1977); (c) P. Binger and M. J. Doyle, *ibid.*, **162**, 195 (1978); (d) R. J. DePasquale, *ibid.*, **32**, *J. Chem. Soc., Dalton Trans.*, 2491 (1973).

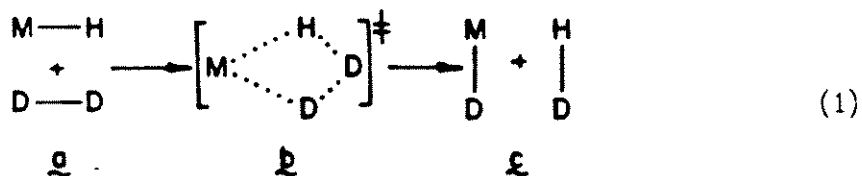
- (33) J. Ashley-Smith, M. Green, and F. G. A. Stone, *J. Chem. Soc. (A)*, 3019 (1969).
- (34) Reference 9, p. 106.
- (35) C. F. Fischer, "The Hartree-Fock Method for Atoms", Wiley & Sons, New York, 1977.
- (36) (a) K. Clauss and H. Bestian, *Justus Liebigs Ann. Chem.*, **654**, 8 (1962); (b) H. Sinn and W. Kaminsky, *Adv. Organomet. Chem.*, **18**, 99 (1980).
- (37) (a) Y. Wakatsuki, T. Kiramitsu, and H. Yamazaki, *Tetrahedron Lett.*, 4549 (1974); (b) J. P. Collman, *Acc. Chem. Res.*, **1**, 136 (1968); (c) P. W. Jolly and G. Wilke, "The Organic Chemistry of Nickel", Academic Press, New York, 1974, Vol. II, Chapter II; (d) H. Suzuki, K. Itoh, Y. Ishii, K. Simon, and J. A. Ibers, *J. Am. Chem. Soc.*, **98**, 8494 (1976).
- (38) (a) Reference 1(e), p. 108; (b) J. L. Thomas, *Inorg. Chem.*, **17**, 1507 (1978); (c) J. L. Thomas, *J. Am. Chem. Soc.*, **95**, 1838 (1973); (d) H. Hoberg, D. Schaefer, and G. Burkhardt, *J. Organomet. Chem.*, **228**, C21 (1982); (e) M. Kadonaga, N. Yasuoka, and N. Kasai, *J. Chem. Soc., Chem. Commun.*, 1597 (1971); (f) R. J. DePasquale, *J. Organomet. Chem.*, **32**, 381 (1971).
- (39) The Ti basis set is from A. K. Rappe', T. A. Smedley, and W. A. Goddard III, *J. Phys. Chem.*, **85**, 2607 (1981). The carbon and hydrogen (scaled, double zeta) basis sets can be found in T. H. Dunning, Jr., and P. J. Hay, in "Modern Theoretical Chemistry: Methods of Electronic Structure Theory", H. F. Schaefer, III, Ed., Plenum Press, New York, 1977, Vol. 3, and references therein.

- (40) (a) W. A. Goddard III and A. K. Rappe', in "Potential Energy Surfaces and Dynamics Calculations", D. G. Truhlar, Ed., Plenum Press, New York, 1981, pp. 661-684; (b) A. K. Rappe', T. A. Smedley, and W. A. Goddard III, *J. Phys. Chem.*, **85**, 1662 (1981).
- (41) P. C. Wailes, R. S. P. Coutts, and H. Weingold, "Organometallic Chemistry of Titanium, Zirconium, and Hafnium", Academic Press, New York, 1974, Chapter III.
- (42) This is the overlap of the two GVB orbitals describing the H-H bond in H₂.
- (43) Geometry of this species taken from "Landolt-Börnstein Numerical Data and Functional Relationships in Science and Technology. Group II, Volume 7, Structure Data of Free Polyatomic Molecules", K.-H. Hellwege, Ed., Springer Verlag, Berlin, 1976.
- (44) For these model calculations we kept the Cl₂Ti fragment frozen, assigned $r(\text{Ti-H}) = 1.70 \text{ \AA}$ (ref 12), $r(\text{Ti-C}) = 2.02 \text{ \AA}$ (ref 10), and $\angle(\text{C-Ti-H}) = 75^\circ$ (ref 10).
- (45) $r(\text{Ti-Cl}) = 2.328 \text{ \AA}$ and $\angle(\text{Cl-Ti-Cl}) = 140^\circ$.
- (46) The geometry of this diatomic was taken from K. P. Huber and G. Herzberg, "Molecular Spectra and Molecular Structure. IV. Constants of Diatomic Molecules", Van Nostrand Reinhold Co., New York, 1979. The value $r(\text{Cr-H}) = 1.655 \text{ \AA}$ was used. See also S. P. Walch and C. W. Bauschlicher, Jr., *J. Chem. Phys.*, **78**, 4597 (1983).
- (47) M. L. Steigerwald and W. A. Goddard III, *Organometallics*, to be submitted.

Chapter 4. Reactions of D_2 with Cl_2ZrH

I. Introduction

In the first paper of this series¹ (Paper I), we showed that suprafacial 2 + 2 reactions such as 1



are allowed (i.e., proceed with low activation barriers) if the M-H bond of the reactant "hydride" is a covalent (nonpolar) bond between the two centers and if this bond involves mostly d orbital character on M. We compared three reactions (1, M = Cl₂Ti⁺, Cl₂Ti, and Cl₂Sc) of hydrides of transition metals of the first series and showed that the activation barrier for these allowed reactions varied in an understandable way. In the second paper of the series,² we presented the main-group counterpoint, indicating that in one case (reaction 1, M = H₂B) valence p orbitals on M could afford sufficient stability to the MH₂ transition state to allow the *nonpolar* 2_s + 2_s reaction to occur but that, in general, *polar* transition states are found in these reactions that cannot take advantage of valence d orbitals on M. In this report we extend our studies to transition metals of the second series and show that in the case of zirconium (reaction 1, M = Cl₂Zr) the reaction is again allowed, that it proceeds through a *nonpolar* transition state, and that the difference in activation barrier between strictly analogous titanium- and zirconium-centered reactions can be related to fundamental differences between the titanium and zirconium atoms.

II. Results

We have calculated the activation barrier for the reaction of Cl_2ZrH with D_2 (reaction 1, $\text{M} = \text{Cl}_2\text{Zr}$). These calculations were based on the generalized valence bond (GVB) technique,³ using the method described in Paper I. The geometries of Cl_2ZrH and the transition state $\text{Cl}_2\text{Zr(H)(D)}_2$ were optimized, and the optimum geometries are reported in Tables I and II. Included for comparison are the geometries optimized previously for Cl_2TiH and $\text{Cl}_2\text{Ti(H)(D)}_2$ (reaction 1, $\text{M} = \text{Cl}_2\text{Ti}$).

The reaction at zirconium is 4.3 kcal/mol lower in energy than the reaction at titanium. In Table III we list activation barriers and Mulliken population data for the two reactions. These data show that the two reactions are similar not only in their low activation energies but also in the nonpolarity of their transition states. Thus, in general terms, zirconium responds just as scandium and titanium: the $2_s + 2_s$ reaction is a "direct hydrogen transfer"⁴ as opposed to the "hydride transfer", which is characteristic of the alkali metal hydrides.²

In Figure 1 we show plots of the four *one-electron* GVB orbitals,⁵ which are active in the $\text{Cl}_2\text{ZrH} + \text{D}_2$ reaction. Just as in the case of $\text{Cl}_2\text{TiH} + \text{D}_2$, the active orbitals here are seen to delocalize to form two three-center, two-electron bonds in the transition state. Bond 1 starts the reaction as the D-D bond, becomes the $\text{H} \cdots \text{D} \cdots \text{D}$ three-center bond at the transition state and completes the reaction as the new H-D bond. Bond 2 starts the reaction as the Zr-H bond, delocalizes to form the *unspiegel*⁶ $\text{H} \cdots \text{Zr} \cdots \text{D}$ three-center bond at the transition state and subsequently *relocalizes* to form the new Zr-D bond in the product. For comparison we show the corresponding set of active orbitals for the $\text{Cl}_2\text{TiH} + \text{D}_2$ reaction in Figure 2. This corroborates the conceptual similar-

ity of the two reactions.

There is a fifth "pseudo-active" electron in each of these two reactions since Cl_2TiH and Cl_2ZrH (and the related transition states) are radicals. In each case this unpaired electron is in an orbital that must remain orthogonal to the bonds that are in motion during the reaction. In Figure 3 we display the orbitals that contain the unpaired electron in the reactants and transition states for each reaction. In Table IV we show how the energies of these orbitals change during the reaction. The plots in Figure 3 show that the singly-occupied orbital in both Cl_2ZrH and Cl_2TiH is in the plane of the four-center reaction. Since the orthogonalization of this orbital to the orbitals of the reaction is not obviated by symmetry, it is possible that it will raise the activation barrier for the pericyclic reaction.

In order to understand the difference in activation barriers between the two reactions, we have studied Cl_2ZrH_2 and Cl_2TiH_2 .⁷ In Table V we compare the optimum geometries for the two molecules and include Mulliken population data that indicate the M-H bonds are not significantly polar toward hydrogen in either case. The fact that these M-H bonds should *not* be viewed as hydridic⁸ is highlighted by the orbital descriptions of these bonds, which are given in Figures 4 and 5.

III. Discussion

The outstanding difference between the titanium and zirconium atoms is that the valence s and valence d orbitals are closer in size in zirconium than in titanium⁹ (Figure 6). This is simply due to the requirement that the 4d orbitals in zirconium be orthogonal to the closed shell of 3d orbitals, while the 3d orbitals of titanium have no such core orbitals to avoid. This orthogonality requirement forces the incorporation of a radial node in the 4d orbitals of zirconium, resulting in their increased size. Since this requirement applies to the valence d orbitals of atoms in both the second and third transition series, d orbitals in atoms of the first series may be thought of as being undersized in the same way that the valence p orbitals are undersized in atoms of the first (main group) row of the periodic table.^{9,10} Since there is such a disparity in relative sizes, the energy of the 4s orbital on titanium is quite high (3.1 eV)¹¹ *vis-à-vis* the 3d orbitals, while in zirconium the energies of the 5s and 4d orbitals are close by comparison (1.8 eV).¹¹ In Table VI we report s and d ionization potentials for the two atoms, showing the 70 kcal/mol energetic separation of 3d and 4s in titanium and the 40 kcal/mol separation of 4d and 5s in zirconium.

In cases such as titanium, in which there are two atomic orbitals in the valence region of an atom that are of markedly different energy, the more electronegative "one-electron" ligands will use the orbital that is the higher in energy of the two, leaving the lower energy orbital to be used by the less electronegative ligands. This effect can be traced to the polarity of the M-X bond. The greater the electronegativity of X, the more important the M^+X^- component is in the description of the bond. This ionic component will be lower in energy when the orbital on M, which is

ionized, is lower in energy. Thus, the greater electronegativity of X will result in the greater tendency of X to bond to the more easily ionized orbital.^{10a} Thus, in Cl_2TiH_2 , the chlorine ligands bond preferentially to the 4s orbital on titanium, while the hydrogen atoms bond to the 3d orbitals that remain. This is to be distinguished from the case of Cl_2ZrH_2 in which there is less discrepancy in the natures of the Zr-Cl and Zr-H bonds. Hence, while the titanium-centered orbital of the Ti-H bond in Cl_2TiH_2 is 74% Ti-d, the corresponding zirconium orbital in Cl_2ZrH_2 is only 58% Zr-d¹² (in each case the remainder of the orbital is metallic valence s and p in character). Stated in other terms, the energetic closeness of the zirconium 5s and 4d orbitals allows s/d hybridization to occur more freely (in Pauling's terms, the promotion energy is smaller¹³).

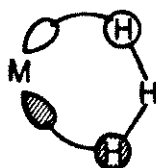
One result of this free mixing is the larger H-M-H angle in Cl_2ZrH_2 than in Cl_2TiH_2 . This may be rationalized by noting that simplest valence bond ideas predict that the angle between two covalent σ bonds to two d orbitals on the same metal will be 54.74° (or 125.26°)^{7,14} (ignoring steric effects and electron correlation). Similarly, the angle between two σ bonds to two s^1p^1 hybrid orbitals in the same metal is predicted to be 180° .^{10a} In the limit of no sp-d hybridization (and ignoring steric and correlation effects), the Cl-M-Cl angle in Cl_2MH_2 (M = Ti, Zr) is thus predicted to be 180° and the H-M-H angle 54.74° (or 125.26°). Increased sp-d hybridization will lead to four bonds that are more equivalent and a concomitant tendency of the bond angles toward the tetrahedral average.

The energetic disparity between valence s and valence d also has an effect on the electronic structure of Cl_2MH . The metal-centered orbital in the Ti-H bond in Cl_2TiH is 65% d, while the corresponding orbital in the zirconium case is only 52% d.¹² Interestingly, the singly-occupied orbital in

Cl_2TiH is 94% d, while the zirconium-centered singly-occupied orbital is only 74% d. This further evinces the ease of s-p-d hybridization in Zr and the energetic difficulty of this in the case of Ti.

In Paper I we asserted that the $2_s + 2_s$ reaction, 1, would be lower in energy for the M-H bonds, which are more d-like on the metal. Here we present a case that violates that prescription. The reaction at Cl_2ZrH is lower in energy than the reaction at Cl_2TiH , even though the Zr-H bond has less d character than the Ti-H bond (Table I). The simple rule postulated in Paper I must be amended to account for the fact that an atom such as zirconium is able to form strong bonds with its valence d orbitals as well as with its valence s and p orbitals. In the discussion in Paper I, it was *assumed* that the removal of metallic s and p components of the M-H bond when the M-H₃ bond was formed would be energetically quite costly. This was due to our belief that "d" bonds are intrinsically weaker than "s" bonds. This appears to be not so much the case with transition metals of the second row, owing to the similarity in radial extent of the s and d orbitals. In the case of titanium, the overlap of the atomic 4s orbital with a 1s orbital on a hydrogen atom 1.7 Å¹⁵ away is 0.444, and the overlap of an atomic 3d_{z²} orbital with that same hydrogen 1s orbital is 0.199.¹⁶ In the case of zirconium, the overlap of the atomic 5s orbital with the 1s orbital on a hydrogen atom is 1.87 Å¹⁷ away is 0.402, while that of the atomic 4d_{z²} is 0.304. Thus, the zirconium valence d orbitals are expected to bond to "one-electron ligands" as effectively as the valence s.¹⁸

In Paper II, we proposed that the barrier for reaction 1 depended on the ability of M to form an "unspiegel"⁶ bond with the H₃ radical. This bond is drawn schematically in (2).



(2)

In this structure, the two fragments of the transition state (M and H_3) are held together by a bond between the antisymmetric (unspiegel) one-electron orbital on M and the *delocalized* and antisymmetric (unspiegel) orbital on H_3 . Thus we showed that the activation barrier for reaction 1 could be dissected into its components, one of which is the ability of the unspiegel orbital on M to form strong π bonds. Comparison of Figures 1 and 2 and the overlaps in Tables I and III bespeaks the greater ability of zirconium than titanium to form such π bonds. This is because the antisymmetric (unspiegel) zirconium 4d orbital that mediates the M- H_3 bond is larger (in proportion) than the corresponding orbital in $Cl_2Ti(H)(D)_2$. This provides for greater overlap of the two orbitals of the $H \cdots M \cdots D$ bond in the zirconium reaction than in the titanium reaction, and this in turn leads to a lower activation barrier. In this way, even though more s and p character is quenched from the Zr-H bond at the $Cl_2Zr(H)(D)_2$ transition state, the comparable strengths of the Zr "s" and "d" bonds makes the activation barrier for the zirconium-mediated $2_s + 2_2$ reaction lower.

The unpaired electron on M (Table IV and Figure 3) has less effect on reaction 1 for $M = Cl_2Zr$ than for $M = Cl_2Ti$, as evidenced by the changes in orbital energies. Apparently, in neither case is the orthogonalization of this orbital to the incoming D_2 unit energetically prohibitive.

IV. Conclusion

In this paper we have shown that

- 1) the suprafacial $2 + 2$ reaction between Cl_2ZrH and D_2 is allowed and proceeds with an activation barrier lower than that for the corresponding reaction at Cl_2TiH ;
- 2) this lower activation barrier is due to the greater ability of Cl_2Zr than Cl_2Ti to form an *unspiegel* " π -bond" with H_3 ; and
- 3) this ability is due to the greater radial extent of the Zr (4d) orbital than the Ti (3d) orbital.

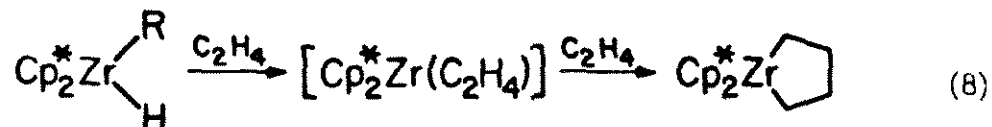
We have also shown that the s-to-d rehybridization about zirconium, which is necessary for the process of the $2_s + 2_s$ reaction is low in energy because the valence s and d orbitals on Zr are close in size,⁹ energy,¹¹ and in their ability to overlap the bonding orbitals of a one-electron ligand such as H.

We have also shown that the Zr-H bond in Cl_2ZrH is quite similar to the Zr-H bond in Cl_2ZrH_2 , and that the singly-occupied orbital on zirconium in Cl_2ZrH is not severely affected during the $2_2 + 2_s$ reaction. Given these data, we suggest that these results [reactions of Cl_2ZrH , an example of "organometallic" Zr(III)] can be used in the analysis of the reactions of the "organometallic" reactions of Zr(IV) complexes.¹⁹

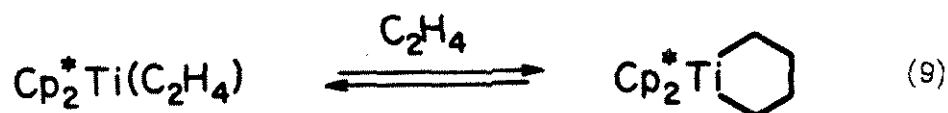
Reactions of Zr(IV) complexes with H_2 (D_2) have been observed by Bercaw [(3)²⁰ and (4)²¹] and Schwartz [(5)²²].

(3)

Finally, we believe that these results can be extended to the description of the reaction shown in (8)²¹



In Paper III of this series,²⁵ we described the electronic structure of $\overline{\text{Cl}_2\text{Ti}-\text{CH}_2-\text{CH}_2}$, indicating the strain in the metallacyclopropane ring. We claimed that the reaction shown in (9)²⁶



should be viewed as a ring-expanding migratory insertion reaction that is pushed by this strain. We suggest that the same mechanism is operative in the zirconium case (8). Owing to the greater radial extent of the valence d orbitals on zirconium, the ethylene complex of Cp_2^*Zr is even more likely to be a metallacyclopropane than is the ethylene complex of Cp_2^*Ti .

Appendix: Details of the Calculations

These calculations were performed at the fully ab initio level.²⁷ All electrons were included in the calculations save the ten core electrons on each chlorine. These electrons were replaced by an ab initio effective potential.²⁸ The valence electrons on chlorine were described by a minimal basis set that was optimized for molecular environments.²⁹ This basis emphasizes the chloride character of these ligands. The metals were described by valence double zeta basis sets,³⁰ and the hydrogen atoms by a triple zeta set.³¹ The geometries of the two titanium species involved in the 2 + 2 reaction were described in Paper I. The geometry of the Cl_2ZrH_2 molecule was optimized in a point-by-point fashion using GVB(2/4) wavefunctions in which the two Zr-H bonds were described by pairs of GVB orbitals.³² The geometry of Cl_2ZrH was optimized at the GVB(1/2) level,³³ keeping the Cl_2Zr fragment fixed at that of the Cl_2ZrH_2 molecule. The geometry of the $\text{Cl}_2\text{Zr(H)(D)}_2$ molecule was optimized at the HF level in a point-by-point way.

The height of the activation barrier for the $2_s + 2_s$ reaction (ΔE in Table III) was determined by the method described in Paper I. In Table VII we report the final total energies for the species pertinent to reaction 1.

Table I. Geometries of Cl_2MH .^{a, b}

Molecule	r(M-Cl)	r(M-H)	$\theta(\text{Cl-M-Cl})$	Mulliken Populations in M-H Bond Pair		
				M (valence d)	M (valence s and p)	H
Cl_2ZrH	(2.450 Å)	1.901 Å	(127.2°)	0.55	0.43	1.03
Cl_2TiH	(2.328 Å)	1.70 Å	(140°)	0.70	0.37	0.87

^a Values in parentheses were fixed at those from Cl_2MH_2 . Other parameters were optimized using a GVB(1/2) wavefunction.

^b Both molecules were found to be planar.

Table II. Geometries of $\text{Cl}_2\text{M} \begin{array}{c} \text{H} \\ \theta \\ \alpha \\ \text{D} \end{array}$. ^{a, b}

Molecule	r_1	r_2	θ	α
$\text{Cl}_2\text{Zr}(\text{H})(\text{D})_2$	2.008 Å	1.032 Å	60.2°	155°
$\text{Cl}_2\text{Ti}(\text{H})(\text{D})_2$	1.8459 Å	1.0284 Å	65°	148°

^a The geometry of the Cl_2M fragment was fixed at that of the Cl_2MH_2 molecule.

^b C_{2v} symmetry was assumed for both complexes.

Table III.



M	ΔE (kcal/mol)	Mulliken Populations					GVB Pair Overlaps	
		Transition State D...M...H Bond			Total on hydrogen in MH_2		sym	antisym
		s	p	d	terminal	central		
Zr	17.4	0.0	0.12	0.60	1.02	0.86	0.85	0.80
Ti	21.7	0.0	0.11	0.72	0.93	0.82	0.84	0.70

Table IV. Orbital Energies of Singly-Occupied Orbitals.^a

Molecule	Orbital Energy of Singly-Occupied Orbital (hartree)
Cl ₂ ZrH	-0.3857
Cl ₂ TiH	-0.5314
Cl ₂ Zr(H)(D) ₂	-0.3718
Cl ₂ Ti(H)(D) ₂	-0.5153

^a All values are results of GVB(1/2) or GVB(2/4) calculations.

Table V. Cl_2MH_2 .^a

M	Geometry			
	r(M-H)	r(M-Cl)	$\theta(\text{Cl-M-Cl})$	$\theta(\text{H-M-H})$
Zr	1.86 Å	2.450 Å	127.2°	102.1°
Ti	1.70 Å	2.328 Å	142°	74.9°

^a Reference 31.

Table VI. Ionization Potentials of Zr and Ti Atoms. ^{a, b}

Ionization	Energy	Δ (= "d" IP - "s" IP)
Zr [³ F; (5s) ² (4d) ²] \rightarrow Zr ⁺ [4F; (5s)(4d) ²]	6.95 eV	39.7 kcal/mol
\rightarrow Zr ⁺ [² D; (5s) ² (4d)]	8.67 eV	
Ti [³ F; (4s) ² (3d) ²] \rightarrow Ti ⁺ [4F; (4s)(3d) ²]	6.86 eV	70.3 kcal/mol
\rightarrow Ti ⁺ [² D; (4s) ² (3d)]	9.91 eV	

^a Quantities averaged over J states.

^b From ref 11.

Table VII. Total Energies.

A. Cl_2MH		Total Energy (hartree)	
M	HF	GVB(1/2)	GVB(1/2)-RCI * single excitations
Zr	-4455.32441	-4455.34308	-4455.34474
Ti	-1767.095723	-1767.12376	-1767.12784

B. $\text{Cl}_2\text{M(H)(D)}_2$			
Zr	-4456.42531	-4456.44556	-4456.46519
Ti	---	-1768.21804	-1768.24138

Figure 1. GVB orbitals active in the reaction of Cl_2ZrH with D_2 . (i) Reactants. (ii) Transition state. (iii) Products. The separation between adjacent contours is 0.05 a.u., and the dimension of each plot is 6 a.u.

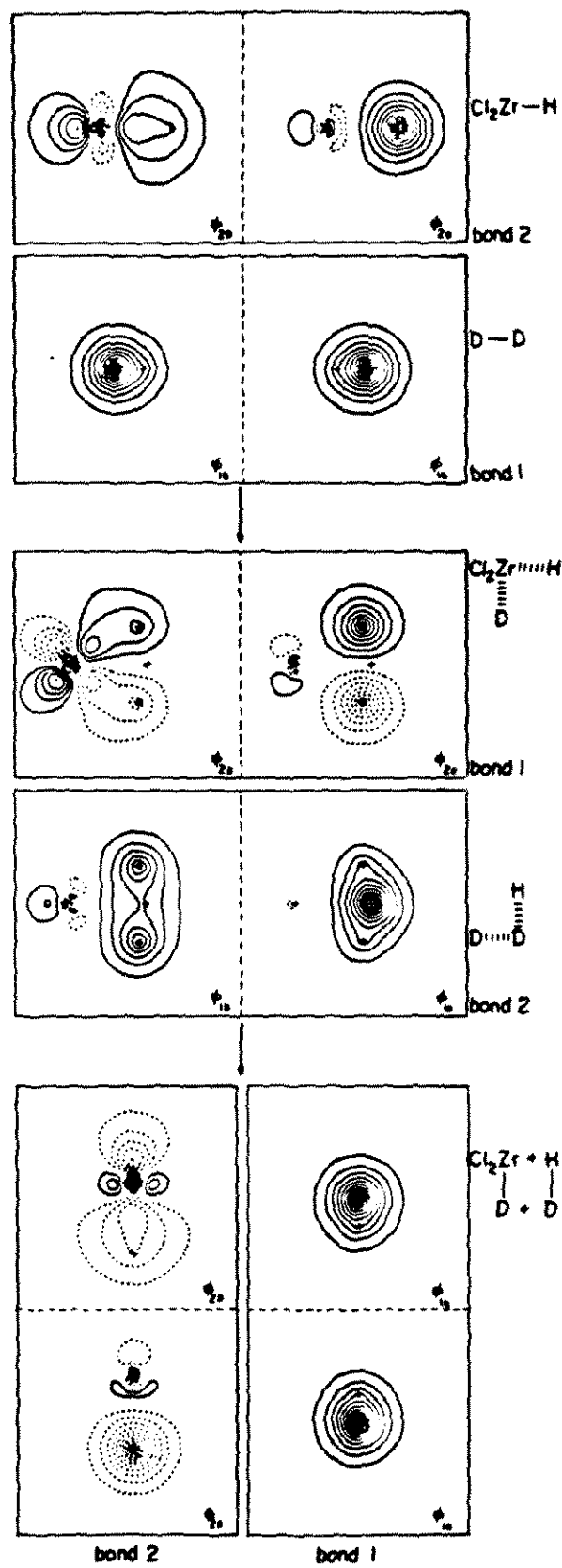


Figure 2. GVB orbitals active in the reaction of Cl_2TiH with D_2 . (i) Reactants. (ii) Transition state. (iii) Products. The separation between adjacent contours is 0.05 a.u., and the dimension of each plot is 6 a.u.

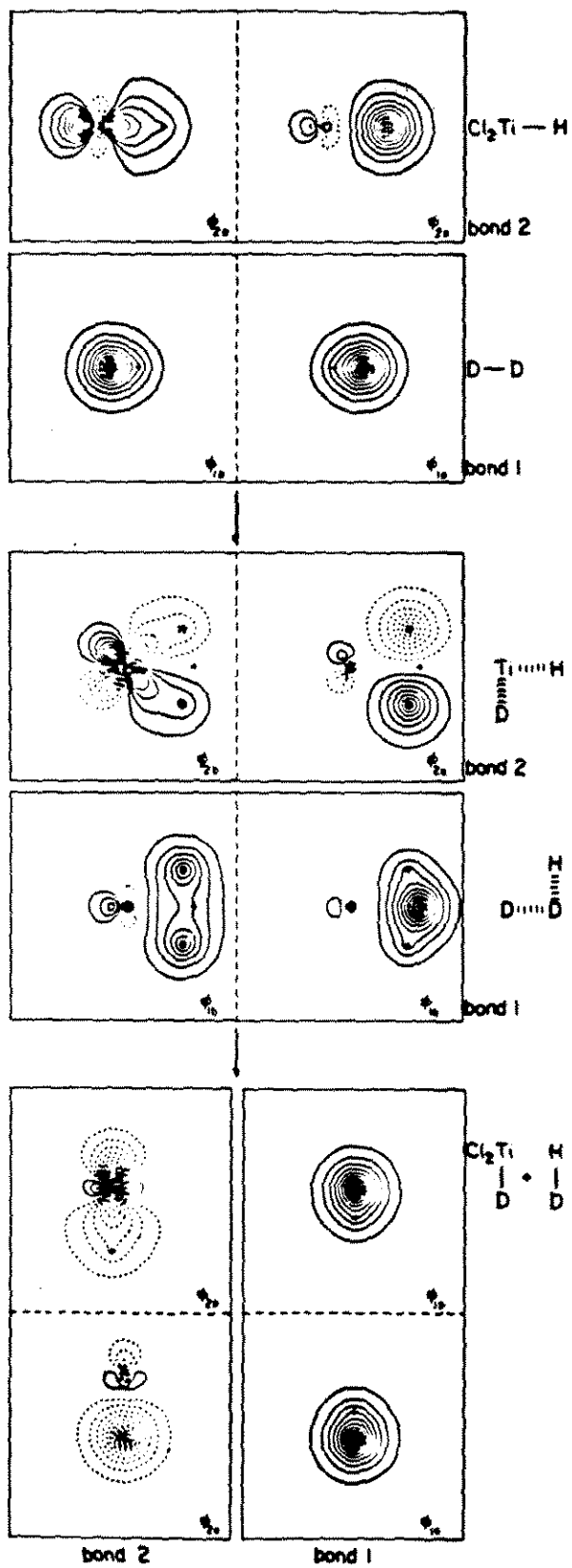


Figure 3. Plots of the singly-occupied orbitals in Cl_2ZrH , Cl_2ZrH_3 , Cl_2TiH , and Cl_2TiH_3 . The separation between adjacent contours is 0.05 a.u., and the dimension of each plot is 6 a.u.

Singly - Occupied Orbitals

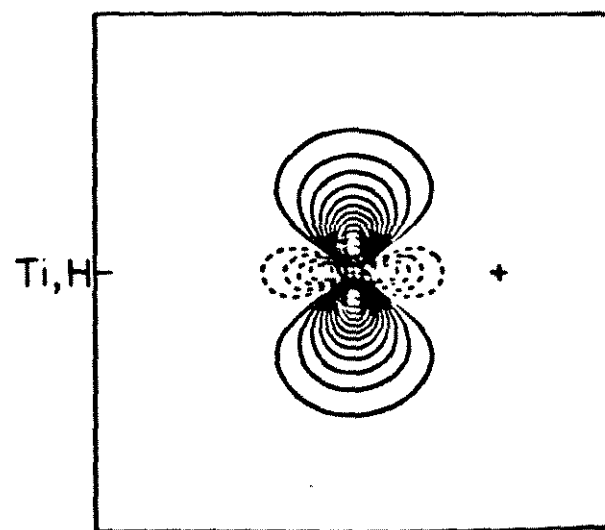
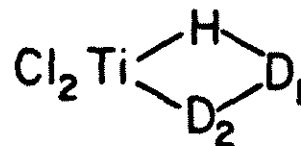
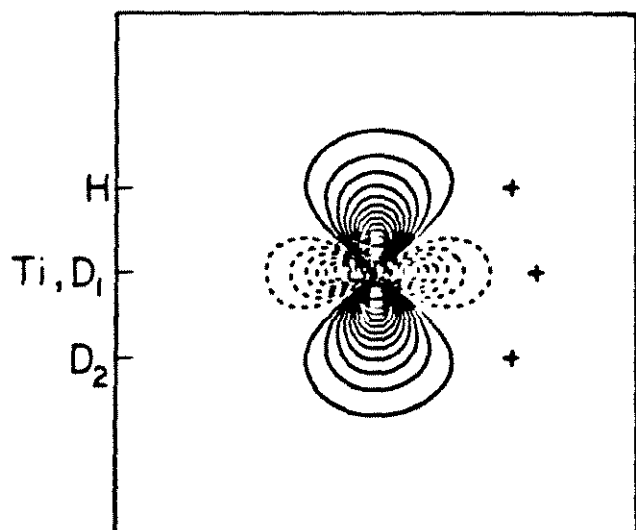
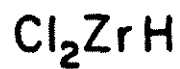
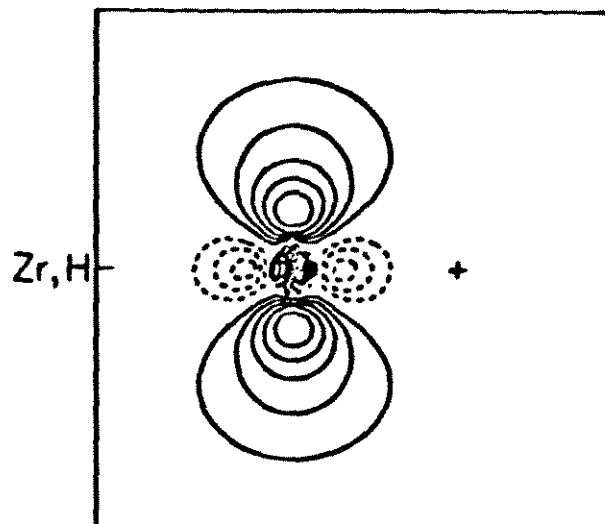
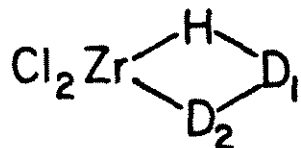
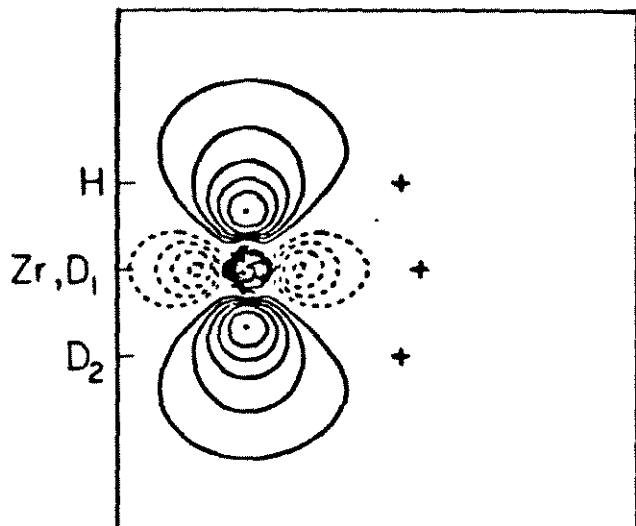


Figure 4. GVB orbitals describing the Zr-H bonds in Cl_2ZrH_2 . The separation between adjacent contours is 0.05 a.u., and the dimension of each plot is 6 a.u.

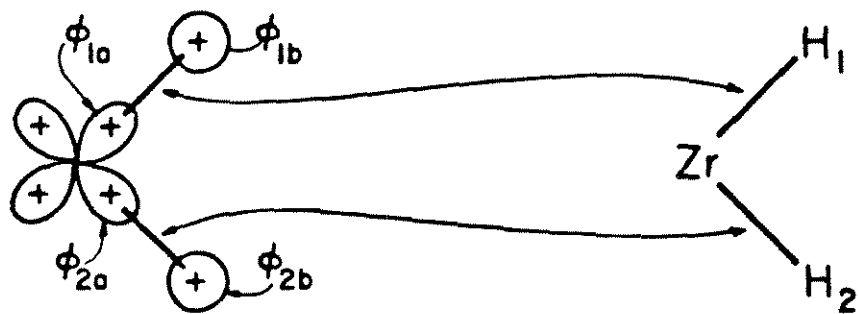
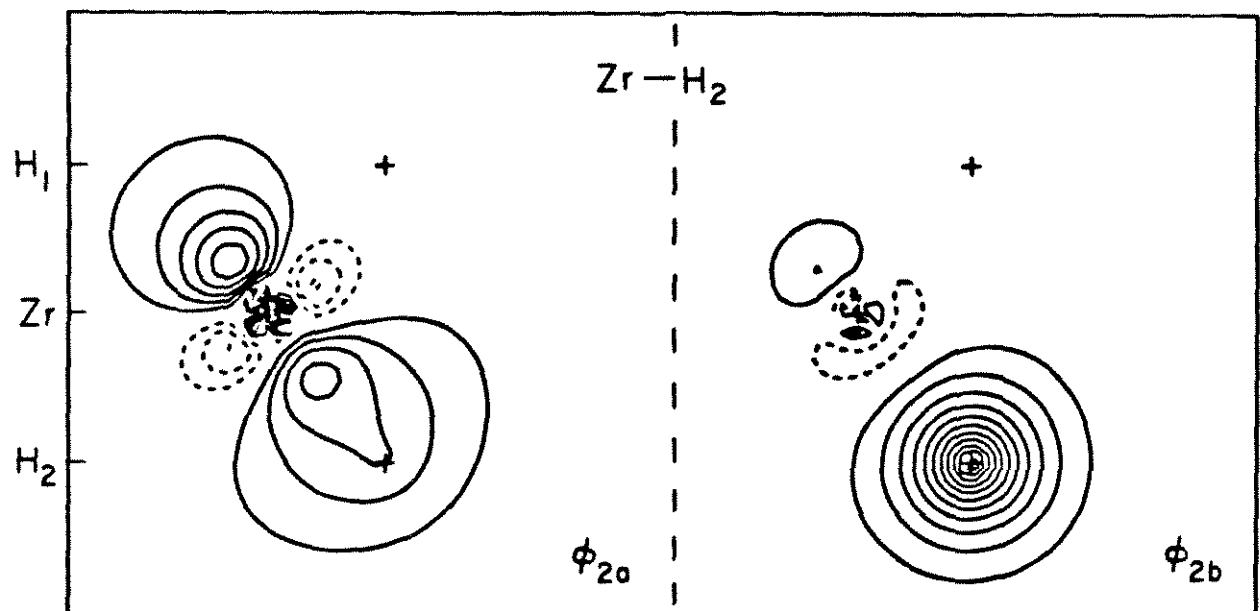
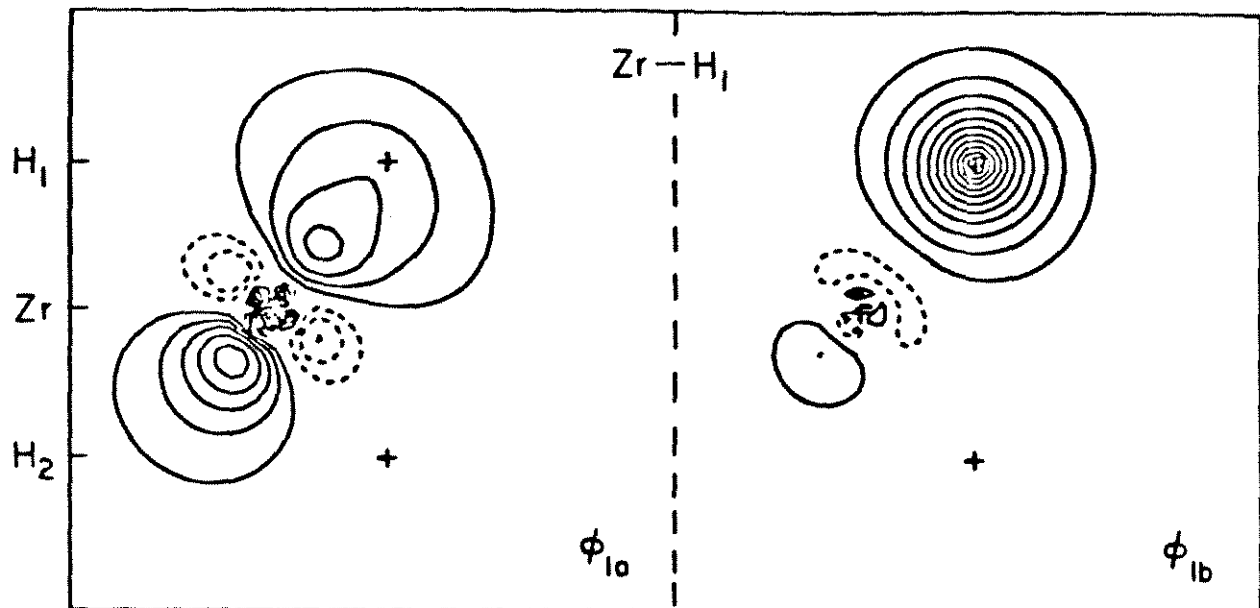
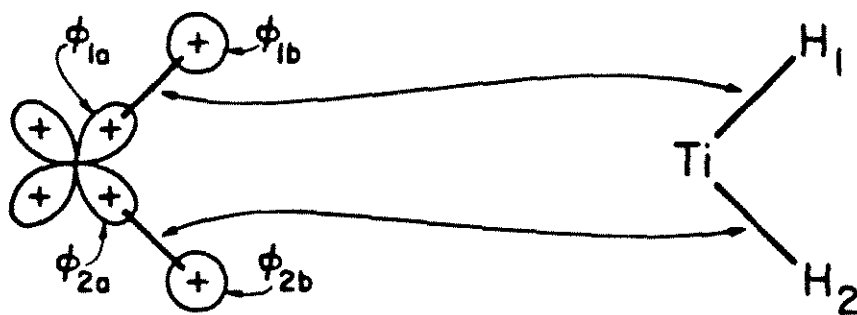
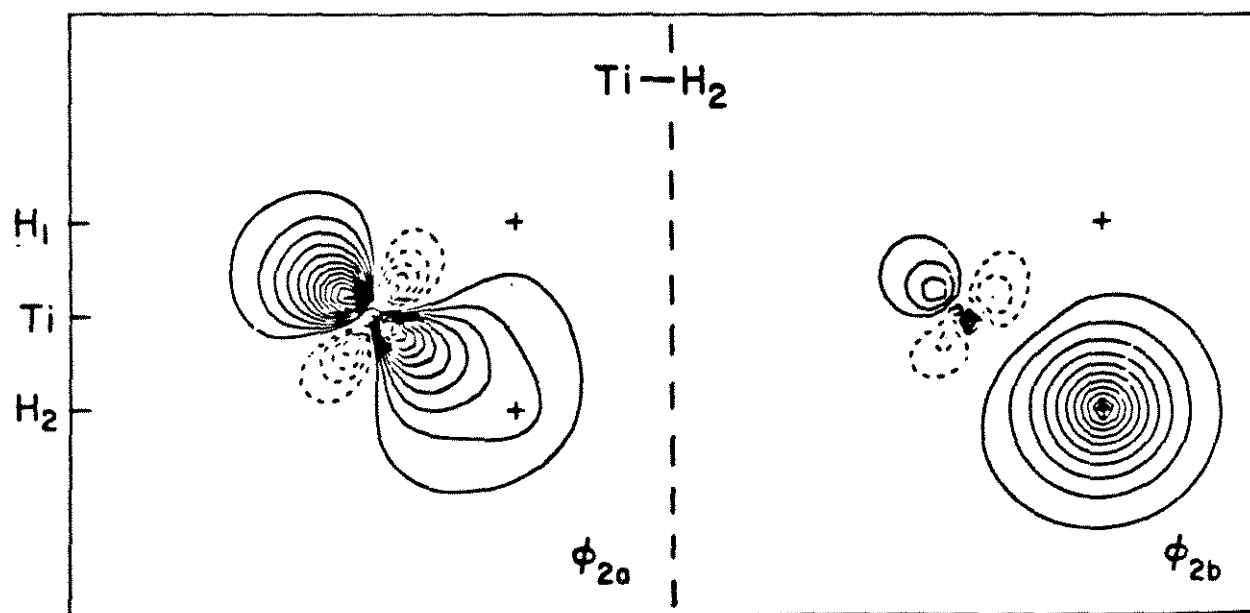
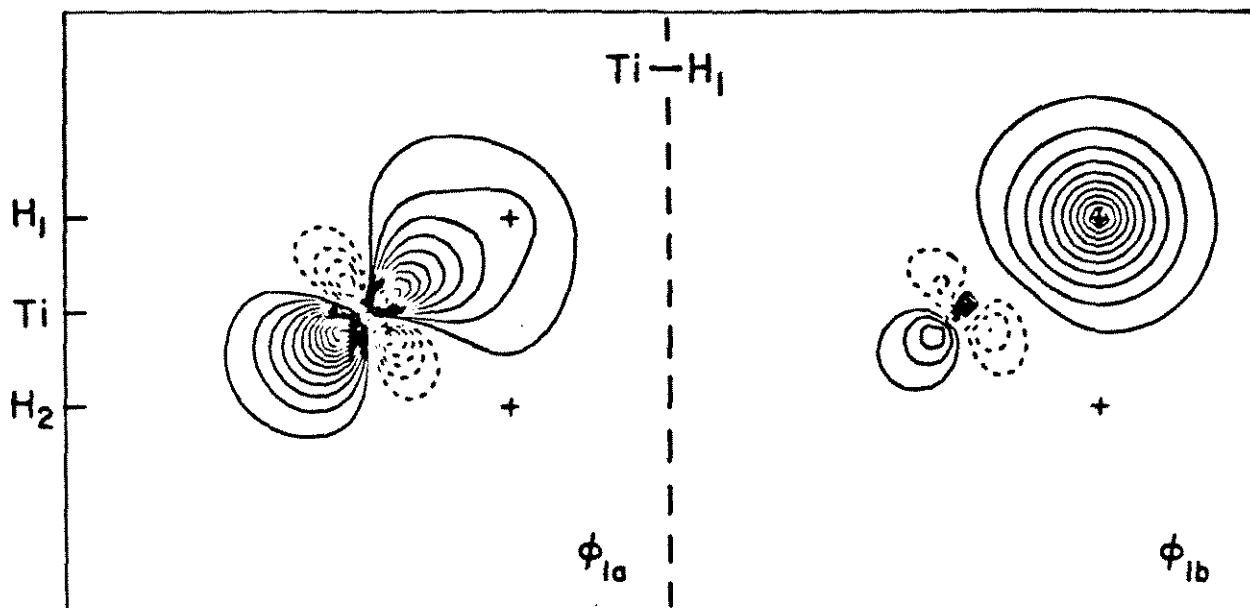
Zr-H bonds in Cl_2ZrH_2 

Figure 5. GVB orbitals describing the Ti-H bonds in Cl_2TiH_2 . The separation between adjacent contours is 0.05 a.u., and the dimension of each plot is 6 a.u.

Ti-H bonds in Cl_2TiH_2 

Titanium and Zirconium Atomic Orbitals

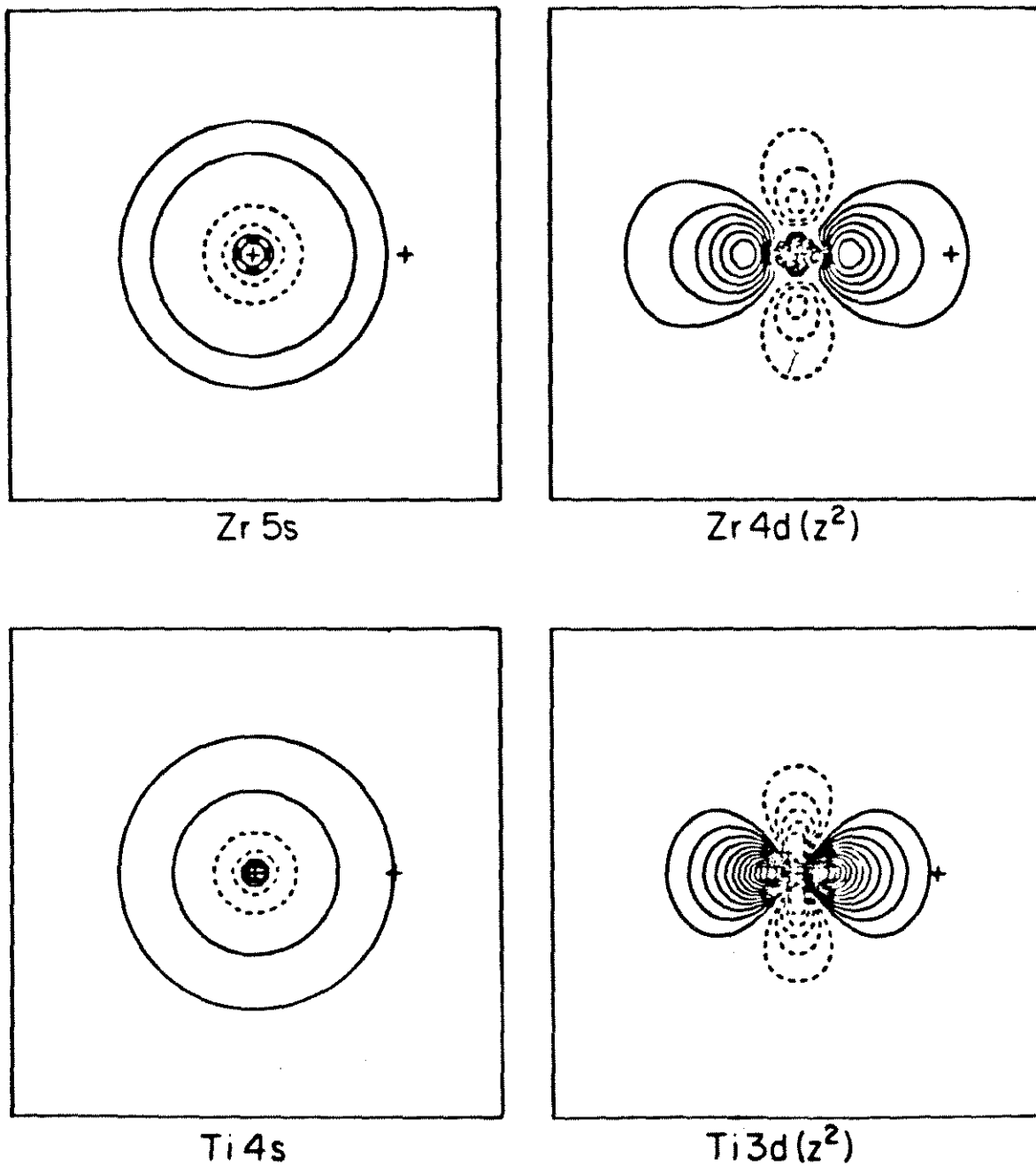


Figure 6. Valence s and d_{z²} orbitals for the zirconium and titanium atoms. The separation between adjacent contours is 0.05 a.u., and the dimension of each plot is 6 a.u.

References and Notes

- (1) M. L. Steigerwald and W. A. Goddard III, (Paper I) *J. Am. Chem. Soc.*, in press.
- (2) M. L. Steigerwald and W. A. Goddard III, *J. Am. Chem. Soc.*, to be submitted.
- (3) W. A. Goddard III, T. H. Dunning, Jr., W. J. Hunt, and P. J. Hay, *Acc. Chem. Res.*, **6**, 368 (1973).
- (4) (a) P. J. Brothers, *Prog. Inorg. Chem.*, **2**, 1-67 (1981); (b) H. H. Brintzinger, *J. Organomet. Chem.*, **171**, 337-344 (1979).
- (5) Recall in GVB that bonds are formed from *overlapping*, singly-occupied orbitals; ref 3; also W. A. Goddard III, *J. Am. Chem. Soc.*, **94**, 793-807 (1972).
- (6) In Paper II (ref 2), we defined an orbital or bonding pair of orbitals to be *spiegel* if they were symmetric under reflection in a given plane and *unspiegel* if antisymmetric. These terms are the generalization of sigma and pi, respectively.
- (7) A. K. Rappe and W. A. Goddard III, *J. Am. Chem. Soc.*, **104**, 297-299 (1982).
- (8) Examples of hydridic species are shown in ref 2.
- (9) C. F. Fischer, "The Hartree-Fock Method for Atoms", Wiley & Sons, New York, 1977.
- (10) W. A. Goddard III and L. B. Harding, *Ann. Rev. Phys. Chem.*, **29**, 363-396 (1978).
- (11) C. E. Moore, "Atomic Energy Levels", NBS Ref. Data Series, NBS 35, U. S. Government Printing Office, Washington, DC, 1971.

- (12) These hybridizations are based on relative Mulliken populations of d and s + p functions on the metal.
- (13) L. Pauling, "The Nature of the Chemical Bond", Third Edition, Cornell University Press, Ithaca, New York, 1960; §4.5.
- (14) (a) Reference 13, p. 152; (b) J. W. Lauher and R. Hoffmann, *J. Am. Chem. Soc.*, **98**, 1729-1742 (1976).
- (15) The value of R(Ti-H) of 1.70 Å is found for both Cl₂TiH₂ (ref 7) and Cl₂TiH (ref 1).
- (16) These overlaps are of *atomic* orbitals, i.e., not self-consistently optimized. The atomic orbitals came from HF calculations on the appropriate (s²d²) state of the Zr and Ti atoms, and a similar calculation on the ground state of the hydrogen atom.
- (17) This value of R(Zr-H) is based on results shown in Tables I and V.
- (18) We believe that this feature of zirconium, as well as the fact that the unpaired electron in Cl₂ZrH is in an orbital which, in comparison to the corresponding orbital in Cl₂TiH, has such a large component of valence s character, accounts for the dearth of examples of *organometallic* complexes of zirconium(III); see Ref. 19.
- (19) P. C. Wailes, R. S. P. Coutts, and H. Weingold, "Organometallic Chemistry of Titanium, Zirconium, and Hafnium", Academic Press, New York, 1974.
- (20) J. E. Bercaw, "Transition Metal Hydrides", Advances in Chemistry Series of the American Chemical Society, 1978, pp. 136-148.
- (21) D. R. McAlister, D. K. Erwin, and J. E. Bercaw, *J. Am. Chem. Soc.*, **100**, 5966-5968 (1978).

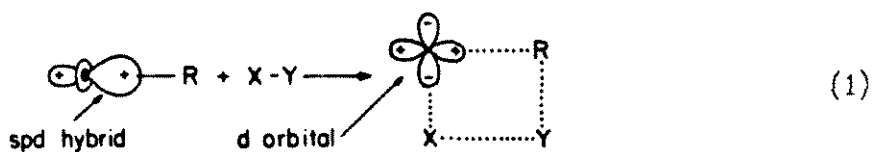
- (22) K. I. Gell and J. Schwartz, *J. Am. Chem. Soc.*, **100**, 3256 (1978).
- (23) This refers to the similarity of the two bonds when they are involved in a $2_s + 2_s$ -type reaction; see ref 2.
- (24) J. Schwartz and J. A. Labinger, *Angew. Chem. Int. Ed. Engl.*, **15**, 333-340 (1976).
- (25) M. L. Steigerwald and W. A. Goddard III, (Paper III), *J. Am. Chem. Soc.*, to be submitted.
- (26) S. A. Cohen, P. R. Auburn, and J. E. Bercaw, *J. Am. Chem. Soc.*, **105**, 1136-1143 (1983).
- (27) R. A. Bair, W. A. Goddard III, A. F. Voter, A. K. Rappe', L. G. Yaffe, F. W. Bobrowicz, W. R. Wadt, P. J. Hay, and W. J. Hunt, GVB2P5 Program, unpublished. See R. A. Bair, Ph.D. Thesis, California Institute of Technology (1980); F. W. Bobrowicz and W. A. Goddard III, "Methods in Theoretical Chemistry", H. F. Schaefer, Ed., Plenum Press, New York, 1979; Vol. 3, p. 77; W. J. Hunt, P. J. Hay, and W. A. Goddard III, *J. Chem. Phys.*, **57**, 738 (1972).
- (28) A. K. Rappe', T. A. Smedley, and W. A. Goddard III, *J. Phys. Chem.*, **85**, 1662 (1981).
- (29) W. A. Goddard II and A. K. Rappe', in "Potential Energy Surfaces and Dynamics Calculations", D. G. Truhlar, Ed., Plenum Press, New York, 1981, pp. 661-684.
- (30) A. K. Rappe', T. A. Smedley, and W. A. Goddard III, *J. Phys. Chem.*, **85**, 2607 (1981).
- (31) T. H. Dunning, Jr., and P. J. Hay, in "Modern Theoretical chemistry: Methods of Electronic Structure Theory", H. F. Schaefer III, Ed., Plenum Press, New York, 1977, Vol. 3 and references therein.

- (32) The HZrH angle was optimized at the HF, GVB(2/4), and GVB(2/4)-RCI levels. The optimum angles were found to be 104.8°, 103.0°, and 102.1°, respectively. At the GVB(2/4)-RCI level, the difference in energy for $\vartheta = 105^\circ$ and $\vartheta = 75^\circ$ is 2.2 kcal/mol, and at the HF level, this difference is 3.1 kcal/mol. For Cl_2TiH_2 , the energy difference between $\vartheta(\text{HTiH}) = 75^\circ$ and $\vartheta = 105^\circ$ is 3.2 kcal/mol (at the HF level).
- (33) For Cl_2TiH , GVB(1/2), and GVB(1/2)-RCI calculations gave the same Ti-H bond length to within 0.004 Å. This leads us to believe that the GVB(1/2) level sufficiently accounts for the Zr-H bond length optimization in Cl_2ZrH .

Chapter 5. The Effect of Hybridization on Reactions at Transition Metals.

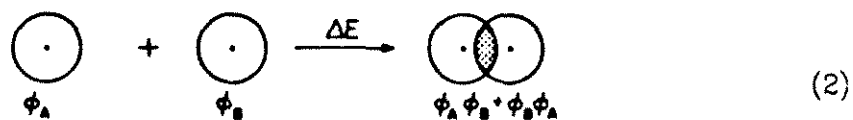
I. Hybridization of Atomic Orbitals on Transition Metals

In the preceding chapters we have shown that suprafacial $2 + 2$ reactions at transition metals can occur with low activation barriers. We have also shown two examples in which the $2_s + 2_s$ reaction does not proceed at low energy, even though transition metals are involved. We showed graphically that the trend in transition metal $2_s + 2_s$ reactivity is related to the ability of the metal to use its valence d orbitals during the concerted reaction. We now turn to the direct study of how atomic s, p, and d orbitals on transition metals mix to form hybrid orbitals that are the optimum orbitals for bonding in the reactants, transition states, and products of reactions. The goal is to appreciate the effects that dictate hybridization in transition metal covalent bonding and how demanding these effects are. In particular, it is important to understand the energetics of (1).



What is the cost of the rehybridization that allows the $2_s + 2_s$ reaction to take place?

We have found simple valence bond ideas¹ and calculations quite useful in these studies. Recall simple valence bond claims that bonds are formed by the overlap of simple atomic orbitals--there is no self-consistent optimization of the sizes and shapes of the bonding orbitals. The simple valence bond description of (2)



indicates that²

$$\Delta E = \frac{2S\hat{\tau}}{1 + S^2} \quad (3)$$

where

$$S = \text{overlap of orbitals } \phi_A \text{ and } \phi_B = \langle \phi_A | \phi_B \rangle \quad /$$

$$\hat{\tau} = H_{AB} - \frac{S}{2}(H_{AA} + H_{BB})$$

and

$$H_{ij} = \langle \phi_i | H | \phi_j \rangle$$

It has been claimed that changes in overall electronic kinetic energy dominate chemical bonding (see Appendix).³ For process (2), the change in total electronic kinetic energy is given by

$$\Delta E_T = \frac{2S\hat{\tau}_T}{1 + S^2} \quad (4)$$

where

$$\tau_T = T_{AB} - \frac{S}{2}(T_{AA} + T_{BB})$$

and

$$T_{ij} = \langle \phi_i | T | \phi_j \rangle ; \quad T = \text{kinetic energy operator}$$

In this study we calculate ΔE_T as a function of the spd hybridization of the metal orbital for process (2) in which ϕ_A is a transition metal-centered orbital and ϕ_B is either a hydrogen or carbon orbital. The use of simple

valence bond wavefunctions allows the effect of hybridization to be tested directly; and the ΔE_T parameter is a useful one because it is a one-electron quantity and is thus easily calculated. The results of this work indicate that, considering the exchange kinetic energy (ΔE_T) along, the optimum mixture of valence s/valence p valence d in transition metal-hydrogen and -carbon bonds is 40% (s and p)/60% d; and that the discrimination in use between valence s and valence p_z in the spd hybridization is not strong.

II. Shapes of the Hybrid Orbitals

An spd hybrid orbital may be defined as in (5),

$$\varphi_{\text{hybrid}} = \frac{\alpha_s \varphi_s + \alpha_p \varphi_{p_z} + \alpha_d \varphi_{d_{z^2}}}{(\alpha_s^2 + \alpha_p^2 + \alpha_d^2)^{1/2}} \quad (5)$$

in which φ_s is the metal valence s orbital, φ_{p_z} is the metal valence p_z orbital, and $\varphi_{d_{z^2}}$ is the metal-valence d_{z^2} orbital.⁴ In the present work we used φ_s , φ_{p_z} , and $\varphi_{d_{z^2}}$ for the metals that came from self-consistent field (Hartree-Fock) calculations on the appropriate atomic states. Thus, for a particular metal and a particular parameter set $(\alpha_s, \alpha_p, \alpha_d)$, the hybrid orbital is completely specified.

In Figure 1 we show φ_s , φ_{p_z} , and $\varphi_{d_{z^2}}$ for titanium. The s and d orbitals are taken from the $4s^2 3d^2$ state and the p orbital from the $4s^1 4p^1 3d^2$ state of the atom. In Figure 2 we show five orbitals that are linear combination of φ_s and $\varphi_{d_{z^2}}$ (φ_{hybrid} , $\alpha_p = 0$, α_s and α_d varied, $\alpha_s + \alpha_d = 1$). In Figure 3 we show φ_{hybrid} (again for Ti) with $\alpha_s/\alpha_p = 1.17$,⁵ varying the $(\alpha_s + \alpha_p)/\alpha_d$ ratio. In Figure 4 we show a third set of titanium hybrid orbitals, those with $(\alpha_s + \alpha_p)/\alpha_d$ set at 4/6, with the α_s/α_p ratio varying.⁶ In Figures 5, 6, and 7, we show hybrid orbitals for zirconium, manganese, and nickel, all with $\alpha_p = 0$ and a varying α_s/α_d ratio.⁷

These orbital plots show what spd hybrid orbitals on transition metals look like. They show that even though the s and p orbitals are significantly more diffuse than the valence d orbitals, the sp hybridization is quite effective in changing the shape of the d orbital. The diffuseness of the s and p orbitals is apparent not only from Figure 1 but also from the fact that the spd hybrids look so much like the parent d orbital until $(\alpha_s + \alpha_p)/\alpha_d$ is large. The effects of hybridization are clear: adding s

character to the d orbital diminishes the "doughnut" of the d orbital, and addition of p character "points" the sd hybrid to one side or the other.

III. Bonding to Hybrid Orbitals

We assessed the importance of hybridization to chemical bonding in a direct way. We prepared simple valence bond between a hybrid orbital on the metal and an atomic 1s orbital on a hydrogen atom located at a bonding distance from the metal. We calculated the orbital overlap [S in (3) and (4)] and the kinetic energy matrix elements, T_{ij} , for this simple valence bond.⁸ Combination of these quantities gives the exchange kinetic energy, ΔE_T . If we assume that this kinetic energy quantity dominates the chemical bond, then a plot of ΔE_T as a function of metal orbital hybridization will indicate what orbital shape is optimum (all else being equal) for bonding to the metal in question.

In Figure 8 we plot ΔE_T as a function of (α_s/α_d) ($\alpha_p = 0$) for Ti-H [$r(\text{Ti-H}) = 1.70 \text{ \AA}$].⁹ This curve indicates that ΔE_T does discriminate on hybridization, and that the optimum ratio is $(\alpha_s/\alpha_d) = 41/59$. Hence, kinetic energy dictates an optimum sd hybrid that is 60% d. Figure 9 shows the corresponding plot of ΔE_T versus hybridization for orbitals formed from the Ti valence d_{z^2} orbital and not a 4s orbital, as in Figure 8, but a 4s-4p hybrid that has $\alpha_s/\alpha_p = 1.17$.⁵ Here again, the optimum bonding orbital is 57% d in character. Although inclusion of this p character does decrease the value of ΔE_T by roughly 50% and increase the bonding overlap by 20%,¹⁰ it does not alter the amount of d "required" by ΔE_T . In Figure 10 we show the plot of ΔE_T versus hybridization for a varying α_s/α_p ratio, keeping $(\alpha_s + \alpha_p)/\alpha_d = 4/6$. This plot shows the comparatively small effect of changes in sp hybridization.

In Figure 11 we show how the value of the valence-bond orbital overlap changed with hybridization. It should be noted that s, p, and d contributions are needed to realize the optimum overlap. The greater

directionality of the d orbital compensates for its smaller radial extent, making "d bonding" competitive with "s or p bonding".

In Figures 12, 13, and 14, we show plots analogous to Figure 8 for the Zr-H,¹¹ Mn-H,¹² and Ni-H¹³ bonds. In each case the optimum value of (α_s/α_d) is close to the value of 41/59 observed in Ti-H (37/63 for Zr-H, 45/55 for Mn-H, and 43/57 for Ni-H). Owing to this similarity for metals as varied as Ti, Zr, Mn, and Ni, we conclude that the kinetic energy criterion selects $\alpha_s/\alpha_d \approx 40/60$ for all transition metal hydrides.

In Figure 15 we show the valence bond orbital overlaps versus α_s/α_d for the Zr-H, Mn-H, and Ni-H bonds. These curves show the expected variation¹⁴ and indicate the geometrical feasibility of sd hybridization.

In Figure 8 we also show ΔE_T as a function of (α_s/α_d) for the two-electron valence bond in Ti-C (carbon located 2.02 Å from titanium; carbon p_z orbital from a Hartree-Fock calculation on *planar* CH₃).¹⁵ Here the optimum hybridization of the titanium bonding orbital is 44/56--quite close to the value of 41/59 observed in Ti-H. This indicates that the 40/60 ratio is persistent in M-R *covalent* bonds.

In the above discussion, only the d_{z^2} orbital was considered. In molecular situations, it may also be possible to covalently bond to metal orbitals shaped like $d(s^2 - y^2)$, i.e., a d orbital having four equivalent lobes. In Figure 8 it is shown that in bonding H(1s) to Ti($3d_{z^2}$), $\Delta E_T = -0.131$ hartree (= 82 kcal/mol). If instead the Ti[$3d(z^2 - y^2)$] orbital is used, $\Delta E_T = -0.099$ hartree (= 62 kcal/mol). There is, at this level of approximation, a 20 kcal/mol bias in favor of bonding to the d_{z^2} orbital. Since $T_{AA} = T_{BB}$ for $\varphi_A = 3d_{z^2}$ and $\varphi_B = 3d(z^2 - y^2)$, this difference in ΔE_T is due to differences in T_{AB} and in overlap. The d_{z^2} orbital has an overlap with the

H(1s) orbital of 0.199; the $d(z^2 - y^2)$ has an overlap of 0.172. The difference in the off-diagonal kinetic energy matrix element is 10 mhartree ($= 6.3$ kcal/mol). Thus the change in overlap dominates this $\Delta(\Delta E_T)$, and a " d_{z^2} " preference in bonding is expected.¹⁶

IV. The Nature of the Chemical Bond

The estimation of the chemical bond based on kinetic energy alone is crude but instructive. Pauling advanced that the strength of the chemical bond is proportional to the square of the valence bond orbital overlap,¹⁷ thus postulating that $\frac{\hat{r}}{1+S^2}$ is proportional to S. Our studies imply that the relationship is more complicated,¹⁸ but that there is a monotonic relationship between S and the bond energy.

The kinetic energy studies show that there is a powerful force urging that ligands bond covalently to metallic d orbitals. This force is the high kinetic energy that is intrinsic to the shape of d orbitals.¹⁹ The kinetic energy of an electron in the $3d_{z^2}$ orbital of Ti atom is 3.76 h (= 2360 kcal/mol), while the kinetic energy of an electron in the 4s orbital is only 0.54 h (= 340 kcal/mol)! The tremendous kinetic energy is decreased when a bond is formed. (Optimum hybridization gives $\Delta E_T = -0.63 \text{ h} = -395 \text{ kcal/mol}$ for Ti-H.)

Based on atomic spectroscopy,²⁰ the energy of the Ti (3d) orbital is roughly 3 eV (= 69 kcal/mol) *lower* than the energy of the Ti (4s) orbital. There is therefore a huge difference in the electrostatic potential (one- and two-electron) felt by the 3d and 4s orbitals. Future work will indicate the effect of hybridization on the potential energy terms in the bond, but at this point we can observe that the virial theorem²¹ indicates that electrons in valence orbitals of complicated atoms do not feel a central force. If they did, the difference in intrinsic kinetic energies of the 4s and 3d orbitals on titanium would be equal to the difference in 4s and 3d ionization potentials. This is not the case.

The kinetic energy analysis suggests that the optimum hybridization

of the metal orbital in an M-R covalent bond should be 40% s and p and 60% d. The method of analysis ignores any polar contributions to the bond. Bonds that do demonstrate significant polarity will not be described usefully by the described scheme and the 60/40 ratio is unimportant.

Bonds that are nonpolar still are observed to have metal-centered hybridization that varies markedly from 60/40.²² This is due not only to the potential energy terms that were neglected above but also to the presence at the metal of more than one ligand and to promotion energy.

In a case such as Cl_2TiH^+ (Chapter 1), the chlorine ligands bond preferentially to the titanium "4s electrons" (see the discussion in Chapter 4). This means that the valence s and p space on Ti is not available for free use by the nonpolar Ti-H covalent bond. This leads to a hybridization in the Ti-H bond with accentuated d character.

Pauling defined the term promotion energy²³ in reference to hybridization. Promotion energy is the energy required to prepare the bonding configuration of an atom. Pauling claimed, for example, that the H-H bond in H_2 would be stronger if the 3d orbital on each hydrogen were used rather than the 1s, but that the energy necessary to prepare the $(3d)^1$ state of H atom precluded this. In the same way, a 60% d/40% s metal orbital may be of the optimum shape for bonding, but if it cost too much to prepare the corresponding state of the atom (as it would in ClMn or Cu ; see Chapter 2), the mentioned hybridization would not prevail.

V. Conclusion

We have studied how the transition metal-to-ligand covalent bond changes with changes in spd hybridization of the metal orbital. We have presented plots of the hybrid orbitals for Ti, Zr, Mn, and Ni, showing pictorially how hybridization effects changes in the shapes of atomic orbitals. We have shown how both the overlap of the metallic orbital with the bonding orbital of a one-electron ligand and the exchange kinetic energy (ΔE_T) change with changes in metallic orbital hybridization. We have found that the decrease in electronic kinetic energy realized on forming a two-electron chemical bond predicts the optimum hybridization of the metallic orbital of the M-R bond to be 60% valence d and 40% valence s and valence p.

A more practical conclusion of this work is shown in Figure 8. There it is apparent that the hybridization of the metallic orbital of a metal-carbon bond is more flexible than the hybridization of the analogous orbital in a metal-hydrogen bond. Based on the process shown in (1) this implies that, all else being equal, a metal-carbon bond is more reactive (in 2 + 2 reactions) than a metal-hydrogen bond.

Appendix: Kinetic Energy and the Chemical Bond

Perhaps the simplest visualization of the chemical bond relies on the quantum mechanical particle-in-a-box. A particle in a one-dimensional box of infinite energy walls and of dimension a is described by a hamiltonian of kinetic energy alone. In the ground state, this particle has an (kinetic) energy of $-\frac{1}{a^2}$ (arbitrary units). Two such systems taken together have $E = -\frac{2}{a^2}$. Now consider bringing these two boxes together; i.e., make the separation between the boxes zero and destroy the coincident wall. This gives a single box of characteristic dimension $2a$, which contains two particles. If the particles are noninteracting, this scenario has a total (kinetic) energy of $\left[-\frac{1}{2a^2}\right]$. Therefore, the "bond energy" of the two boxes is $\left[\frac{3}{2a^2}\right]$. This is the mathematically simplest realization of the bonding question and is the basis of the molecular orbital model of molecules. Obviously, if the particles interact with one another (e.g., electrostatically), or if there is an external potential (e.g., an electrostatic central field) that is more complicated than the one-dimensional square well, the problem will assume greater complexity, but as it stands, this represents the gross features of the quantum mechanics of the chemical bond.

A "valence bond" representation of the bond between two potential "boxes" can be formulated with similar felicity. The results are less immediately obvious but equally simply, varying only slightly from those given in the text of this chapter.

Titanium Atomic Orbitals

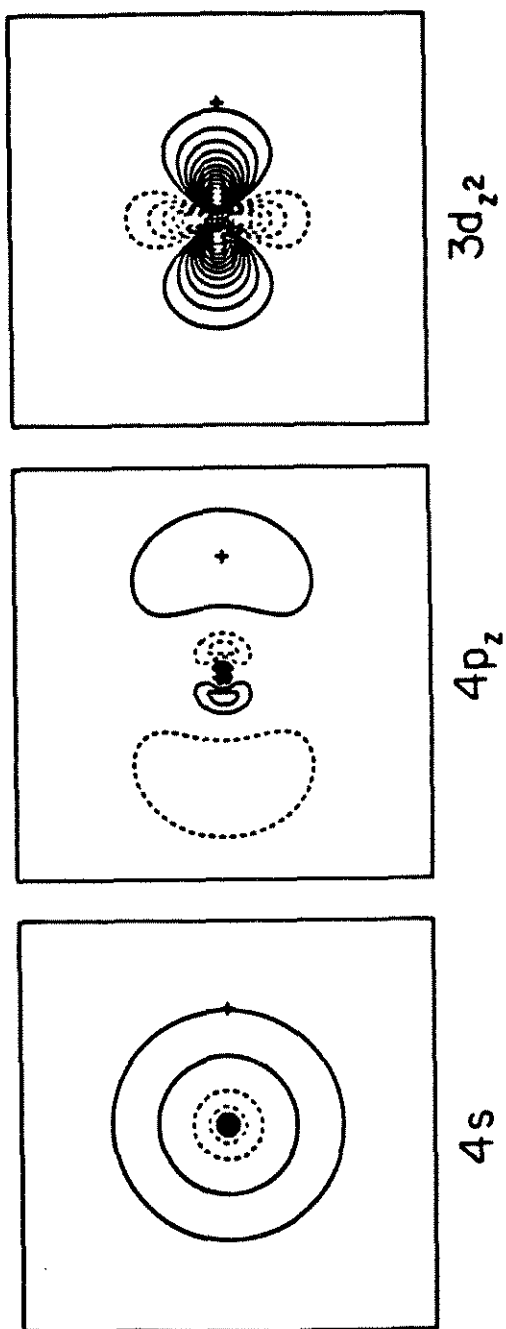


Figure 1. Valence atomic orbitals for titanium. (a) 4s, (b) 4p_z, (c) 3d_{z²}.

The cross represents the location of the hydrogen atom in the model calculations. The separation between adjacent contours is 0.05 a.u.

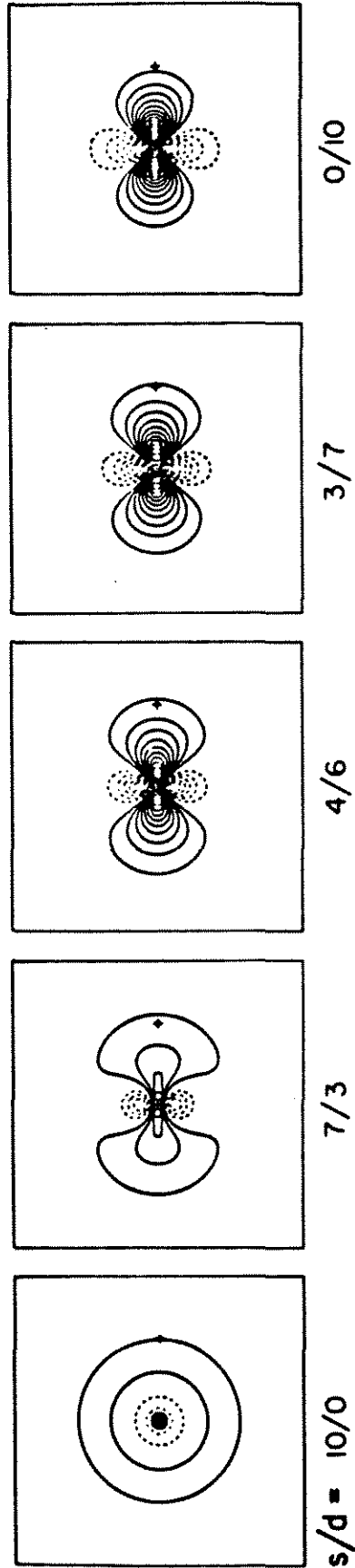
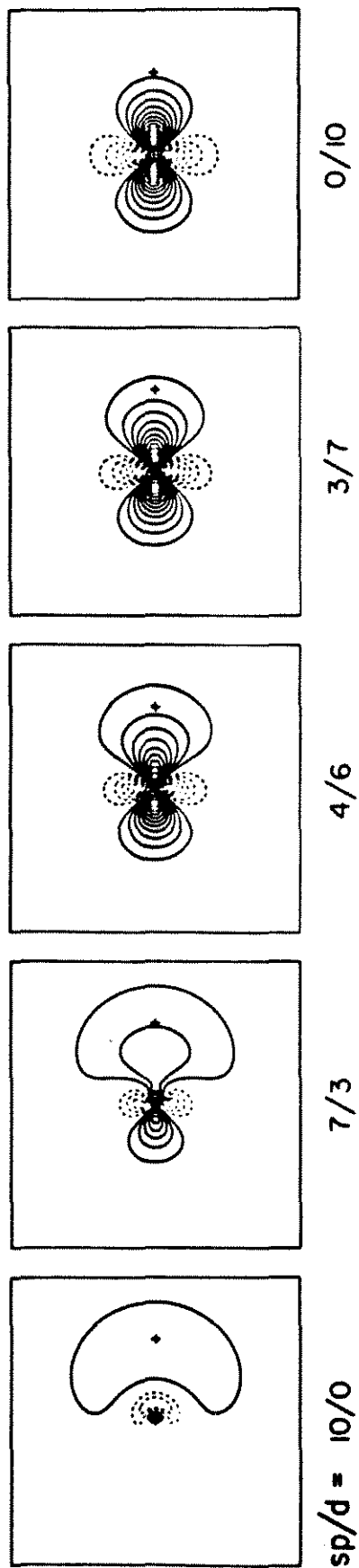
Titanium Atomic Hybrids: $4s/3d_z^2$ 

Figure 2. Titanium atomic sd hybrids. (a) $4s$, (b) $(\alpha_s/\alpha_d) = 7/3$; (c) $(\alpha_s/\alpha_d) = 4/6$; (d) $(\alpha_s/\alpha_d) = 3/7$; (e) $3d_z^2$. The separation between adjacent contours is 0.05 a.u.

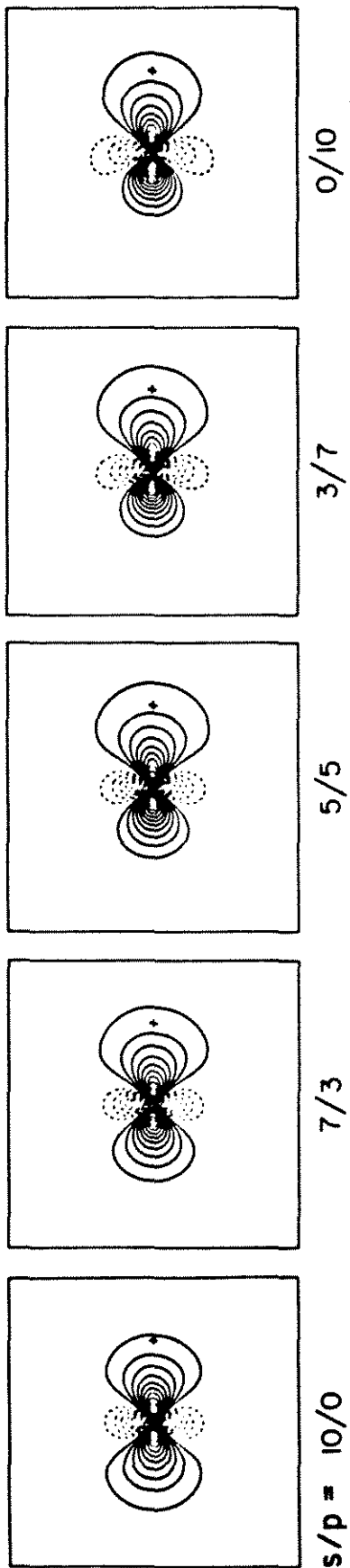
Titanium Atomic Hybrids: $4s/4p_z/3d_{z^2}$ *



* ratio of $4s/4p = 1.17/1$

Figure 3. Titanium atomic spd hybrids, $(\alpha_s/\alpha_p) = 1.17$. (a) sp hybrid $[(\alpha_s/\alpha_p) = 1.17, \alpha_d = 0]$, (b) $(\alpha_{sp}/\alpha_d) = 7/3$; (c) $(\alpha_p/\alpha_d) = 4/6$; (d) $(\alpha_{sp}/\alpha_d) = 3/7$; (e) $3d_{z^2}$.

Titanium Atomic Hybrid: $4s/4p_z/3d_{z^2}^*$



* ratio $(s+p)/d = 4/6$

Figure 4. Titanium atomic spd hybrids, $(\alpha_{sp}/\alpha_d) = 4/6$. (a) 4s; (b) $(\alpha_s/\alpha_p) = 7/3$; (c) $(\alpha_s/\alpha_p) = 5/5$; (d) $(\alpha_s/\alpha_p) = 3/7$; (e) 4p.

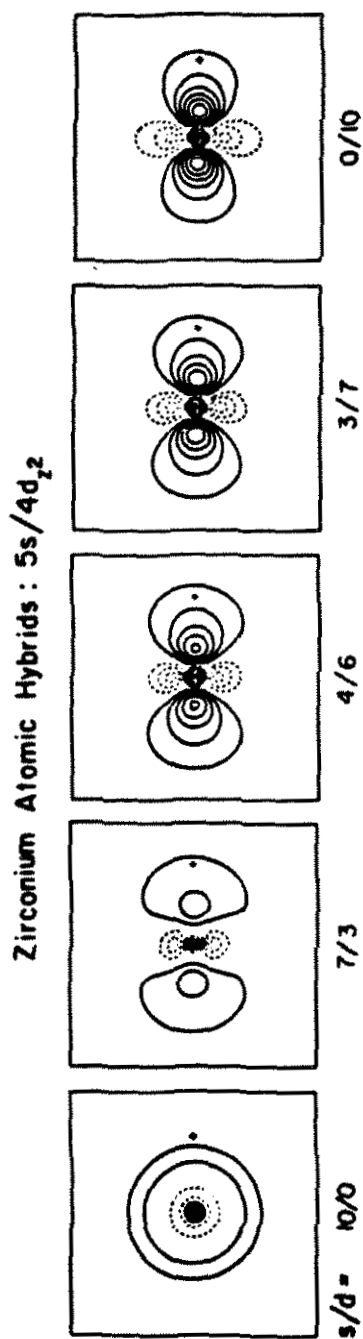


Figure 5. Zirconium atomic sd hybrids. (a) $5s$, (b) $(\alpha_s/\alpha_d) = 7/3$; (c) $(\alpha_s/\alpha_d) = 4/6$; (d) $(\alpha_s/\alpha_d) = 3/7$; (e) $4d_z^2$. The separation between contours is 0.05 a.u. The cross is the location of the hydrogen atom in the model calculation (1.86 Å).

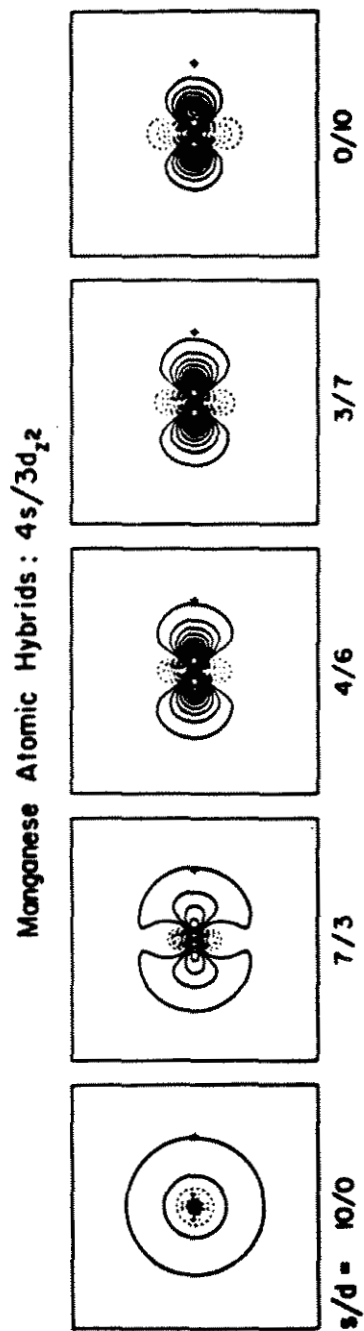


Figure 6. Manganese atomic sd hybrids. (a) $4s$; (b) $(\alpha_s/\alpha_d) = 7/3$; (c) $(\alpha_s/\alpha_d) = 4/6$; (d) $(\alpha_s/\alpha_d) = 3/7$; (e) $3d_{z^2}$. The separation between adjacent contours is 0.05 a.u. The cross is the location of the hydrogen in the model calculations (1.731 \AA).

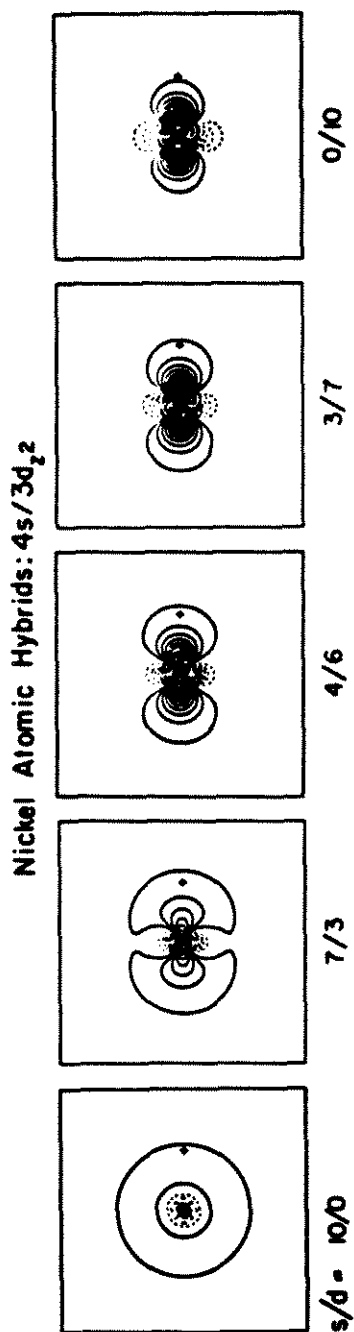


Figure 7. Nickel atomic sd hybrid orbitals. (a) $4s$; (b) $(\alpha_s/\alpha_d) = 7/3$; (c) $(\alpha_s/\alpha_d) = 4/6$; (d) $(\alpha_s/\alpha_d) = 3/7$; (e) $3d_{z^2}$. The cross indicates the location of the hydrogen atom in model calculations (1.475 \AA). The separation between adjacent contours is 0.05 a.u.

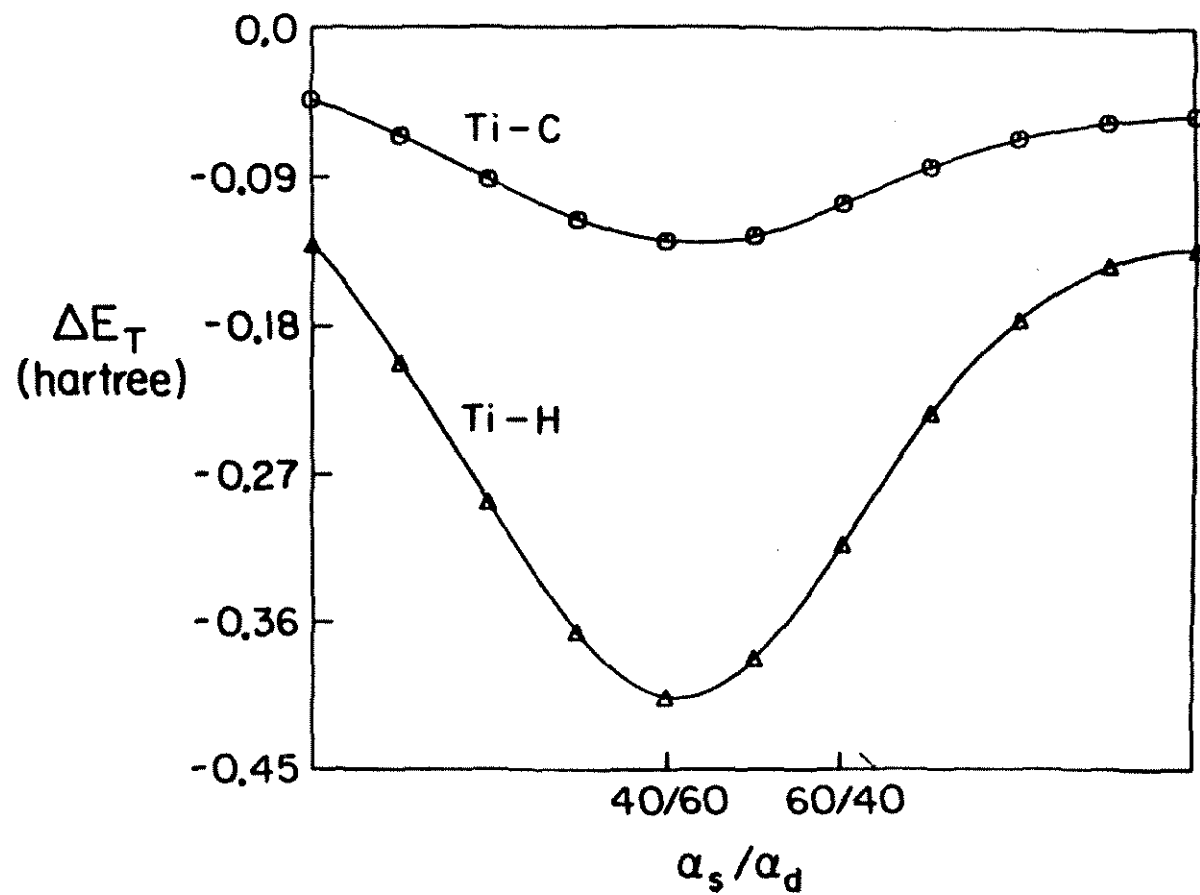


Figure 8. ΔE_T as a function of (α_s/α_d) for the (a) Ti-H and (b) Ti-C two-electron valence bond. Units on the abscissa are increments of $\alpha_s/(\alpha_s + \alpha_d)$.

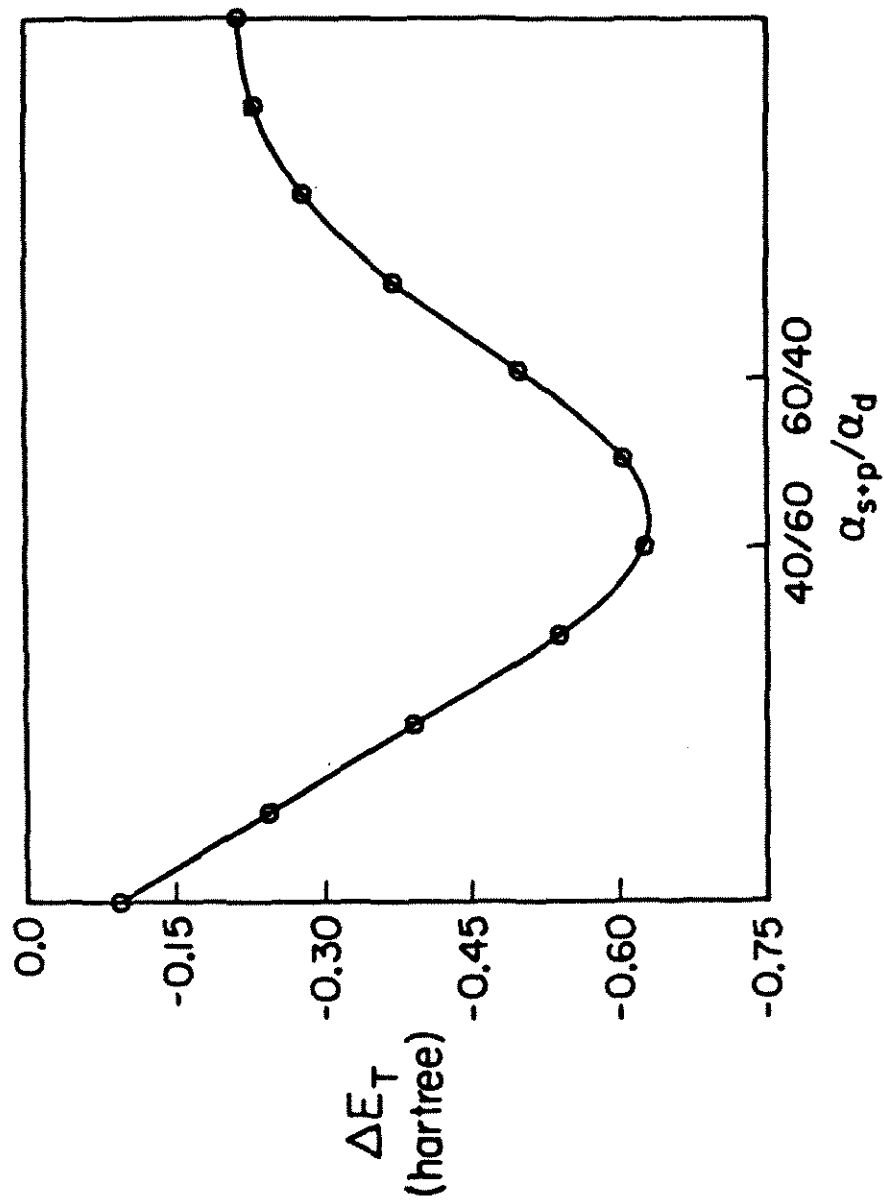


Figure 9. ΔE_T as a function of (α_{sp}/α_d) for the two-electron valence bond in Ti-H. Here $(\alpha_s/\alpha_p) = 1.17$ for all hybrids. Units on the abscissa are increments of $\alpha_{sp}/(\alpha_{sp} + \alpha_d)$.

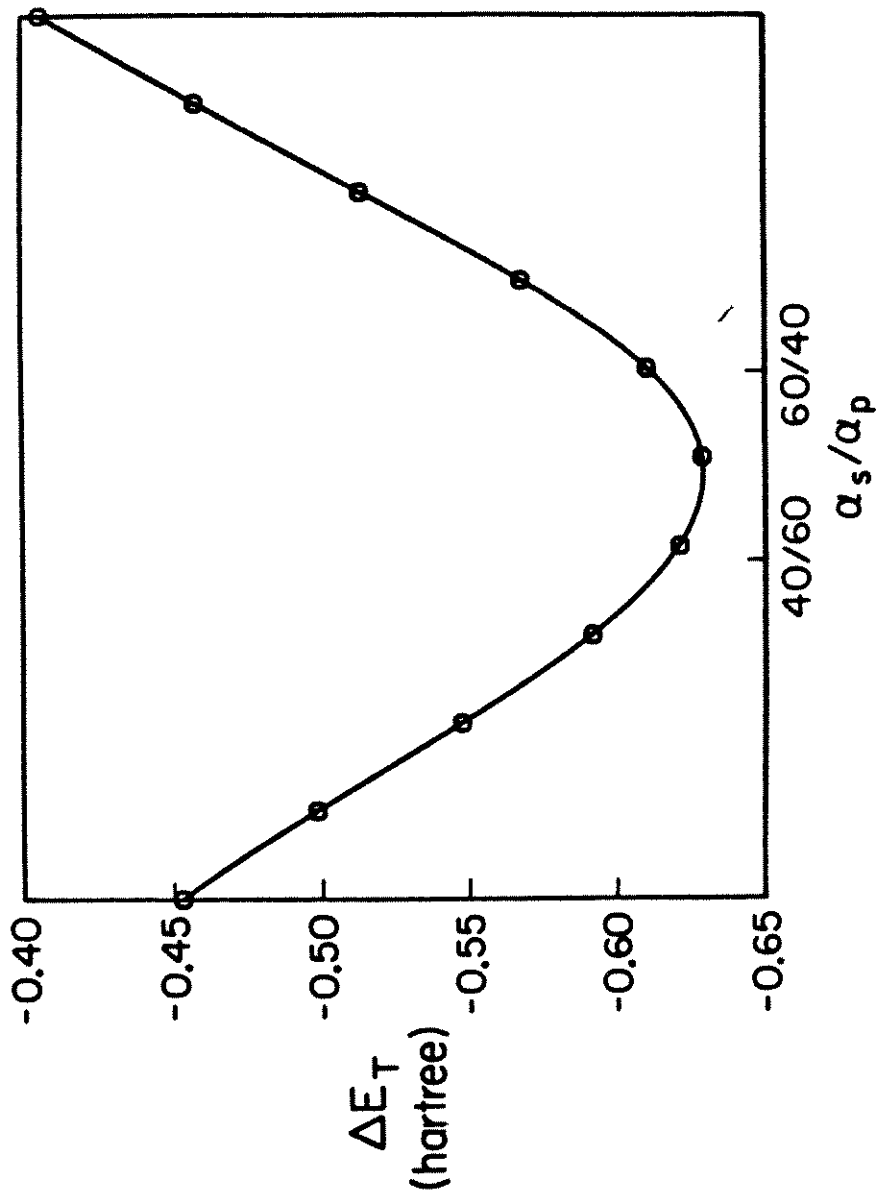


Figure 10. ΔE_T as a function of (α_s/α_p) for the two-electron valence bond in Ti-H. Here $\alpha_d/(\alpha_s + \alpha_p) = 6/4$. Units on the abscissa are increments of $\alpha_s/(\alpha_s + \alpha_p)$.

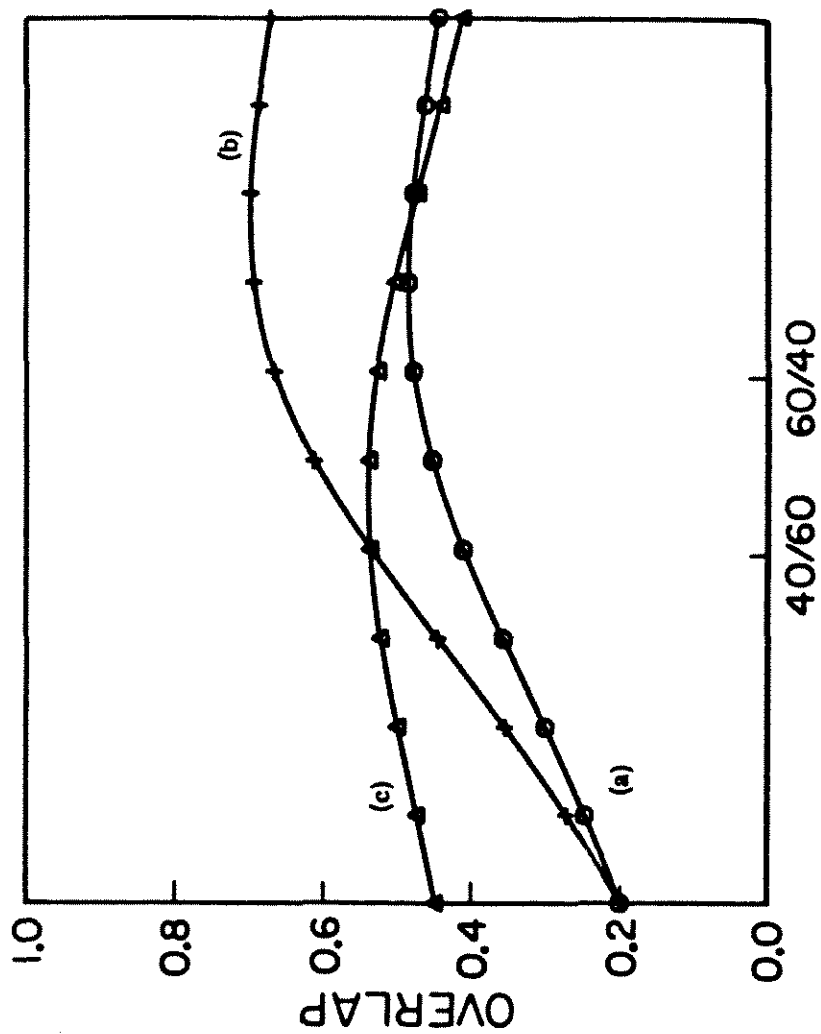


Figure 11. Bond orbital overlap in Ti-H as a function of hybridization for (a) hybrids of the form $(\alpha_s\varphi_s + \alpha_d\varphi_d)$; (b) hybrids of the form $(\alpha_{sp}\varphi_{sp} + \alpha_d\varphi_d)$, where φ_{sp} is a titanium $4s/4p$ hybrid with $(\alpha_s/\alpha_p) = 1.17$; (c) hybrids of the form $(\alpha_s\varphi_s + \alpha_p\varphi_p + \alpha_d\varphi_d)$ with $(\alpha_s + \alpha_p)/\alpha_d = 4/6$ and α_s/α_p varied.

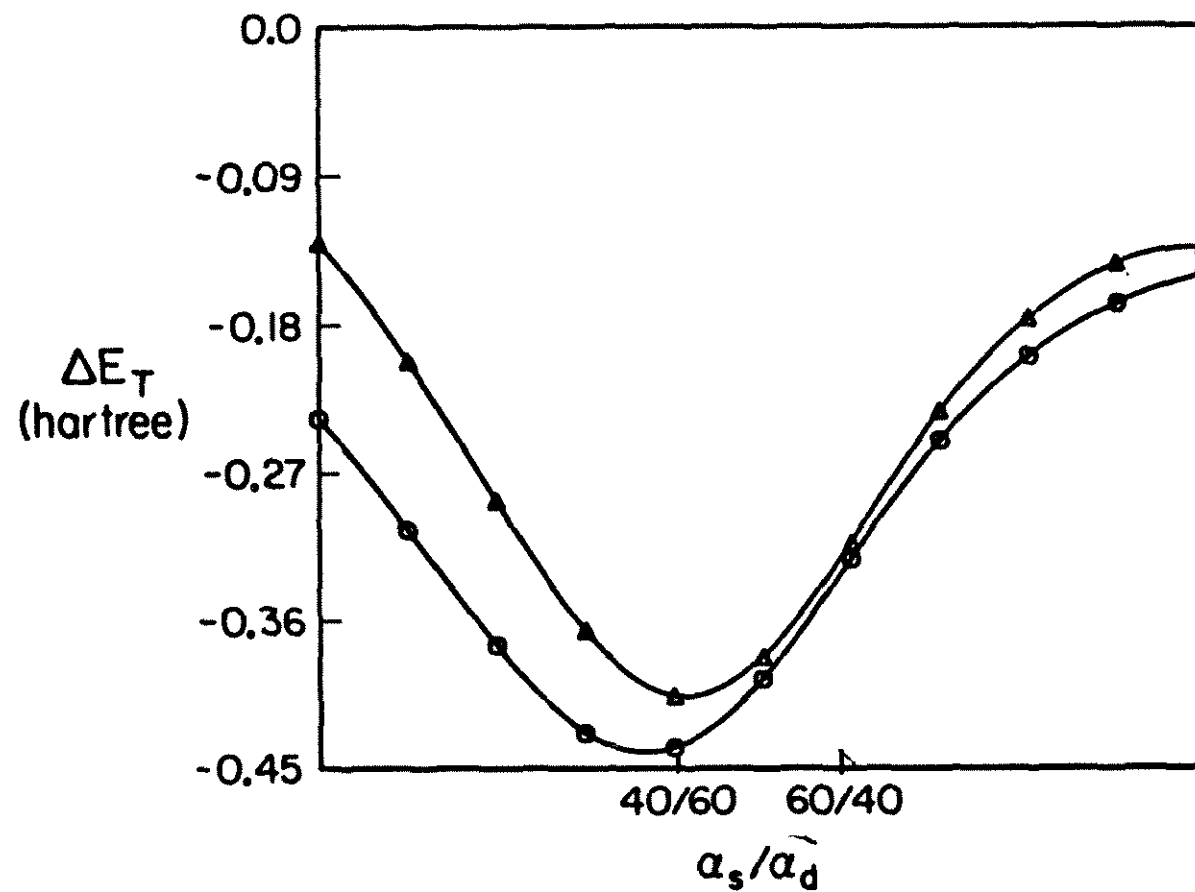


Figure 12. ΔE_T as a function of (α_s/α_d) for the two-electron valence bond in Zr-H. Added for reference (upper curve) is the Ti-H curve from Figure 8.

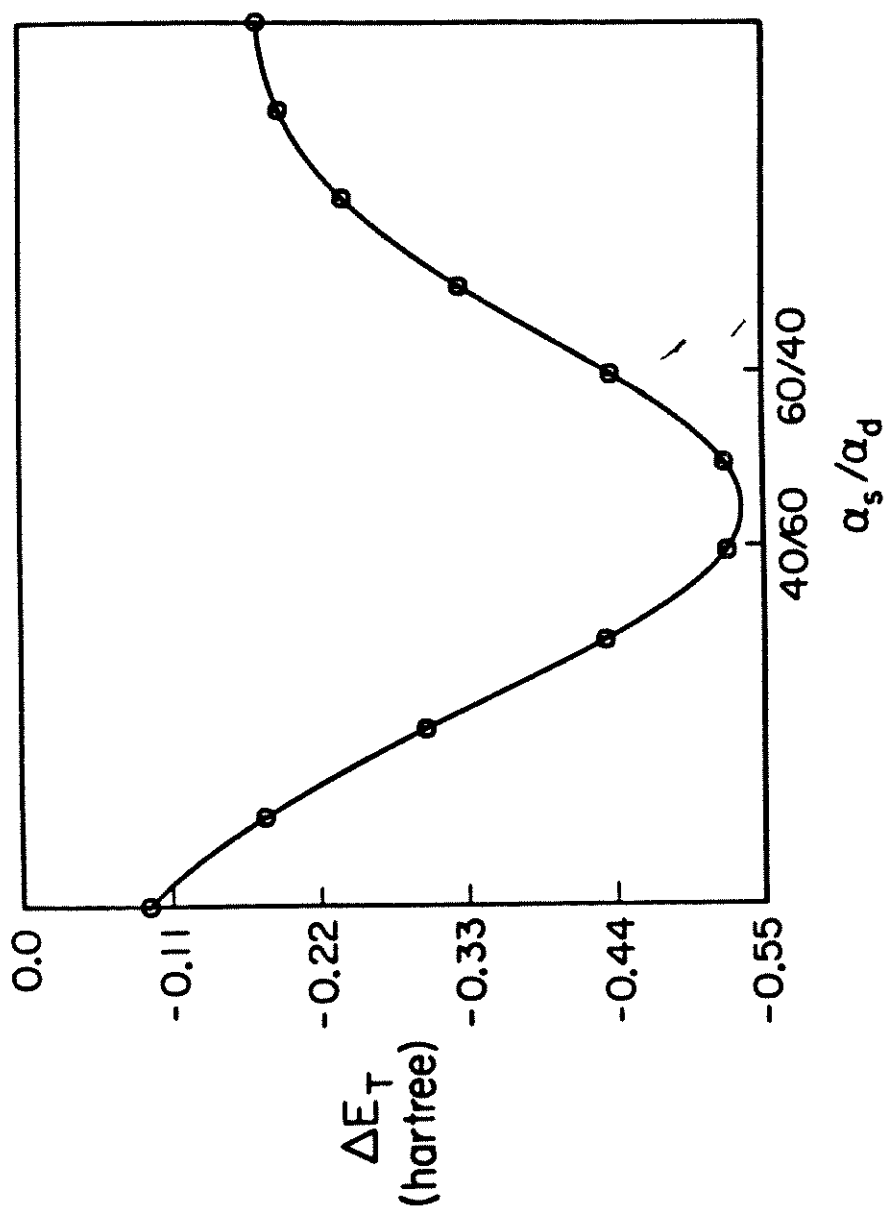


Figure 13. ΔE_T as a function of (α_s/α_d) for the two-electron valence bond in Mn-H.

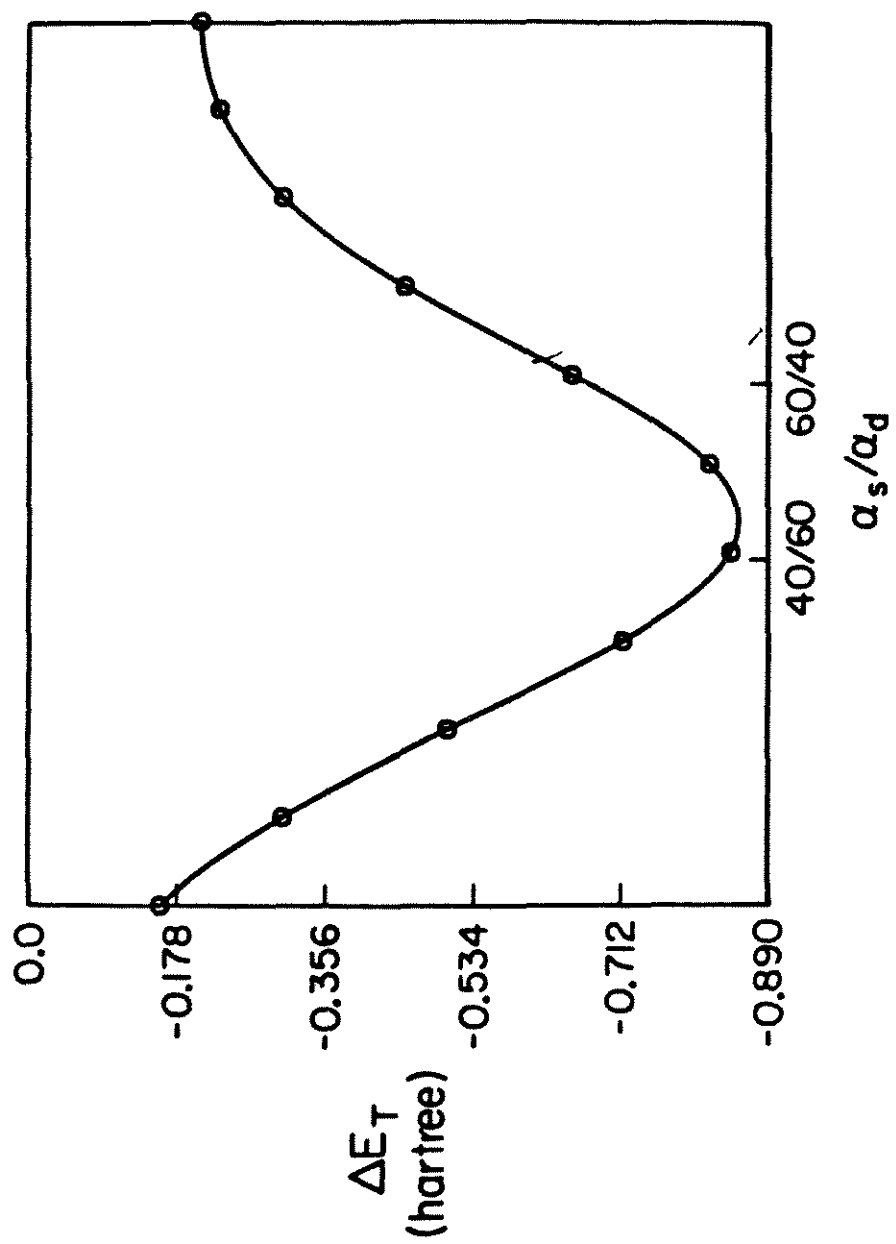


Figure 14. ΔE_T as a function of (α_s/α_d) for the two-electron valence bond in Ni-H.

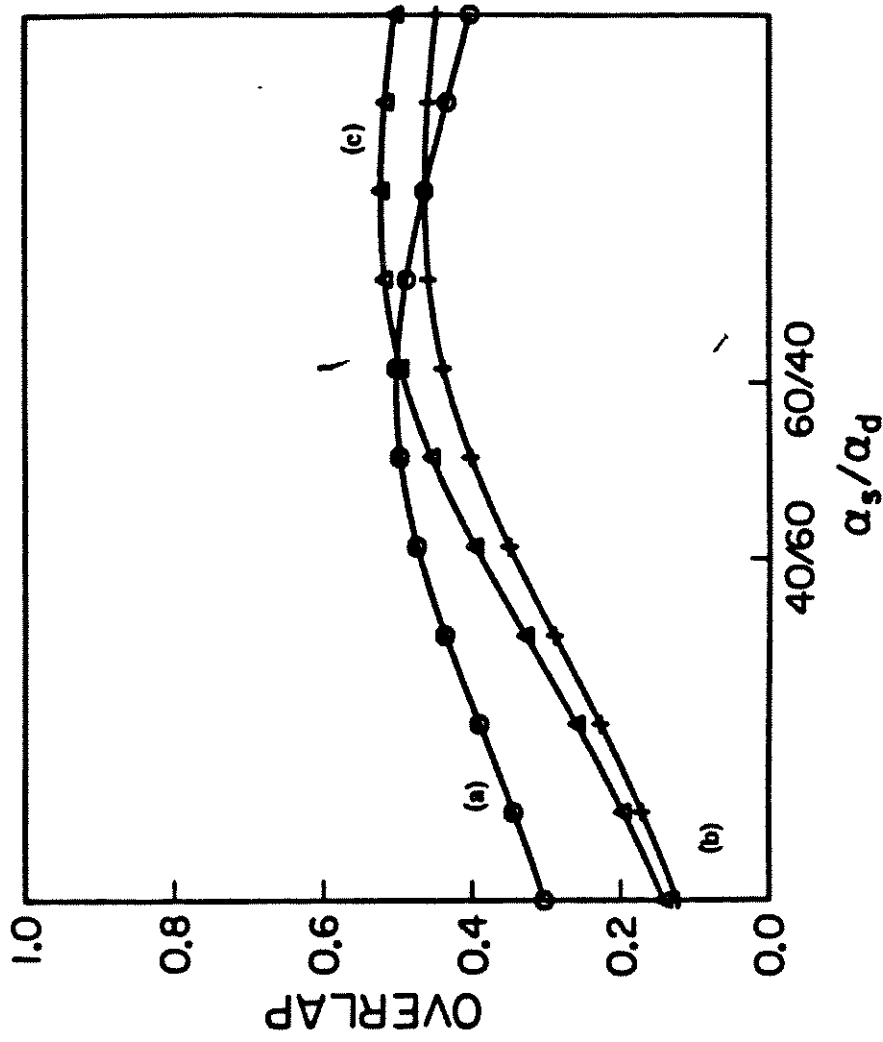


Figure 15. Valence bond orbital overlaps as a function of (α_s/α_d) for the two-electron valence bond in (a) Zr-H, (b) Mn-H, and (c) Ni-H. Units on the abscissa are increments of $\alpha_s/(\alpha_s + \alpha_d)$.

References and Notes

- (1) L. Pauling, "The Nature of the Chemical Bond", Third Edition, Cornell University Press: Ithaca, New York, 1960; p. 25.
- (2) Assume a (valence bond) wavefunction of the form

$$\psi^{VB} = \varphi_A \varphi_B + \varphi_B \varphi_A$$

Then

$$\begin{aligned} E^{VB} &= \langle \psi^{VB} | \mathbf{H} | \psi^{VB} \rangle / \langle \psi^{VB} | \psi^{VB} \rangle = \left[\frac{1}{1+S^2} \right] (\langle \varphi_A \varphi_B | \mathbf{H} | \psi^{VB} \rangle) \\ &= \left[\frac{1}{1+S^2} \right] (\langle \varphi_A \varphi_B | \mathbf{H} | \varphi_A \varphi_B \rangle + \langle \varphi_A \varphi_B | \mathbf{H} | \varphi_B \varphi_A \rangle) \\ &= E(A,B) + \left[\frac{-S^2}{1+S^2} \right] (\langle \varphi_A \varphi_B | \mathbf{H} | \varphi_A \varphi_B \rangle) + \left[\frac{1}{1+S^2} \right] (\langle \varphi_A \varphi_B | \mathbf{H} | \varphi_B \varphi_A \rangle) \end{aligned}$$

where $E(A,B)$ is the nonquantum mechanical energy of atom A and atom B placed at a bonding distance. This gives

$$E^{\text{bond}} = E^{VB} - E(A,B) = \left[\frac{1}{1+S^2} \right] (H_{AB,BA} - S^2 H_{AB,AB}) \equiv \frac{2s\hat{t}}{1+S^2}$$

where

$$\hat{t} \equiv \frac{(H_{AB,BA} - S^2 H_{AB,AB})}{2S}$$

If $\mathbf{H} \equiv \mathbf{T}_1 + \mathbf{T}_2$ (i.e., hamiltonian \equiv sum of kinetic energy operators), then

$$E^{\text{bond}} = \frac{2s}{1+S^2} [T_{AB} - \frac{S}{2}(T_{AA} + T_{BB})] \equiv \frac{2S\hat{t}_T}{1+S^2}$$

- (3) (a) H. Hellman, *Z. Physik*, **85**, 180 (1933); (b) K. Ruedenberg, *Rev. Mod. Phys.*, **34**, 326 (1962).

- (4) The term $(\alpha_s^2 + \alpha_p^2 + \alpha_d^2)^{-1/2}$ insures normalization.
- (5) The ratio of $(\alpha_s/\alpha_p) = 1.17$ was observed for the self-consistently optimized Ti-H bond in Cl_2TiH .
- (6) Since the optimum ratio of sp-hybrid-to-d was found to be 41/59 for the case described by Figure 3, the ratio of $(\alpha_s + \alpha_p)/\alpha_d$ was kept at 40/60 throughout this test.
- (7) The metal bases used were taken from A. K. Rappea, T. A. Smedley, and W. A. Goddard III, *J. Phys. Chem.*, **85**, 2607 (1981). The hydrogen basis set is a six-gaussian triple zeta set found in T. H. Dunning, Jr., and P. J. Hay, In "Modern Theoretical Chemistry: Methods of Electronic Structure Theory", H. F. Schaefer, Ed., Plenum Press: New York, 1977; Vol. 3 and references therein.
- (8) These calculations were performed using the LTRAN program for the Caltech Molecular Quantum Mechanics Program Library.
- (9) The value of $r(\text{Ti-H}) = 1.70 \text{ \AA}$ was found for the Ti-H bond in Cl_2TiH (a) (Chapter 1 of this thesis) and in Cl_2TiH_2 , (b) [A. K. Rappea and W. A. Goddard III, *J. Am. Chem. Soc.*, **104**, 297 (1982)].
- (10) For $\varphi_{\text{hybrid}} = (4\varphi_s + 6\varphi_d)/N$, $S = 0.412$ and $\Delta E_T = -0.406 \text{ h}$. For $\varphi_{\text{hybrid}} = \left[4 \left(\frac{\varphi_s + \varphi_p}{\sqrt{2}} \right) + 6\varphi_d \right] / N$, $S = 0.540$ and $\Delta E_T = -0.629 \text{ h}$.
- (11) $R(\text{Zr-H}) = 1.86 \text{ \AA}$; see Chapter 4 of this thesis.
- (12) $R(\text{Mn-H}) = 1.7311 \text{ \AA}$; see K. P. Huber and G. Herzberg, "Molecular Spectra and Molecular Structure. IV. Constants of Diatomic Molecules", Van Nostrand-Reinhold: New York, 1979.
- (13) $R(\text{Ni-H}) = 1.475 \text{ \AA}$; see ref. 12.

(14) If

$$\varphi_M = (\alpha_s \varphi_s + \alpha_d \varphi_d) / (\alpha_s^2 + \alpha_d^2)^{1/2}$$

and if

$$\langle \varphi_s | \varphi_H \rangle \equiv \sigma \quad \text{and} \quad \langle \varphi_d | \varphi_H \rangle \equiv \delta$$

then

$$S = \langle \varphi_M | \varphi_H \rangle = \left(\frac{1}{\alpha_s^2 + \alpha_d^2} \right)^{1/2} (\alpha_s \sigma + \alpha_d \delta)$$

Once σ and δ are calculated, the variation of S with α_s/α_d is determined.

- (15) The value of $r(\text{Ti-C})$ is taken from ref 9b.
- (16) This effect has been observed. A. K. Rappe, Ph.D. thesis California Institute of Technology, 1981.
- (17) Reference 7, p. 121.
- (18) Preliminary results of an examination of simple valence bond wavefunctions of H_2 at variable internuclear separations indicate that, phenomenologically, the strength of the H-H bond is proportional to the $\frac{3}{2}$ power of the bonding pair overlap.
- (19) Recall the kinetic energy of a particle in an orbital φ is the (unweighted) average of the gradient of that orbital; hence the more curved the orbital, the higher the kinetic energy of the particle in that orbital.
- (20) C. E. Moore, "Atomic Energy Levels", NBS Reference Data Series, NBS 35, U. S. Government Printing Office, Washington, DC, 1971.

- (21) H. Goldstein, "Classical Mechanics", Addison-Wesley, Reading, Massachusetts, 1950, p. 69.
- (22) See Chapters 1, 2, and 4 of this thesis.
- (23) Reference 1, p. 127.

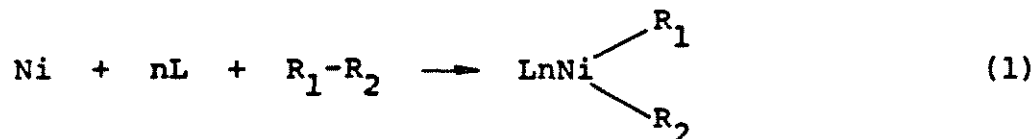
Chapter 6. Carbon-Carbon Bond Cleavage in Nickelacyclopentanes

I. $2_s + 2_s$ Reactions in the Organic Chemistry of Nickel

The organic chemistry of nickel¹ is dominated by reactions which, at least formally, are suprafacial 2+2 reactions. Oxidative addition, reductive elimination, migratory insertion of coordinated ligands into nickel-carbon bonds and the corresponding de-insertion comprise the set of "normal" reactions of the organometallic complexes of the Group VIII metals. These simple reactions have been cited as the fundamental transformations which govern homogeneous catalysis,² and have been studied in that light. One of the goals of physical organometallic chemistry must be to gain a detailed understanding of these reactions so that they may be used in a selective way.

A) Oxidative Addition

Oxidative addition is a standard way to prepare ligand-stabilized alkyl complexes of nickel³ (eq. 1). In the

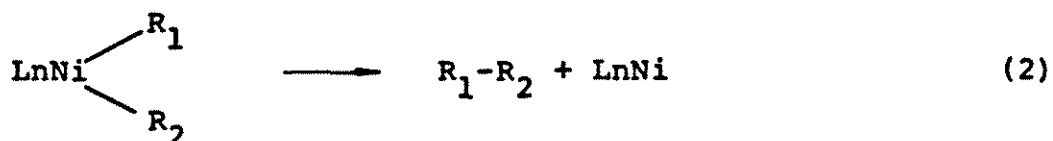


typical case, $\text{R}_1\text{-R}_2$ is an alkyl halide, pseudo-halide or ether,⁴ although oxidative addition of C-H and C-C bonds has been occasionally observed in the nickel triad.⁵ It is also claimed⁶ that the oxidative addition of weak carbon-carbon π bonds begins the "oxidative-cycloaddition" sequence which has been of use to the synthetic chemist.⁷

The mechanics of oxidative addition are understood in a general way, but a detailed physical explanation of the reaction is available only in isolated instances.⁸ There are undoubtedly several mechanisms operative in the process,⁹ some involving a concerted, three center addition,¹⁰ other involving S_N2-type displacement of the leaving group in R₁-R₂,¹¹ and still others involving an intermediate electron-transfer step.¹² The phenomenology is comprehensive in a practical sense: the more electron-rich the metal center, the more facile the addition¹³ - assuming the peripheral steric and electronic effects are not pathological. Although the oxidative addition reaction is formally a suprafacial 2+2 reaction, the absence of data precludes the widespread invocation of this intimate electronic mechanism.

B) Reductive Elimination

If oxidative addition in the step with which catalytic processes at many Group VIII metal sites begin (by introducing the organic substrate to the metal), reductive elimination is the step by which they end.² Reductive elimination is quite well documented in the chemistry of dialkyl complexes of nickel (eq. 2). This process, also a



formal $2_s + 2_s$ reaction, also apparently occurs via several distinguishable mechanisms. It has been claimed that simple metal-carbon bond homolysis initiates the sequence in many cases.¹⁴ The incipient radical then "captures" the carbon fragment of the remaining metal-carbon bond, leading to C-C bond formation and the observed alkane. On the other hand, very thorough studies, particularly on palladium dialkyls, imply the existence of a direct, three-center pathway for the elimination.¹⁵

As with the oxidative addition reaction, in the case of organometallic complexes of nickel, an extensive empirical understanding of reductive elimination exists.^{1,9} Reductive eliminations occur upon thermolysis, oxidation and/or photolysis. In thermal reactions, it has been observed that more basic ligands (L in eq. 2) lead to higher barriers to decomposition.¹⁶ This has been rationalized by the citation of the necessary dissociation of one of these donor ligands at the initial stages of the decomposition,^{15,17} although this has yet to be conclusively demonstrated in the case of nickel dialkyl complexes. Oxidative induction of reductive elimination is well-known. Although the mechanism of the reaction between nickel dialkyls and O_2 is not well understood, it is observed that reductive elimination of alkane is the ultimate result.¹ It is quite tempting to suggest the intermediacy of a nickel (III) dialkyl cation, and there is some electrochemical evidence for this.¹⁸ Other examples of oxidatively-

induced reductive elimination are less obvious. Treatment of stable and isolated dialkyl complexes of nickel with Lewis acids such as AlCl_3 results in the low-temperature elimination of alkane via a mechanistic pathway which is not understood.¹⁹ Treatment of isolated dialkyl complexes of nickel with strongly " π -acidic" olefins such as acrylonitrile also results in the low-temperature decomposition of the dialkyl complex,²⁰ this time resulting in activated-olefin complexes of nickel which certainly deserve more attention. The mechanism of this reaction is also not well known, but it has been claimed that the olefin simply oxidizes the dialkyl complex. It is also possible that this reductive elimination is not a simple 2+2 reaction, but a more complicated six-electron "isovalent" (not reductive) elimination.

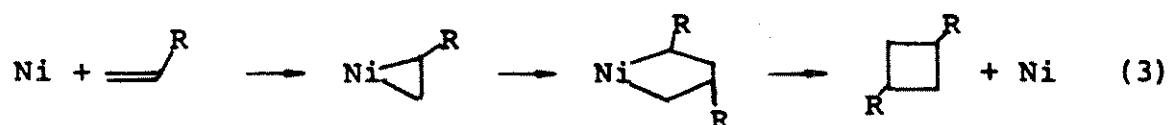
Photochemically-induced reductive elimination has been observed in rare instances.²¹ The details of this process are also unknown, but a functional photo-oxidation seems likely.

C) Migratory Insertion and De-insertion

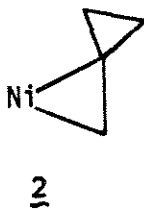
The migratory insertion reaction pervades the chemistry of nickel. Aside from the oligomerization of olefins and diolefins²² and the coupling of Grignard reagents and aryl halides,²³ carbonylation of organic substrates (alkenes, alkynes, organic halides, etc.)²⁴ is the most useful transformation mediated by organonickel reagents. The heart of this process is the insertion of CO

into the nickel-carbon bond of an intermediate nickel-alkyl complex. Although this step of the catalytic sequence has been modeled extensively,²⁵ many details of the insertion remain unknown. The simplest electronic interpretation of the insertion is as a suprafacial, three-center 2+2 reaction.

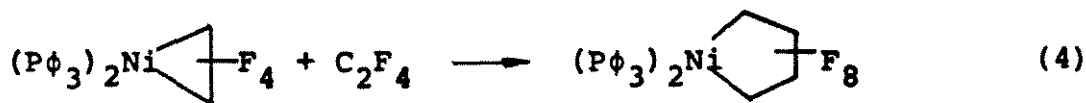
The present author believes that a migratory insertion occurs in the zerovalent nickel catalyzed cyclodimerization of activated olefins (eq. 3). The stepwise nature of this



coupling has been definitely demonstrated only in the case of tetrafluoroethylene reacting with $(\text{P}\phi_3)_2\text{Ni}(\text{C}_2\text{H}_4)$,²⁶ even though other olefins can be cyclized by this procedure. This is presumably because complexes such as 2 are too



reactive to be isolated.²⁷ In the case of tetrafluoroethylene, it has been suggested that the ring expansion reaction (4)



is a dipolar (nucleophilic) insertion reaction, although this has not been clearly demonstrated.

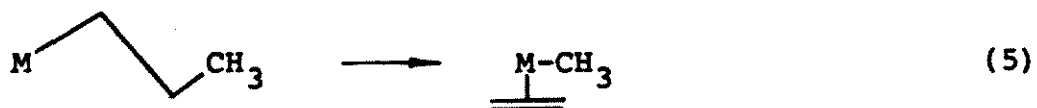
Despite the widespread importance of these nickel-mediated migratory insertion reactions, the detailed electronics of the processes are not known. In particular, the structure of the nickel-carbon bond is still the subject of some not unreasonable controversy. In particular, the degree of polarity of the nickel-carbon bond has not been established unambiguously. Since the ground state of the nickel atom is $^3F (s^2d^8)$ two reasonably polar "s bonds" seem likely for the nickel-carbon bonds of nickel dialkyls,²⁸ but this must be established more rigorously. If these bonds are significantly polar toward carbon, and if they are bonds to the 4s orbitals of the nickel atom, then the migratory insertion reactions at nickel will be of the polar type.²⁹ A detailed study of the migratory insertion reaction at the nickel-carbon bond will yield answers to significant questions such as how to best prepare the nickel atom to carry out insertion reactions and how to best prepare the nickel atom to suppress unwanted insertions.

One migratory insertion reaction which is only rarely of practical value is the β -hydrogen transfer reaction. This reaction is crucial to the olefin isomerization reaction of Tolman,³⁰ the Wacker oxidation sequence,³¹ and the productive activation of saturated hydrocarbons,³² but in preparative organometallic chemistry, the β -hydrogen reaction is best suppressed. Study of the nickel-based β -hydrogen reaction

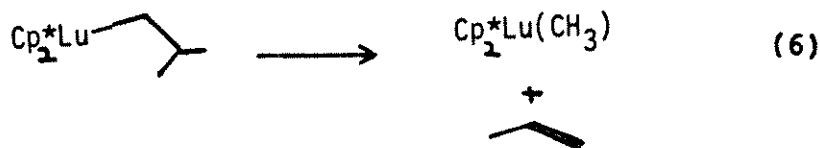
has been limited, owing to the paucity of nickel complexes which have β -hydrogens and are nonetheless stable enough to study in the synthetic laboratory,¹ and decompose at amenable rates via β -hydrogen transfer pathways. Very elegant studies on bis(phosphine)diethylpalladium complexes have shown that the *cis*-square planar complex decomposes via reductive elimination, while the *trans*-square planar complexes decomposes via β -hydrogen elimination.³³

Although the different reactivity is easily explained on geometrical grounds, it would be of interest to see if other inroads exist for controlling the reactivity of such complexes. Are there other ways to direct the trans complex toward reductive elimination? It is curious that one of the very few diethyl complexes of nickel which is stable is (bpy)NiEt₂. This complex thermolyzes to give a mixture of n-butane, ethane and ethylene.³⁴ A detailed study of this reaction is in order.

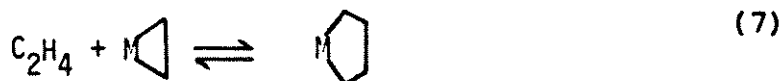
A final reaction at nickel which is of considerable interest, and is best explained as a $2_s + 2_s$ reaction, is the β -alkyl transfer reaction, 5. Despite the simplicity



of this reaction, and its gross similarity to the β -hydrogen transfer reaction, it has been seen only rarely: (1) Watson³⁵ has reported that the isobutyl complex 3 will react as in



(6). (2) Equilibrium of the form (7) have been observed or implied for $M = \text{Cp}_2\text{Ti}$,³⁶ Cp_2^*Ti ,³⁷ Cp_2^*Zr ³⁸ and CpCl_2Ta .³⁹



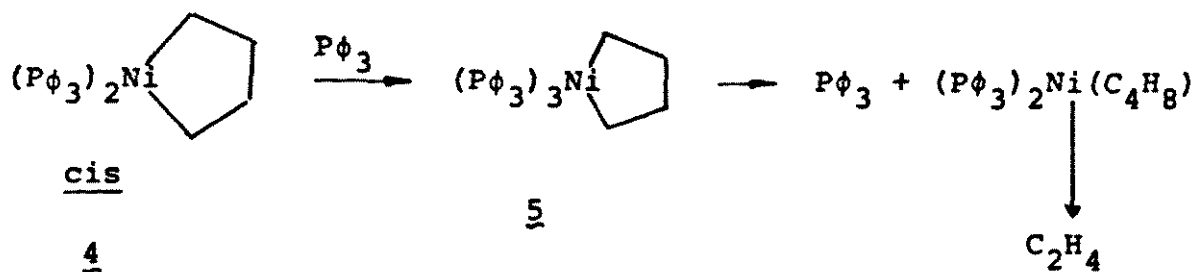
(3) Decarbonylation reactions⁴⁰ have been postulated to proceed through retrograde $2_s + 2_s$ reactions. (4) Tris-(triphenylphosphine)nickelacyclopentane decomposes by an apparent $2_s + 2_s$ process to give ethylene.⁴¹ This is the only example of simple β -alkyl transfer (or phenomenological equivalent thereof) in the organic chemistry of nickel, and served as the initial point for all of the investigations reported in this thesis.

The β -alkyl transfer reaction is of interest for several reasons: (1) The Ziegler-Natta polymerization of simple olefins occurs via the reverse of the β -alkyl transfer.⁴² Conclusions reached concerning the β -alkyl transfer can

easily be inverted to give insight into the polymerization process. (2) The stereospecificity of the polymerization of propylene remains a mechanistic mystery.⁴³ In particular, it is not known whether the Ziegler-Natta systems have the ability to correct their stereochemical mistakes. The most obvious "self-correcting" capacity invokes the removal of the last unit of substituted olefin from the growing polymer chain (a β -alkyl transfer), stereochemical readjustment, then reinsertion to give the proper polymer chain. Characterization of β -alkyl transfer in independent systems would lend support to this mechanistic twist to the polymerization process. (3) Several studies of the homogeneous activation of saturated hydrocarbons have been disappointing, because the organometallic complexes resulting from initial insertion into the saturated C-H bond are too stable.⁴⁴ In other cases, such as that described by Crabtree,³² products resulting from β -hydrogen transfer reactions are too stable. If we knew how to direct β -alkyl transfer generally, perhaps solutions to these problems in C-H activation could be devised. (4) Reactions which are best rationalized as β -alkyl transfer reactions have been observed to proceed at naked transition metal cations in the gas phase.⁴⁵ Studies of active metal complexes in the homogeneous phase could aid in the interpretation of these results.

Despite the utility of the β -alkyl transfer reaction, and owing to its apparent rarity, it has not been extensively

studied. I undertook the examination of the nickel-based reaction in eq. 9.



(9)

The questions of interest were: (1) What is the force behind the cleavage of the carbon-carbon bond, and (2) can this force be controlled and directed.

II. Previous Work

Grubbs and coworkers reported that bis(triphenylphosphine)nickelacyclopentane, 4, could be prepared from the corresponding bis(phosphine)nickeldichloride and 1,4-dilithiobutane.⁴¹ Based on the available data, it was concluded that this complex is a cis-square planar complex of Ni(II). When a large excess of phosphine is added to a solution of the metallacyclo in toluene, a new complex results, tris(triphenylphosphine)nickelacyclopentane.⁴⁶ When this complex is isolated and excess phosphine removed, a dissociative equilibrium may be observed between 5, free phosphine, and a new complex, 6, which has the stoichiometry, but not the identity of 4 (thus observed by ³¹P NMR). These workers found ethylene to be the major organic product of thermolysis of 5. They suggested that the new complex, 6, is the tetrahedral isomer of the cis square-planar complex 4.

The chemistry observed from this set of nickel complexes must be compared to that of the corresponding palladium and platinum complexes. Bis(phenyldimethylphosphine)palladacyclopentane is observed to decompose at 70° in toluene to give predominantly 1-butene.⁴⁷ Bis(tri-n-butylphosphine)platinacyclopentane decomposes in various solvents to give a variety of products, but the predominating

product in all cases is also 1-butene.⁴⁸ It should be mentioned that the dominant product of photolysis of either the nickel (II) or palladium (II) is ethylene. One must then be able to explain: what is the practical difference between Ni, Pd and Pt?

The electronic difference between nickel, palladium and platinum is immediately apparent. While the ground state of the nickel atom is 3F , the ground state of the palladium atom is $^1S(4d^{10})$.⁴⁹ (For comparison, the 3F state in palladium is above the 1S by 3.4 eV, with the $^3D(5s^14d^9)$ between the two, at an energy of 0.9 eV.) In the platinum atom LS coupling is no longer useful, but it is helpful to note that the $^3D(6s^15d^9)$ state (averaged over L and S) is still the ground state, lying roughly 0.1 eV below the $^1S(5d^{10})$ and 0.3 eV below the $^3F(6s^25d^8)$. Thus, the elementary difference between Ni, Pd and Pt is the ground electronic state. The nickel atom adopts the doubly occupied valence-s configuration in its ground state. In this way nickel acts like Be, Mg, Ca, Sr, etc., and is expected to act, in a general way, like a Group IIA metal. In particular, the directed valence associated with a (valence-s)² state predicts a bond angle at the central atom of 180°. Hence, divalent beryllium, divalent magnesium, divalent calcium, etc., and divalent nickel should show covalent bond angles of 180°.⁵⁰

In cases where the geometries of isolated complexes have been determined, this obtains. In fact, in all crystallographic studies of complexes of the form L_2NiR_2 (L = donor base ligand, R = alkyl ligand; neither L_2 nor R_2 chelating), the covalent bond angle (i.e., the R-Ni-R angle) is 180° . This is to say that all complexes of this form are trans-square planar complexes.⁵¹

The atomic arguments made above imply that this geometric peculiarity should not persist throughout the nickel triad. Palladium and platinum, being ground state d^{10} and s^1d^9 atoms, respectively, should make covalent bonds at roughly 90° to one another (i.e., cis square planar complexes). This should be particularly pronounced in palladium since the s^2d^8 state is so high in energy. Detailed studies have shown that bis(phenyldimethylphosphine)-dimethyl palladium prefers to adopt the cis orientation of the alkyl ligands by a factor of 7/3.⁴⁷ Thus, the prediction of geometry based on atomic states is verified, in a relative way, by comparing organometallic complexes of Pd(II) and Ni(II). These geometrical predictions have also been verified with ab initio electronic structure calculations.⁵² Theoretical studies have predicted NiH_2 to be a linear molecule with a $^3\Delta$ ground state (characteristic of the s^2d^8 state of the nickel atom), and PdH_2 to be a bent molecule ($\theta \cong 90^\circ$) with a 1A_1 ground state characteristic of the s^1d^9 state of the Pd atom.

III. Hypothesis

The above argument suggests that the driving force for the β -alkyl transfer in (9) is the ability of the nickel atom to adopt the lower energy s^2d^8 configuration if the C-Ni-C angle is 180° , or, conversely, that the geometrical distortion of the C-Ni-C angle from the 180° optimum is energetically costly and the β -alkyl transfer relieves the strain in the five-membered ring. The fact that the β - β' carbon-carbon bond is cleaved rather than simply stretched is due to the facility of the $2_s + 2_s$ reaction at nickel - recall the nickel valence d orbitals are already involved in the two nickel-carbon sigma bonds.

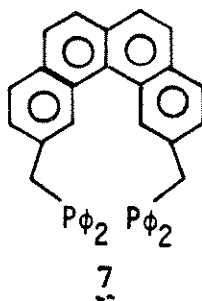
It is apparent that the bis(phosphine)nickelacyclopentane, 4, is stable (vis-a-vis β -alkyl transfer) because of the method of synthesis. This complex is prepared from the corresponding nickel dichloride - an inorganic complex which has previously coordinated (and static) phosphines. As the metallacycle is formed, the phosphines must adjust to accommodate the ring, and the metallacycle which is isolated has the cis orientation of the phosphines. The stereochemistry of the complex is locked, owing to the observed inability of the coordinated phosphines to dissociate.⁵³ Thus, even though the β -alkyl shift is thermodynamically favorable, it is kinetically forbidden.

If the contention that the β -alkyl shift is due to the $4s^23d^8$ ground state of the nickel atom is correct, any nickelacyclopentane which is formed under circumstances

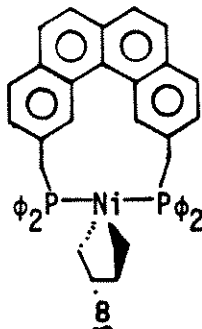
which allow for the adoption of the trans geometry will do so, resulting in the production of ethylene as the primary decomposition product. In particular, if a bis(donor ligand)nickelacyclopentane is formed in which the two donor ligands are forced to be trans, that nickelacycle should decompose to give ethylene. The attempt was made to prepare such a complex and study its decomposition.

IV. Transphos - 2,11-bis(diphenylphosphinomethyl)benzo[c]-phenanthrene

Venanzi and coworkers have shown that the title ligand, transphos (abbreviated tp), 7, is an effective bidentate



ligand, and that the chelating bite angle when it is complexed to a group VIII metal is 180° .⁵⁴ This ligand has been used by Venanzi and by Stille in complexes in which the trans orientation was desired. For this reason, we attempted to prepared 8.



This complex will have the desired trans orientation of the phosphines, allowing the C-Ni-C angle to open to the "s²d⁸" value.

The synthesis of 7 has been described,⁵⁶ and the ligand was prepared by this route (Scheme 1). The only bothersome step in the process is the aromatization of the dibenzodecalin to the benzo[c]phenanthrene. Venanzi reported the use of DDQ in a minimum amount of benzene to carry out the aromatization. This procedure resulted in consistently low yields (42% reported by Venanzi). Our attempted aromatization by palladium in carbon in refluxing naphthalene was not successful; however, aromatization using $\phi_3\text{CBF}_4$ in acetic acid was quite convenient and yielded only two products (by NMR): 2,11-dimethylbenzo[c]phenanthrene and triphenyl methane. Repeated crystallizations, chromatographies and sublimations failed to separate these compounds. This effort thus gave no better avenue to the desired product; however, it did lead to the discovery that the product is best isolated from the DDQ reaction by removal of solvent followed by sublimation (150°, 1 μm Hg) of the crude material.

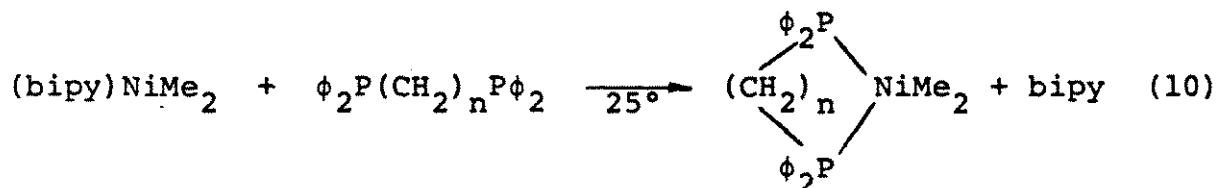
The rest of the synthetic sequence is convenient, giving an overall 5% yield based on starting p-tolualdehyde.

V. Attempted Synthesis of (transphos)nickelacyclopentane, 8.A) Alkylation of (tp)NiCl₂

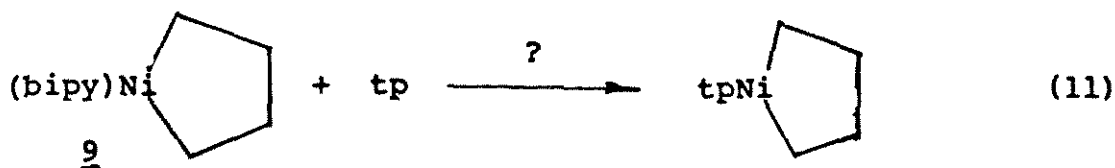
The dichloride of (tp)Ni is easily prepared.⁵⁷ The corresponding complex of palladium was alkylated by Stille with methyllithium to give (tp)PdMe₂ - presumably with the trans stereochemistry. Treatment of tpNiCl₂ with excess methylmagnesium bromide resulted in a complex mixture of products (Figure 1). Owing to this and to the difficulty anticipated in preparing 8 in this fashion, other syntheses of bis(ligand)nickeldialkyls were sought.

B) Exchange of transphos for bipy in (bipy)NiR₂

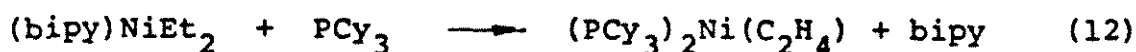
Yamamoto and coworkers have shown⁵⁸ that the 2,2'-bipyridyl ligand can be replaced by chelating diphosphines in (bipy)NiMe₂ (eq. 10). For n=2 or 3 in eq. 10



this reaction proceeds smoothly as shown, but for n=1 or 4 reductive elimination of ethane resulted in the production of phosphine-stabilized Ni(O). We attempted the generalization of this procedure shown in (11). The bipyridyl-stabilized nickelacycle has been reported,⁵⁹ and is quite easily prepared and handled.

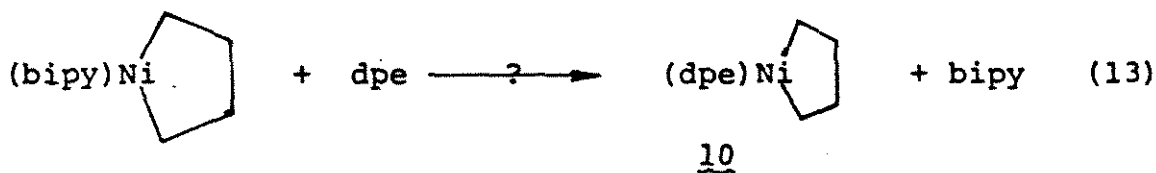


Although the ligand replacement (eq. 10) occurs smoothly for (bipy)NiMe₂, a similar ligand replacement is not facile for (bipy)NiEt₂.⁶⁰ Instead, reaction 12 is observed. Therefore, it was necessary to check the



feasibility of bipyridiyl replacement by phosphines in 9.

The complex [1,2-bis(diphenylphosphine)ethane]nickelacyclopentane, 10, has been reported;⁴¹ therefore, reaction (13) was studied (dpe ≡ 1,2-bis(diphenylphosphino)ethane).



Since 10 is slightly thermally labile, this reaction must proceed at room temperature or below if it is to be useful. This reaction did occur at a very convenient rate at room temperature in toluene. Treatment of 9 with 1.25 equivalents of dpe at room temperature resulted in a change in sample color from the deep forest green of 9 to the bright yellow of 10 almost immediately. ³¹P NMR indicated the conversion of 9 to 10 and a small amount of (dpe)₂Ni. The

ratio of 10 to Ni(0) was 17/1. Proton NMR is less useful in these complexes, but the proton NMR spectra for this reaction are consistent with the products shown. Further confirmation of eq. 13 comes from thermolysis of the products. ^{31}P spectroscopy indicated the conversion of 10 to $(\text{dpe})_2\text{Ni}$ after prolonged heating to 70° . Reductive elimination of cyclobutane has been reported for the thermal decomposition of 10, and cyclobutane is suggested in the proton NMR spectrum of this thermolysis. The proton NMR spectrum of the displacement reaction and of the thermolysis of the products indicates 1-butene also. This product is also reported in the thermal decomposition of 10. (Attempted displacement of bipyridyl from $(\text{bipy})\text{NiEt}_2$ has resulted⁶⁰ in the β -hydrogen decomposition to $\text{L}_2\text{Ni}(\text{C}_2\text{H}_4)$. An analogous side-reaction in (13) would produce 1-butene.)

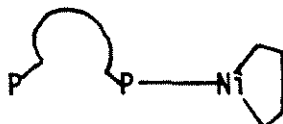
We conclude that treatment of 9 with dpe results in the production of 10 and a small amount (<10%) of reduction to Ni(0).

Reaction of 9 with transphos was very sluggish. While the reaction with dpe was complete in less than 10 minutes, the reaction with transphos (eq. 11) was not obviously complete after 5 days. At the end of 5 days at room temperature, the proton NMR spectrum of a mixture of 9 and 1.5 equivalents of transphos showed a significant amount of 9 remaining and the only apparent organic product of the reaction to be 1-butene. The color of the reaction mixture changed very slowly from the dark green of 9 to a dark

olive green (~5 days) and finally to a dark red-brown (two weeks). After two weeks at room temperature, the mixture showed a ^{31}P NMR spectrum having no free transphos, and only one significant peak. At this time, the proton spectrum of the reaction mixture showed a small amount of 9 remaining, two peaks characteristic of the protons in complexed transphos, no ethylene, and a preponderance of 1-butene.

We conclude that treatment of 9 with transphos at room temperature results in the β -hydrogen decomposition to 1-butene and a transphos-complexed Ni(0) species. Reaction at below room temperature will be too slow to be conveniently observed and therefore this route to 8 is not satisfactory.

The production of 1-butene from this reaction is best explained by noting that the thermolysis of $(\text{Cy}_3\text{P})\text{Ni}(\text{CH}_2)_4$ yields 1-butene. If it is assumed that three-coordinate nickelacycloalkanes decompose via β -hydrogen pathways, the claim may be made that the 1-butene resulting from the reaction of transphos with 9 comes from a complex such as 11.

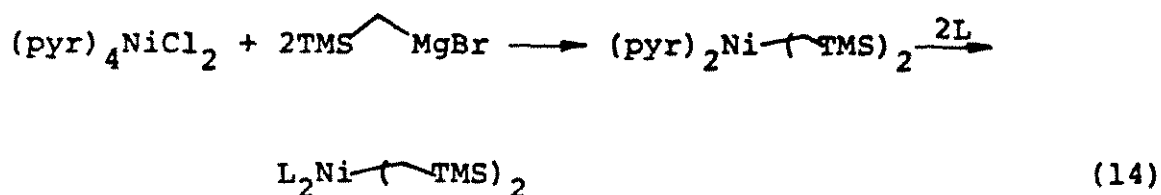


11

The phosphine can displace the bipyridyl,^{58,60} and this three-coordinate complex decomposes before the second phosphine can complex to the nickel. If this is the case, the ligand displacement reaction must be run at lower temperature.

C) Synthesis of L_2NiR_2 from $(pyr)_4NiCl_2 + L + RMgBr$

It was recently reported⁶¹ that $L_2Ni(CH_2SiMe_3)_2$ (L = two electron donor ligand) could be prepared by treating $(pyr)_4NiCl_2$ with Me_3SiCH_2MgCl , and subsequently displacing the loosely coordinated pyridine ligands in $(pyr)_2Ni(CH_2SiMe_3)_2$ (eq. 14). There are four attractive



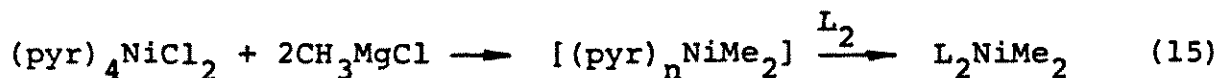
features of this sequence: (1) Although the ligand displacement was usually carried out at room temperature, in one case (eq. 14, $L_2 = dpe$) this step was carried out at $-30^\circ C$. The major drawback with the displacement of bipyridyl from 9 is the high temperature required. If the transphos ligand could be attached to the nickel complex at low temperatures, there is a better chance of isolating the transphos nickelacycle. (2) The displacement of pyridine ligands presumably occurs sequentially, hence if this process were used to prepare nickelacycloalkanes, it is not

likely that three-coordinate species would be formed and β -hydride decomposition would be suppressed. (3) Grignard reagents are used rather than the alkyl lithium reagents which have been used to synthesize nickelacycles. Digrignard reagents⁶² are much more easily prepared and handled than dilithium reagents. (4) In common with route (B) (vide supra), in this process, the nickelacyclopentane is prepared before the trans-directing ligand is attached. If we know that the nickelacycle is intact before the ligand is added, we will obviously know the direct effect of the ligand additive.

We tested the generality of this synthetic sequence by using it in the preparation of (bipy)NiMe₂,⁶³ (dpe)NiMe₂,⁶⁴ (bipy)NiEt₂³⁴ and (bipy)Ni(CH₂)₄.⁵⁹ Since these compounds have all been reported independently, prepared by alternate routes, their preparation from (pyr)₄NiCl₂ represents a valid and simple test of the method.

1) Preparation of L₂NiMe₂ (L₂ = dpe, bipy)

The title dimethyl complexes of L₂Ni for L₂ = bipy and L₂ = dpe have been prepared from Ni(acac)₂ + AlMe₂(OEt) + bipyridyl, and (dpe)NiCl₂ and methyllithium, respectively. We have prepared these complexes as in eq. 15. These reactions are best performed in tetrahydrofuran



in view of the greater solubility of the digrignard reagents in this solvent,⁶² although in syntheses designed to isolate intermediate 12 diethylether was used for easier solvent removal. The preparative reactions are performed at low temperature. Warming the reaction above 0°C for prolonged periods (15-30 minutes) resulted in the decomposition of the organonickel species to nickel black. Several equivalents of free pyridine were added at the outset of each synthesis. This presumably prevented the production of ligand-free NiMe₂ (followed by decomposition).⁶¹ Withholding of this pyridine did lead to the production of nickel black at lower temperatures. The (pyr)₄NiCl₂, excess pyridine, methymagnesium chloride and solvent were combined at -70°, the mixture was allowed to warm slowly to -20° and held at this temperature until the inorganic starting material was consumed. An excess of Grignard reagent was required; use of less Grignard resulted in excessive reaction times. The excess Grignard is necessarily quenched before addition of the replacement ligand (specifically in the case of bipyridyl). Isopropanol, water and trimethylsilylchloride were all used as quenching agents. Trimethylsilylchloride proved to be the most convenient in view of its volatility, but isopropanol was also practiced.

Significantly, the replacement of the pyridine in (pyr)_nNiMe₂ by bipyridyl was apparent at temperatures as low as -78°! The (pyr)_nNiMe₂ reaction mixture shows a bright

orange to bright yellow color. When bipyridyl (2 eq. in thf) is added to this mixture (at -78°), there is an immediate color change which slowly gives complete predominance to the bright green color characteristic of $(\text{bipy})\text{NiMe}_2$. Although the kinetics of this process have not been studied, it is certainly apparent that this ligand exchange is synthetically useful owing to its tolerance for low reaction temperatures.

NMR spectra of $(\text{bipy})\text{NiMe}_2$ and $(\text{dpe})\text{NiMe}_2$ prepared via 15 are shown in Figures 2, 3 and 4. In Figure 3 note the $X_2\text{AA}'X_2'$ and $X_3\text{AA}'X_3'$ patterns characteristic⁶⁴ of the $-\text{CH}_2-$ and $-\text{CH}_3$ protons, respectively, in $(\text{dpe})\text{NiMe}_2$. The ^{31}P NMR spectrum of $(\text{dpe})\text{NiMe}_2$ in Figure 4 is important, because it indicates the virtual absence of $\text{Ni}(0)$ products.

2) Preparation of $(\text{bipy})\text{Ni}(\text{CH}_2)_4$

Complex 9 has been synthesized by a rather circuitous route,⁵⁹ but not spectroscopically characterized. In Figure 5 we show the proton NMR spectrum of 9 prepared in this way, showing the two distinct protons of the metallacyclic ring. Integration shows the expected 1:1 ratio, and decoupling irradiation (Figures 6 and 7) shows the coupling of the two proton sets. Integration relative to the bipyridyl resonances indicates the expected 2:4:2:4:4 ratio.

This nickelacyclopentane can also be prepared by the method of eq. 14. Using 1,4-di(bromomagnesia)butane, $(\text{pyr})_4\text{NiCl}_2$ and bipyridyl and the method outlined above, a

complex was isolated whose ^1H NMR spectrum is identical to that of Figure 5. Although the yield is low (10%), the conditions have not been optimized and the literature preparation also results in a modest yield (21%). Most importantly, the result indicates the feasibility of this procedure for general synthesis of nickelacycles.

3) Isolation of $(\text{pyr})_n\text{NiMe}_2$

The most convenient method for studying the formation and decomposition of 8 is NMR spectroscopy. It would thus be valuable to isolate the pyridine stabilized "naked" nickelacyclopentane as a solid. Carmona and coworkers⁶¹ reported the isolation and crystallographic characterization of $(\text{pyr})_2\text{Ni}(\text{CH}_2\text{TMS})_2$, the isolation of the corresponding dimethylnickel and nickelacyclopentane complexes appeared possible.

The complex $\text{NiMe}_2 \cdot n(\text{pyr})$ was isolated. Treatment of $(\text{pyr})_4\text{NiCl}_2$ in diethyl ether at -70° with 5 equivalents of methylmagnesiumchloride (as a thf solution) resulted in the production of a bright orange suspension in a red solution. This mixture was treated with several equivalents of trimethylsilylchloride to quench unreacted Grignard reagent. Filtration and repeated extraction of the solids gave a deep red solution. Removal of solvent and washing with pentane gave an ochre solid. Proton NMR (Figure 8)⁶⁵ shows resonances characteristic of pyridine (free and complexed) and a singlet at $\delta(-0.83)$. Treatment of this solid with bipyridyl in d_8 -thf gives bipyNiMe_2 . When the

ochre solid and solid bipyridyl are placed in an NMR tube, even the solids mix and begin to turn green (characteristic of $(\text{bipy})\text{NiMe}_2$). Solvent (d_8 -thf) is transferred onto this at -196° , and the color change to green is complete when the thf melts (-65°C). Thus, the ligand replacement reaction to give $(\text{bipy})\text{NiMe}_2$ is extremely fast.

If a sample of the ochre solid in thf is kept at room temperature, there appears a good deal of brown-green precipitate and the resonance of $\delta(-0.83)$ in the proton NMR broadens and diminishes, the peak at $\sim\delta 0.0$ broadens, and a new peak at $\delta 0.85$ appears. I interpret this as the reductive elimination of ethane and deposition of metallic nickel.

These data indicate that the ochre solid produced in the above reaction is $\text{NiMe}_2 \cdot n(\text{pyr})$. The value of n is difficult to determine since excess pyridine is necessary in the preparation of the complex. These data also indicate that for practical purposes the complex may be considered the functional equivalent of simple dimethyl metal. The pyridine ligands are so loosely coordinated that they are easily displaced even in the solid state. Although the analogous pyridine-stabilized nickelacyclopentane has not been isolated, there is no apparent reason to believe that it cannot be. These pyridine-stabilized nickel alkyls will prove to be very useful in organonickel synthesis. Structural characterization and independent chemical studies will yield a good deal of information about the

character of "ligand-free" metal alkyls. It is curious and unexpected that the complex $(\text{pyr})_2\text{Ni}(\text{TMS})_2$ is the only complex of the form L_2NiR_2 (in which L_2 and R_2 are not chelating) which shows cis stereochemistry.⁶¹ It is not known whether this is due to selective crystallization, packing forces, etc., or to a distinct change in electronics about nickel. Chemical studies should help explain this.

4) Reaction of transphos with $(\text{pyr})_n\text{NiR}_2$

The reaction of transphos with $\text{NiMe}_2 \cdot n(\text{pyr})$ gave discouraging results. Treatment of the isolated organonickel complex with transphos is d_8 -thf led to the immediate (<20 minutes at -70°C) disappearance of the Ni-CH_3 resonances in the proton NMR. Concomitant with this is the growth of a resonance at $\delta(0.86)$ which may be assigned to ethane. A new peak at $\delta 10.1$ may be assigned to transphos bound to nickel.⁵⁷ After 8 hours at -70° and 15 minutes on $+60^\circ$, the resonance at $\delta(0.86)$ is the dominant peak in the proton spectrum. This peak could be assigned to the Ni-CH_3 resonance in $(\text{tp})\text{Ni}(\text{CH}_3)_2$, but for the absence of the expected phosphorus-hydrogen coupling.

These results indicated that it will be quite difficult to prepare organonickel complexes of transphos. Since the dimethyl nickel complex is so difficult to prepare, the metallacyclopentane complex is expected to be even more challenging.

The obvious problem with this trans-directing ligand is its great bulk. It must be that the ligand displaces

both pyridine units before complexing both phosphorus atoms to the metal. In future work, I suggest either performing the preparative ligand exchange reactions in neat pyridine or use of a different trans-directing ligand. Use of neat pyridine will cause trouble: (1) the high melting point forbids low temperature reactions, (2) the high boiling point makes removal difficult, and (3) unless all of the pyridine is removed from the reaction medium, there will still be ambiguity in assignment of the active nickel species in the reaction.

Replacement of the four bulky phenyl rings in transphos with methyl groups provides an attractive alternative trans-directing ligand. The "tetramethyl transphos" will be able to complex more easily to the nickel atom, allowing the ligand displacement to proceed at lower temperatures. Finally, there will be the obvious technical benefit of having the molecular weight of the trans-directing ligand reduced by 50%.

VI. Conclusions

The force behind and mechanism of the β - β' carbon-carbon bond cleavage reaction in the organic chemistry of nickel is still not understood. The possibility of stereoelectronic control in organometallic chemistry is very attractive and must be more thoroughly investigated. The carbon-carbon bond cleavage reaction in nickelacyclopentanes may be an example of a reaction which is so-controlled, but the question is technically difficult to answer.

Alkyl complexes of nickel whose stabilizing ancillary ligands are pyridine have been prepared, isolated and used in the synthesis of organonickel complexes having more complicated ligands. These ligand-replacement syntheses proceed at very low temperatures and are quite convenient. Generalization of the process described here will allow the formation of a variety of complicated organonickel complexes which have not been prepared to date.⁶⁶

Experimental

All operations involving organometallic complexes of nickel were carried out either in vacuo or under inert atmosphere. Toluene, diethyl ether, tetrahydrofuran, benzene and all hydrocarbon solvents were dried over sodium benzophenone ketyl and vacuum transfer distilled before use. Pyridine was dried over calcium hydride. $\text{Ni}(\text{COD})_2$ was either prepared via the published procedure,⁶² or purchased from Strem Chemicals and used without further purification. Tetrakis(pyridine)nickel dichloride was prepared as in the literature,⁶⁸ as were the bis(phosphine)nickel dihalides used in this study.⁶⁷ 1,4-dichlorobutene and 1,4-dibromobutane were dried over Linde 4A molecular sieves and vacuum-distilled before use. 2,2'-bipyridyl and 1,2 bis(diphenylphosphino)ethane were purchased (Aldrich Chemicals and Strem Chemicals, respectively) and used without further purification. Unless otherwise noted, all spectra were recorded at room temperature.

2,11-bis(diphenylphosphinomethyl)benzo[c]phenanthrene (7)

This compound was prepared via the literature route, although the following modifications of the aromatization step were attempted.

1) Aromatization with palladium on carbon.⁷⁰

1.0 g (3.8 mMole) of 2,11-dimethyl-5,6,6a,7,8,12b-hexahydrobenzo[c]phenanthrene, 17 g of naphthalene, 100 mg of palladium on carbon and 5 equivalents (based on

hydrocarbon) of indene were refluxed (218°C) for 20 hr. Thin layer chromatography (silica plates; pentane elution solvent), and proton NMR showed no aromatization at all.

2) Aromatization using triphenylmethyl cation.⁷¹

1.0 g (3.8 mMole) of 2,11-dimethyl-5,6,6a,7,8,12b-hexahydrobenzo[c]phenanthrene and 1.5 g triphenylmethyl-tetrafluoroborate were refluxed in glacial acetic acid until the initial yellow-brown reaction color is replaced with a bright burgundy and TLC indicates the absence of starting hydrocarbon. The reaction mixture was poured into water and extracted with benzene. The benzene extract was thoroughly washed and dried over MgSO_4 . Removal of solvent gave a crystalline solid which proved (by NMR) to be a mixture of triphenylmethene and the desired aromatic produced. Crystallization from benzene/ethanol (1:1) removed a good deal of $\phi_3\text{CH}$, but left a mixture of the two products of $\approx 1:1$ ratio. Chromatography (diethyl-ether, or benzene, or pentane or pentane/diethyl ether as eluting solvents) gave no separation at all. The two products co-sublime, thus sublimation/distillation was not effective in separation. Crystallization from ethanol, pentane, petroleum ether, diethyl ether, benzene or toluene gave little success. A low temperature crystallization from toluene gave a mixture of triphenylmethane/dimethylbenzo[c]phenanthrene of 1/3 (NMR).

Separation not being fruitful, the triphenylmethane impurity was carried through the bromination step.

Unfortunately, fickle bromination of the dimethyl hydrocarbon to give $-\text{CHBr}_2$ and $-\text{CH}_3$ are serious side reactions and accurate use of NBS is necessary, thus triphenylmethane (which is also brominated) led to a mixture of bromination products.

Even though the aromatization went to apparent completion, this method is not useful.

(2,2'-bipyridyl)nickelacyclopentane

This synthesis follows the method of Hagihara and coworkers.^{3a} 5.0 g (18 mMole) $\text{Ni}(\text{COD})_2$ and 5.7 g 2,2'-bipyridyl are degassed in a schlenk vessel. 75 ml cold (0°) THF is added, resulting in a fast (but not immediate) ligand replacement to give soluble, purple $(\text{bipy})\text{Ni}(\text{COD})$. After all of the $\text{Ni}(\text{COD})_2$ has reacted and the nickel species dissolved, 1.35 ml (2.4 g, 11 mMole) 1,4-dibromobutane is added all at once to the mixture. This mixture is stirred at 0° for approximately 3 hr. At this point, the purple solution has turned green and a good deal of precipitate (pink-colored $(\text{bipy})_3\text{NiBr}_2$) has separated. The solvent is removed (in vacuo, 0°C) to give a grey solid. This solid is washed with several aliquots of cold n-pentane to remove excess dibromobutane.⁷² The resulting grey solid is extracted with fresh tetrahydrofuran until the extracting solvent is colorless. In the absence of excess alkyl halide, the nickelacycle is stable at room temperature. Removal of solvent gives a powder which is crystallized from THF/pentane to give dark green (black)

crystals. Recrystallized yield 500 mg (21%). Spectra of this material are shown in the text.

Reaction of (bipy)Ni(CH₂)₄ with 1,2-bis(diphenylphosphino)ethane (dpe).

In an NMR sample tube, 12 mg (44 μMole) (bipy)Ni(CH₂)₄ and 22 mg (55 μMole) dpe were added to 300 μl dry toluene-d₈ at room temperature (sample prepared in an inert atmosphere box). There was a quick color change from green to yellow. This reaction seemed to be limited by the rate of dissolution of the fairly insoluble organo-nickel complex. After 15 minutes at room temperature, ¹H and ³¹P spectra were recorded. The proton spectrum showed free bipyridyl, free and complexed dpe (P-CH₂ at δ2.1), peaks at δ1.85 and δ1.67 which have been assigned⁴¹ to the ring protons in (dpe)Ni(CH₂)₄, and peaks in the alkyl and vinyl regions consistent with 1-butene. The (proton-decoupled) ³¹P NMR spectrum shows free phosphine, and (dpe)₂Ni(O) and (dpe)Ni(CH₂)₄ in a ratio of ~20:1. These resonances are consistent with those of independently prepared samples of (dpe)₂Ni(O) (from Ni(COD)₂ and dpe) and (dpe)Ni(CH₂)₄ (from (dpe)NiCl₂ and 1,4-dilithiobutane).

Thermolysis of this sample (+70°, 36 hours) gave complete conversion to (dpe)₂Ni(O) (³¹P NMR). The protons in cyclobutane (the reported organic product of thermolysis), the ethylene protons in dpe and the methyl protons of toluene appear at ~ δ2.0 in the proton NMR so assignment of the organic products of this decomposition

is not possible using proton NMR, but the resonances assigned to the ring protons in $(dpe)Ni(CH_2)_4$ are absent in the thermolyzed sample.

Reaction of transphos with $(bipy)Ni(CH_2)_2$

Transphos (7; 36 mg, 58 μ Mole) and $(bipy)Ni(CH_2)_4$ (8 mg, 30 μ Mole) were added to an NMR tube (sample prepared in inert atmosphere box). Tetrahydrofuran- d_8 (0.5 ml) was vacuum-distilled into this tube which was subsequently sealed. Immediately upon the melting of solvent, the ^{31}P and 1H NMR spectra were recorded. The ^{31}P spectrum showed a large peak (free transphos) plus a small impurity (the phosphine-oxide) in a ratio of 220:1. The proton spectrum showed only unreacted starting materials and a small unidentified impurity at $\delta(0.13)$. The reaction was monitored periodically for two weeks, during which time the color of the reaction mixture changed very slowly from bright green to red-brown. At commensurate rates, a new resonance in the ^{31}P -NMR (20.5 ppm downfield from free transphos) and resonances due to 1-butene in the proton NMR appear. (A third ^{31}P resonance (34.3 ppm downfield from free transphos) appeared after the first day of reaction, but did not grow in size and represented only ~3% of the entire phosphorus spectrum, hence it is unimportant.) During the course of two weeks, the signal due to free transphos both broadened and lost intensity until it disappeared altogether. At the end of two weeks, no free phosphine was observed in the ^{31}P NMR and only a

small amount remained in the proton NMR. At this time, the proton NMR showed small peaks due to $(bipy)Ni(CH_2)_4$ which remained, a large amount of 1-butene and a new broad peak in the alkyl region which is relatively small and may be assigned to n-butane. This reaction is therefore not of synthetic utility in this case.

Preparation of $(bipy)NiMe_2$ from $(pyr)_4NiCl_2$ and methylmagnesium halide.

Tetrakis(pyridine)nickel dichloride (1.0 g, 2.2 mMole), 20 ml dry THF and 4 ml dry pyridine were added to a schlenk vessel which had previously been purged with argon. The suspension was cooled to $-70^\circ C$. Slowly (over the space of 3-5 minutes) 11 ml of a 0.64 M THF solution of methylmagnesium chloride was delivered (via syringe) into the reaction vessel. There was an immediate color change from aquamarine to pale yellow-green. The reaction was allowed to warm to $-20^\circ C$ which vigorous stirring was maintained. The reaction was stirred at -20° until the inorganic starting material was no longer evident. This gave a rich orange-colored suspension. The mixture was cooled to -70° and 230 μl degassed isopropanol was added to quench any unreacted Grignard reagent.⁷³ Stirring was maintained until gas-evolution ceased.

2,2'-bipyridyl (0.6 g; 3.8 mMole) was degassed, then dissolved in 5 ml dry tetrahydrofuran. This solution was cooled to -40° and then transferred via syringe to the $(pyr)_n NiMe_2$ reaction mixture which was kept at -70° .

Immediately a color change was apparent. The -70° bath was replaced with a -20° bath and the reaction mixture stirred at this temperature until the color change was apparently complete (1-2 hr).

The solvent was removed in vacuo from this green suspension. The bipyNiMe_2 was extracted from the resulting grey solution with 20 ml refluxing benzene. Hot filtration gave a dark green homogeneous solution from which purple-black needles form. After cooling ($\sim +10^{\circ}$) the crystalline product was isolated and washed several times with n-pentane and dried in vacuo. Recrystallized yield 116 mg (22%). Proton NMR in acetone- d^6 : $\delta 7.65$ (integral = 2.0, bipyridyl), $\delta 8.2$ (integral = 4, bipyridyl), $\delta 9.05$ (integral = 2, bipyridyl), $\delta 0.0$ (integral = 6, Ni- CH_3).

Preparation of $(\text{dpe})\text{NiMe}_2$ from $(\text{pyr})_4\text{NiCl}_2$ and methyl-magnesium halide.

The same procedure was used here as was used to prepare $(\text{bipy})\text{NiMe}_2$, the only change being that, owing to solubility the dpe ligand was added to the $[(\text{pyr})_n\text{NiMe}_2]$ as a solution in toluene rather than thf. The crude material was purified using the literature procedure.⁶⁴ This resulted in the isolation of 210 mg of material whose spectra were identical to those of independently prepared dpeNiMe_2 and $(\text{dpe})_2\text{Ni}$. The dpeNiMe_2 was contaminated by 10% with $(\text{dpe})_2\text{Ni}$ (based on ^{31}P NMR).

Preparation of (bipy)Ni(CH₂)₄ from (pyr)₄NiCl₂ and
Di-Grignard reagent.

The preparation of 1,4-dibromomagnesiumbutane followed literature methods.^{48,62}

Tetrakis(pyridine)nickeldichloride (1.0 g, 2.2 mMole) was suspended in 15 ml tetrahydrofuran and 2 ml pyridine. This mixture was cooled to -70°. A solution of 1,4-dibromomagnesiumbutane (33 ml, 0.1 M solution) was added slowly to the well-stirred suspension. The reaction was allowed to warm slowly to -10°. When all of the (pyr)₄-NiCl₂ had reacted, the mixture was cooled to -70° and 180 µl degassed isopropanol was added. A solution of 0.7 g bipyridyl in 5 ml tetrahydrofuran was added to this cooled mixture which was subsequently allowed to warm to -30° until the color change (orange-to-green) was complete. Most of the solvent was removed in vacuo at room temperature. The resulting slurry was washed with 2x50 ml dry pentane. The dried solid was extracted with toluene at +40° until the extractions were colorless. The solvent was removed from this extracted material. Two recrystallizations (toluene/pentane) gave 60 mg (10%) (bipy)Ni(CH₂)₄. This sample gave proton spectra identical to the material prepared from Ni(COD)₂, 1,4-dibromobutane and bipyridyl.

Attempted preparation of (bipy)NiEt₂ from (pyr)₄NiCl₂ and ethylmagnesium chloriate.

The preparation of (bipy)NiEt₂ using the ligand replacement on (pyr)_nNiEt₂ was attempted several times. In each case a procedure similar to that described above for (dpe)NiMe₂, (bipy)NiMe₂ and (bipy)Ni(CH₂)₄ was used, with small variations. In each case, the ligand replacment appeared to proceed properly, giving the expected orange-to-green color change. In each case, however, decomposition to a pale brown material occurred during the work-up of the reaction. The green suspension is stable, even at room temperature; therefore, the product is isolable, but appears to be much more sensitive than the dimethyl complex.

Reaction of methylmagnesium bromide with tpNiCl₂

The synthesis of (tp)NiCl₂ is reported.⁵⁷ A suspension of this material (100 mg, 0.13 mMole, in 5 ml tetrahydrofuran) was cooled to -60°. Methylmagnesium bromide (1.6 ml of 0.64 M solution in tetrahydrofuran) was added over 10 minutes. The mixture was stirred, warming slowly to room temperature. The purple suspension reacted to give a bright red solution. When no tpNiCl₂ was apparent, the mixture was cooled to -60° and 60 µl of degassed isopropanol added to quench the excess Grignard. Solvent was removed to give a sticky orange solid which was extracted with 5 ml benzene. This extract was filtered through a celite pad to give a clear homogeneous red-orange

solution. Removal of solvent in vacuo gave a vermillion powder. The ^1H NMR and ^{31}P NMR spectrum of this powder are shown in Figure 1.

Preparation of $(\text{pyr})_n\text{NiMe}_2$

Tetrakis(pyridine)nickeldichloride (1.0 g, 2.2 mMol) was degassed in a schlenk vessel. Solvent (75 ml diethyl ether/7 ml pyridine) was added to this. The suspension was stirred and cooled to -40° . Methylmagnesium-chloride (4.0 ml of a 2.9 M solution in tetrahydrofuran) was added dropwise to the mixture. After the addition was complete, the mixture was warmed to 0° and stirred vigorously until the $(\text{pyr})_4\text{NiCl}_2$ had reacted (circa 3 hr). The mixture was cooled to -10° and 2 ml of dry (sieves), degassed trimethylsilylchloride was added. After stirring for 15 minutes, the mixture was filtered under argon through a chilled frit. This gave a red-orange solution and a very pale solid. The solid was extracted once with 25 ml diethyl ether/5 ml pyridine. Filtration and combination of filtrates gave a bright orange solution and colorless powder (MgX_2 , discarded). The solvent was removed to give a pasty yellow-red solid. This solid was washed with pentane (0°) and dried in vacuo. The proton NMR of this product is shown in Figure 8.

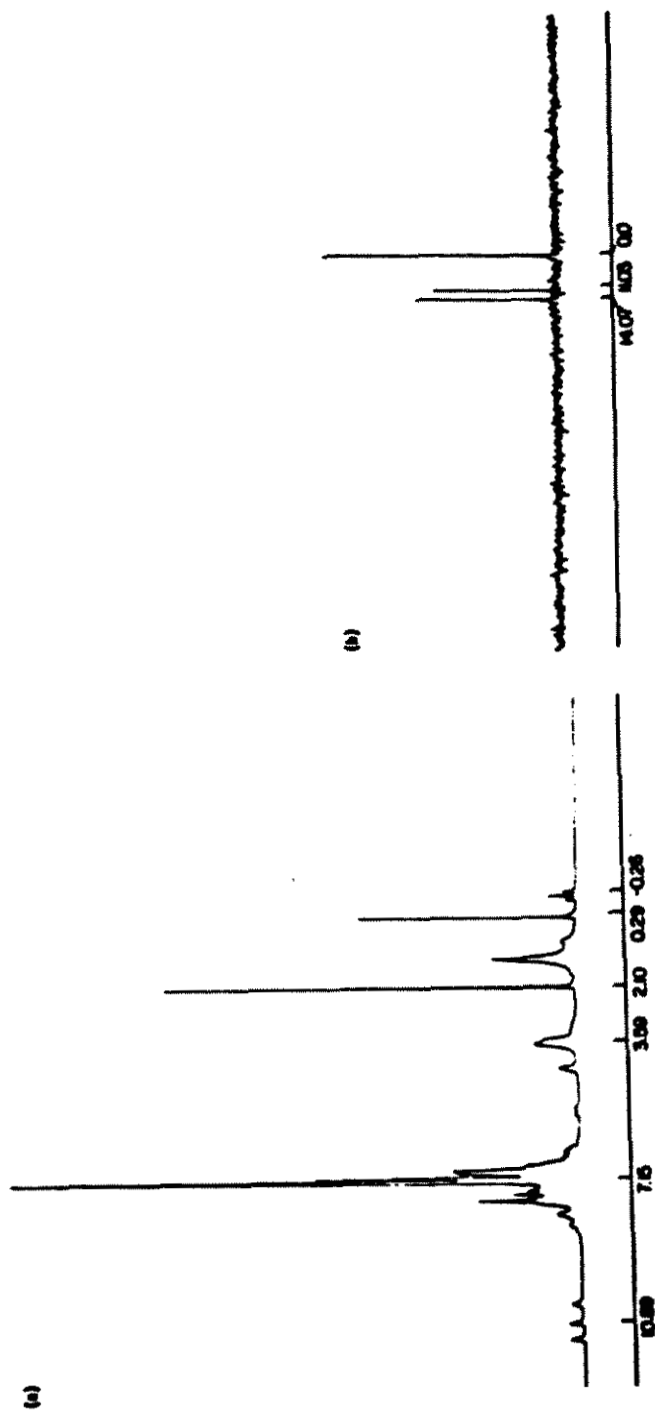


Figure 1. NMR spectra (JEOL FX-90Q; C_6D_6 solvent) of the products of the reaction: transphos + excess $MeHgBr$. (a) 1H , shifts relative to C_6D_5H at δ 7.15. (b) ^{31}P , shifts relative to free transphos at δ 0.0.

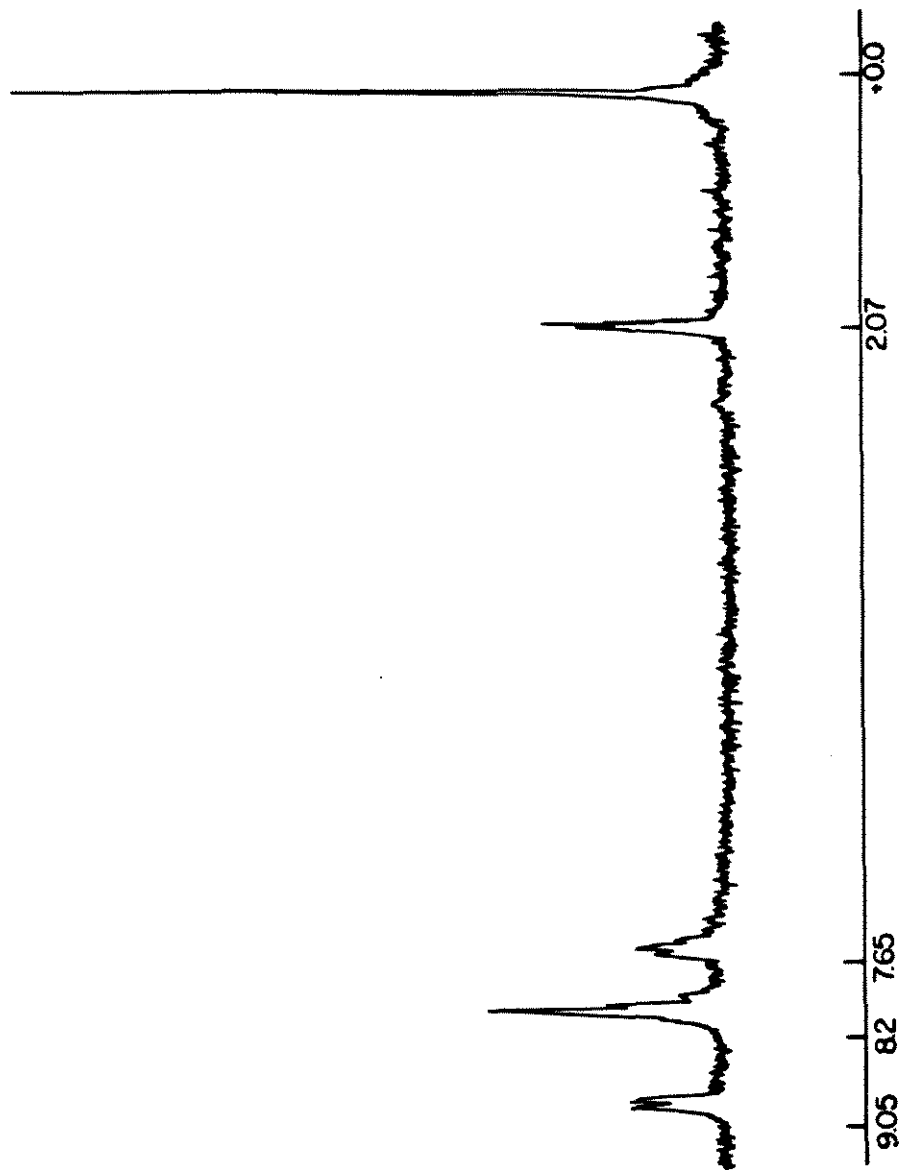


Figure 2. ^1H NMR spectrum (EM-390; d_6 -acetone solvent) of $(\text{bipy})\text{NiMe}_2$. Shifts relative to residual proton in d_6 -acetone at $\delta 2.07$.

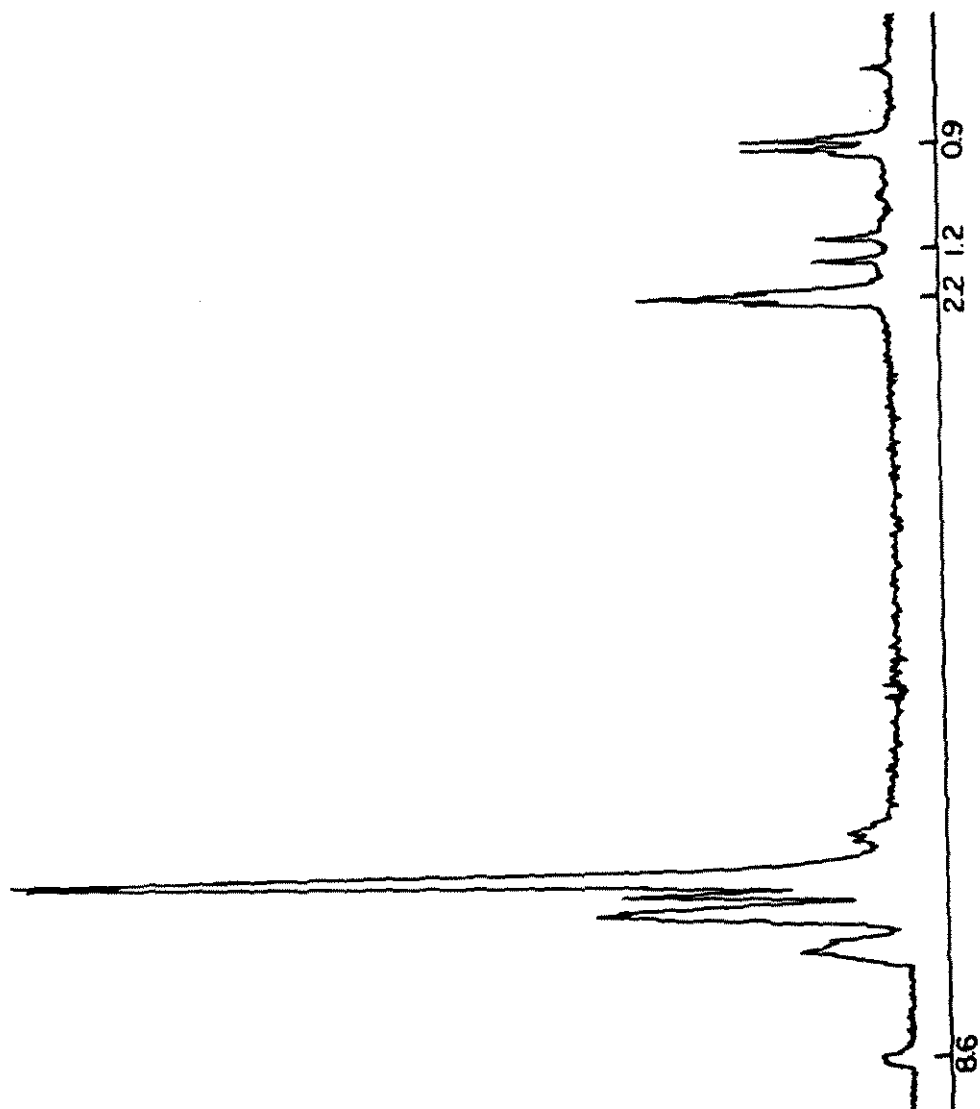


Figure 3. ^1H spectrum (JEOL FX-90Q; C_6D_6 solvent) of $(\text{dpe})\text{NiMe}_2$. Shifts relative to $\text{C}_6\text{D}_5\text{H}$ at $\delta 7.15$.

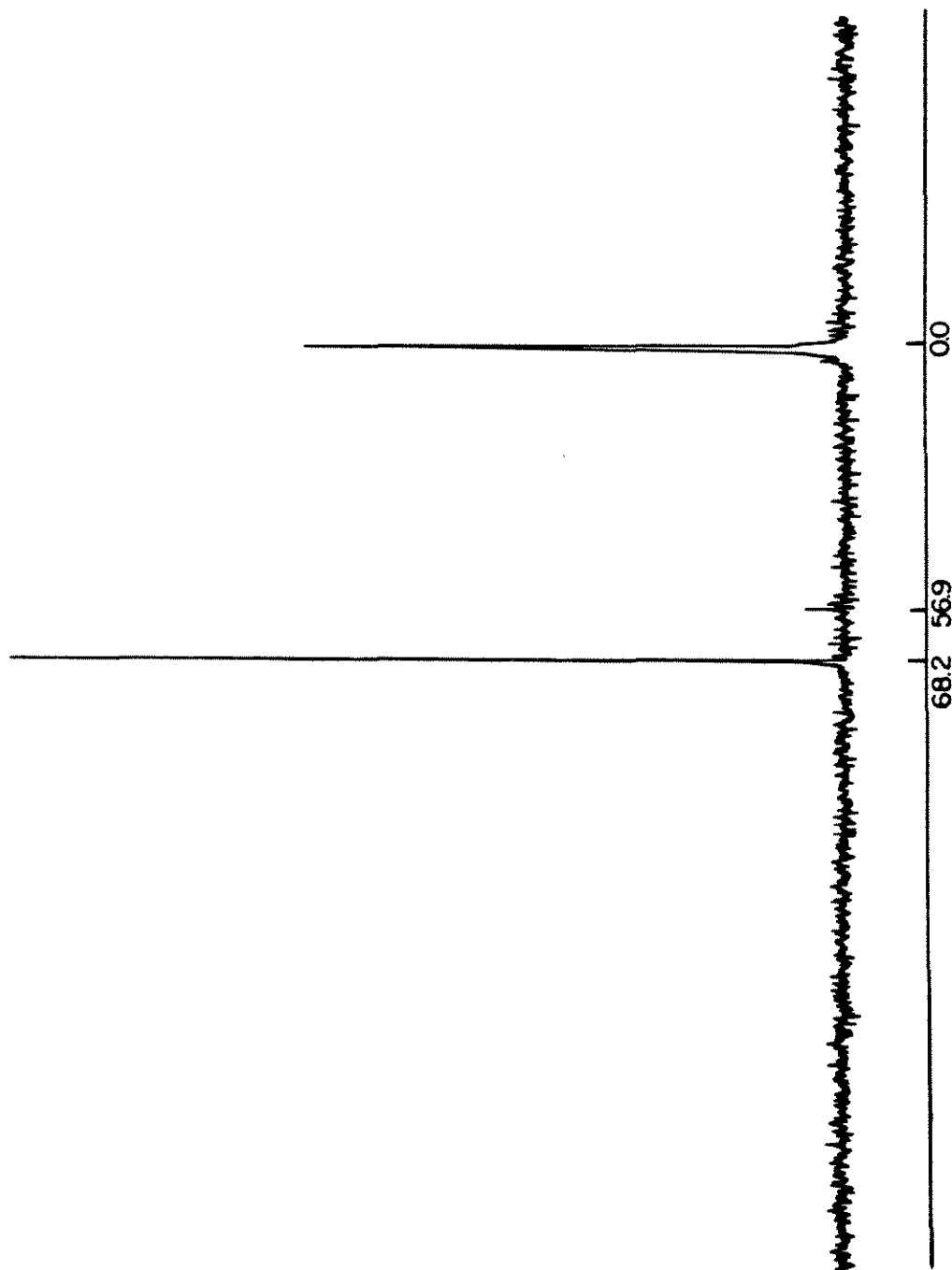


Figure 4. ^{31}P NMR spectrum (FX-90Q; C_6D_6 solvent) of $(\text{dpe})\text{NiMe}_2$. Shifts relative to free dpe at 60.0.

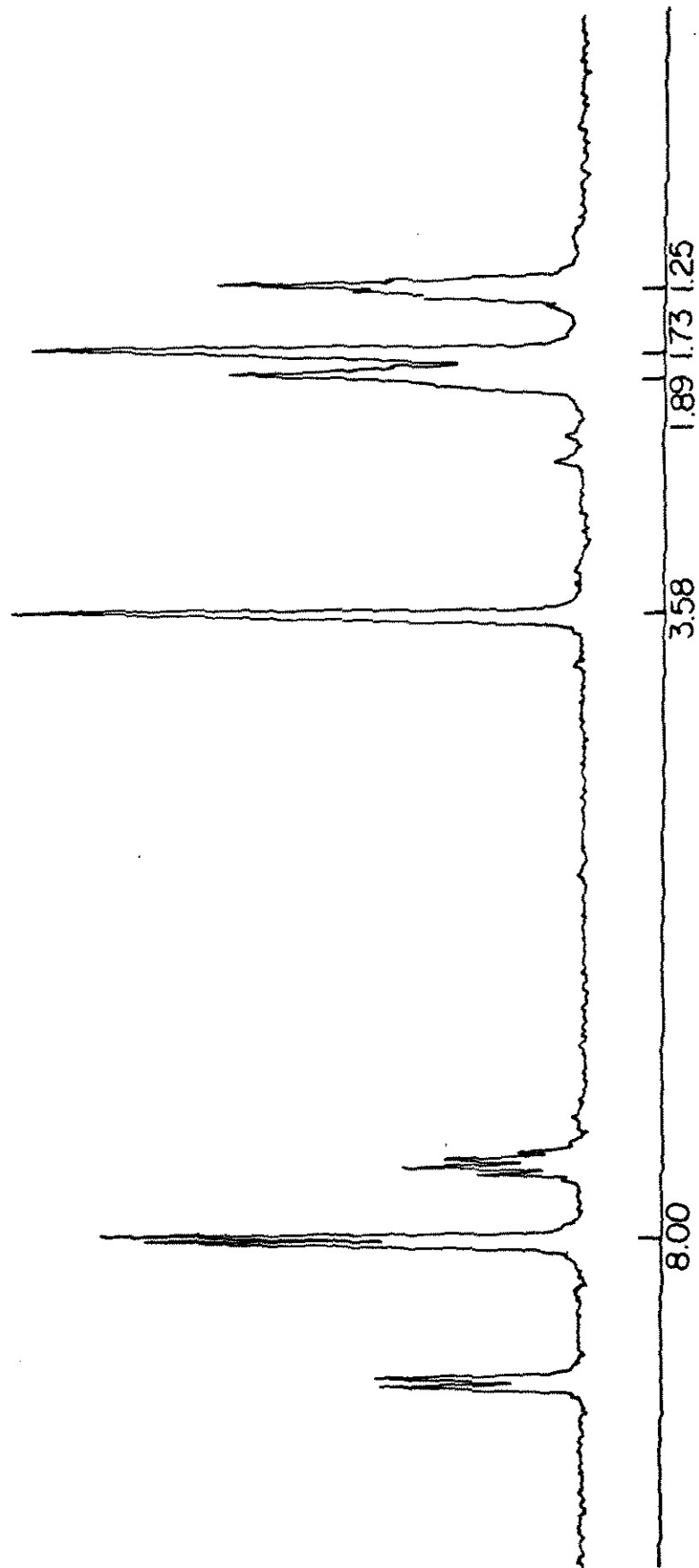


Figure 5. ^1H NMR spectrum (JEOL FX-90Q; d_8 -thf solvent) of (bipy)nickelcyclopentane. Shifts relative to residual protons in the solvent.



Figure 6. Spectrum from Figure 5. Here the signal at $\delta 1.89$ was decoupled from the remainder of the spin system.

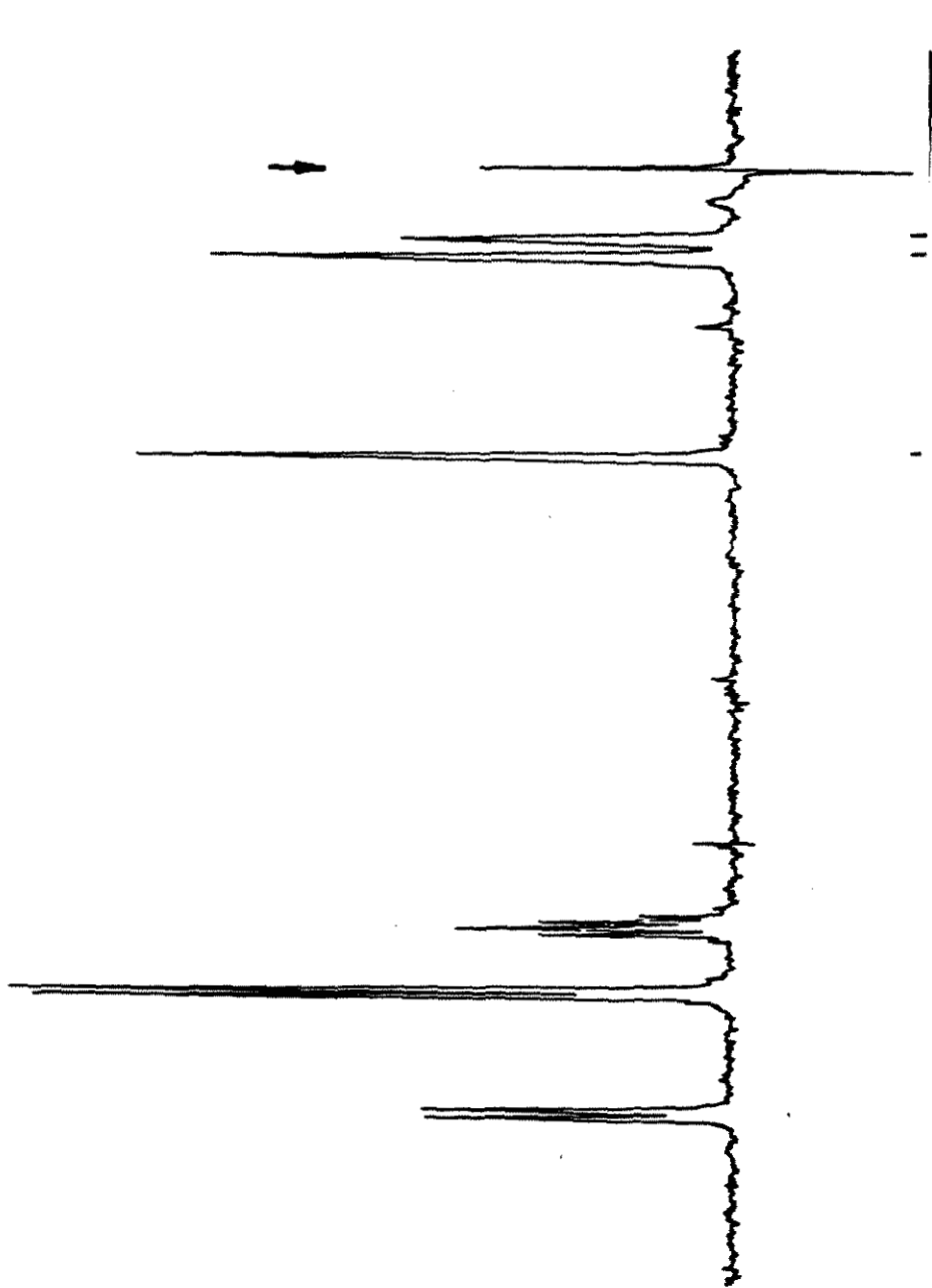


Figure 7. Spectrum from Figure 5. Here the signal at $\delta 1.25$ was decoupled from the remainder of the spin system.

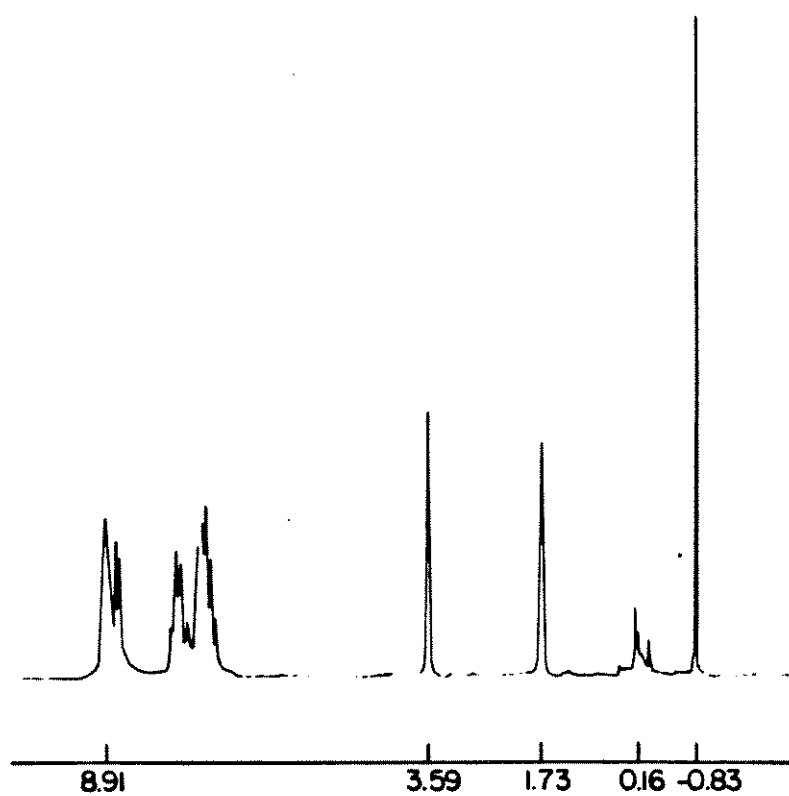
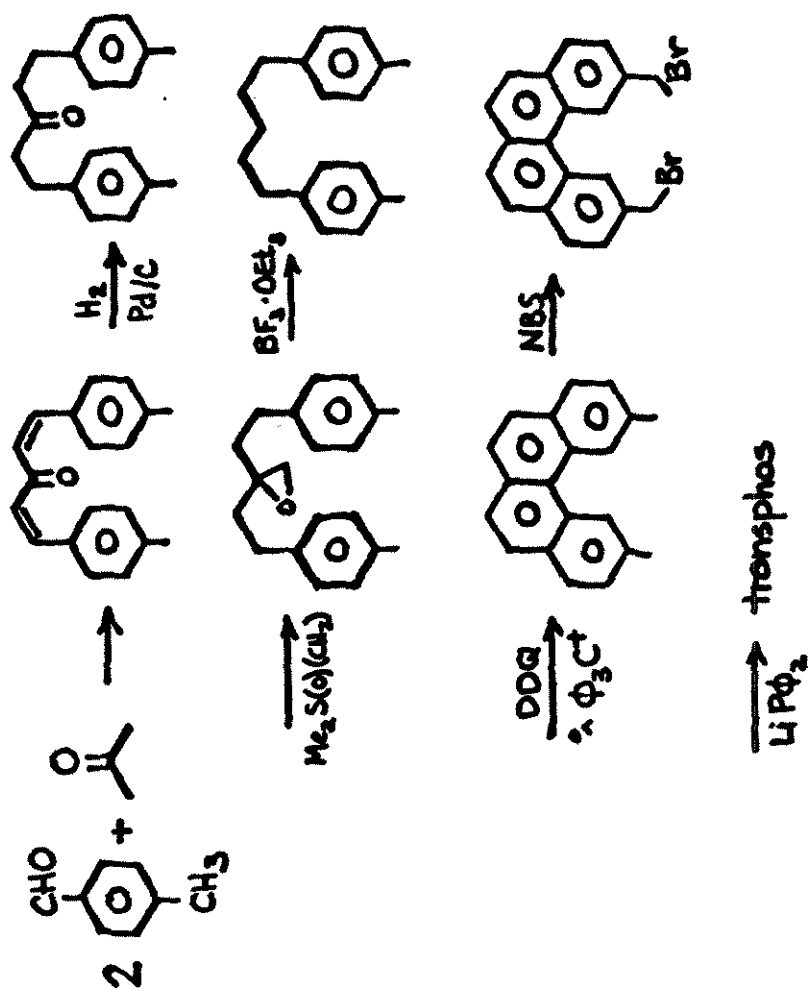


Figure 8. ^1H spectrum (JEOL FX-90Q, d_8 -thf solvent) of $(\text{pyr})_n\text{NiMe}_2$. All shifts are relative to the residual protons in the solvent. Signal at ≈ 0.0 are due to silyl impurities remaining after the TMSCl quench.



Scheme 1. The synthesis of 2, 11-bis(diphenylphosphinomethyl)benzo[c]phenanthrene

REFERENCES

1. P. W. Jolly and G. Wilke, "The Organic Chemistry of Nickel", Academic Press, N.Y., 1974 (V. 1), 1975 (V. 2).
2. G. W. Parshall, "Homogeneous Catalysis", Wiley-Interscience, N.Y., 1980.
3. S. Takahashi, Y. Suzuki and N. Hagihara, Chem. Lett., 1974, 1363. (b) M. F. Semmelhack, Org. Reactions, 1972, 19, 115-198. (c) M. F. Semmelhack, P. M. Helquist and J. D. Gorzynski, J. Am. Chem. Soc., 1972, 94, 9234-9236. (d) M. F. Semmelhack, P. M. Helquist and L. D. Jones, J. Am. Chem. Soc., 1971, 93, 5908-5910. (e) M. F. Semmelhack and S. J. Brickner, J. Am. Chem. Soc., 1981, 103, 3945-3947.
4. T. Yamamoto, J. Ishizu, T. Kohara, S. Komiya and A. Yamamoto, J. Am. Chem. Soc., 1980, 102, 3758-3764; see also reference 6.
5. G. Wilke and H. Schott, Angew. Chem. Int. Ed. Engl., 1966, 5, 583.
6. Chapter 3 of this thesis.
7. (a) P. Binger, M. J. Doyle, J. McMeeking, C. Krüger and Y.-H. Tsay, J. Organomet. Chem., 1977, 135, 405-414. (b) P. Binger and M. J. Doyle, J. Organomet. Chem., 1978, 162, 195-207.
8. (a) J. K. Kochi, "Organometallic Mechanisms and Catalysis", Academic Press, N.Y., 1978; Section 7.IV. (b) J. J. Low and W. A. Goddard, III., to be published.

9. J. P. Collman and L. S. Hegedus, "Principles and Applications of Organotransition Metal Chemistry", University Science Books, Mill Valley, CA, 1980, Chapter 4.
10. L. H. Sommer, J. G. Lyons and H. Fujimoto, J. Am. Chem. Soc., 1969, 91, 7051; see also reference 13.
11. A. E. Jukes, Adv. Organomet. Chem., 1974, 12, 215-322.
12. T. T. Tsou and J. K. Kochi, J. Am. Chem. Soc., 1979, 101, 6319-6332.
13. E. Uhlig and D. Walther, Coord. Chem. Rev., 1980, 33, 3.
14. D. R. Fahey, Organometal. Chem. Rev., 1972, 7, 245-294; see also reference 34 and reference 19.
15. K. Tatsumi, R. Hoffmann, A. Yamamoto and J. K. Stille, Bull. Chem. Soc. Japan, 1981, 54, 1968.
16. C. A. Tolman, Chem. Rev., 1977, 77, 313-348.
17. F. Ozawa, T. Ito, Y. Nakamura and A. Yamamoto, Bull. Chem. Soc. Japan, 1981, 54, 1868-1880.
18. M. Almemark and B. Akermark, J. Chem. Soc., Chem. Comm., 1978, 66.
19. T. Yamamoto and A. Yamamoto, J. Organomet. Chem., 1973, 57, 127-137.
20. T. Yamamoto, A. Yamamoto and S. Ikeda, J. Am. Chem. Soc., 1971, 93, 3350-3359.
21. T. Ikariya, personal communication.

22. K. Fischer, J. Jonas, P. Misbach, R. Stabba and G. Wilke, Angew. Chem. Int. Ed. Engl., 1973, 12, 943-1026. (b) B. Bogdanovic, B. Henc, H.-G. Karmann, H. G. Nüssel, D. Walter and G. Wilke, Ind. and Eng. Chem., 1970, 62, 34-44.
23. (a) E.-I. Negishi, Accts. Chem. Res., 1982, 15, 340.
(b) D. G. Morrell and J. K. Kochi, J. Am. Chem. Soc., 1975, 97, 7262-7270.
24. A. Wojcicki, Adv. Organometallic Chem., 1973, 11, 88-145.
25. T. C. Flood, J. E. Jensen and J. A. Statler, J. Am. Chem. Soc., 1981, 103, 4410-4414.
26. J. Ashley-Smith, M. Green and F. G. A. Stone, J. Chem. Soc. (A), 1969, 3019-3023.
27. P. Binger, personal communication.
28. B. Åkermark, H. Johansen, B. Roos and U. Wahlgren, J. Am. Chem. Soc., 1979, 101, 5876-5883.
29. Chapter 2 of this thesis.
30. C. A. Tolman, J. Am. Chem. Soc., 1972, 94, 2994-2999.
31. Reference 2, Chapter 6.
32. R. H. Crabtree, M. F. Mellea and J. M. Quirk, J. Chem. Soc., Chem. Commun., 1981, 1217-1218.
R. H. Crabtree, J. M. Mihelcik and J. M. Quirk, J. Am. Chem. Soc., 1979, 101, 7738-7740.
33. F. Ozawa, T. Ito and A. Yamamoto, J. Am. Chem. Soc., 1980, 102, 6457-6463.
34. T. Saito, Y. Uchida, A. Misono, A. Yamamoto, K. Morifuji and S. Ikeda, J. Am. Chem. Soc., 1966, 88, 5198-5201.

35. P. L. Watson and D. C. Roe, J. Am. Chem. Soc., 1982, 104, 6471-6473.
36. J. X. McDermott, M. E. Wilson and G. M. Whitesides, J. Am. Chem. Soc., 1976, 98, 6529-6536.
37. S. A. Cohen, P. R. Auburn and J. E. Bercaw, J. Am. Chem. Soc., 1983, 105, 1136-1143.
38. D. R. McAlister, D. K. Erwin and J. E. Bercaw, J. Am. Chem. Soc., 1978, 100, 5966-5968.
39. R. Schrock, S. McLain and J. Sanchi, Pure and Appl. Chem., 1980, 52, 729-732. S. J. McLain, C. D. Wood and R. R. Schrock, J. Am. Chem. Soc., 1979, 101, 4558-4570.
40. (a) Reference 1, Volume 2, page 365.
(b) Reference 4.
41. R. H. Grubbs, A. Miyashita, M. Liu and P. Burk, J. Am. Chem. Soc., 1978, 100, 2418-2425.
42. (a) P. Cossee, Recueil, 1966, 85, 1151-1160.
(b) J. Boor, Jr., Macromol. Rev., 1967, 2, 115-268.
(c) J. Soto, M. L. Steigerwald and R. H. Grubbs, J. Am. Chem. Soc., 1982, 104, 4479-4480.
43. P. Pino and R. Mülhaupt, Angew. Chem. Int. Ed. Engl., 1980, 19, 857-875.
44. A. H. Janowicz and R. G. Bergman, J. Am. Chem. Soc., 1983, 105, 3929-3939.
45. (a) J. Allison, R. B. Freus and D. P. Ridge, J. Am. Chem. Soc., 1979, 101, 1332-1333. (b) D. B. Jacobson and B. S. Freiser, J. Am. Chem. Soc., 1983, 105, 736-742.
(c) L. F. Halle, P. B. Armintrout and J. L. Beauchamp, Organometallic, 1982, 1, 963-968.

46. The kinetics of this process have been described.
K. C. Ott, personal communication.
47. F. Ozawa, A. Yamamoto, T. Ikariya and R. H. Grubbs,
Organometallics, 1982, 1, 1481-1485.
48. (a) J. X. McDermott, J. F. White and G. M. Whitesides,
J. Am. Chem. Soc., 1976, 98, 6521-6528. (b) G. B. Young
and G. M. Whitesides, J. Am. Chem. Soc., 1978, 100,
5808-5815.
49. C. E. Moore, "Atomic Energy Levels", National Bureau
of Standards NSRDS 35, Government Printing Office,
Washington, D.C., 1971.
50. F. A. Cotton and G. Wilkinson, "Advanced Inorganic
Chemistry", 4th Ed., Wiley-Interscience, N.Y., 1980.
51. Reference 1, Volume 1, Chapter 4; see reference 6
for the only exception.
52. (a) M. L. Steigerwald and W. A. Goddard, III.,
unpublished results. (b) M. Blomberg, U. Brandemark,
L. Petterson and P. Siegbahn, personal communication.
53. The ³¹P NMR spectrum of a mixture of bis(triphenyl-
phosphine)nickelacyclopentane and free triphenyl shows
no exchange of phosphine between the two sites.
54. (a) L. M. Venanzi, Pure and Appl. Chem., 1980, 52,
1117-1129. (b) F. Bachechi, L. Zambonelli and
L. M. Venanzi, Helv. Chim. Acta, 1977, 60, 2815-2823.
55. A. Gillie and J. K. Stille, J. Am. Chem. Soc., 1980, 102,
4933.

56. N. J. DeStefano, D. K. Johnson, R. M. Lane and L. M. Venanzi, Helv. Chim. Acta., 1976, 59, 2674-2682.
57. N. J. DeStefano, D. K. Johnson and L. M. Venanzi, Helv. Chim. Acta., 1976, 59, 2683-2690.
58. T. Kohara, T. Yamamoto and A. Yamamoto, J. Organomet. Chem., 1980, 192, 265-274.
59. M. J. Doyle, J. McMeeking and P. Binger, J. Chem. Soc., Chem. Comm., 1976, 376-377.
60. E. Dinjus, I. Gorski, E. Uhlig and H. Walther, Z. Anorg. Allg. Chem., 1976, 422, 75-79.
61. E. Carmona, F. Gonzáles, M. L. Poveda, J. L. Atwood and R. D. Rogers, J. Chem. Soc. Dalton, 1981, 777-782.
62. (a) C. D. Nenitzesen and I. Necsoiu, J. Am. Chem. Soc., 1950, 72, 3483-3486. (b) I. T. Millar, H. Heaney, Quart. Rev. Chem. Soc., 1950, 11, 109-120.
63. G. Wilke and G. Herrmann, Angew. Chem. Int. Ed. Engl., 1966, 5, 581.
64. M. L. H. Green and M. J. Smith, J. Chem. Soc. (A), 1971, 639-641.
65. The multiplet at $\delta(0.0)$ is due to unremoved silyl products of the trimethylsilyl quench. Later studies found these contaminants to be innocuous and easily removable.
66. (a) J. W. F. L. Seetz, F. A. Hartog, H. P. Böhm, C. Blomberg, O. S. Nekerman and F. Bickelhaupt, Tet. Lett., 1982, 23, 1497-1500. (b) L. C. Costa and G. M. Whitesides, J. Am. Chem. Soc., 1977, 99, 2390-2391.

67. Reference 3b, p. 178.
68. F. Reizenstein, Z. Anorg. Chem., 1896, 11, 254.
69. (a) L. M. Venanzi, J. Chem. Soc., 1958, 719-724.
(b) C. R. C. Coussmaker, M. H. Hutchinson, J. R. Mellor, L. E. Sutton and L. M. Venanzi, J. Chem. Soc., 1961, 2705-2713. (d) P. J. Stone and Z. Dori, Inorg. Chem. Acta, 1971, 5, 434-438.
70. P. P. Fu and R. G. Harvey, Chem. Rev., 1978, 78, 317-336.
71. P. P. Fu and R. G. Harvey, Tet. Lett., 1974, 3217-3220; and references.
72. Complexes of the form $(\text{bipy})\text{Ni}(\text{R}_1)(\text{R}_2)$ are known to react with $\text{R}'\text{-X}$ to give $\text{R}_1\text{-R}'$ and $\text{R}_2\text{-R}'$.
(a) S. Takahashi, Y. Suzuki, K. Sonogashira and N. Hagihara, J. Chem. Soc., Chem. Comm., 1976, 839-840.
(b) Reference 7b. This reaction is observed to proceed at $0^\circ - 25^\circ$; hence, the preparation of $(\text{bipy})\text{Ni}(\text{CH}_2)_4$ from $\text{Ni}(\text{COD})_2$ and $\text{Br}(\text{CH}_2)_4\text{Br}$ is something of an art.
73. Failure to quench the Grignard reagent is particularly detrimental when bipyridyl is introduced to the reaction, owing to the rapid formation of the radical anion $[\text{bipy}]^{\cdot-}$. (a) W. Kaim, J. Organomet. Chem., 1981, 222, C17-C20. (b) E. C. Ashby, A. B. Gock and R. N. DePriest, J. Am. Chem. Soc., 1980, 102, 7779-7780.

**Chapter 7. Concerning the Mechanism of Ziegler-Natta Polymerization
of Simple Olefins.**

Concerning the Mechanism of Ziegler-Natta Polymerization: Isotope Effects on Propagation Rates

Jorge Soto, Michael L. Steigerwald, and Robert H. Grubbs*

Contribution No. 6591 from the Laboratories of Chemistry
California Institute of Technology
Pasadena, California 91125

Received January 25, 1982

Ziegler-Natta polymerization, a major industrial organometallic process, is poorly understood at the molecular level. Several sets of molecular descriptions have been proposed for this reaction which differ fundamentally from one another.¹⁻⁴ The source of this disagreement is the very mode of carbon-carbon bond formation. Before the more subtle distinctions between and within these sets of mechanisms can be elucidated, this most crucial and elementary aspect of the polymerization process must be understood.

Two of the most clearly defined proposals among the many sets suggested are the carbene-to-metallacycle mechanism of Green and Rooney⁵ (Scheme 1, a) and the direct four-center olefin insertion mechanism of Cossee and Arlman (Scheme 1, b).⁷ Neither of these schemes is inconsistent with the known kinetic and stereochemical aspects of the process,⁶ and known reactions have been cited as models in justifying each step of both proposals.⁷⁻¹⁰ The important difference between the two suggestions is the involvement of hydrogen migration in a (Scheme 1). This mobility implies a large primary kinetic isotope effect on chain propagation in a and related reactions but no such effect in b. In this paper we report our efforts to determine this isotope effect and conclude that if such an effect exists it is quite small.

Earlier workers have examined¹¹ the rates of polymerization of C₂D₄ and C₂H₄ and concluded these rates are the same. However, this work allows for k_H/k_D of between 0.7 and 1.4. Since isotope effects on the rate of catalyst generation were also observed even wider variations can not be ruled out.

Recent studies provide values expected for titanocene systems that involve carbenoid intermediates. The abstraction of an α hydrogen by an aluminum alkyl is modeled by the formation of Cp₂TiCH₂Al(CH₃)₂Cl from Cp₂TiCl₂ and (CH₃)₃Al.¹² The isotope effect for this reaction is 3. Other related α abstractions fall between 3 and 3.5.¹³ Even if the α -hydrogen migration is not a part of the rate-determining step, the reverse of eq 3 provides an expected secondary isotope effect for reactions involving titanium carbene intermediates. The secondary isotope effect determined in these systems is large, ranging from 1.2 to 1.4.¹⁴ Since few models exist for direct insertion into a metal-carbon bond, good values are not available. However, since this reaction does not involve hydrogen migration or major hybridization

Scheme 1.

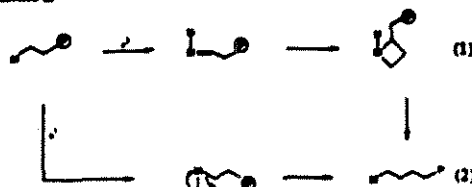


Table I. Relative Concentration of *n*-Alkanes from Ethylene-d₂:Ethylene-d₀ Mixtures

<i>n</i> -alkane produced	<i>d₂:d₀</i>			
	1:0	1.03:1	0:1	1.03:1
C ₁₁	1.00	1.00	1.00	1.00
C ₁₂	1.43	1.34	1.06	1.19
C ₁₃	2.18	1.38	1.03	1.31
C ₁₄	1.55	1.24	0.89	1.06
C ₁₅	1.21	1.08	0.87	0.81
C ₁₆	1.04	0.99	0.67	0.67

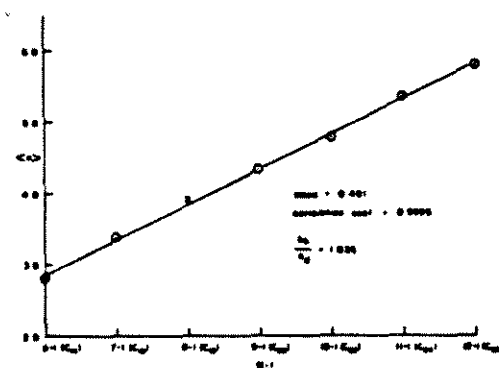
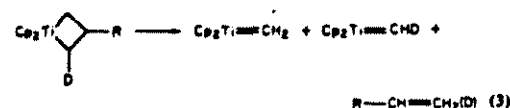


Figure 1. Average number of C₂D₄ units, (*n*), as a function of total number of monomer units, *N*, in an oligomer.



changes at the growing polymer terminus, we expect $k_H/k_D \approx 1$ for this process.

In these catalytic systems, as well as many other, comparisons between different polymerization runs are dangerous, owing to a lack of absolute reproducibility from one preparation to the next. Furthermore, the concentration of the active sites can be affected by the monomer (as in Shilov's study), and in some systems the catalytic activity is diffusion limited. Consequently, experiments designed for precise isotope-effect measurements must be copolymerizations. Due to the ease of analysis and the availability of homogeneous catalyst systems, the polymerization of ethylene and perdeuterioethylene was chosen for study. So that precise measurements on the copolymers could be obtained, the reaction was studied by using a stopped-flow apparatus similar to that developed by Fink and co-workers.¹⁵ Suitable conditions were developed to obtain sufficient material of the C₂H₄ to C₂₀H₄₀ molecular weight range for GC/MS-Cl analysis.¹⁴

(1) Cossee, P. *J. Catal.* 1964, 3, 80-82; Arlman, E. J. *Ibid.* 1964, 3, 89-96; Arlman, E. J.; Cossee, P. *Ibid.* 1964, 3, 99-104.

(2) McKinney, R. J. *J. Chem. Soc., Chem. Commun.* 1980, 491-492. This mechanism requires growth by two olefin units/insertion step. Hence, only C₂, C₄, C₆, C₈, C₁₀, ... would be expected. The results presented in Table I ruled out this mechanism.

(3) Ivin, K. J.; Rooney, J. J.; Stewart, C. D.; Green, M. L. H.; Mahab, R. *J. Chem. Soc., Chem. Commun.* 1978, 604-606; Green, M. L. H. *Pure Appl. Chem.* 1978, 50, 27-35.

(4) Bank, R., unpublished results. Ruled out by experiments in ref. 5.

(5) Finn, P.; Mathias, R. *Angew. Chem., Int. Ed. Engl.* 1980, 19, 857-875.

(6) Sinn, H.; Kaminsky, W. *Adv. Organomet. Chem.* 1980, 18, 99-149.

(7) Evtlt, E. R.; Bergman, R. G. *J. Am. Chem. Soc.* 1980, 102, 7003-7011; 1979, 101, 3973-3974.

(8) Maurignat, J. M.; McAllister, D. R.; Sanner, R. D.; Barrow, J. E. *J. Am. Chem. Soc.* 1978, 100, 2716-2724.

(9) Watson, P. L. *J. Am. Chem. Soc.*, in press.

(10) Tobbs, F. N.; Parshar, G. W. *J. Am. Chem. Soc.* 1971, 93, 3793-3795.

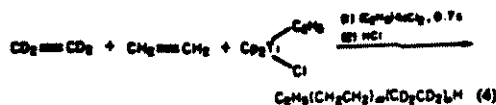
(11) Origyan, E. A.; Drozhkovskii, P. S.; Shilov, A. Ye. *Polymer Sci. Ser. A* 1966, 7, 145-149.

(12) Ott, K., unpublished results.

(13) Schrock, R. R. *Acc. Chem. Res.* 1979, 12, 98.

(14) Liu, B.; Ott, K.; Grubbs, R. H., unpublished results.

(15) Schnell, D.; Fink, G. *Angew. Makromol. Chem.* 1974, 30, 131.



If the catalyst activation is fast and the chain transfer slow relative to chain propagation, then the results for the copolymerization can be analyzed precisely. It can be shown that the average number of deuterated units, $\langle n \rangle$, in a chain is related to the total number of units, N , by the following expression:¹⁷

$$\langle n \rangle = (N - 1) \left(\frac{c\alpha}{1 + c\alpha} \right) + \frac{c}{1 + c}$$

where $c = k_{\text{CD}}[\text{C}_2\text{D}_4]/(k_{\text{CH}}[\text{C}_2\text{H}_4])$ and $\alpha = k_{\text{CD}}/k_{\text{CH}}$, $k_c =$ rate of complexation, and $k_p =$ rate of propagation.

The distribution of products in Table I shows a bell-shaped curve.¹⁸ This demonstrates that the catalyst is formed at a much faster rate than polymer growth. Only traces of olefin are formed in the reaction, i.e., little chain transfer is taking place.¹⁹ Hence the two boundary conditions are met. The plot of $\langle n \rangle$ vs. $(N - 1)$ in Figure 1 shows an excellent agreement with eq 2 (correlation factor 0.9996) with a slope of 0.49, which corresponds to a $k_{\text{CH}}/k_{\text{CD}}$ of 1.04 ± 0.03 .

Although this is derived from only one catalyst system which is not a propylene polymerization catalyst,²⁰ these data strongly support an insertion mechanism that does not involve a hydrogen migration during the rate-determining step of propagation. It is possible that the growing alkyl chain is interacting with a bridging Lewis acid center which does not leave the catalyst site during reaction or that the α -CH bonds are always distorted toward the metal center. Such cases would not necessarily show an isotope effect but could have a pronounced influence on the stereoselectivity. Such systems are now under investigation.

Registry No. Ethylene, 74-85-1; ethylene- d_2 , 683-73-8.

(16) Typically, the experiments were carried out by mixing 50 mL of a solution of $\text{Cp}_2\text{Ti}(\text{C}_2\text{H}_5)_2\text{Cl}$ (1 mmol in toluene) saturated with the desired monomer with an equal volume of $\text{Al}(\text{C}_2\text{H}_5)_2\text{Cl}$ (10 mmol in toluene) saturated with the same monomer in a stop-flow tube. After leaving the initial chamber, the reaction stream was delivered to a solution of HCl , CH_3OH , and toluene in a second mixing chamber. The contact time for the reaction was 0.7 s. The reaction mixture was washed with aqueous base (1M NaOH), dried, and concentrated by using a spinning band column to remove most of the solvent. The product was analyzed by capillary GC (10 m SE-30 column) and GC/MS-Cl (methane). The monomer mix was ethylene- d_2 /ethylene- d_0 = 1/1.033 (high-resolution MS). The ethylene mixture recovered after reaction showed no deuterium scrambling.

(17) Given the assumptions mentioned in the text, the probability of producing (in the given reaction time) a polymer chain N units long, n of which are deuterated units, is proportional to

$$P(N,n) = \frac{(c\alpha)^{n-1}(k_{\text{CH}})^{N-n-1}}{(k_{\text{CH}} + c\alpha)^{N-1}} \left\{ k_{\text{CH}} \left(\frac{c}{1+c} \right) \left(\frac{N}{(n-1)(N-n-1)} \right) + \left(\frac{1}{1+c} \right) (c\alpha) \left(\frac{N-1}{n(N-n-1)} \right) \right\}$$

Then $\langle n \rangle$ is given by

$$\langle n \rangle = \frac{\sum n P(N,n)}{\sum P(N,n)} = (N-1) \left(\frac{c\alpha}{1+c\alpha} \right) + \frac{c}{1+c}$$

(18) As seen in Table I, the average carbon number is similar for each monomer mix, while the spread in variance changes with monomer. The average is related to propagation rate while the spread is a function of catalyst formation rate. Both molecular and macroscopic factors will influence catalyst formation.

(19) Lack of chain transfer was demonstrated by the following: (a) polymerizing pure ethylene- d_0 and - d_2 resulted in no detectable olefin (capillary GC, authentic standards); (b) from the polymerization of ethylene- d_2 , only those oligomers of formula $\text{C}_n\text{D}_{2n-2}\text{H}_2$ were produced. None of the H, or H₂ isomers were observed by GC-MS.

(20) Rev. John, Jr. "Ziegler-Natta Catalysts and Polymerizations", Academic Press: New York, 1979.

Appendix: Elaboration on Footnote 17.

The probability of propagation to a chain of N links before termination is given by

$$P_N = \left(\frac{k_T}{k_T + k_P} \right) \left(\frac{k_P}{k_T + k_P} \right)^{N-1} \quad \text{that is, } N-1 \text{ propagations and one termination} \quad (1)$$

At a given time, assuming equilibrium of steady state is achieved, the number average degree of polymerization is given by

$$\langle N \rangle = \sum_{N=1}^{\infty} N P_N = \sum_{N=1}^{\infty} N \left(\frac{k_T}{k_T + k_P} \right) \left(\frac{k_P}{k_T + k_P} \right)^{N-1}$$

define $r = \left(\frac{k_P}{k_T + k_P} \right)$ and an arbitrary variable λ

$$\sum_{N=1}^{\infty} (r\lambda)^{N-1} \cdot N = \frac{1}{r} \frac{d}{d\lambda} \left(\sum_{N=1}^{\infty} (r\lambda)^N \right) = \frac{1}{r} \frac{d}{d\lambda} \left(\frac{r\lambda}{1-r\lambda} \right) \quad r\lambda < 1$$

$$\left(\frac{(1-r\lambda) + r\lambda}{(1-r\lambda)^2} \right) = \left(\frac{1}{1-r} \right)^2$$

$$\text{Set } \lambda=1, \text{ and } \sum_{N=1}^{\infty} N r^{N-1} = \left(\frac{1}{1-r} \right)^2 = \left(\frac{k_T + k_P}{k_T} \right)^2$$

$$\text{So } \langle N \rangle = \left(\frac{k_T}{k_T + k_P} \right) \left(\frac{k_T + k_P}{k_T} \right)^2 = \frac{k_T + k_P}{k_T}$$

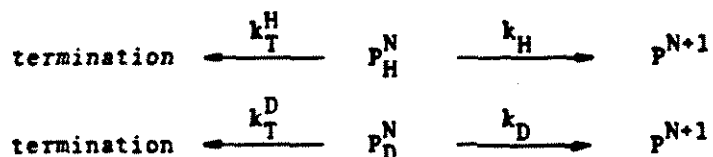
This result agrees with that predicted by standard methods.

Now consider the co-polymerization of two species: a deuterated and an undeuterated monomer. The fate of growing chains depends on the nature of the terminal unit, so split the problem to a consideration of each case: H-terminated and D-

terminated growing chains

(P_D^N = N-link chain which is D-terminated, P_H^N = N-link chain, H-terminated).

Each chain can either grow or terminate (temporarily ignore isotope effects on complexation).



We know that

$$\begin{aligned} r_H &= \text{rate of propagation past an H-terminus} \\ &= k_H (P_H) \text{ (olefin)} \end{aligned}$$

$$\begin{aligned} r_T^H &= \text{rate of chain transfer at an H-terminus} \\ &= k_T^H (P_H) \text{ (olefin)}. \end{aligned}$$

Similarly

$$\begin{aligned} k_D &= k_D (P_D) \text{ (olefin)} \\ r_T^D &= k_T^D (P_D) \text{ (olefin)}. \end{aligned}$$

The probabilities of a given H-rxn (i.e., H-terminus reaction) being propagation or termination are

$$\frac{r_H}{r_H + r_T^H} = k_H / (k_H + k_T^H) \quad \text{and} \quad \frac{r_T^H}{r_H + r_T^H} = k_T^H / (k_H + k_T^H)$$

respectively; and similarly for D-rxns.

The probability of a given reaction being an H-rxn is simply

$$\frac{r_H + r_T^H}{r_H + r_T^H + r_D + r_T^D} = \frac{(k_H + k_T^H) (P_H)}{(k_H + k_T) (P_H) + (k_D + k_T^D) (P_D)} \equiv \alpha_H$$

Similarly for α_D (= prob. that a rxn is a D-rxn). So we have

$$\begin{aligned} \pi_H &= \text{prob. that a rxn is a propagation past an H-terminus} \\ &= \alpha_H \left(\frac{k_H}{k_H + k_T} \right) \end{aligned}$$

Similarly

$$\pi_T^H = \alpha_H \left(\frac{k_T^H}{k_T + k_H} \right) = \text{probability that a rxn is termination after an H-terminus}$$

$$\pi_D = \alpha_D \left(\frac{k_D}{k_D + k_T^D} \right)$$

and

$$\pi_D^T = \alpha_D \left(\frac{k_T^D}{k_T^D + k_D} \right)$$

Now it is assumed that the ratio of the concentration of D-terminated chain (growing) to H-terminated is a constant (call it c).

$$\frac{(P_D)}{(P_H)} \equiv c \equiv \text{constant.}$$

So the probability of terminating a chain by chain transfer after an H-monomer terminus after growing a chain of N units, n of which are D is

$$H_{P(n)}^N = \binom{n}{D} \pi_D^{N-n-1} \pi_H \binom{N-1}{n} \pi_T^H$$

Similarly for transfer after a D terminus:

$$D_{P(n)}^N = \left(\pi_D^{n-1} \pi_H^{N-n} \pi_T^D \right) \binom{N-1}{n-1}$$

Thus the probability of generating a chain N units long, n of which are deuterated is given by:

$$P_{(n)}^N = H_{P(n)}^N + D_{P(n)}^N$$

$$P_{(n)}^N = \left(\pi_D^{n-1} \pi_H^{N-n-1} \right) \left\{ \pi_D \pi_T^H \binom{N-1}{n} + \pi_H \pi_T^D \binom{N-1}{n-1} \right\}$$

In order to simplify, note that

$$\pi_H = \frac{(P_H)}{R} (k_H) \quad \pi_D = \frac{(P_D)}{R} (k_D)$$

$$\pi_T^H = \frac{(P_H)}{R} (k_T^H) \quad \pi_T^D = \frac{(P_D)}{R} (k_T^D)$$

where

$$R = (k_H + k_T^H) (P_H) + (k_D + k_T^D) (P_D)$$

So,

$$\begin{aligned} P_{(n)}^N &= \left(\frac{1}{R} \right)^N \left\{ [(P_H)k_H]^{N-n-1} [(P_D)(k_D)]^{n-1} \right\} \\ &\quad \left\{ (P_D)(P_H) \left[k_D k_T^H \binom{N-1}{n} + k_H k_T^D \binom{N-1}{n-1} \right] \right\} \\ &= \left(\frac{1}{R} \right)^N (P_D)^n (P_H)^{N-n} \left\{ k_D^{n-1} k_H^{N-n-1} \left[k_D k_T^H \binom{N-1}{n} + k_H k_T^D \binom{N-1}{n-1} \right] \right\} \end{aligned}$$

$$\begin{aligned}
&= \underbrace{\left(\frac{1}{k_H + k_T^H + C(k_D + k_T^D)} \right)^N}_{\equiv (R')^{-N}} \left\{ (Ck_D)^{n-1} k_H^{N-n-1} \right. \\
&\quad \left. \left(Ck_D k_T^H \binom{N-1}{n} + k_H (Ck_T^D) \binom{N-1}{n-1} \right) \right\} \\
&= \left(\frac{1}{R'} \right)^N (k_T^H + k_T^D C) (Ck_D + k_H)^{N-1} \cdot F_{(n)}^N \quad (2)
\end{aligned}$$

Where

$$F_{(n)}^N = \frac{(Ck_D)^{n-1} k_H^{N-n-1} \left[(Ck_D) k_T^H \binom{N-1}{n} + k_H (Ck_T^D) \binom{N-1}{n-1} \right]}{(k_T^H + k_T^D C) (Ck_D + k_H)^{N-1}}$$

In this form, the relationship of eqⁿ (2) to eqⁿ (1) is obvious. It only remains to be shown that

$$\sum_{n=0}^N F_{(n)}^N = 1$$

x

$$\begin{aligned}
\sum_{n=0}^N F_{(n)}^N &= \left(\frac{1}{k_T^H + k_T^D C} \right) \sum \left(\frac{Ck_D}{Ck_D + k_H} \right)^{n-1} \left(\frac{k_H}{Ck_D + k_H} \right)^{N-n-1} \left\{ \right. \\
\sum_{n=0}^N F_{(n)}^N &= \sum_{n=0}^{N-1} \left(\frac{Ck_D}{Ck_D + k_H} \right)^n \left(\frac{k_H}{Ck_D + k_H} \right)^{N-n-1} k_T^H \binom{N-1}{n} \\
&\quad + \sum_{n=1}^{N-1} \left(\frac{Ck_D}{Ck_D + k_H} \right)^{n-1} \left(\frac{k_H}{Ck_D + k_H} \right)^{N-n} (Ck_T^D) \binom{N-1}{n-1} \\
&= k_T^H + Ck_T^D
\end{aligned}$$

Thus

$$\sum_{n=0}^N F_{(n)}^N = 1 \text{ as required.}$$

Thus equation (2) represents the generalization of equation (1) to the case of two component polymerization, if the new definitions are made

$$k_p' = k_H + Ck_D$$

$$k_T' = k_T^H + Ck_T^D$$

That is,

$$P_{(n)}^N = \left(\frac{k_T'}{R}\right) \left(\frac{k_p'}{R}\right)^{N-1} \cdot F_{(n)}^N \quad (2a)$$

Then, summing on n for a given N and determining the average N ($\equiv \langle N \rangle$),

$$\begin{aligned} \langle N \rangle &= \sum_{N=0}^{\infty} \left(\sum_{n=0}^N N P_{(n)}^N \right) = \frac{k_T' + k_p'}{k_T'} \\ &= \frac{k_T^H + k_H + C(k_T^D + k_D)}{k_T^H + k_T^D C} \end{aligned}$$

Now find $\langle n \rangle$ as a function of N

$$\langle n \rangle = \sum_{n=0}^N n P_{(n)}^N = \left(\frac{1}{R}\right)^N (Ck_T^D + k_T^H) (Ck_D + k_H)^{N-1} \sum n F_{(n)}^N$$

$$\begin{aligned} \sum n F_{(n)}^N &= \left(\frac{1}{k_T'}\right) \left(\frac{1}{k_p'}\right)^{N-1} \sum n \left[(Ck_D)^{n-1} k_H^{N-n-1} \right. \\ &\quad \left. \left[(Ck_D) k_T^H \binom{N-1}{n} + k_H (Ck_T^D) \binom{N-1}{n-1} \right] \right] \end{aligned}$$

$$= \sum_n \left[\theta^n (1-\theta)^{N-n-1} \binom{N-1}{n} \frac{k_T^H}{k_T} + \theta^{n-1} (1-\theta)^{N-n} \frac{ck_T^D}{k_T} \binom{N-1}{n-1} \right]$$

here

$$\theta = \frac{ck_D}{k_P}$$

$$\begin{aligned} \sum_n F_{(n)}^N &= \left[\sum_{n=0}^{N-1} n \theta^n (1-\theta)^{(N-1)-n} \binom{N-1}{n} \right] \frac{k_T^H}{k_T} \\ &\quad + \left[\sum_{n=1}^N n \theta^{n-1} (1-\theta)^{N-n} \binom{N-1}{n-1} \right] \frac{ck_T^D}{k_T} \\ &= (N-1) \left(\theta \frac{k_T^H}{k_T} \right) + \left[\sum_{v=0}^{N-1} \theta^v (1-\theta)^{(n-1)-v} (v+1) \binom{N-1}{v} \right] \frac{ck_T^D}{k_T} \\ &= (N-1) \left(\theta \left[\frac{k_T^H}{k_T} + \frac{ck_T^D}{k_T} \right] \right) + \frac{ck_T^D}{k_T} \\ &= (N-1) (\theta) + \frac{ck_T^D}{k_T} \end{aligned}$$

So

$$\langle n \rangle = \left(\frac{1}{R'} \right)^N (k_P')^{N-1} (k_T') \left[(N-1) \theta + \frac{ck_T^D}{k_T} \right]$$

Recall

$$R' = k_H + k_T^H + C(k_D + k_T^D) = k_P' + k_T'$$

Therefore

$$\langle n \rangle = \frac{(k_p')^{N-1} (k_T')}{(k_T' + k_p')^N} \left[\left(\frac{Ck_D}{k_p'} \right)^{N-1} + \frac{Ck_T^D}{k_T'} \right]$$

For a given N , the distribution of n is given by

$$n(N) = \frac{p^N(n)}{\sum_{n=1}^N p^N(n)} = F^N(n)$$

where $F^N(n)$ is defined (as earlier) as

$$F^N(n) = \frac{(Ck_D)^{n-1} (k_H)^{N-n-1}}{k_T' (k_p')^{N-1}} \left\{ Ck_D k_T^H \binom{N-1}{n} + Ck_H k_T^D \binom{N-1}{n-1} \right\}$$

Now define

$$\alpha = \frac{Ck_D}{k_H} \quad \text{and} \quad \beta = \frac{Ck_T^D}{k_T^H}$$

$$\begin{aligned} F^N(n) &= \left(\frac{\alpha^{n-1}}{k_H (1+\alpha)^{N-1} k_T'} \right) \left(Ck_D k_T^H \binom{N-1}{n} + Ck_T^D k_H \binom{N-1}{n-1} \right) \\ &= \left(\frac{1}{1+\alpha} \right)^{N-1} \left(\alpha^n \binom{N-1}{n} \left(\frac{1}{1+\beta} \right) + \left(\frac{\beta}{1+\beta} \right) \alpha^{n-1} \binom{N-1}{n-1} \right) \\ &= \left(\frac{1}{1+\beta} \right) \left(\frac{1}{1+\alpha} \right)^{N-1} \left\{ \alpha^n \binom{N-1}{n} + \alpha \beta^{n-1} \binom{N-1}{n-1} \right\} \end{aligned}$$

So define

$$G_{(n)}^N = (1+\beta) (1+\alpha)^{N-1} F_{(n)}^N$$

$$= \left\{ \alpha^n \binom{N-1}{n} + \beta \alpha^{n-1} \binom{N-1}{n-1} \right\}$$

Here $G_{(n)}^N$ represents the unnormalized distribution of n .

Examples

Suppose $c=1$, and let:

$$\alpha = \frac{k_D}{k_H} = 0.9 \quad \text{and} \quad \beta = \frac{k_T^D}{k_H^T} = 2.0$$

Let $N = 8$

N	$G_{(n)}^N$
0	1
1	8.3
2	29.61
3	59.54
4	24.00
5	58.33
6	28.52
7	7.92
8	0.96

$$\langle n \rangle = \frac{\beta}{1+\beta} + \left(\frac{\alpha}{1+\alpha} \right) (N-1)$$

$$= \frac{2}{3} + 7 \left(\frac{0.9}{1.9} \right) = 3.98$$

Distribution for $c=1$, $\alpha=0.9$, $\beta=2$ and $N=20$

$$\langle n \rangle = \frac{2}{3} + 19 \left(\frac{0.9}{1.9} \right) = \boxed{9.67}$$

$$G_{(n)}^N = \alpha^n \binom{19}{n} + \beta \alpha^{n-1} \binom{19}{n-1}$$

$$= (0.9)^n \binom{19}{n} + 2 (0.9)^{n-1} \binom{19}{n-1}$$

<u>N</u>	<u>G_(n)²⁰</u>
0	1.00
1	19.1
2	172.71
3	983.42
4	3.96 x 10 ³
5	1.20 x 10 ⁴
6	2.82 x 10 ⁴
7	5.29 x 10 ⁴
8	8.07 x 10 ⁴
9	1.009 x 10 ⁵
10	1.04 x 10 ⁵
11	8.81 x 10 ⁴
12	6.17 x 10 ⁴
13	3.54 x 10 ⁴
14	1.65 x 10 ³
15	6.12 x 10 ³
16	1.78 x 10 ²
17	3.88 x 10 ¹
18	5.99 x 10 ¹
19	5.84
20	0.27

CONCLUSION

In this thesis the results of a study of the suprafacial $2 + 2$ reaction have been presented. The electronics of the transformation have been described in terms of the motion of four singly-occupied electronic orbitals. If these orbitals are able to change their shapes in continuous ways from reactants to products, and if these shape changes do not result in the cleavage of either of the two active bonds (as judged as orbital overlaps), then the suprafacial reaction can occur.

The stipulation that both bonds be retained during the entire reaction engenders severe restrictions. In the nonpolar four-center process, the participation of an orbital which is antisymmetric with respect to the reaction is demanded. The energy of this orbital and its ability to form a covalent bond which is antisymmetric with respect to the reaction determine the energetic barrier to the electronic reorganization implied by the $2_s + 2_s$ reaction.

One very common example of the $2_s + 2_s$ reaction is the organometallic migratory insertion reaction - a cornerstone in the chemistry of homogeneous catalysis. The principle of maximum bonding upon which the Woodward-Hoffmann rules are based, coupled with the description of the migratory insertion as a concerted process, and the notion that a given ligand environment around a given metal supports one state of covalency at the expense of the alternatives suggests a simple rule for the design of homogeneous catalysts.

During a homogeneously catalytic cycle, the number of covalent bonds to the metal at the active site of the catalysis should remain constant.

Odi et amo! Quare id faciam fortasse requiris.

Nescio, sed fieri sentio et excrucior.

Gaius Valerius Catullus

"Carmina Catulli" 85